

Parker, Laura Louise (2003) *Macrocyclic nitrogen mustard prodrugs as hypoxia selective anti-cancer agents*. PhD thesis.

<http://theses.gla.ac.uk/5364/>

Copyright and moral rights for this thesis are retained by the author

A copy can be downloaded for personal non-commercial research or study, without prior permission or charge

This thesis cannot be reproduced or quoted extensively from without first obtaining permission in writing from the Author

The content must not be changed in any way or sold commercially in any format or medium without the formal permission of the Author

When referring to this work, full bibliographic details including the author, title, awarding institution and date of the thesis must be given



**UNIVERSITY
of
GLASGOW**

Scheme 1

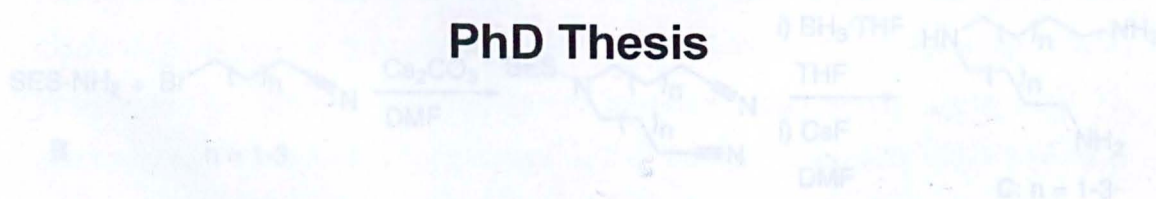
Macrocyclic nitrogen mustard prodrugs as hypoxia selective anti- cancer agents

The (2-trimethylallylthio)ethylsulfonyl (TES) protecting group is very versatile. It is removed under mild conditions using fluoride. The published synthesis of the sulfonyl chloride **A** gave variable yield and purity, but we have improved the conditions to give consistently pure material in high yield (70-86% overall) (Scheme 1).

Scheme 2

Laurie Louise Parker

PhD Thesis



Triamines

Department of Chemistry

Supervisor: Prof. David J. Robins

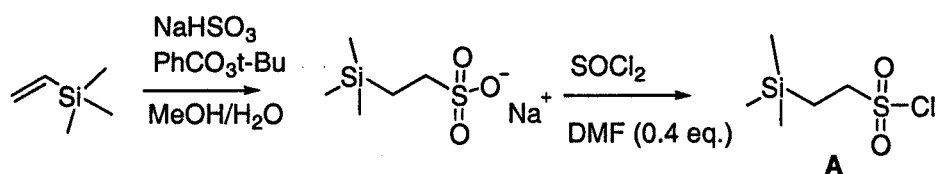
November 2003

A variation on the Robinson-Aikens synthesis has been exploited to reach known and novel triazamacrocyclic compounds **D** (Scheme 3), in order to explore their structure-activity relationship as *N*-mustard drugs **E** (made as shown in Scheme 4). Eight novel macrocyclic triamines **D** were prepared and found to be potent DNA cross-linking agents (nM range). Three of the novel triamines were tested *in vitro* for anti-parasitic

Summary

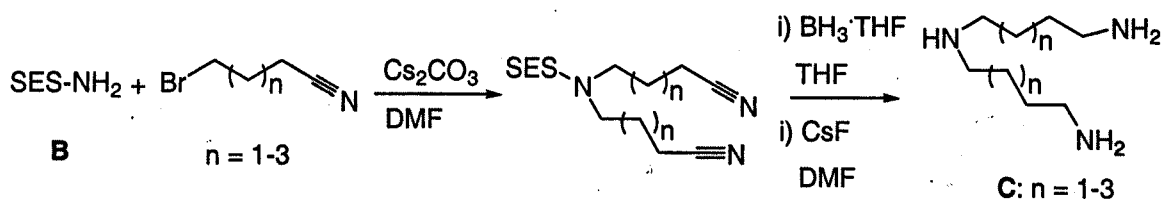
The low selectivity of chemotherapy is an ongoing problem in the treatment of cancer. Prodrugs that are activated *in vivo* provide a therapeutic advantage for selective cytotoxicity. Here we have designed redox-active compounds that are electrochemically reduced in hypoxic (poorly oxygenated) tissue, resulting in release of a nitrogen mustard cytotoxin. This thesis describes the synthesis of novel macrocyclic *N*-mustard drugs and the development of their Cu(II) complexes as hypoxia-selective prodrugs.

Scheme 1



The (2-trimethylsilyl)ethanesulfonyl (SES) protecting group is very versatile. It is removed under mild conditions using fluoride. The published synthesis of the sulfonyl chloride **A** gave variable yield and purity, but we have improved the conditions to give consistently pure material in high yield (70-86% overall) (**Scheme 1**).

Scheme 2

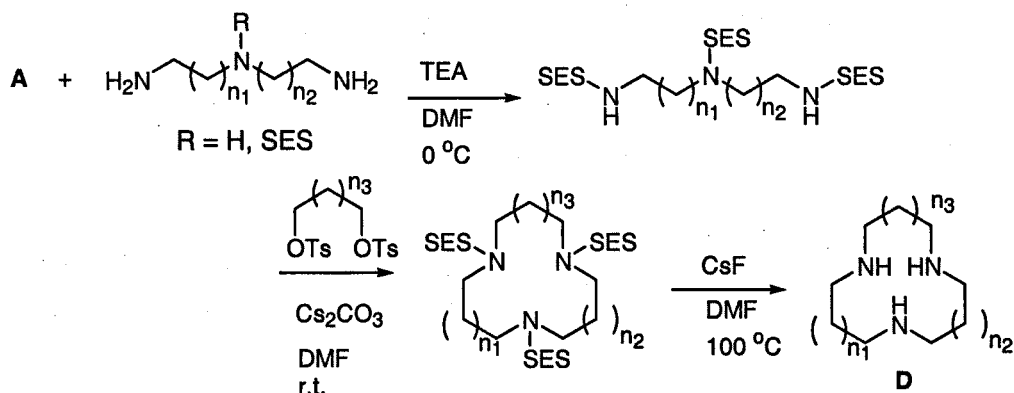


Triamines with carbon bridges longer than three are difficult to prepare, often requiring multistep syntheses. A route was developed to synthesize linear triamines, using the SES-amide **B**. This route produces these triamines in relatively high yields (60-80% overall), via simple reactions with little purification necessary (**Scheme 2**).

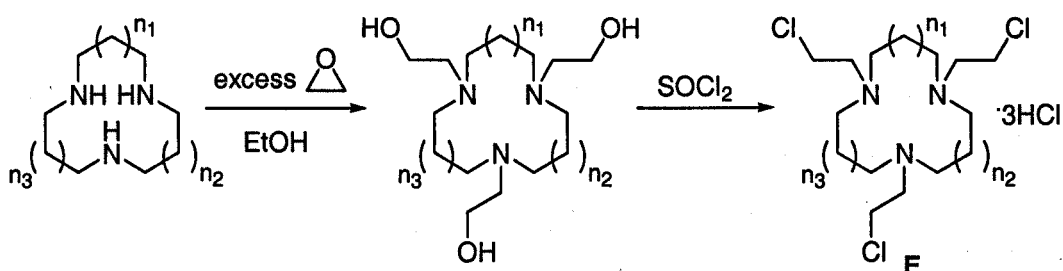
A variation on the Richman-Atkins synthesis has been exploited to reach known and novel triazamacrocyclic compounds **D** (**Scheme 3**), in order to explore their structure-activity relationship as *N*-mustard drugs **E** (made as shown in **Scheme 4**). Eight novel macrocyclic *N*-mustards **E** were found to be potent DNA cross-linking agents (nM range) by Prof. John Hartley at University College London. Three of the novel triazamacrocycles **D** were assessed *in vitro* for anti-parasitic

activity by Dr. Michael Barrett at the University of Glasgow. They showed moderate activity against *Leishmania mexicana* and *Trypanosoma brucei*.

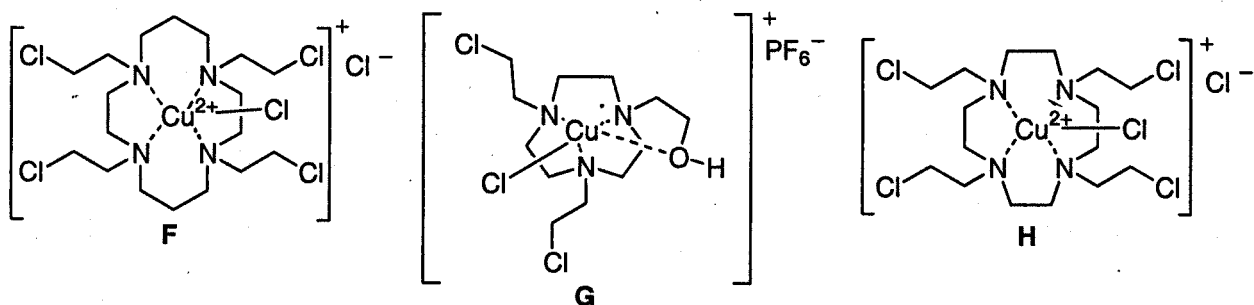
Scheme 3



Scheme 4



Water soluble Cu(II) complexes of cytotoxic macrocyclic nitrogen mustards have been prepared and their structures have been determined using X-ray crystallography by Dr. Louis Farrugia in this department. The redox behaviour and reduction potentials (Cu[II] to Cu[I]) of the complexes in phosphate buffer were assessed using cyclic voltammetry. The thermodynamic stabilities of the Cu(II) complexes in aqueous solution were analysed qualitatively using UV-Vis spectroscopy. The mustard complexes **F** and **G** showed irreversible redox behaviour and low thermodynamic stability, and were not hypoxia-selective but behaved as typical mustard drugs. The cyclen-based mustard complex **H** showed reversible redox behaviour and had high thermodynamic stability under aqueous conditions. **H** exhibited excellent hypoxia selectivity (the best so far in the lung tumour cell line tested) and is an attractive lead compound for further development of this novel approach to cancer chemotherapy.



Acknowledgements

First and foremost, I thank my supervisor, Prof. David Robins, for giving me the opportunity to live in Scotland for three years and study for a PhD. It wouldn't have happened without his help.

I also thank my co-workers in the Henderson lab for support and camaraderie, especially Isabel Freer and the other members of the Robins group: Gary (we attracted all the weird people in New Orleans...), Jill, Sam, Kathryn and Stephen. Special gratitude goes to Stephen Jones and Nicholas Gowans for having tried out various experiments for me during their fourth-year projects. Special thanks to Alex Pickering for proofreading this thesis. A huge thank-you goes to all the staff members who have given me technical help and advice, including Jim Gall and Dr. David Rycroft (NMR spectroscopy), Jim Tweedie and Tony Ritchie (mass spectrometry), Dr. Louis Farrugia and Dr. Cameron Evans (X-ray crystallography), Dr. Lee Cronin (and the Cronin group) and Dr. De-liang Long (cyclic voltammetry and understanding inorganic chemistry), Kim Wilson (microanalysis) and Stuart Mackay (for IT help when my laptop was driving me crazy)—as well as those who helped me with biological testing: Dr. Michael Barrett, David Laughland (leishmania) and Janice Brock (trypanosomes), and Prof. Stephen Phillips (malaria) of the University of Glasgow; Prof. John Hartley of University College London (DNA-crosslinking assays and *N*-mustard cytotoxicity); and Prof. Ian Stratford, Dr. Mohammed Jaffar and Natasha Wind (bioelectrochemical testing).

I need to thank all my friends here in Glasgow for their moral support and companionship during my time so far away from home. In particular I want to thank the Fraser sisters (especially Kirstie), Linda Jordan (for being a perfect flatmate!), Megan Read (for singing with me), Rod Ashley (for giving me songs to sing), all the Hartleys: Richard, Lucy, Sarah, Hannah and Stephen (you'll always be very special to me), and Nicola Meenan and Gordon McKiernan (for being my gym buddies and rant outlets).

I express my love and gratitude to all my family (Mom, Dad, Sarah, Amy) for being my best friends (and for flying me home to visit them!), and to Tom Hutton for being my emotional support and for not letting me take things too seriously.

Preface

This thesis represents original synthetic work carried out by Laurie Louise Parker at the University of Glasgow in the Henderson Laboratory, under the supervision of Prof. David Robins, during the period of December 2000 to November 2003. This work was funded by the University of Glasgow (University 2001 Scholarship) and Universities UK (ORS Award). Portions of the work described herein have been published elsewhere as listed below.

L. L. Parker, N. D. Gowans, S. W. Jones and D. J. Robins, *Tetrahedron*, in press (2003)

Abbreviations

18-crown-6	1,4,7,10,13,16-tetraoxocyclooctadecane
Å	Ångstrom
Ac	acetyl
AcOH	acetic acid
ADEPT	antibody-directed enzyme prodrug therapy
aq.	aqueous
Ar	aryl
Bn	benzyl
Boc	<i>tert</i> -butoxycarbonyl
CDI	carbonyldiimidazole
CI	chemical ionisation
COSY	<u>C</u> orrelation <u>S</u> pectroscop <u>Y</u>
CPI	cyclopropylpyrroloindolo-quinone
Cu-ATSM	Cu(II)-diacetyl-bis(N-4-ethylthiosemicarbazone)
CV	cyclic voltammetry
cyclam	1,4,8,11-tetraazacyclotetradecane [2,3,2,3]
cyclen	1,4,7,10-tetraazacyclododecane [2,2,2,2]
d	days
DCC	dicyclohexylcarbodiimide
DFMO	difluoromethylornithine
DMF	<i>N,N</i> -dimethylformamide
DMSO	dimethylsulfoxide
DNA	deoxyribonucleic acid
$E_{1/2}$	$(E_{pa}+E_{pc})/2$ (redox potential)
e^-	electron
EC	electrochemical-chemical
ECE	electrochemical-chemical-electrochemical
EDTA	ethylene-1,2-diamine- <i>N,N,N',N'</i> -tetraacetic acid
EI	electron impact
E_{pa}	anodic peak potential (oxidation potential)
E_{pc}	cathodic peak potential (reduction potential)
eq.	equivalents
Et	ethyl
Et ₂ O	diethyl ether
FAB	fast atom bombardment
FAD	flavin adenine dinucleotide
FCA	ferrocenecarboxylic acid
Fc/Fc+	ferrocene/ferrocenium couple
g	gram
GDEPT	gene-directed enzyme prodrug therapy
h	hour
HIF-1	hypoxia inducible factor 1
HMBC	<u>H</u> eteronuclear <u>M</u> ultiple <u>B</u> ond <u>C</u> orrelation
HMQC	<u>H</u> eteronuclear <u>M</u> ultiple <u>Q</u> uantum <u>C</u> orrelation
homocyclen	1,4,7,10-tetraazacyclotridecane [2,2,2,3]
HIV	human immunodeficiency virus

<i>hν</i>	ultraviolet light
IC ₅₀	concentration of drug to inhibit 50% of growth
IR	infrared
λ _{max}	maximum ultraviolet-visible absorbance
M	molar
mAChRs	muscarinic acetylcholine receptors
Me	methyl
MeCN	acetonitrile
mesyl	methanesulfonyl
MHz	megaHertz
min	minute
ml	millilitre
mmol	millimole
MMPs	matrix metalloproteinases
mp	melting point
MPA	mercaptopropionic acid
MRI	magnetic resonance imaging
Mts	mesitylene (i.e. 1,3,5-trimethylbenzene)sulfonyl
NADH	nicotinamide adenine dinucleotide phosphate (oxidised form)
NADPH	nicotinamide adenine dinucleotide phosphate (reduced form)
NBS	<i>N</i> -bromosuccinimide
NHE	normal hydrogen electrode
NMR	nuclear magnetic resonance
<i>N</i> -mustard	<i>N</i> -bis(2-chloroethyl)
<i>N</i> -half mustard	<i>N</i> -mono(2-chloroethyl)
nosyl	nitrobenzenesulfonyl
2-Ns	2-nitrobenzenesulfonyl
4-Ns	4-nitrobenzenesulfonyl
OMs	methanesulfonyl
OTs	<i>para</i> -toluenesulfonyl
Pg	protecting group
Ph	phenyl
PNA	peptide nucleic acid
Pr	propyl
PTR1	pteridine reductase 1
RNA	ribonucleic acid
rt	room temperature
SES	(2-trimethylsilyl)ethanesulfonyl
tacn	1,4,7-triazacyclononane [2,2,2]
TBAF	tetra- <i>N</i> -butylammonium fluoride
TBAOH	tetra- <i>N</i> -butylammonium hydroxide
TEA	triethylamine
TEAF	tetra- <i>N</i> -ethylammonium fluoride
TEBACl	triethylbenzylammonium chloride
THF	tetrahydrofuran
TLC	thin layer chromatography
TMAF	tetra- <i>N</i> -methylammonium fluoride
tosyl	<i>para</i> -toluenesulfonyl

Tr
TRYR
UV-Vis
VEGF
VHL

triflate (trifluoromethanesulfonic acid)
trypanothione reductase
ultraviolet-visible
vascular endothelial growth factor
von-Hippel Lindau protein

Table of contents

Chapter 1.....	5
1. Introduction	5
1.1. Cancer	5
1.1.1. Biology of cancer development	5
1.1.2. Cancer therapy	8
1.2. Bioreductive drugs	9
1.2.1. Hypoxia	9
1.2.2. Exploiting tumour hypoxia	11
Gene therapy approach.....	11
Bioreductive drug approach	12
<i>Release systems</i>	13
<i>Direct activation systems</i>	15
1.2.3. Enzymology of bioreduction	22
1.2.4. Electrochemistry of bioreduction	23
1.2.5. Bioreductive drug design	25
1.3. Nitrogen mustard alkylating agents	25
1.3.1. Biological effects.....	25
1.3.2. Previous developments in mustard drugs.....	27
1.4. Synthesis of macrocyclic polyamines.....	33
1.4.1. Cyclisation.....	33
High dilution cyclisations	33
Templated cyclisations.....	35
<i>Metal ion templates</i>	35
<i>Carbon templates</i>	36
Richman-Atkins cyclisation of sulfonamides	39
<i>p-Toluenesulfonamide cyclisation</i>	39
<i>Alternative sulfonamides</i>	42
1.5. Other biological considerations.....	43
1.5.1. Polyamine analogues.....	44
1.5.2. Catalysts and enzyme mimics	46
Carboxyesters	47

Phosphate esters	47
Peptide bonds	49
Chapter 2.....	51
2. Synthesis of parent macrocycles	51
2.1. Initial strategy using the mesitylenesulfonyl protecting group	51
2.2. Alternative protecting group strategies	53
2.3. Synthesis of (2-trimethylsilyl)ethanesulfonyl chloride	56
2.4. SES-triamines	57
2.5. Cyclisation and deprotection	62
2.6. Purification of parent macrocycles	68
2.7. Alternative fluoride sources	68
2.8. Synthesis of triazacyclophanes	72
2.9. Alternative routes to polyazamacrocycles	74
2.10. Conclusions	76
Chapter 3.....	78
3. Synthesis of polyazamacrocyclic nitrogen mustard derivatives	78
3.1. Unsuccessful routes: reductive alkylation; chloroacetamides	78
3.1.1. Reductive alkylation	78
3.1.2. Chloroacetamides	79
3.2. Poly- <i>N</i> -(2-hydroxyethyl) derivatives	80
3.3. Macrocyclic nitrogen mustard derivatives	83
Chapter 4.....	86
4. Coordination chemistry of novel polyazamacrocycles.....	86
4.1. Synthesis of metal complexes	86
4.2. Stability of polyazamacrocyclic metal complexes	95
4.2.1. Discussion of stability	95
4.2.2. 'Aqueous stability' of mustard macrocycle complexes	97
4.2.3. Electrochemistry and complex stability	98

4.3. Electrochemistry of novel mustard complexes	103
4.4. Aqueous stability of novel complexes	111
4.5. Additional complexation	113
4.5.1. Co(II) complex of cyclen mustard	113
4.5.2. Complexation of novel parent triazamacrocycles	115
4.6. Conclusions	118
Chapter 5.....	119
5. Biological testing and results.....	119
5.1. DNA-crosslinking and cytotoxicity of uncomplexed mustards	119
5.2. Hypoxia selectivity of Cu(II) complexes of selected macrocyclic mustards	121
5.3. Anti-parasitic activity of polyazamacrocycles and selected Cu(II) complexes	123
5.4. Conclusions	127
5.5. Future Work	128
Chapter 6.....	132
6.1. Experimental to Chapter 2.....	132
General procedures 2a-l	132
Experimental details.....	137
6.1.1. Diol ditosylate formation	137
6.1.2. Mesitylenesulfonamides.....	139
6.1.3. Cyclisation of mesitylenesulfonamides.....	140
6.1.4. Deprotection of mesitylenesulfonamides	142
6.1.5. Synthesis of SES-chloride.....	142
6.1.6. Building triamines from sulfonamides.....	143
6.1.7. SES-amide synthesis	148
6.1.8. Cyclisation of SES-amides.....	151
6.1.9. Deprotection of SES-amides	158
6.1.10. Synthesis of cyclophanes	164
6.1.11. Carbon template routes.....	167

6.2. Experimental to Chapter 3	170
General procedures 3a-c	170
Experimental details	171
6.2.1. Chloroacetamides	171
6.2.2. Hydroxyethyl derivatives	173
6.2.3. Synthesis of chloroethyl derivatives	179
6.3. Experimental to Chapter 4	185
6.3.1. Formation of Cu(II) complexes	185
6.3.2. X-ray crystallography	190
6.3.3. UV-Vis spectroscopy	191
6.3.3.1. Characterisation: λ_{max} and ϵ_{coeff}	191
6.3.3.2. Aqueous stability of complexes	191
6.3.4. Cyclic voltammetry	192
6.3.5. Complexation of novel triazamacrocycles	195
6.4. Experimental to Chapter 5	197
6.4.1. Anti-cancer testing	197
6.4.1.1. Cytotoxicity of free mustard ligands (Prof. Hartley)	197
6.4.1.2. Cytotoxicity and hypoxia-selectivity of complexes (Prof. Stratford)	197
6.4.2. Anti-parasitic testing	198
6.4.2.1. Cytotoxicity against <i>Leishmania mexicana</i> (Dr. Barrett)	198
6.4.2.2. Cytotoxicity against <i>Trypanosoma brucei</i> (Dr. Barrett)	198
References	199
Appendix 1	210
Appendix 2	215

Chapter 1

1. Introduction

1.1. Cancer

Cancer is the second most frequent cause of death in the western world. One in three people contract cancer at some point in their lives. Roughly two-thirds of those people die as a result of their cancer, bringing the total death toll by cancer to one in four people.¹ For decades we have been searching for 'the cure;' but it became apparent long ago that things were not going to be that simple.

A wealth of data exists describing the biological and environmental origins and characteristics of cancer. The post-genomic era provides a new environment in which to seek out and understand the genetic basis for tumour development. As we come to grips with the biological mechanisms inherent in cancer development, new strategies in the fight against it emerge. Better aims in tissue targeting, fewer side effects and improved length and quality of life for cancer sufferers bring us closer to the holy grail of complete treatment and control. However, like a mathematical asymptote, we will probably never reach that ultimate goal; cellular evolution will always be one step ahead of us.

1.1.1. Biology of cancer development

The biological irregularities that eventually lead to cancer are extremely complex. Many steps are involved, beginning with genetic changes and culminating in regulatory defects that allow the uncontrolled proliferation of cells. The process has been compared to Darwinian evolution: genetic mutations allowing a better chance for survival and thus being carried on to further generations.² Advanced tumours are almost perfect examples of 'the survival of the fittest.' Cancer cells have forgotten they are an integral part of an organism. With an adequate supply of nutrients, they can continue to grow and reproduce virtually indefinitely, even being

termed 'immortal.' One of the first samples of human tumour cells, the Hela cell line isolated in 1951, is still alive and growing today.

Cells have built-in obstacles that must be overcome in order for them to become cancerous. Hanahan and Weinberg³ describe the six major traits that must be acquired to begin tumour development: self-sufficiency in growth signals; insensitivity to growth-inhibitory signals; evasion of apoptosis (programmed cell death); limitless replicative potential; sustained angiogenesis (blood vessel growth); and tissue invasion and metastasis (aggressive spread of cancer *via* release and migration of tumour tissue to other tissues).

Cell growth is regulated by countless pathways within the cell, but also importantly by the cell's external environment. For example, cells in normal tissue are mostly instructed to replicate or cease replication by contact with their neighbours.³ Some tumours are able to co-opt their neighbouring normal cells into abnormal growth.⁴ Ignoring growth-inhibitory signals also involves a combination of inter- and intra-cellular factors. Normally the tissue environment tells its cells to stop multiplying. The commands are carried out *via* signalling pathways within the cell. Unrestricted growth requires circumvention of those pathways. Essentially, cancerous cells stop responding to the messages telling them not to replicate.

Evasion of apoptosis is a hallmark of almost every type of cancer. Tumour cell populations explode because far more cells are being produced than destroyed. Apoptosis usually occurs in old and abnormal cells *via* a cascade of proteases called caspases.⁵ Caspases cause cell death by taking apart the genome and various organelles and sub-cellular structures. Cancer cells acquire resistance to apoptosis through genetic mutations, losing genes for key apoptosis-inducing responses.

Limitless replicative potential goes beyond the combined abilities to ignore cell-growth messaging and to avoid self-degradation. Normal cells have built-in restrictions on their replicative potential. Each cell cycle results in the shortening of telomeres (protective sequences of DNA at the ends of the chromosomes). Eventually the telomeres have been shortened to a critical length, causing disadvantageous chromosomal fusion, disarray and widespread cell death (the 'crisis' state). However,

those cells that have adapted to maintain the length of their telomeres survive past the crisis state and become 'immortalised',⁶ replicating indefinitely.

Another requirement for cancer development is the ability to sustain continuous angiogenesis to supply the tumour tissue with blood. Regulation of angiogenesis is carried out through an array of homeostatic pathways. Vascular endothelial growth factor (VEGF) is closely involved in the stimulation of angiogenesis. These relationships have been demonstrated using anti-VEGF antibodies to impair the growth of implanted tumours in mice.⁷ Integrins (cell-surface proteins that participate in cellular adhesion and intercellular communication) are also essential to the process of angiogenesis and interfering with their signalling pathways can have an inhibitory effect. Many proteases are also involved in controlling the levels of various activating and inhibiting factors in the angiogenic response.

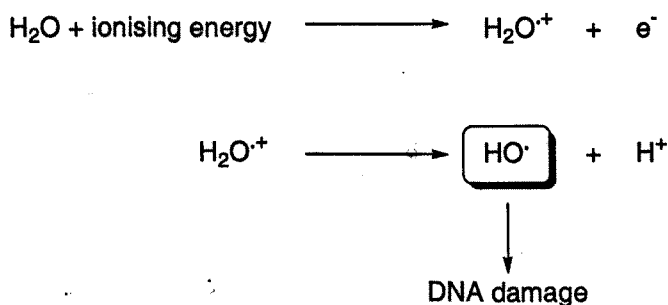
Lastly, 90% of lethal cancers develop the ability to invade and colonise other tissues.⁸ This activity, called metastasis, is the culmination of the tumour's progress towards 'survival of the fittest.' Its enhanced speed of growth and facility to use nutrients gives it an advantage over the normal tissues it invades. In order to begin metastasis, tumour cells must be able to release themselves from their extracellular matrix and eventually create entrances into new tissue. These processes involve the impairment of integrins and other cell-adhesion proteins, as well as stimulation of extracellular proteases to degrade the matrix. Without metastasis, the tumour would eventually use all the nutrients in its immediate area and its growth would be halted. With this process, it can keep its progeny cells alive by sending them to distant territories with plentiful resources; that is, until the cancer completely overwhelms the organism it has invaded and destroys its own environment.

Since all of the above processes are highly complex and no one instigator for any of them can be identified, it is important to maintain a holistic mindset when developing cancer treatment.³ The disciplines of biochemistry, immunology, genetics, molecular biology, pharmacology and synthetic chemistry all need to be considered in a comprehensive cancer treatment strategy. This thesis discusses our synthetic chemistry approach to drug design in the struggle against cancer.

1.1.2. Cancer therapy

Classical cancer therapy takes on a number of forms. Sometimes various therapies are applied concurrently. When the cancer takes the form of a solid tumour, physical removal of the tumour is common. However, when tumours are difficult to access surgically or have already begun to metastasise, chemical or radiotherapies are employed. Radiotherapy takes advantage of the damaging hydroxyl radicals produced following the exposure of water to ionising radiation (Scheme 1.1.2.1). Unfortunately the damage is difficult to localise, resulting in damage to healthy tissues and highly unpleasant side effects. Occasionally radiotherapy induces secondary cancers, especially in children. Chemotherapy uses toxic chemicals to kill the tumour cells, often focusing on rapidly proliferating cells by targeting the cell cycle.⁹ Recent chemotherapy advances have exploited the cytotoxic effects of a number of natural products, e.g. daunorubicin¹⁰ and taxol.¹¹ Other strategies employ toxic analogues of cellular components, such as 5-fluorouracil.^{12,13} Again, toxicity is often unselective, resulting in side effects especially to fast-growing cells like hair follicles and bone marrow.

Scheme 1.1.2.1



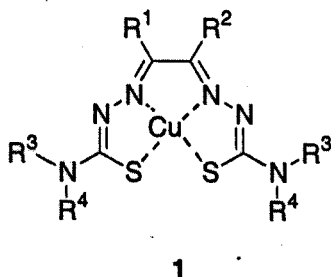
Cellular hypoxia (lowered intracellular oxygen concentration) is common in solid tumours.¹⁴⁻¹⁶ The rapid proliferation of cancer cells and the resulting insufficient growth of supporting vasculature creates an environment in which the cells adapt to survive under anaerobic conditions. This often results in resistance to normal chemo- and radio-therapy. However, it advantageously provides a key difference between cancer cells and normal cells, offering opportunities for more directed targeting of tumour cells, as well as allowing for therapeutic differentiation

between types of cancers *via* the specific enzyme profiles of the various cell types.¹⁷ The targeting of hypoxic cells with bioreducible alkylating agents, through the exploitation of tumour hypoxia, is the principal aim of this project. Therefore, the discussion of cancer therapies herein will focus on the use of these drugs.

1.2. Bioreductive drugs

1.2.1. Hypoxia

Tumour hypoxia is highly heterogeneous, changing with tumour size, stage of development, extent of necrosis and histological environment.^{18, 19} Almost all solid murine tumours (commonly used for *in vivo* drug studies) contain large proportions of hypoxic cells.²⁰ There is also a large body of experimental evidence for the existence of hypoxia in human tumour cells.¹⁴⁻¹⁶ Hypoxic environments have been found in cervical cancer, squamous cell carcinoma of the head and neck, melanoma, breast cancer, prostate cancer and brain tumours. Lactate levels give an indication of the degree of anaerobic metabolism present and thus the degree of oxygenation of tissue, but are less quantitative for determination of hypoxia.²¹⁻²⁴ Oxygen levels can be detected quantitatively by electrode methods, although electrodes are unable to distinguish between cell viabilities and cell types.^{23, 25} Chemical marker methods are more reliable, such as radiolabelled or fluorescently labelled nitroimidazoles, which bind to hypoxic cells *in vitro* and *in vivo*.²⁶⁻²⁸ In addition, bis(thiosemicarbazone) ligands (e.g. 1) act as vectors for bioreducible Cu(II) isotopes which are deposited in hypoxic cells upon reduction to Cu(I).²⁹



Tumour hypoxia has been linked to the unsuccessful outcome of therapeutic treatments, especially radiotherapy. The dose of radiation required to kill hypoxic

cells is three times that necessary to kill well-oxygenated cells; therefore at safe levels of radiation for treatment, most hypoxic cells survive. Chemotherapy is often inhibited in hypoxic cells due to the requirement for molecular oxygen in the toxicity of many anti-cancer agents (e.g. bleomycin). In addition, cell proliferation is greatly reduced as a result of lowered oxygen concentration, so agents that specifically target the mechanism of fast proliferation are less toxic in hypoxic cells. Lastly, since hypoxia often occurs as a result of insufficient vasculature and oxygen delivery, drug delivery through these same channels is also affected and can result in lower effective doses to the hypoxic regions.³⁰

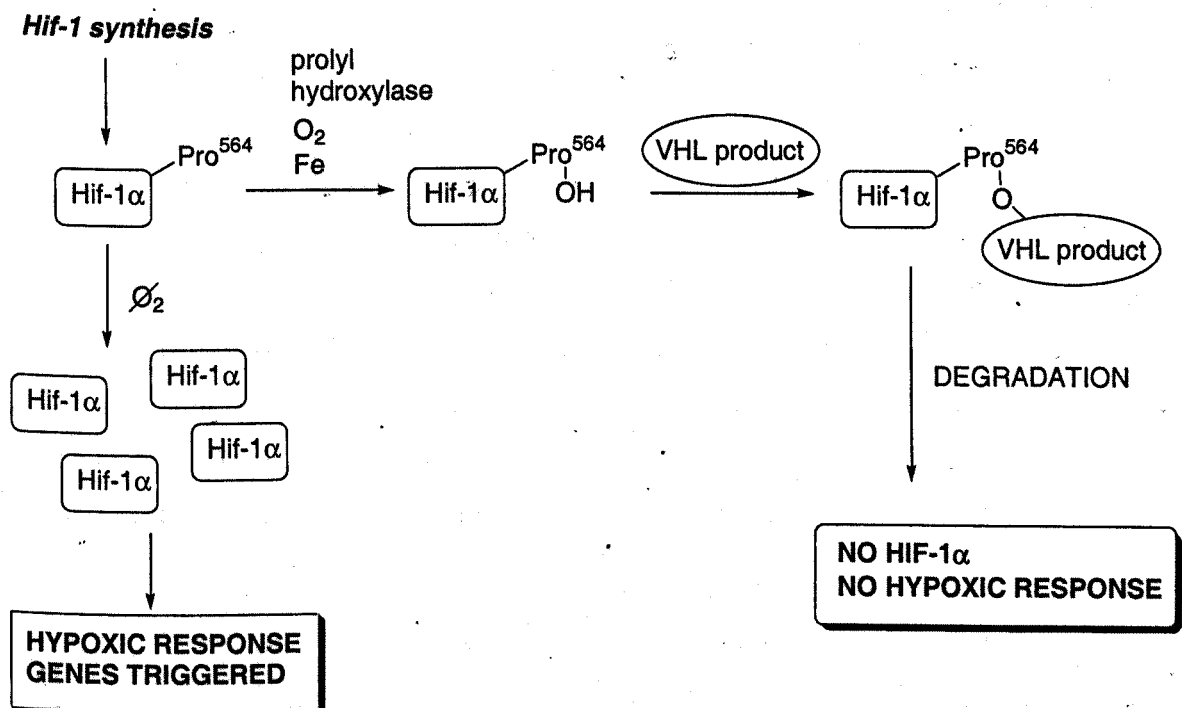
Aside from contributing to treatment resistance, hypoxia also contributes to adverse malignant effects within the tumour microenvironment by promoting metastasis and angiogenesis. Metastasis is promoted through the increased expression of matrix metalloproteinases (MMPs) under hypoxic conditions.^{31, 32} MMPs are essential to the metastasis process.^{33, 34} They degrade the basement membrane and extracellular matrix to facilitate the release of migrating tumour cells. There is some evidence that hypoxia contributes to cell adhesion processes required for metastasis, by reducing the levels of cell surface integrins and allowing the migration of cells from their original location.^{35, 36} Hypoxia also increases the levels of interleukin-8, an inflammatory factor associated with tumourigenicity, angiogenesis and metastasis in many types of tumours. The same processes (MMP production, cell adhesion changes) are important in the beginning of angiogenesis. Angiogenesis begins when the cells respond to the initiation of production of VEGF and its receptors (mediated by hypoxia inducible factor [HIF-1] which is described later).³⁰

Clinically, hypoxia is known to affect adversely the average success of treatment for a population, specifically resulting in lower levels of two-year local control of the cancer, disease-free survival and survival.^{30, 37} Because hypoxia opens up numerous avenues for the promotion of tumour malignancy, there is a need to target hypoxia both as a cellular process and as an opportunity to differentiate between normal healthy cells and cancer cells.³⁰

1.2.2. Exploiting tumour hypoxia

Gene therapy approach³⁸

The adaptation of cells to hypoxic conditions is dependent upon the induction of key genes that regulate for glucose transporters, glycolytic enzymes, production of red blood cells and stimulation of angiogenesis. The products of these genes all participate in the viability of anaerobic metabolism either directly (glycolysis participants) or indirectly (by increasing oxygen delivery). Hypoxia inducible factor-1 (HIF-1) is the primary activator protein for transcription in one of the key genes involved in the hypoxic response.³⁹⁻⁴¹ The protein is a heterodimer comprised of a novel subunit, HIF-1 α , and a previously identified subunit, HIF-1 β , identical to a protein involved in the xenobiotic response.⁴² Under oxic conditions, the proline-564 residue in HIF-1 α is normally hydroxylated by a prolyl hydroxylase enzyme with an absolute requirement for oxygen and iron, enabling its binding to the product of the Von Hippel Lindau (VHL) tumour suppressor gene which targets the HIF-1 protein for proteolysis.⁴³ Thus, in the presence of normal oxygen levels, induction of the hypoxia response genes is inhibited *via* the breakdown of their activator, HIF-1. If oxygen levels are lowered, the prolyl hydroxylase protein is unable to perform its crucial proline-564 hydroxylation; HIF-1 will no longer bind to the VHL protein; and HIF-1 is able to accumulate in sufficient quantities to activate the hypoxic response.



HIF-1 is a target for cancer therapies in its own right. Without activation of the hypoxic response, cells without sufficient oxygen for aerobic metabolism cannot survive. Some strategies have been proposed such as blocking of HIF-1 α production through anti-sense and have met with moderate success.^{44, 45}

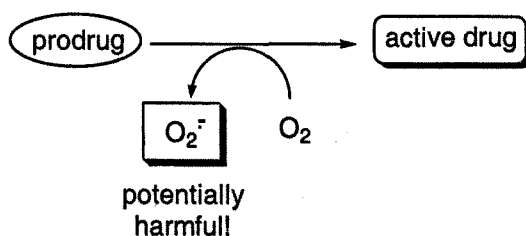
Another way to exploit the HIF-1 response involves placing a gene for a therapeutic protein under the transcriptional regulation of HIF-1. Following the hypoxia-specific production of HIF-1, the therapeutic enzyme will be expressed. The enzyme could be therapeutic in itself, or it could be used to activate a prodrug. In the case of the expressed enzyme being a prodrug activator, the process is called gene directed enzyme prodrug therapy (GDEPT).^{38, 46} Although promising, the classic problems of gene therapy arise in the development of suitable gene delivery vectors. A related but possibly less problematic approach involves the use of antibodies as therapeutic enzyme delivery systems (called antibody directed enzyme prodrug therapy [ADEPT]).^{17, 38, 47} In ADEPT, the therapeutic enzyme is attached to an antibody that can bind to a cell-surface protein expressed during hypoxia (e.g. angiogenic proteins such as flk-1).⁴⁸ The prodrug would only be activated in the immediate vicinity of the targeted cell, with the aim of diffusion of the active drug into the desired location.

Bioreductive drug approach

Bioreductive drug activation operates on the principle that hypoxic cells provide an environment in which reductive electron transfer can occur in one direction, without subsequent back oxidation by molecular oxygen. The electron affinity of radiosensitising drugs allows them to act as substitutes for the molecular oxygen required for the production of the hydroxyl radical (key to the toxicity of ionising radiation). Other hypoxia selective cytotoxins employ prodrug strategies to mask their effects until reductase enzymes in the hypoxic tissue can activate them. The optimum redox potential for cellular reduction has been suggested to be between -200 and -400 mV vs. the normal hydrogen electrode (NHE),⁴⁹ but many bioreductive drugs with different potentials still have useful clinical activity.⁵⁰

Various problems appear in the bioreductive approach to prodrug design. Because of the heterogeneous nature of tumour hypoxia, important activation factors, such as pH, level of oxygen concentration, blood flow and enzyme levels, can differ even between neighbouring hypoxic cells within a tumour.⁴⁷ Additionally, it can be very difficult to predict the efficiency of bioreductive activation in human cells, as they often exhibit much slower rates of bioreduction than rodent cells.³⁸ Even when some human cell lines show appropriate levels of bioreduction, *in vivo* reduction behaviour for individual patients could be completely different due to the inherent genetic polymorphism in enzyme expression displayed between different people.⁵¹ Even in the best-case scenario of hypoxia selective drug activation, the aerobic back-oxidation may provide unwanted side effects through the production of superoxide radicals (Scheme 1.2.2.1).³⁸ However, in life-threatening diseases such as cancer, some chances can be taken and the practical goal is to minimise side effects rather than completely eliminate them.

Scheme 1.2.2.1



There are two possibilities for bioreductive drug delivery systems: a) designing the prodrug as a release system, which masks the activity of a drug that is released under the bioreductive conditions; or b) designing the prodrug as an inactive form of a drug, which can be converted directly into an active form. For either type of delivery system, Denny and Wilson propose a three-component design involving trigger (deactivating functionality) and effector (active drug) units joined by a linker (method for activation, either conceptual or chemical).⁵² Their terminology will be used in this review.

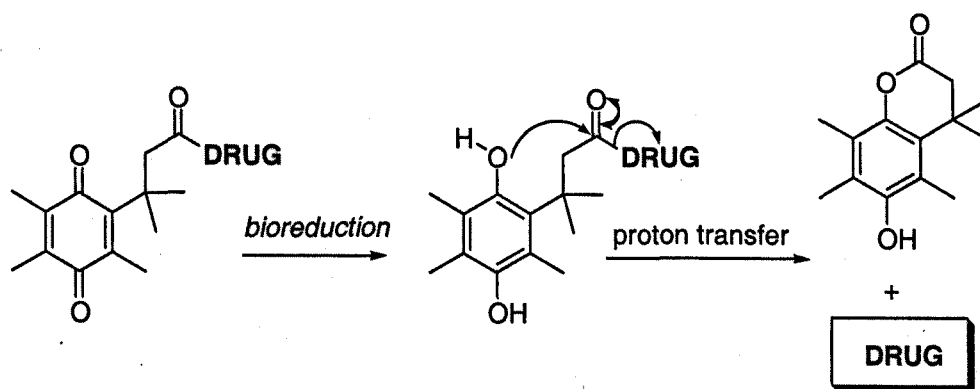
Release systems

The release systems (termed 'self-inactivating' delivery systems by Naughton)⁵³ involve attaching the effector by a molecular linker to a separate trigger

molecule, which masks the drug's activity. This method often avoids some of the unwanted side effects of cytotoxicity in the intermediates of the bioreductive process. There are three main types of self-inactivating delivery systems: the quinone lactonisation system; the self-alkylating bioreductives; and vitamin E analogues.

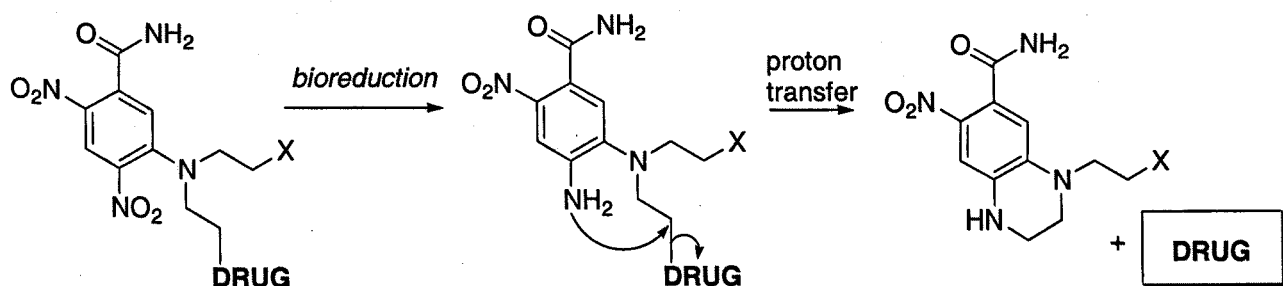
Quinone lactonisation systems contain a quinone moiety attached to a propionic acid linker, which is easy to attach to alcohol or amine functionality on the desired drug.⁵³ Reduction of the quinone triggers lactonisation of the masked acid, resulting in release of the drug. Gem-dimethyl substitution on the propionic acid chain, along with a methyl substituent on the quinone ring (called a 'trimethyl lock'), imparts a Thorpe-Ingold-type effect on the drug-linked ester or amide, encouraging lactonisation (**Scheme 1.2.2.2**).⁵³ Generally, the lability of quinone delivery systems is not well controlled under biological conditions and they require further development in order to be clinically useful.⁵³

Scheme 1.2.2.2



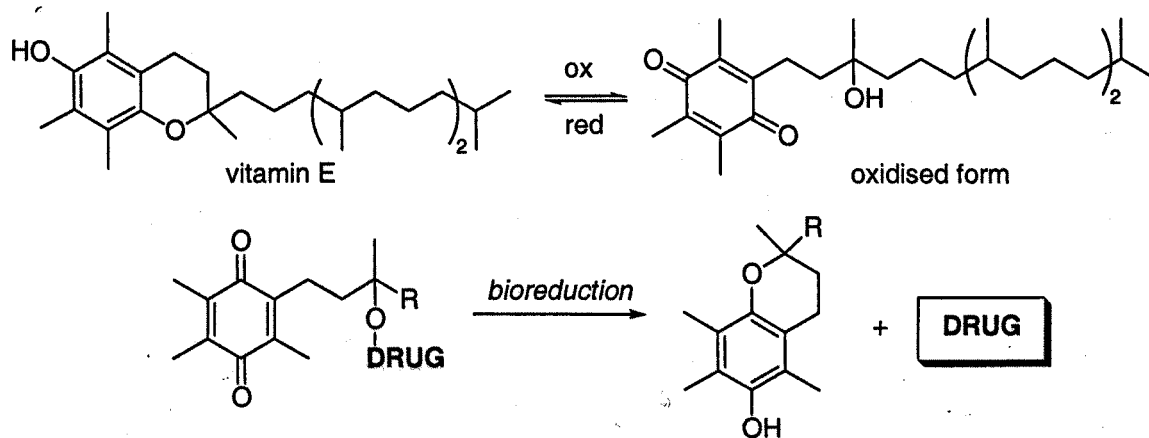
Most bioreductive agents form alkylating intermediates which can react with DNA and other biological macromolecules, which is not advantageous in diseases where the hypoxic tissue is to be preserved (e.g. arthritic tissue) rather than destroyed (as for tumour tissue). The self-alkylating bioreductives are similar to the 'deactivated drug'-type prodrugs, but are designed to undergo intramolecular alkylation upon reduction, to avoid the generation of cytotoxic intermediates. One such system uses the active drug as a leaving group, linking it to a nitroaniline that releases the drug upon reduction of the nitro group to a dianiline and cyclisation to a benzopiperazine (**Scheme 1.2.2.3**).³⁸

Scheme 1.2.2.3



Vitamin E analogues exploit the propensity of vitamin E to undergo reductive cyclisation to a hydroquinone derivative. The hydroxyl group is ejected as a result of the cyclisation, offering the opportunity to attach and mask a drug moiety to oxidised vitamin E analogues (**Scheme 1.2.2.4**). Trolox[®], in which a water-soluble vitamin E analogue has been oxidised and conjugated to aspirin, shows effective release of aspirin in chemical model systems.⁵⁴

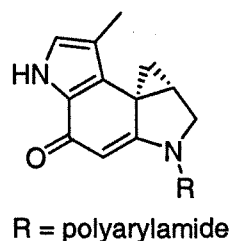
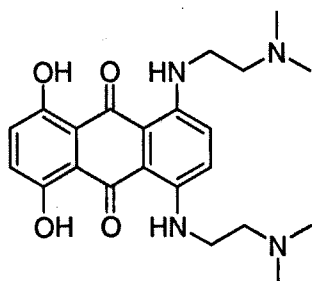
Scheme 1.2.2.4



Direct activation systems

When limiting damage to the hypoxic tissue is not an issue, the delivery system can ignore or even exploit the formation of toxic intermediates upon bioreduction. For this type of targeting, the direct conversion of the molecule from trigger-deactivated prodrug into activated effector is usually employed. The linkers are usually conceptual, for example intramolecular electron release to change electron density within the molecule, or intramolecular fragmentation to generate more than one cytotoxic product. The prodrugs can be activated by endogenous enzymes in the

tumour environment, by enzymes introduced or exploited using ADEPT or GDEPT, or by radiotherapy utilising the reducing species produced from water in the presence of ionising radiation and absence of oxygen. DNA affinic agents and alkylating agents (quinone methides, cyclopropyldienone precursors and nitrogen mustards) are the most commonly employed effectors.⁵²



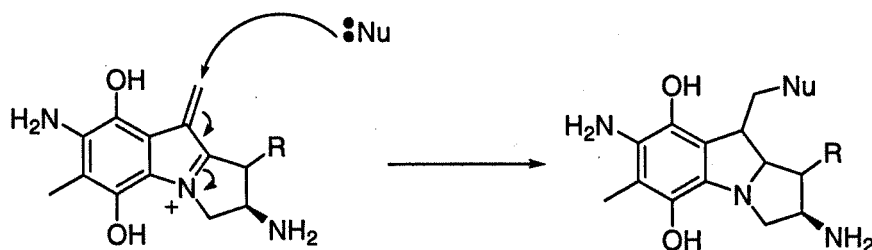
Effectors

DNA affinic agents such as AQ4 (2) are excellent DNA intercalators, binding tightly to DNA and inhibiting topoisomerase II. Usually this type of compound has little effect on non-cycling cells, as topoisomerase II activity is specific to the cell cycle. However, in the case of AQ4, although the binding capability is activated under hypoxic conditions, the effector binds tightly enough to be retained by the DNA for a long time, until the cells are reoxygenated and recommence their normal cycle and topoisomerase II resumes activity.⁵⁵

Cyclopropyldienone precursors deliver highly potent DNA alkylating agents upon bioreduction, with IC₅₀ values in the picomolar range.^{56, 57} They are based on the cyclopropylpyrroloindoles, e.g. CPI (cyclopropylpyrroloindoloquinone [3]), which react solely with the N-3 of adenine in the minor groove of double stranded DNA.⁵⁸ They do not react with proteins, RNA, or single-stranded DNA; therefore their selectivity is easier to control. Upon reduction, the cyclopropyl moiety opens and alkylates DNA. The active effector in carzelesin (another cyclopropylpyrroloindole drug) reacts too quickly, preventing useful absorption into tissues. The cyclopropyl group is masked as a chloromethyl substituent, which is hydrolysed to the hydroxymethyl followed by cyclisation to the cyclopropyl ring.⁵⁷ This allows the drug to be adequately distributed throughout tumour tissues before conversion into the active cyclopropyl analogue and subsequent alkylation. One disadvantage is that the

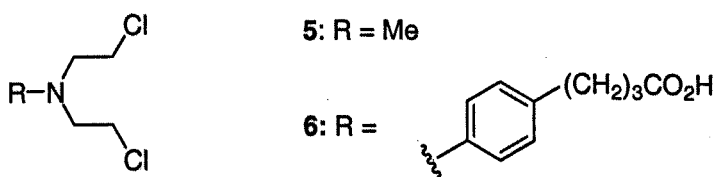
trigger is not very tumour-specific, with activation occurring under most cellular conditions.⁵⁷

Scheme 1.2.2.5



4 R = DNA, cysteinyl

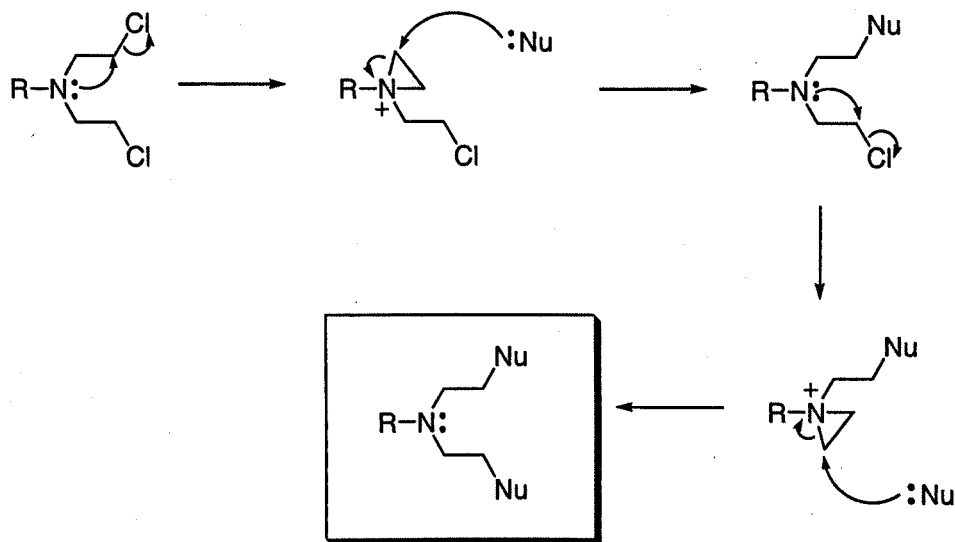
Quinone methides are reactive intermediates generated from the reduction of quinones. They are activated *via* an elimination β - to the quinone, usually of a hydroxyl group. The activated species (4) of mitomycin C, formed after nucleophilic attack of a nucleophile (nucleophilic sites in DNA or proteins) on an aziridinium ion, is a quinone methide. It can bond covalently with nucleophiles (Scheme 1.2.2.5), e.g. N-7 of guanine in DNA or thiol-containing proteins.⁵⁹



Nitrogen mustards, such as mechlorethamine (5) and chlorambucil (6) have historically-proven clinical effectiveness. They were developed from the analogous sulfur mustard gas after World War II and present a number of advantages for therapeutic use. Their cytotoxicity is fairly indiscriminate, giving them the ability to kill almost all types of tumour cells, both cycling and non-cycling. Without prodrug deactivation, this can be a disadvantage, as they generally exhibit cytotoxicity in normal cells as well. The mechanism of action of nitrogen mustards *via* aziridinium ion intermediates is shown in Scheme 1.2.2.6.⁶⁰ The reactivity of these compounds is almost completely dependent on the electron density on the nitrogen. This allows for versatile and stable deactivation through the manipulation of the electronic properties of the molecule around the central nitrogen. The traditional nitrogen mustard

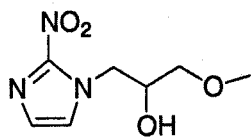
effectors present challenges, since they generally exhibit lower potency when activated; but design of more potent nitrogen mustards would allow for further clinical investigation of these compounds. These compounds will be discussed further in a later section.

Scheme 1.2.2.6

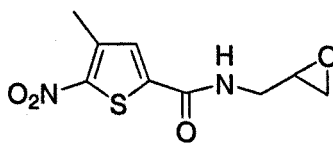


Triggers

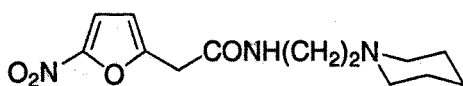
A variety of trigger functionality has been used for the activation of the common effectors. Previously studied triggers include nitroaromatics (as functionality within the parent drug compound and also as quaternary nitrobenzyl salts of active amines), *N*-oxides (aromatic and aliphatic), quinones and transition metal complexes.^{52, 61, 62} Nitroaromatics have been extensively studied as bioreductive drugs, mostly due to their potential as radiosensitisers. Numerous nitroimidazole, nitrothiophene and nitrofuran derivatives (such as misonidazole [7], and others [8 and 9]) have shown promising radiosensitisation activity *in vitro*, but



7



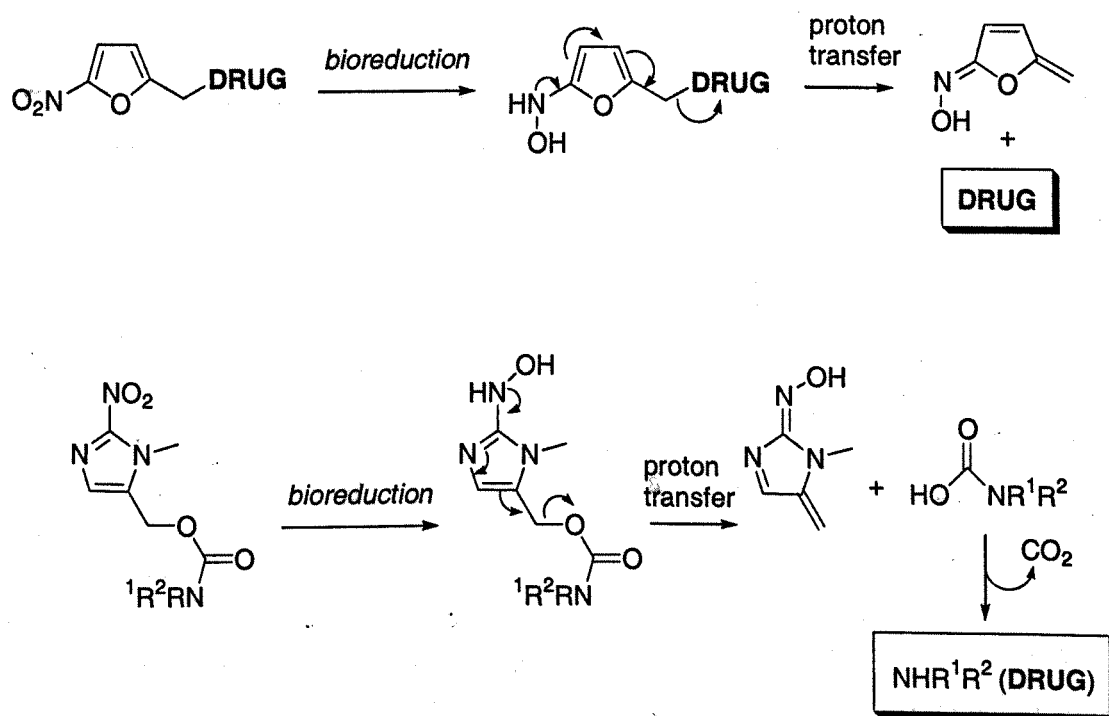
8



9

solubilities and systemic toxicities have slowed their development as clinical agents.^{63, 64} Other nitrofuran and nitroimidazole derivatives can be used as release systems (Scheme 1.2.2.7).^{65, 66} Nitroaromatic nitrogen mustards, such as nitroaniline and nitrobenzamide derivatives,⁶² have reduced electron density on the central nitrogen atom, affecting the formation of the active aziridinium ion and thus the activity. Reduction of the nitro group to the amino group shifts the electron density back onto the mustard nitrogen, re-establishing its potential for alkylation. Nitroaryl quaternary salts of tertiary nitrogen mustards take advantage of the propensity of the nitroaryl functionality to fragment upon one-electron reduction of the nitro group.⁶⁷ These prodrugs have high hypoxia selectivity *in vitro* (up to 10,000 fold),⁶⁸ but exhibit unpredictable cytotoxicity *in vivo*. Nitrobenzyl salts have low activities,⁶⁸ and other nitroaryl salts show non-specific toxicity to normal cells.⁶⁹

Scheme 1.2.2.7

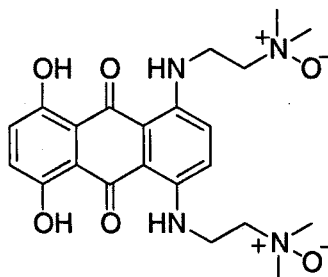


N-Oxides provide three types of prodrug trigger. The tirapazamine prodrug **10** can undergo oxygen-reversible fragmentation upon reduction, generating reactive drug species and hydroxyl radicals under hypoxic conditions, causing DNA damage.⁷⁰ DNA affinic agents, such as AQ4, can be masked as their *N*-oxides (e.g. **11**) to prevent DNA binding until they reach hypoxic tissues. *N*-Oxides of nitrogen mustards also have their activity masked by changing the electron density of the

central nitrogen, as previously described for nitroaromatic mustards.⁷¹ So far, only tirapazamine derivatives are being investigated for clinical use.⁷⁰

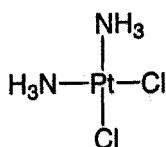


10

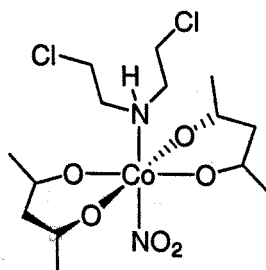


11

Transition metal ions are common components of anticancer drugs, e.g. cis-platin **12**. However, their use as trigger agents has only emerged within the past 13 years. Some metal ions can be reduced from stable complexes (e.g. Co[III]) to less stable ones (Co[II]) by reductase enzymes.⁷² Molecular oxygen should reverse this process, as with other hypoxia selective drugs. However, if the reduced complex is too labile, the active agent may be released before reoxidation of the complex and this may reduce the selectivity.⁵² Thermodynamic lability of the oxidised form of the complex may also cause problems. This is discussed in more depth in Chapter 4.



12

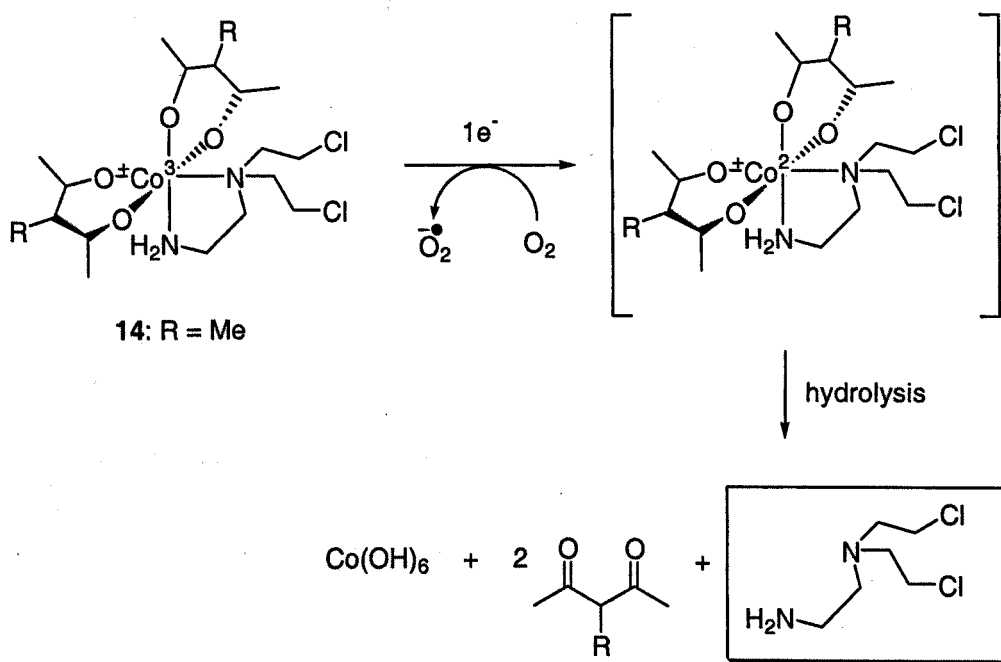


13

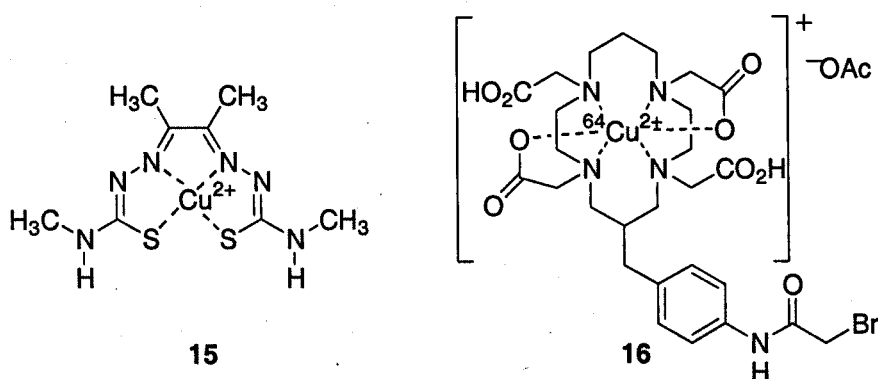
One of the first nitrogen mustard metal complexes **13** was designed as a radiosensitiser, not as a masked alkylating agent. It showed mild hypoxic activity (although it was actually more active in oxygenated cells) and evidence of alkylating activity as compared to a similar non-alkylating complex.⁷³ Soon after, Denny, Wilson and Ware published a series of Co(III) complexes of bifunctional alkylating agents. Their use of ethylenediamine mustards as chelating ligands increased the stability of the reduced Co(II) complex sufficiently to provide the first transition metal complex with bioreducible hypoxia selectivity (~six-fold).⁷⁴ Originally, a

one-electron mechanism was suggested for the hypoxic activation of these complexes (Scheme 1.2.2.8).

Scheme 1.2.2.8



These promising results were followed by a rapid succession of further characterisation studies of similar Co(III) complexes. Correlations were found between ligand structure, redox potential and activity. Hypoxia selectivity was increased to approximately 20-fold with SN 24771 (**14**). It was subjected to more detailed investigations into the oxygen dependence of its cytotoxicity.⁶¹ The released mustard showed extensive killing in multi-cellular spheroids, demonstrating its ability to diffuse into surrounding tissue. Pulse radiolysis studies to determine the kinetics of reduction revealed an unexpected result: the activation mechanism did not appear to follow the one-electron pathway common to other hypoxia selective drugs (as in Scheme 1.2.2.8).⁷⁵ Instead, it appears that **14** may compete with O₂ for available reductants, with low oxygen concentrations freeing those reductants to activate the Co(III) complex. Since this result in 1996, there have been few reports of these complexes in the literature. Problems with their aqueous solubility and selectivity (compared to some other *N*-oxides etc.) could be the reason for the lack of development.



Cu(II) complexes of bis(thiosemicarbazone) ligands have also shown hypoxia selectivity.⁷⁶ Their redox potentials are easily tuned by changing the ligand substituents and the complexes with the lowest reduction potentials are the most selective.⁷⁷ These complexes have cytotoxic properties, but so far have been primarily employed as vectors for Cu(II) radionucleotides for hypoxia-targeted radiotherapy. Radiolabelled ⁶⁰Cu- and ⁶²Cu- ATSM (e.g. **15**) are used in the imaging of hypoxic tissue.⁷⁸⁻⁸⁰ Macrocyclic Cu(II) complexes of cyclen and cyclam derivatives (e.g. **16**) have also been shown to release ⁶⁴Cu into tumour tissue, suggesting lower stability of the bioreduced complex.⁸¹ All of these Cu(II) complexes are water-soluble and bioreducible, as shown clinically. Generally, the bioreduction of Cu(II) to Cu(I) shows great versatility, practicality and promise for new bioreductive drug development.

1.2.3. Enzymology of bioreduction

A number of enzymes have been implicated in the activation of bioreductive drugs, including cytochrome p450, cytochrome p450 reductase, NQO1 and xanthine oxidase.⁸² The activation generally proceeds *via* a one-electron reduction, with the exception of NQO1, which can also utilise an aerobic two-electron reduction pathway in the reduction of quinones, causing possible loss of selectivity.⁸² Within key enzymatic pathways, different enzymes activate particular drugs to various extents. For example, mitomycin C and other quinone drugs are often activated by NQO1 (albeit sometimes in the presence of oxygen), while cytochrome p450 reductase and cytochrome p450 isozymes dominate in the hypoxia selective activation of nitroimidazoles.⁴⁹ Although the relationships between drug activation and enzymology are highly complex, they do offer some useful opportunities for drug

development. Occasionally, bioreductive drugs can be targeted specifically to different types of cancer by combining knowledge of the role of a specific enzyme in the activation of a particular drug with an understanding of tumour cell lines that express elevated levels of that enzyme.⁸³

NQO1 has been extensively studied, due to its overexpression in many cancers.⁸⁴⁻⁸⁷ However its behaviour is widely variable depending on the tumour type and cell line. Diaphorases such as NQO1, called "coenzyme factors," catalyse electron transfer between reduced pyridine nucleotides and redox indicators. NQO1 is a two- or four-electron reductase flavoprotein (using FAD as a cofactor) that is unique in its ability to use both NADH and NADPH as cofactors as well.^{88, 89} Given its propensity to activate bioreducible drugs under oxic as well as hypoxic conditions and the complexity of its *in vivo* behaviour, NQO1 can be a difficult enzyme to target in predictive bioreducible drug design. The one-electron reductases, such as xanthine oxidase and cytochrome p450 reductase, perform much more predictably and correlations can be made between reduction potentials and rates of reduction/activation of drugs.⁸² However, NQO1 activity still needs to be considered in any screening regime, as it is commonly overexpressed in tumours.⁴⁹

The enzyme profile of hypoxia, along with computerised databases of tumour enzyme expression and enzymatic drug activation,⁹⁰ provide a unique opportunity to target tumours without extensive toxicity to healthy cells.

1.2.4. Electrochemistry of bioreduction⁵⁰

Thorough investigation of electrochemical properties can be useful in predicting the activity of bioreductive drugs. Many factors influence the fate and mode of action of such drugs *in vivo*, so it is dangerous to base assumptions on *in vitro* electrochemical data. However, techniques such as cyclic voltammetry (CV) can provide information on important parameters such as ionisation potentials, electron affinity and redox potentials. The conditions and standards used for analysis must be carefully considered in order to obtain biologically relevant information. As yet, there are no standardised procedures for assaying bioelectrochemical data, but common sense and reference to previous studies can be used to develop possibilities

for suggestive, if not predictive, ways of modelling biological electrochemical activity.

In addition to the parameters listed above, cyclic voltammetry can be used to study the reactivity of reduced chemical species by monitoring the reversibility of the system. Reversible systems indicate that the reduced species is thermodynamically stable and doesn't change chemically before *in vivo* reoxidation under oxic conditions. This positively affects the selectivity of the release of cytotoxin, as well as contributing to bystander effect diffusion into the surrounding tissue before reaction with biomolecules. It is important to evaluate the redox potential in both aqueous and non-protic conditions, as at least one essential reductase enzyme, cytochrome p450, has domains in both the lipophilic cell membrane and the aqueous cytoplasm.⁹¹ Although the redox potential provides a possible starting point for prediction of activity, it is not prudent to use their values as a screening method, since the technique can be less accurate for slower electron transfer reactions and is highly dependent on pH and other unpredictable effects such as *in vivo* metabolism.⁵⁰

The aforementioned ionisation potential and electron affinity provide useful information about the drug's ability to exchange protons and accept electrons, respectively. The pH of hypoxic cells is generally lower than in normal tissues, thus the ionisation potential can be of greater significance to its interaction with biomolecules as well as inter- and intra-cellular transport.⁵⁰ An optimum electron affinity can also be important, as molecules that accept electrons too readily will be quickly metabolised and excreted, while those with lower affinities risk poor levels of activation by reductase enzymes.

The most relevant information that can be obtained from reduction potentials is the comparison of reduction rates under hypoxic and oxic conditions, as it can give a good indication of the selectivity of cytotoxicity based on whether or not it is possible to generate the reactive species under oxic conditions.⁵⁰ So although it is not possible to correlate electrochemical behaviour with bioactivity directly, it is useful to consider electrochemical characterisation when performing a full exploration of *in vitro* bioreductive drug activity. Additionally, knowledge of optimum redox potentials for enzymatic reduction can contribute to directed bioreductive drug design.

1.2.5. Bioreductive drug design

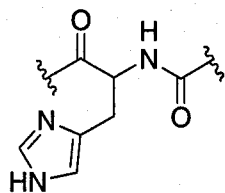
Many aspects of the cellular environment contribute to the efficacy of bioreductive drugs, including the enzymes present, the level of hypoxia and the rate of metabolism of the prodrug and activated drug.⁹² Additionally, the reduction potential of the prodrug and the stability of the activated drug can be significant for the drug's selectivity. It is thought that the reduction potential should fall within an appropriate range for reduction by one of the common enzymatic activation pathways (*ca.* -200 to -400 mV vs. NHE).⁵⁰ The reduced compound must be stable enough to allow for reoxidation in the presence of oxygen in order to prevent activation under aerobic conditions.

There are many approaches available for design. The affinity of drugs for reductase enzymes can be assessed experimentally or by computer modelling of the compounds in the enzyme active sites. The reduction potentials can be estimated using Hammett calculations (based on certain constants for substituents). Metal complexes provide a particularly attractive avenue for bioreducible drug design. Their potential as hypoxia selective agents has only been touched on so far: their redox potentials are easily tuned by changing the metal ion or the ligand substituents; and a wealth of data already exists describing their synthesis and complexation properties.⁹³⁻⁹⁹ Accordingly, the development of cytotoxic ligands for bioreductive release from a redox metal trigger has been the primary focus of the work described herein.

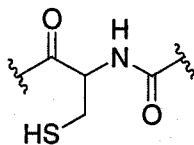
1.3. Nitrogen mustard alkylating agents

1.3.1. Biological effects

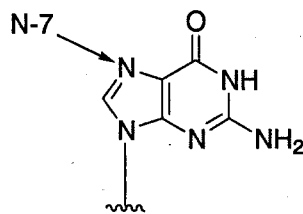
Nitrogen mustard alkylating agents can interact covalently with many cellular components, especially enzymes and DNA. As detailed in **Scheme 1.2.2.6**, the reactive aziridinium ions formed can alkylate nucleophiles such as histidine (**17**) and cysteine (**18**) residues of proteins,¹⁰⁰ or guanine residues (**19**) of DNA.¹⁰¹ Binding to enzyme backbone peptides can cause conformational changes of the active site and



17



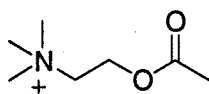
18



19

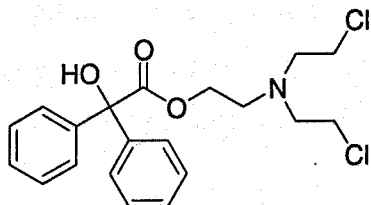
these can result in deactivation of the enzyme. Such is the case for the vesicant (blistering) effect of mustard compounds on skin and mucous membranes.¹⁰⁰

The primary toxicity of mustards upon inhalation or skin contact arises from their vesicant effect. Mustard exposure causes epithelial cells to change shape, detach from each other and form blisters. The mustard agents alkylate muscarinic acetylcholine receptors (mAChRs) in epithelial cells. These receptors control cell adhesion together with acetylcholine (**20**, an important cellular transmitter). Their interaction with mAChR proteins may be enhanced by the similarity of aziridinium ions to the trimethylammonium group of acetylcholine.¹⁰⁰

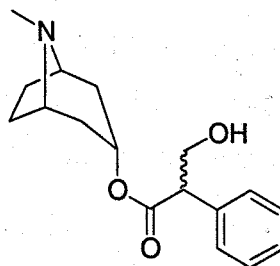


20

Some lipophilic nitrogen mustards (e.g. **21**) are able to cross the blood-brain barrier to bind to neural muscarinic receptors, resulting in cholinergic effects (such as seizures).¹⁰² These compounds bind irreversibly to mAChRs, targeting them for protease degradation. However, the use of reversible cholinergic drugs can moderate the adverse effects of mustards on the cholinergic systems by occupying the active sites of the enzymes and reducing the conformational changes induced by the alkylation. Thus, drugs such as atropine (**22**, the racemate of hyoscyamine) can diminish the adverse vesicant effects of mustard drugs.¹⁰⁰

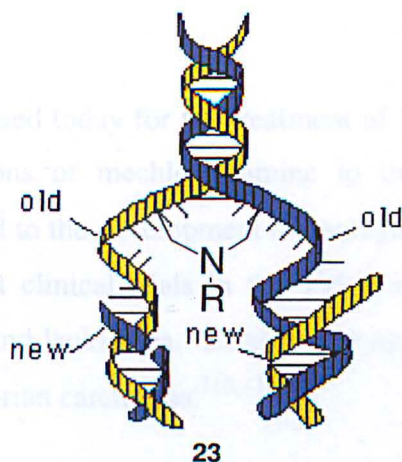


21



22

26

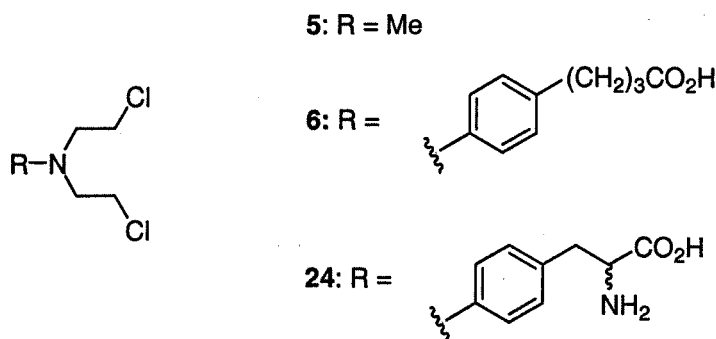


Bifunctional nitrogen mustards are known to form DNA cross-links.^{103, 104} When guanines on different strands of DNA are cross-linked, DNA unwinding is obstructed, triggering apoptosis (23). Resistance can develop through the up-regulation of DNA repair pathways.¹⁰⁵ However, the cytotoxic effects of DNA cross-linking can be enhanced with the concurrent use of DNA repair inhibitors or *via* inactivation of other repair pathways.^{105, 106} Similarly, DNA-repair-deficient mutant cell lines (e.g. UV4) are more sensitive to alkylating agents than cells with normal repair mechanisms. Other pathways of cytotoxicity may arise from the linking of DNA to proteins.¹⁰⁷ Generally, the cytotoxicity of mustard drugs is non-specific and potent (IC₅₀ values around 10⁻⁶ M), which is useful in the design of anti-cancer agents. Specificity of drug action encourages the development of resistance to the treatment.⁴⁷ Non-specific action ensures a multiplicity of pathways for drug activity, all of which must be overcome before resistance will succeed.

1.3.2. Previous developments in mustard drugs

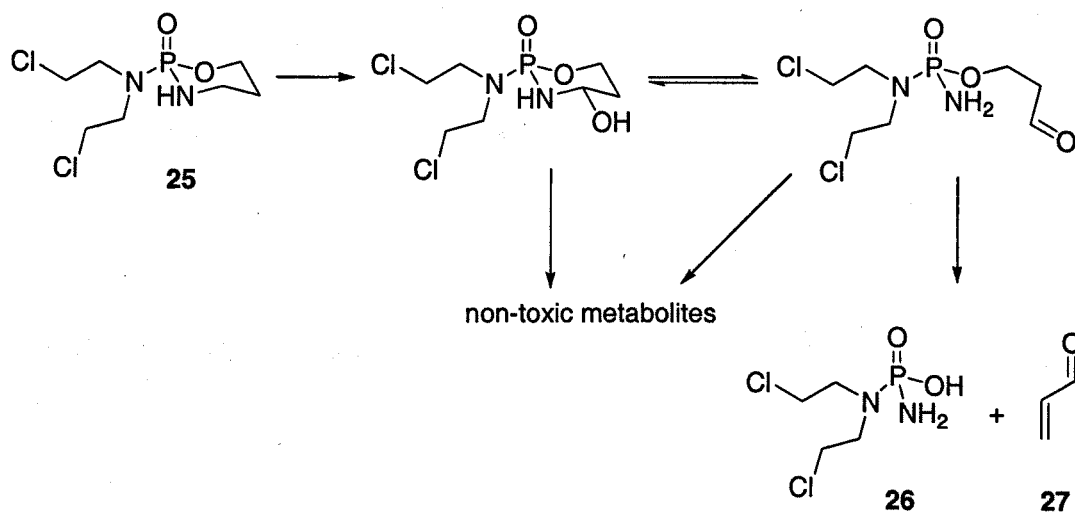
Nitrogen mustard alkylating agents provided an entry into the previously unknown world of cancer chemotherapeutics. One of the first anti-cancer drugs developed was the *N*-mustard mechlorethamine (5). During World War II, medical technicians noticed that exposure to mustard gas dramatically lowered the white blood cell counts of survivors (among other toxic effects). Dr. Cornelius Rhoads, who treated many patients poisoned by mustard gas, postulated that similar drugs might be used to inhibit leukaemia, as it involves the cancerous overproduction of white blood cells.¹⁰⁸ Louis Goodman and Alfred Gilman pioneered the clinical trials of mechlorethamine in the first attempts at chemotherapy in the 1940s.¹⁰⁹ Although the initial trials were not successful, they represented the birth of medical oncology and

mechlorethamine is still used today for the treatment of Hodgkin's disease and other lymphomas. Modifications of mechlorethamine to improve stability, membrane transport and solubility led to the development of analogues such as chlorambucil (**6**). Chlorambucil had its first clinical trials in the 1950s and is currently used in the treatment of lymphomas and leukaemia. Its analogue melphalan (**24**) is used to treat multiple myeloma and ovarian carcinoma.^{110, 111}



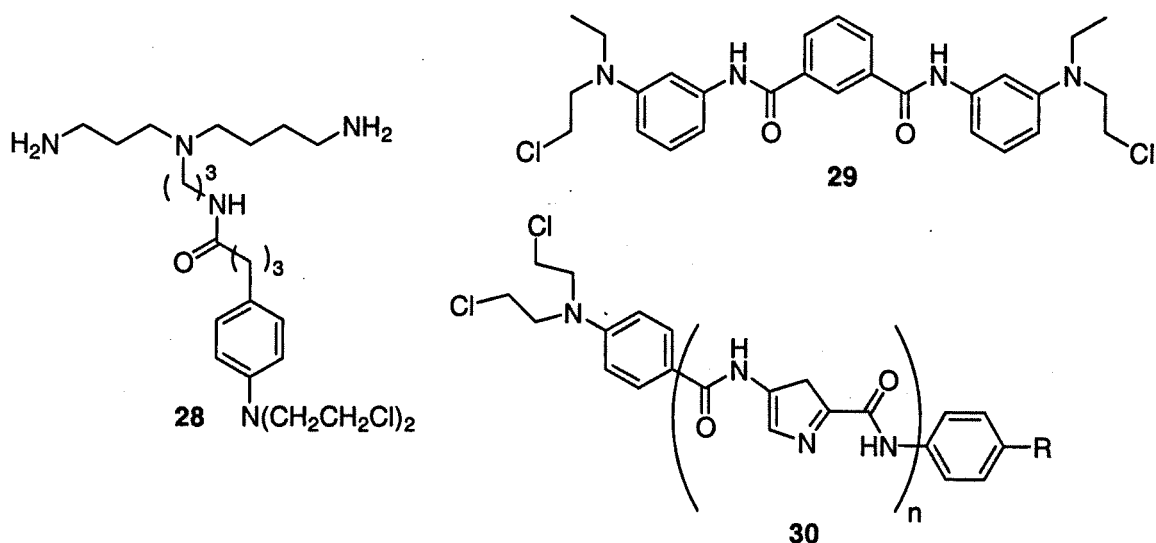
Although mustard drugs have experienced some success in cancer treatment, their side effects can be severe and dangerous. Seizures, reduced immunity, blistering of mucous membranes and instigation of new cancers are unpleasant and potentially life threatening. Therefore, it was a priority to develop prodrugs of these compounds in order to improve their selectivity and minimise the adverse effects to normal tissues. Cyclophosphamide (**25**) was one of the first of these prodrugs.¹¹² Developed in 1958, it was designed for activation by phosphoramidase enzymes *in vivo*, cleaving the mustard moiety from the phosphoramidate.¹¹² Unexpectedly, cyclophosphamide is actually activated *via* hydroxylation by cytochrome p450 and breakdown into phosphoramidate mustard (**26**) and acrolein (**27**) (Scheme 1.3.2.1). The production of acrolein is unfortunate, as it causes cystitis and other bladder problems. However, overall the side effects are less severe than with naked mustard drugs. Accordingly, cyclophosphamide is the most commonly used alkylating agent.¹¹²

Scheme 1.3.2.1



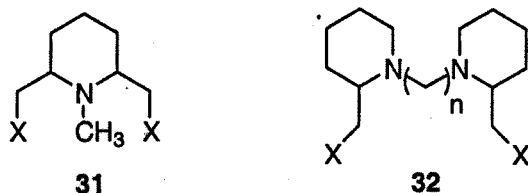
Extensive research has been conducted in the drive to improve the selectivity of alkylating agents and only the most recent developments will be discussed here. Studies on the kinetics of chlorambucil hydrolysis in biological model systems have yielded useful information about the reactivity of mustard drugs. For example, the rates of reaction of mustards at physiological pH with various biologically available nucleophiles proceeded in the following order: water \ll phosphate $<$ imidazole \ll thiol.⁶⁰ This suggests that mustard drugs may have some selectivity towards thiol-containing proteins. Conjugates of chlorambucil with polyamines have been studied^{60, 113} in an attempt to exploit the increased uptake of polyamines by tumour cells. Indeed, a chlorambucil-spermidine conjugate (**28**) exhibited a 10^4 increase in potency over chlorambucil.⁶⁰ It was not clear whether the increase was due to an intrinsic enhancement of the mustard's reactivity, or an increased association of the conjugate with DNA *via* the affinity of polyamines for DNA. If the increase was due to increased DNA interaction, it was non-sequence specific.¹¹⁴

Other nitrogen mustard conjugates have been investigated, including poly-arylamide (**29**) and distamycin-type compounds (**30**).¹¹⁵⁻¹¹⁷ Like polypyrrole antibiotics (e.g. distamycin), these compounds have planar conformations that are complementary to the minor groove of DNA. These mustards are bifunctional, with the alkylating groups on the same nitrogen or on different nitrogens separated by a spacer. The polyamide backbones confer rigidity on the spacer between mustard moieties, allowing for control of the distance between the nitrogens.

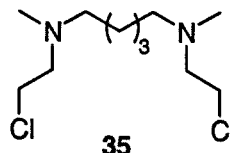
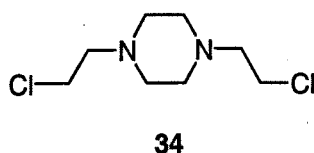
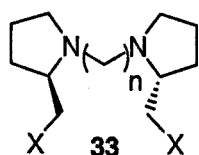


In vitro tests of these compounds showed enhanced DNA-crosslinking activity and IC_{50} values in the micro- to nano-molar ranges against human cancer cell lines.¹¹⁵⁻¹¹⁷ A hairpin polyamide-chlorambucil conjugate was particularly effective against leukaemia, with an IC_{50} value of 2.2 nM.¹¹⁶ Its polyamide sequence targeted a specific sequence of DNA. Distamycin mustard conjugates (e.g. **30**) were also effective against human leukaemia cells *in vitro*, with IC_{50} values in the sub-micromolar range. *In vivo* tests of the polyamide mustard **29** showed a 37% increased lifespan in tumour-bearing animals, which was equal to the activity of chlorambucil.¹¹⁵

Our group began working with alkylating agents in the mid 1990s. In order to prepare *N*-oxide prodrugs, Nicola Henderson first synthesised a series of bifunctional mustards based on piperidine (**31**) during her PhD research.¹¹⁸ It was hoped that the conformational restriction inherent in cyclic nitrogen mustard analogues would temper the reactivity in setting up the necessary conformation for aziridinium ion formation. The best of these compounds showed good cytotoxicity against human colon carcinoma cell lines ($\sim 8 \mu M$).¹¹⁹ However, their *N*-oxide derivatives were inactive under both oxic and hypoxic conditions. Their reduction potentials were probably not within an appropriate range for cellular reduction.

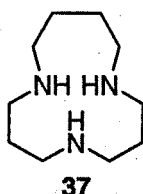
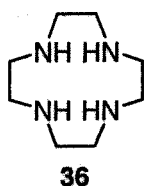


Rather than concentrating on improving the potential for prodrug activation, Henderson focused on further increasing the selectivity of the alkylation. She extended her work to a series of bispiperidine derivatives, e.g. **32**. They showed improved selectivity for N-7 of guanine over melphalan and were cytotoxic in three cisplatin-resistant cell lines.¹²⁰ Although these compounds cross-linked DNA at lower concentrations than melphalan, their IC₅₀ values showed they were not as potent. A relationship began to emerge between the linker chain length and the reactivity. Compound **32**, with an ethylene linker, was twice as reactive as its longer-chain analogues. This suggested that there might be an optimum distance between nitrogens for cross-linking activity.

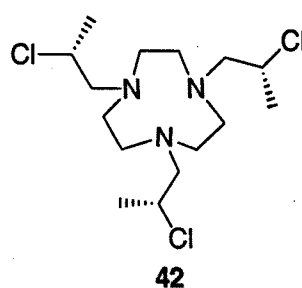
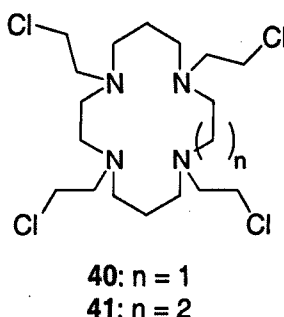
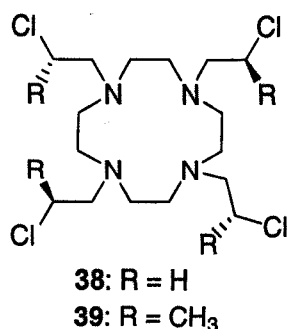


During her PhD research, Fiona Anderson carried out further investigations into this issue.¹²¹ She synthesised a series of homochiral bispyrrolidine mustard derivatives (**33**) and a number of alkyl cyclic and linear mustards (**34** and **35**).¹²² The bispyrrolidine compounds showed a relationship between linker length and alkylating activity, with the 2-, 5- and 6- carbon linkers giving the best alkylation. Surprisingly, the 3- and 4- carbon linkers resulted in no DNA cross-linking activity. Also, in contrast to conventional mustard drugs, there was no clear correlation between alkylating ability and cytotoxicity. None of the linear or cyclic mustards showed cytotoxicity within a useful range (< 100 μ M). The reasons for the lack of activity were not apparent. Perhaps cells did not take up the inactive compounds efficiently, or they may have been more reactive with other cellular components (e.g. thiol-containing proteins).

In order to expand the previous work, macrocyclic polyamines provided an attractive avenue to compounds with multiple alkylating moieties, variable carbon chain lengths and the possibility for metal ion chelation to generate bio-reducible prodrugs. Macrocyclic polyamines (e.g. cyclen **36**) are well known in the field of inorganic chemistry as ligands for chelation.^{97, 98, 123-125} They offer a range of



possibilities for variation of structure, including multiple substituents at carbons and nitrogens, as well as variation in the size of the macrocycle. They also have the biological advantage of being natural polyamine analogues, e.g. cyclic spermidine (37). Linear polyamines show a range of interesting biological activities, including anti-malarial and anti-cancer and will be discussed in a later section.



During his work with the Robins group, Dr. Stephen Lacy synthesized the cyclen derivative 38, which had phenomenal DNA cross-linking activity (100% cross-linked DNA at 0.1 μ M) and higher cytotoxicity (IC_{50} = 22 μ M) than chlorambucil (IC_{50} = 45 μ M) against a human colon carcinoma cell line.¹²⁶ Fiona Anderson followed up this line of work and synthesised a series of poly-2-chloroethylated macrocyclic polyamines such as 39-42, from commercially available starting materials. Some had very promising biological activity (Table 1.3.2.1) and she extended her work to vary ring size, carbon chain length between nitrogens and number of nitrogens in the ring. However, she encountered difficulties in the synthesis of many of these compounds, such that she was unable to reach her targets. As a result, the primary synthetic aims of this project have been to develop a flexible, reliable method to obtain azamacrocycles of variable ring size with different carbon chain lengths between the nitrogen atoms.

Table 1.3.2.1. DNA cross-linking and cytotoxicity data for previously tested macrocyclic N-mustards

Compound	% crosslinked DNA ^a				IC_{50} ^a (μ M)
	0.01 μ M	0.1 μ M	1 μ M	10 μ M	
38	-	100	-	-	22
39	-	64	100	-	10
40	16.4	93.7	100	-	7.5
41	77	100	-	-	9
42	-	30	100	-	13

^a details of testing procedures published previously¹²¹

1.4. Synthesis of macrocyclic polyamines

1.4.1. Cyclisation

Polyazamacrocycles are notoriously difficult to synthesise. As is the case for other types of cyclisation, the reaction conditions must be designed to ensure intramolecular cyclisation as opposed to intermolecular oligomerisation. This can be achieved in a number of ways: using high dilution conditions; templating the starting polyamine with a metal ion or carbon-based backbone; or using sulfonamides for preorganisation in the Richman-Atkins-type synthesis.¹²⁷ The details of these methods, particularly the Richman-Atkins synthesis, will be discussed in this mini-review.

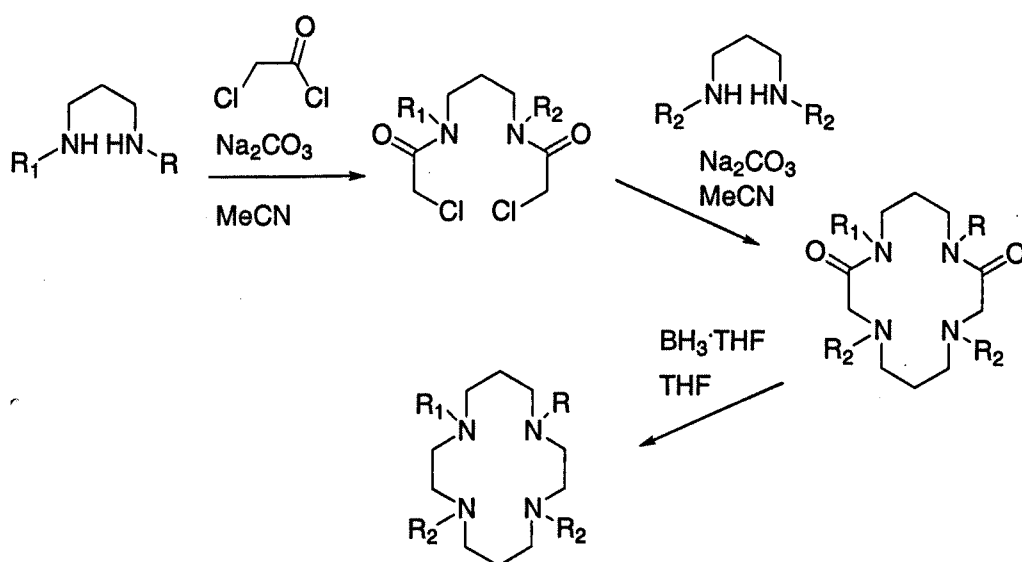
High dilution cyclisations

Up until the 1970s, polyazamacrocycles were typically isolated in low yields from complex mixtures of oligomers formed in simple amine-substitution reactions.¹²⁸⁻¹³⁰ Amines protected as sulfonamides were first used by Stetter and Roos in the 1950s^{131, 132} and by Stetter and Mayer in the 1960s¹³³ with limited success—yields were still very low (<15% overall) and reactions required high dilution to prevent oligomerization. High dilution conditions are usually characterised by maintaining a concentration of less than 0.1 M reactant, under the assumption that fewer collisions will take place between reactants, and thus an intermediate will have time to react with itself in a cyclisation before meeting another reactant molecule. This effect can be achieved either by using a large excess of solvent or by slow addition of reactants (e.g. with a syringe pump). The main disadvantages of this technique are the large volumes of solvent required and the long reaction times necessary. Even on a small scale (0.5-1 g), high dilution cyclisations can take longer than two weeks to reach completion. Still, these conditions often result in high yields and can involve fewer protection-deprotection steps than some other methods.

The 'crab-like' cyclisation is one example of very effective high dilution synthesis of selectively *N*-substituted cyclam derivatives (**Scheme 1.4.1.1**). A wide variety of cyclam derivatives were produced in just three steps giving *ca.* 80% yield

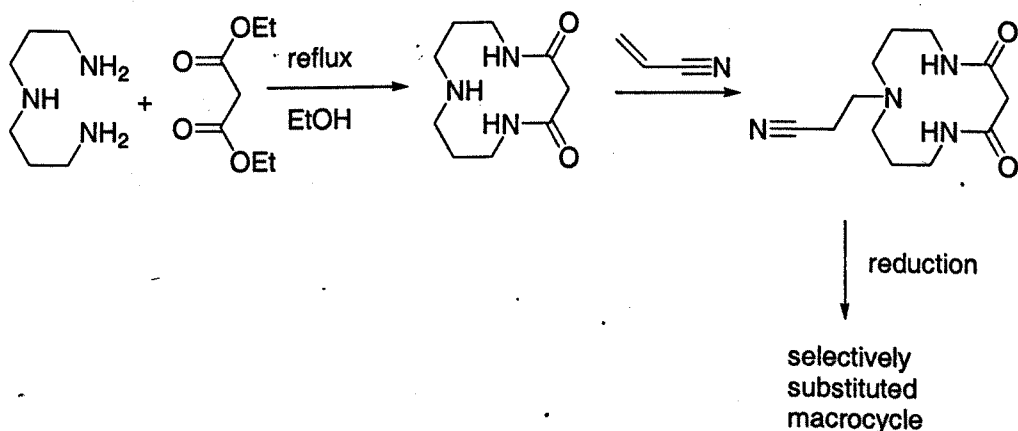
in the cyclisation.¹³⁴ This method still results in the formation of 2:2 and 3:3 cyclisation byproducts; however they are easily separated by filtration through a short silica gel column. The drawback is that the efficiency of the cyclisation is highly dependent on the ring size formed, so it is not very effective for the production of macrocycles other than cyclam. Also, the reduction of the diamide precludes the incorporation of reduction-sensitive functionality.

Scheme 1.4.1.1



Similar diamide cyclisations have analogous problems. Diester-triamine condensations give very low yields (<13%) and require long reaction times (>5 days),^{135, 136} however they do allow the potential for selective alkylation (Scheme 1.4.1.2).

Scheme 1.4.1.2



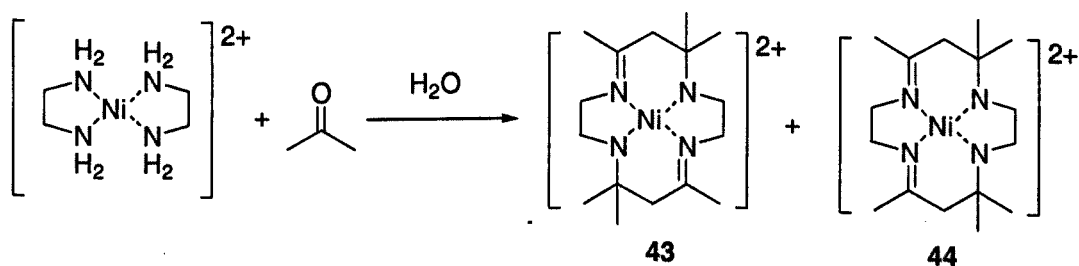
In general, diamide formation is useful in certain situations, especially when selective *N*-substitution is desired. However, it can be lengthy and low yielding and is dependent on the ring size formed so it is not a good general method for producing a range of polyazamacrocycles.

Templated cyclisations

Metal ion templates

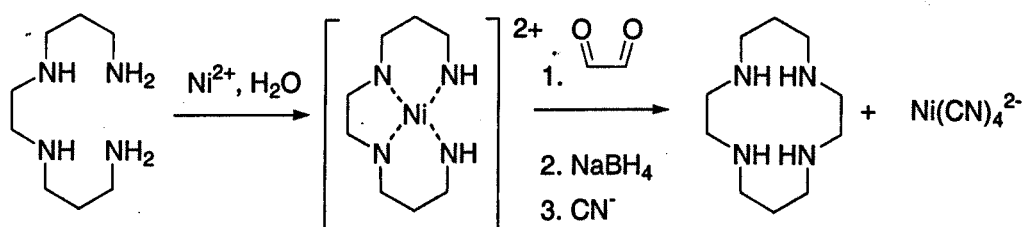
One way to reduce the need for high dilution is to template the polyamine in some way in order to preorganise it for cyclisation. The complexation of amines with metal ions has been exploited for this purpose.¹³⁷⁻¹⁴⁰ The first of these methods used a diamine-Ni(II) complex which was condensed with acetone (**Scheme 1.4.1.3**) to produce two structural isomers of a cyclam derivative (**43** and **44**). The resulting diimine complex must be reduced to the alkylazamacrocycle.¹³⁷

Scheme 1.4.1.3



Another classic example of this type of macrocycle synthesis is the Ni(II)-templated synthesis of cyclam (**Scheme 1.4.1.4**). This method starts from the readily available, low-cost 1,2-bis(3-aminopropyl)-1,2-ethanediamine and gives good yields of cyclam. However, the Ni(II) must be removed *via* displacement of the cyclam ligand with cyanide, so this method is not suitable for industrial production of macrocycles.¹³⁸

Scheme 1.4.1.4

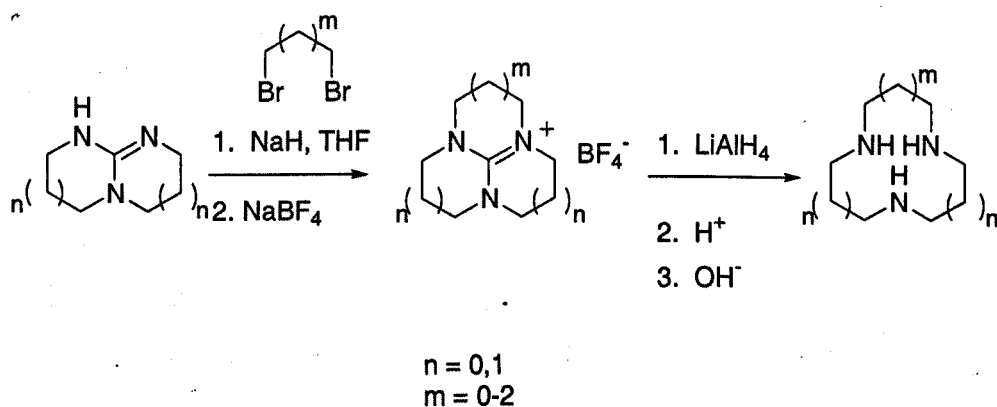


Carbon templates

Carbon-based templates can also be employed for macrocyclic polyamine synthesis. These strategies are also high-yielding and the template is usually removed by simple hydrolysis, avoiding the toxic reagents required for metal-template removal.

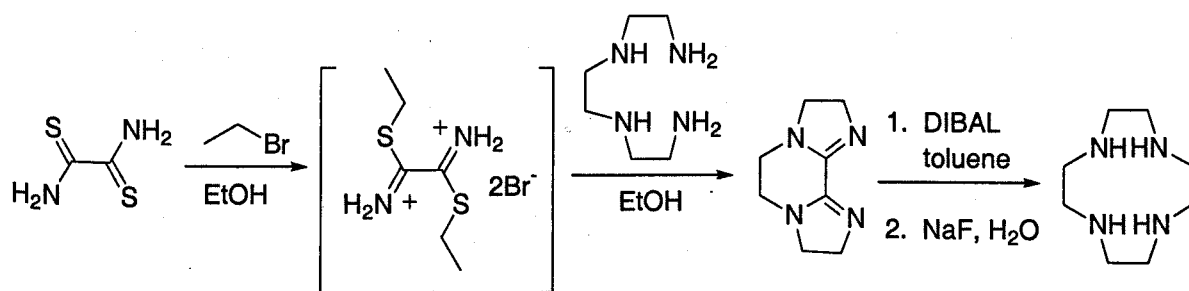
Triazamacrocycles can be synthesised using bicyclic guanidine templates,¹⁴¹⁻¹⁴⁴ as in **Scheme 1.4.1.5**. This allows for reasonably large-scale synthesis of a number of triazamacrocycles (~3 g macrocycle obtained), but the bicyclic guanidines are not commercially available and must be made beforehand. Also, the intermediate tricyclic guanidinium salts can be difficult to purify, as their crystallinity varies with ring size.

Scheme 1.4.1.5



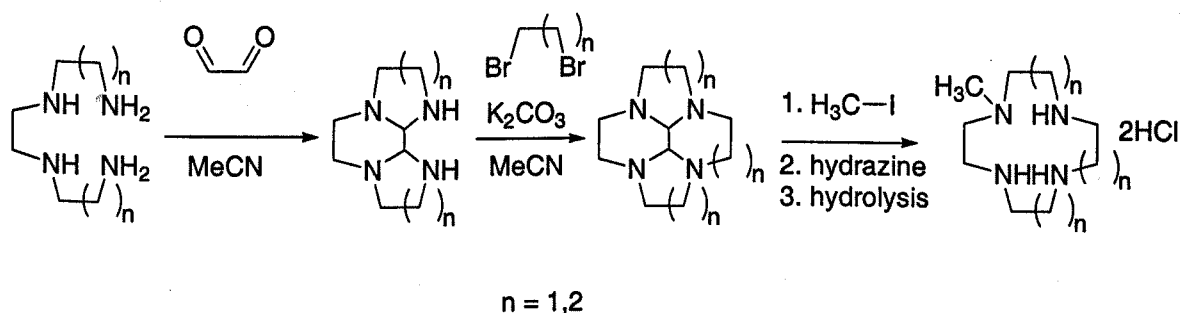
Tetraamines can also be templated using carbon-based structures. Cyclen (**36**) can be synthesised from a tricyclic bisamidine precursor *via* reductive ring expansion (**Scheme 1.4.1.6**).¹⁴⁵ This method produces cyclen in high yields with minimal purification necessary. However the synthesis of the bisamidine precursor produces stoichiometric amounts of ethanethiol, which reduces the industrial viability of this procedure.

Scheme 1.4.1.6



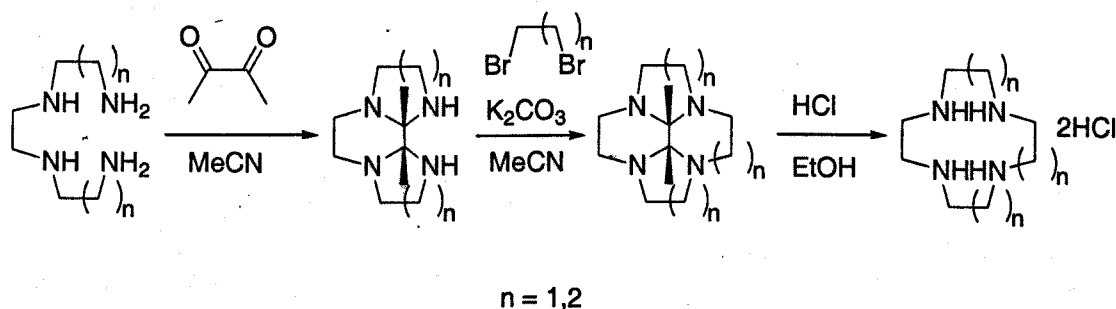
Other similar syntheses using glyoxal as the template, forming the bisaminal, are mostly useful for producing *N*-substituted macrocycles (e.g. **Scheme 1.4.1.7**) due to the difficulties in removing the template from the unsubstituted tetracycle at the end.^{146, 147}

Scheme 1.4.1.7

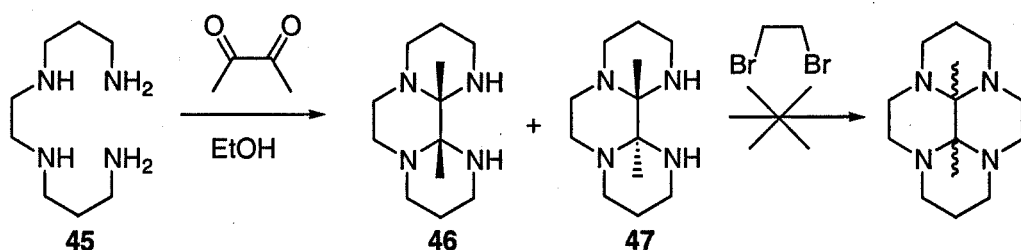


More recently, two very simple carbon-templated tetraazamacrocyclic syntheses have appeared in the literature. The first uses butanedione as the template, forming a rigid tricyclic bisaminal. Once cyclised to the protected macrocycle, the *C*-substituted bisaminal is much easier to remove than the aforementioned glyoxal derivative and the acid salt of the tetraazamacrocyclic can be obtained in good yield by simple hydrolysis (**Scheme 1.4.1.8**).¹⁴⁸

Scheme 1.4.1.8

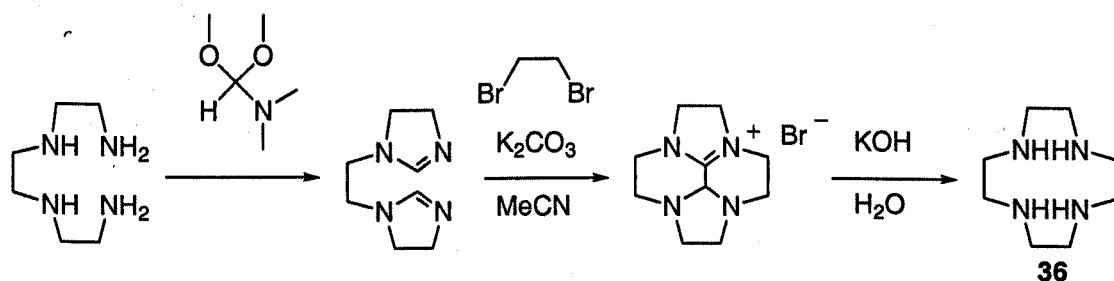


Scheme 1.4.1.9

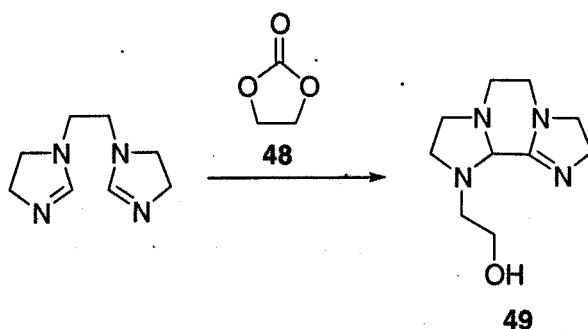


Unfortunately, the success of the cyclisation to the tetracyclic bisamidine is highly dependent on the conformation of the tricyclic compound. The 3,2,3-tetraamine **45** forms two conformational isomers of the tricyclic guanidine (**46** and **47**), neither of which allows the cyclisation of the final six-membered ring (Scheme 1.4.1.9).¹⁴⁸ The 2,3,2-tetraamine does provide access to cyclam, but it is much more expensive than the 3,2,3-tetraamine.

Scheme 1.4.1.10



The second recent method uses a bisimidazoline to form cyclen through a diaminocarbene intermediate (Scheme 1.4.1.10).^{149, 150} This route uses cheap starting materials and gives good overall yield of cyclen (**36**). The diaminocarbene dimerisation mechanism was confirmed by using ethylene carbonate (**48**) as the electrophile, giving the product **49**. Unfortunately, this route was found not to be suitable for the production of other tetraazamacrocycles. This observation is discussed further in Chapter 2.



Template methods can provide good yields and convenient access to polyazamacrocycles, but all are highly dependent on the ring size and the conformation of the templated intermediates. This restricts the range of carbon bridges available to two and three carbons. Although those bridge lengths were useful for some of the macrocycles desired for this project, this restriction was not satisfactory for the production of all of the nitrogen mustard alkylating agents we wished to produce. Thus it was important to investigate other strategies as well.

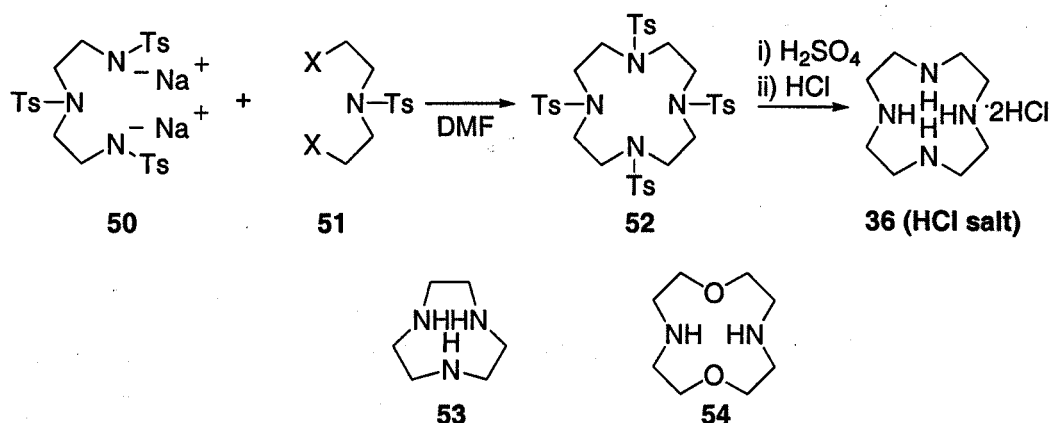
Richman-Atkins cyclisation of sulfonamides

Sulfonamide cyclisation has emerged as the most flexible synthesis of polyazamacrocycles. Variations in type of sulfonamide, base and deprotection strategy have allowed for the production of a wide range of ring sizes and structural features. One disadvantage of the *p*-toluenesulfonamides traditionally used is the harsh conditions required for their deprotection. Usually hydrolysis in H₂SO₄ or HBr/AcOH is necessary, but reductive removal, e.g. with sodium or lithium in ammonia can sometimes be effective. More recent variations have used sulfonamides that are removed under milder conditions, such as the (2-trimethylsilyl)ethanesulfonyl (SES)¹⁵¹ and 2- and 4-nitrobenzenesulfonyl (2- and 4-Ns)^{152, 153} groups.

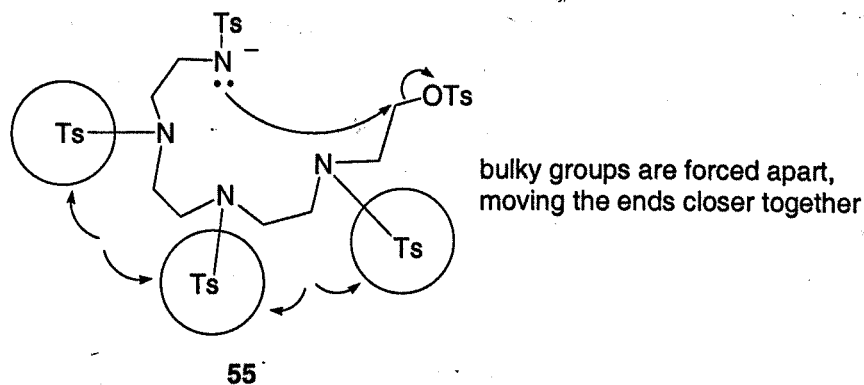
***p*-Toluenesulfonamide cyclisation**

The first efficient cyclisation of sulfonamides was developed in the 1970s by Richman and Atkins.¹²⁷ The initial conditions in the Richman-Atkins cyclisation combined the pre-formed disodium salt of a *p*-toluenesulfonamide in DMF with a diol ditosylate or dihaloalkane, heating at 100 °C for 2 hours, followed by detosylation in conc. sulfuric over two days (**Scheme 1.4.1.11**). This process did not require high dilution and gave very high yields for the synthesis of cyclen (**36**) and other macrocycles including triazamacrocycles (e.g. tacn [**53**]) and dioxodiazamacrocycles (e.g. [**54**]).

Scheme 1.4.1.11



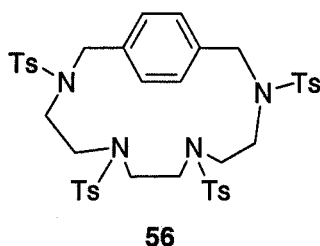
A number of notable observations were reported in this paper. Importantly, ditosylates (or dimesylates) were found to give the best yields in the cyclisation. The rates of reaction were measured for different leaving groups -X (I, Br, OTs, OM and Cl) and found to give second-order kinetics for the disappearance of sulphonamide (suggesting an $\text{S}_{\text{N}}2$ mechanism); however only the dimesylate gave a clean second-order plot. Curvature in the plots for the dihalo-compounds indicated competing processes e.g. elimination and/or oligomerization. Also, Richman and Atkins found that the high yield was not due to a template effect on the cyclisation by the sodium ion. Replacing the sodium with a tetramethylammonium cation did not significantly decrease the yield. However subsequent groups have reported a dependence on the cation suggesting some degree of template effect.^{154, 155} Synthesis of cyclophanes with the modified Richman-Atkins conditions also indicates that there is not a template effect and so it is best to assume that some combination of factors applies.



Although the reasons for the improved intramolecular reaction were not immediately clear, it was later suggested that the sulfonamide groups contributed to the success of the cyclisation in two ways:¹⁵¹ they rendered the amine hydrogens sufficiently acidic

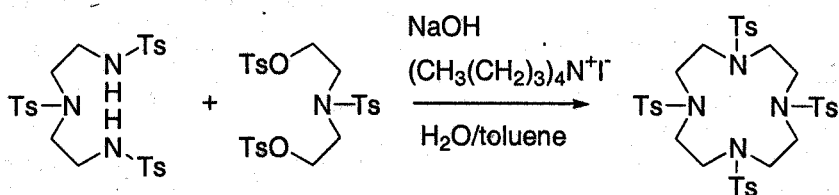
for facile deprotonation; and the steric bulk of the *p*-toluenesulfonyl groups conferred a Thorpe-Ingold-type effect on the intermediate **55**, encouraging intramolecular reaction.

Soon after it was found that the sulfonamide salt could be formed *in situ* using Cs_2CO_3 ¹⁵⁶ or K_2CO_3 .¹⁵⁴ The yields were still good and the reaction no longer required high temperatures (although the reaction time was increased to ~24 h). Using K_2CO_3 gave better yields for smaller rings, allowing improved access to triazamacrocycles. Some cyclophanes (e.g. **56**) were also formed and deprotected with sodium-mercury amalgam. These 'modified Richman-Atkins conditions' using Cs_2CO_3 or K_2CO_3 are now regarded as the most effective for the formation of most polyazamacrocycles. However the yield was still somewhat dependent on the ring size being formed and the deprotection of the alkylazamacrocycles was still difficult with typical hydrolysis procedures.



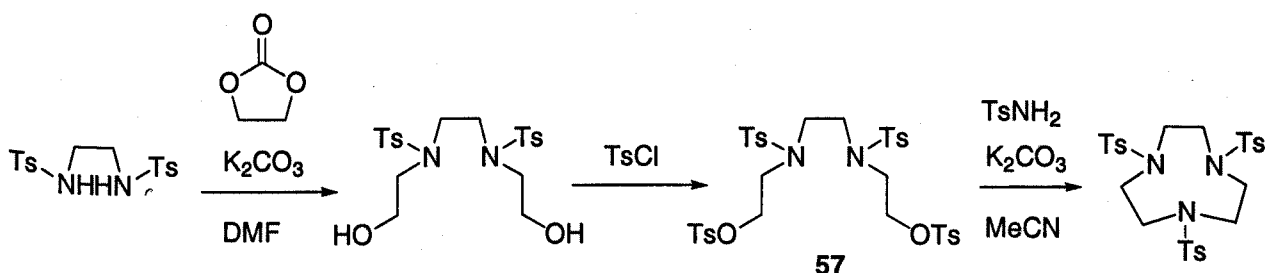
It was apparent that although this method was much more general than template methods and more convenient than high dilution syntheses, there were still problems with inconsistencies in cyclisation and deprotection yields. Numerous adaptations of the Richman-Atkins synthesis have appeared over the years, each providing its own advantages. Although none stands out as the definitive ideal method, a few do provide distinct improvements in protection strategy or practicality.

Scheme 1.4.1.12



For example, use of phase-transfer conditions (**Scheme 1.4.1.12**) improved the cyclisation yields for some ring sizes.¹⁵⁵ Presumably this is because it allows for the use of NaOH, a stronger base, which is also kept separate from the ditosylate (preventing possible elimination of the tosylate groups and loss of this starting material). Another interesting use of the tosyl group involves the synthesis of triazamacrocycles by closing **57** with tosylamide (**Scheme 1.4.1.13**).^{157, 158} With the right solvent and base, this reaction is quantitative for certain ring sizes (e.g. [2,2,2]). This route is amenable to laboratory scale production of some triazamacrocycles. However, this route encounters the same problems with deprotection of the tosylamide macrocycles as for traditional Richman-Atkins synthesis.

Scheme 1.4.1.13

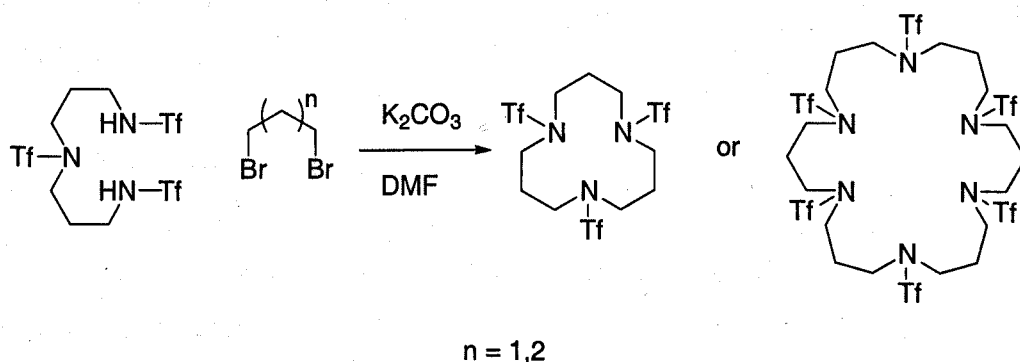


Alternative sulfonamides

Some alternative sulfonamides have been used in attempts to simplify the deprotection. Each has advantages and disadvantages, however they do provide higher yields of some azamacrocycles.

Using trifluoromethylsulfonamides (triflamides) allows for dilution-specific control over the cyclisation process, giving either 1:1 or 2:2 cyclisation products (**Scheme 1.4.1.14**).¹⁵⁹ Reactant concentrations of 0.02 M give predominantly the 1:1 cyclised product, whereas concentrations ~0.5 M result in the 2:2 'dimerised' macrocycle. The process still avoids oligomerisation, so it can be used to prepare certain ring sizes ([3,3,3]; [3,3,4]; [3,3,3,3,3,3]; and [3,3,4,3,3,4]) in a reliable manner. The deprotection is achieved using lithium in ammonia and the macrocycles are obtained as their hydrochloride salts after ion-exchange chromatography.

Scheme 1.4.1.14



The 2- or 4-nitrobenzenesulfonyl (nosyl, Ns) group has also been used. It most specifically provides an advantage in the synthesis of cyclophanes—pyridinophanes, naphthalenophanes and anthracenophanes.^{152, 153} The deprotection is mild enough for the *N*-benzylic functionality to survive. The (2-trimethylsilyl)ethanesulfonyl group is also removed under mild conditions and is also useful for the synthesis of the aforementioned cyclophanes as well as for alkyltriazamacrocycles. The synthesis of polyazamacrocycles using these protecting groups is discussed in more detail in Chapter 2.

Overall, the Richman-Atkins route provides the most flexible, generally applicable synthesis of polyazamacrocycles. It is not as sensitive to ring size and intermediate conformation as the template routes and does not require high dilution and extended reaction times as do diamide condensations. This route was chosen for this project as the primary method with which to prepare a series of triazamacrocycles of various carbon-bridge lengths and ring sizes.

1.5. Other biological considerations

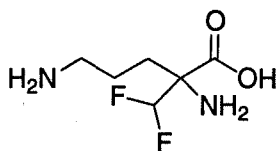
Polyazamacrocycles have numerous interesting biological activities in addition to their potential use as bioreductive prodrugs. As analogues of natural polyamines, they may show anti-fungal and anti-parasitic activity. *N*-Substituted polyazamacrocycles have a range of activities, such as anti-tumour and anti-HIV.¹⁶⁰⁻¹⁶³ As complexes with transition metals, they are useful as magnetic resonance imaging (MRI) contrast agents. They can also act as catalysts and mimics of various enzymes including ribonucleases and proteases. In order to understand

fully the biological characteristics of the novel polyazamacrocycles and complexes produced in this project, it is important to investigate these alternatives for biological activity.

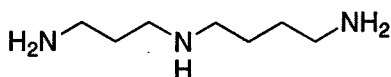
1.5.1. Polyamine analogues

Polyamines are present in all living systems, playing a key role in the replication and proliferation of cells.^{164, 165} Introduction of unnatural polyamines into the natural pathway can have a therapeutically useful impact on stopping the proliferation of cells such as cancer cells, which usually show elevated levels of polyamine activity.¹⁶⁶

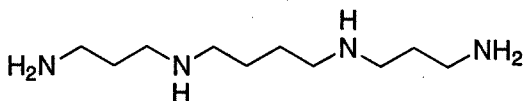
Four key aspects of polyamines could be exploited in the treatment of disease.¹⁶⁷ Firstly, the uptake and transport systems are not highly specific. They will transport polyamine analogues with diverse functionality and structure. Indeed, it is possible to 'tag' compounds with polyamines in order to exploit the transport system for their uptake.¹⁶⁸ Second, certain tissues have increased levels of polyamine transport, including tumours and prostate tissues (as shown by radiolabelling studies). They can be targeted with strategies involving unnatural polyamine analogues. Third, intracellular polyamines can be depleted with drugs such as (+/-) 2-(difluoromethyl)ornithine (DFMO, **58**), further increasing the uptake of artificially introduced analogues by polyamine-dependent cells. DFMO is especially active in tumour cells *versus* normal cells *in vivo*. Last, polycationic polyamines such as spermidine (**59**) and spermine (**60**) have a high affinity for DNA. Drugs based on these structures that are transported by the polyamine system will collect in the nucleus, in high local concentrations near DNA.



58



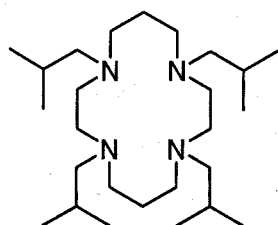
59



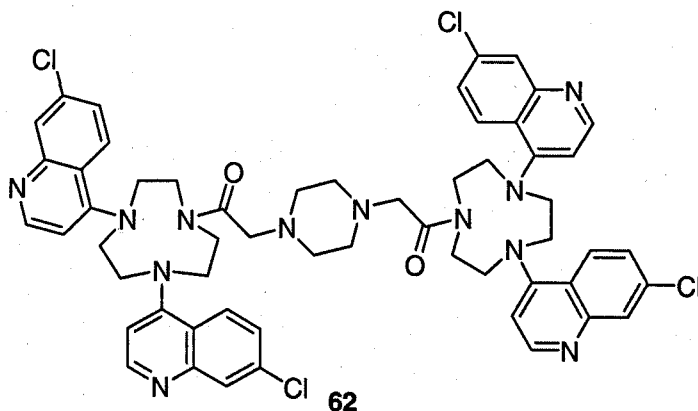
60

Unnatural polyamine analogues (e.g. with unusual chain lengths or substitution) can act in a number of ways: by inhibiting polyamine transport systems and preventing uptake of extra-cellular polyamines; by being incorporated into the cell *via* polyamine transport systems and inhibiting the biosynthetic and metabolic pathway of polyamines (as does DFMO); and by acting as vectors for cytotoxic and imaging agents.¹⁶⁷ Polyamines are essential for cell reproduction, so disrupting these pathways can cause cell death.^{169, 170} Usually it is necessary to combine drugs with complementary effects on the polyamine system to ensure maximum therapeutic viability, e.g. depleting cellular polyamine levels with DFMO combined with a polyamine transport inhibitor disabling the uptake system, preventing extracellular replenishing of polyamine levels.

Bergeron *et al.* showed that even small variations in structure, such as length of carbon bridges between nitrogen atoms, have drastic effects on the biological activity.¹⁶⁹ Polyamine analogues have also shown useful anti-parasitic activity against trypanosomes, leishmania and malaria, as well as anti-fungal activity.¹⁷¹⁻¹⁷³ Polyamine levels and metabolism in these organisms are also susceptible to disruption by unnatural substrate analogues. *N*-Benzyl analogues appear to be especially active, perhaps due to their increased lipophilicity. This would imply that their uptake is not through polyamine transport systems, but instead due to increased ability to cross cell membranes.¹⁶⁷ *N*-Aryl substituted polyamines also function well as anti-cancer agents, probably by interacting with DNA *via* both ionic effects and hydrophobic intercalation.¹⁷⁴ However, if lipophilicity is increased too much the compounds lose some of the selectivity of their cytotoxicity.¹⁶⁷



61



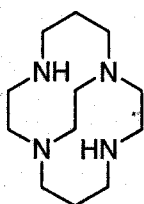
62

N-Substituted polyazamacrocycles have shown a variety of biological activities, including anti-tumour (**61**)¹⁶⁰ and anti-malarial (e.g. **62**).¹⁷³ They are also used commercially for their anti-microbial and anti-fungal properties.¹⁷⁵

There is scope for the use of new polyazamacrocycles as polyamine analogues. It is of interest to consider the polyamine transport system as a target for polyazamacrocyclic drug delivery.¹⁶⁸ It is also important to keep in mind the possible polyamine analogue activity of polyazamacrocyclic drugs targeted towards other systems, in the light of possible side effects or potentiation of cytotoxicity.

1.5.2. Catalysts and enzyme mimics

Metal ions, either alone or complexed to various ligands, are well known as catalysts. They are also essential components of many enzyme active sites. Complexation with peptides holds the metal in place and nearly always contributes to the reactivity of the metal for the desired enzymatic catalysis. Accordingly, small molecule metal complexes can act as artificial enzymes. Polyazamacrocycles have a range of catalytic activities. Manganese complexes of cross-bridged cyclams (e.g. **63**) are peroxide oxidation catalysts used in laundry detergents.¹⁷⁶ Complexes of tetra- and triazamacrocycles with various metals can catalyse the hydrolysis of carboxyesters, phosphate esters and peptide bonds.

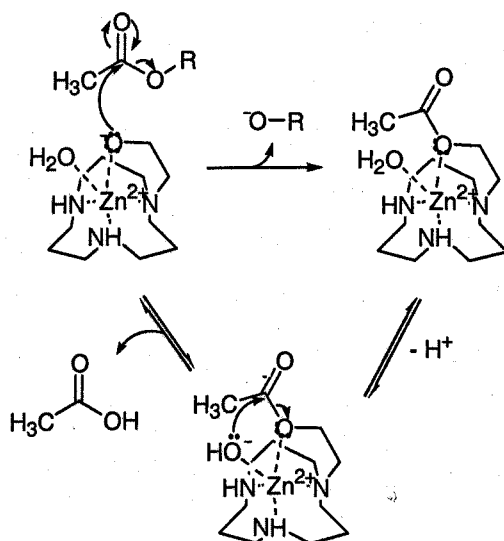


63

Carboxyesters

Experimental evidence from Kimura *et al.* shows zinc to be the best metal ion for hydrolysis of carboxyesters by polyazamacrocyclic complexes.¹⁷⁷ Zinc complexes readily bind water molecules. The nature of the ligand can lower the pK_a of the bound water, facilitating ionisation at neutral pH. For optimum activity, the ligand should have alcohol functionality that can also be deprotonated in order to participate in an initial transesterification reaction. This is followed by hydrolysis of the newly formed ester (Scheme 1.5.2.1) by the bound hydroxyl ion.¹⁷⁸ Dinuclear Zn(II) complexes provide two reactive centres, increasing rate constants by approximately 2.4.¹⁷⁹ These complexes provide useful model systems for elucidating the mechanism of zinc enzyme-catalysed ester hydrolysis.¹⁷⁷⁻¹⁷⁹

Scheme 1.5.2.1



Phosphate esters

The phosphate esters that make up the DNA and RNA backbones are incredibly stable to hydrolysis. With half-lives (under physiological conditions) estimated at 10⁶ and 10³ years, respectively, RNA is relatively less stable to hydrolysis than DNA.¹⁸⁰ However, they are both essentially inert to hydrolysis within biological systems without the catalysis of nuclease enzymes. The anionic charge of the backbone hinders the approach of nucleophiles, so nuclease enzymes often utilise cationic metal centres to neutralise the charge. The complexed metal

can also serve to activate water molecules for deprotonation to hydroxide ions, facilitating the hydrolysis.

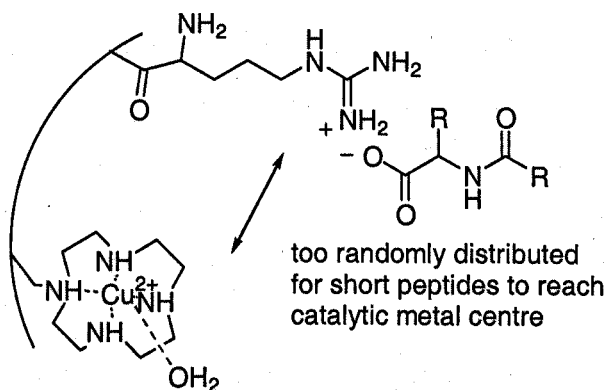
In order to be useful, a catalyst needs to increase the rate of DNA hydrolysis by at least 10^{14} .¹⁸⁰ The efficiency of the catalysis is dependent on a number of factors, such as the attraction of the catalyst to DNA, the strength of the substrate binding and the pKa of the bound water. These properties are all adjusted by changing the nature of the active site. Metal complexes of organic ligands are used as model systems, allowing for broad variation in the active site components and correlation of the behaviour with structure.

Metal complexes of polyazamacrocycles can have artificial nuclease activity,¹⁸¹⁻¹⁸⁵ although so far only limited success has been achieved (increasing hydrolysis rates by up to 7 orders of magnitude). Usually a large excess of complex relative to DNA substrate is required to effect even minimal cleavage. The mechanism is similar to that for carboxyester hydrolysis, however the need for large 'catalyst' excess implies that the cycle may often stop at transesterification. The activity is highly dependent on the substitution around the ligand macrocycle and the metal involved. Lanthanide complexes of substituted cyclen increase the rate of RNA hydrolysis to $\sim 0.65 \text{ M}^{-1}\text{s}^{-1}$. Peptide and peptide-nucleic acid functionality can improve the interaction of the complex with oligonucleotides. For example, a hexapeptide derivatised with two Zn(II) triazacyclononane complexes lowered the pKa of the water bound to zinc to ~ 7.7 , which increased the hydrolysis of DNA by about 10^7 .¹⁸⁰

These are only the more promising of a wide range of results from polyazamacrocycle complex catalysis of phosphate ester hydrolysis. There is still extensive scope for further development in this area, especially given the improvement in macrocycle synthesis and substitution methods. Also, Cu(II) complexes usually need to be reductively activated to Cu(I) in order to function in this way. Thus, it is feasible they could provide another mode of hypoxia selective action, increasing cytotoxicity to tumours while remaining unreactive in normal cells.

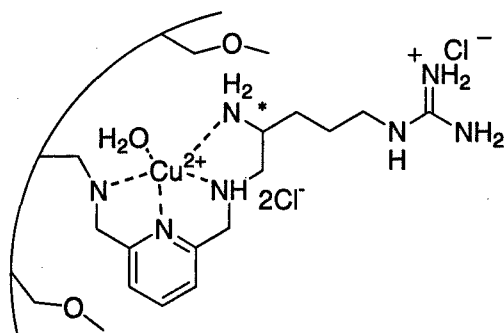
Peptide bonds

Amides are also very stable to hydrolysis under physiological conditions. Peptide linkages normally have half-lives between 500 and 1000 years. Free metal ions can catalyse the hydrolysis of amides, but only if the substrate contains a proximal metal binding site.¹⁸⁶ However, metal complexes are more useful, as they usually avoid the problem of metal hydroxide precipitation (which makes mechanistic studies difficult). Incorporating substrate binding moieties in the ligand can improve the efficiency of amide hydrolysis.



64

The Cu(II) complex of cyclen was randomly attached to polystyrene (**64**), along with guanidinium ions to attract negatively charged protein components (e.g. carboxylate groups of aspartate residues and C-termini of peptide chains). The guanidinium ion made the catalyst a mimic of carboxypeptidase A.¹⁸⁷ The polymer-supported catalyst improved hydrolysis rates by up to 2×10^8 (from normal physiological conditions).¹⁸⁸ However, the active site of the catalyst was too large to bind small peptides for hydrolysis. The guanidinium ions and the metal complex were distributed too widely to bring bound small peptides sufficiently close to the catalytic centre. The catalyst was improved by attaching the guanidinium ion directly to the metal complexing component of the polymer, in order to ensure binding of peptides in close proximity to the active moiety (**65**). This is the first example of a general artificial peptidase.



65

A selective artificial peptidase has been prepared by attaching cyclen complexes to peptide nucleic acid (PNA) chains. A combinatorial selection strategy found PNA sequences that selectively bound myoglobin over bovine serum albumin, γ -globulin, elongation factor P and gelatins A and B. When the sequences were ligated to cyclen complexes, they did selectively cleave myoglobin. The authors claim that this provides a paradigm for the design of drugs to cleave specific disease-related proteins. However, optimisation of catalytic centres and binding sequences for those specific proteins would be necessary in order for this to be practical.^{189, 190}

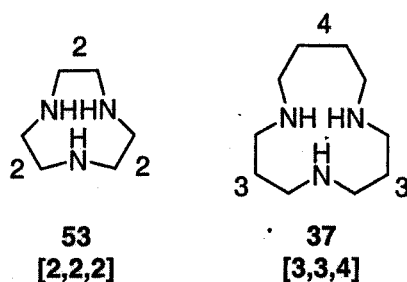
Artificial peptidases are biochemically and pharmaceutically interesting. Very few examples of artificial peptidases based on polyazamacrocycles have been published. As yet, work has focused on the use of commercially available compounds such as cyclen and tacn. A non-specific, high-turnover artificial catalyst to hydrolyse proteins to their component amino acids for analysis would be very useful and so far is not forthcoming. Perhaps new macrocycle synthesis strategies will allow detailed structure-activity investigations, leading to catalysts that are more effective. Very few groups are concentrating work in this area, thus it offers scope for extensive development.

Chapter 2

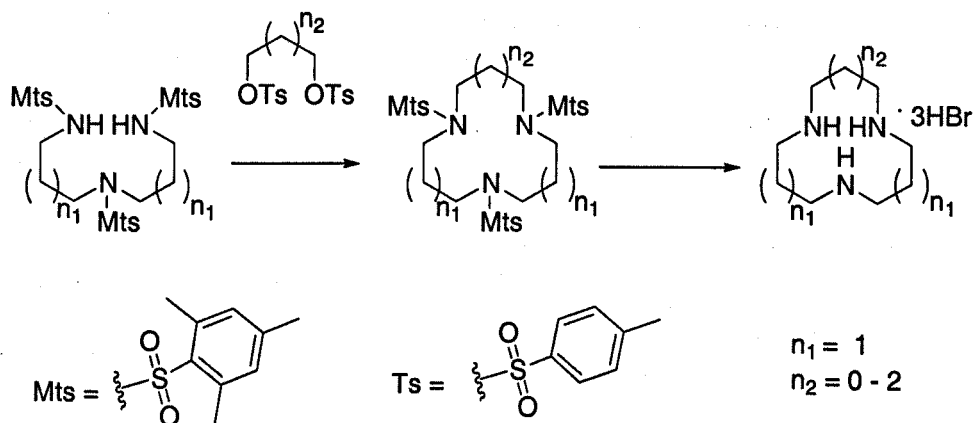
2. Synthesis of parent macrocycles

2.1. Initial strategy using the mesitylenesulfonyl protecting group

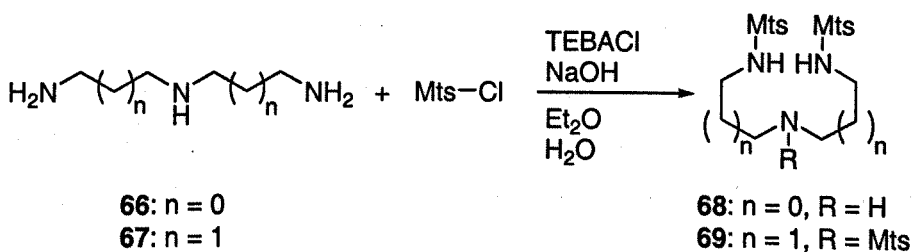
In her PhD project, Fiona Anderson used amines protected with *p*-toluenesulfonyl (tosyl) groups in the Richman-Atkins polyazamacrocyclic synthesis.¹²¹ Her difficulties in the deprotection step indicated that a different protecting group was necessary. Our initial approach involved the use of mesitylenesulfonamides in place of tosylamides (**Scheme 2.1.1**). The deprotection of mesitylenesulfonamides is reported to occur under milder conditions than for tosylamides, e.g. stirring at room temperature with conc. HBr/glacial acetic acid.¹⁹¹ A series of tris-*N*-(mesitylenesulfonyl) (Mts) triazamacrocycles was prepared *via* a modified Richman-Atkins cyclisation, using the required triamines and diol ditosylates. The triamines **66** and **67** were protected under phase transfer conditions using triethyl-benzylammonium chloride (TEBACl) according to **Scheme 2.1.2** giving the Mts-amides **68** and **69** in moderate to good yield (41% and 75%, respectively). Attempts to cyclise **68** always resulted in a complex mixture of oligomers. The yields for cyclisation and deprotection of triazamacrocycles using **69** are listed in **Table 2.1.1**. For simplicity, macrocycle 'ring size' will be described either according to the abbreviations previously listed in this thesis (e.g. **53** = tacn, **36** = cyclen), or by the convention [n_1, n_2, n_3 etc.], where n_1 etc. indicates the length of carbon chain between nitrogens (see **53** and **37** below for examples).



Scheme 2.1.1



Scheme 2.1.2



Unfortunately, the deprotection of mesitylenesulfonyl-protected triazamacrocycles proved to be just as difficult as for tosylamides. Only one compound, the 3,3,3 macrocycle **71**, was successfully deprotected under hydrolysis conditions to give **73** and then only after 14 days of reflux and 14 days of standing at room temperature. Although the yield was good, the unpredictable behaviour and still harsh hydrolysis conditions for the deprotection, were undesirable.

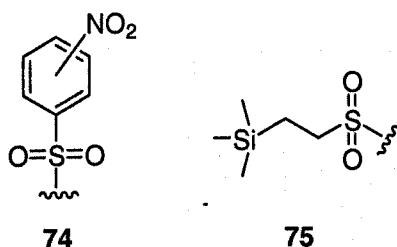
Table 2.1.1

<div style="display: flex; justify-content: space-around; align-items: center;"> <div style="text-align: center;"> </div> <div style="text-align: center;"> </div> </div>			
n_1, n_2	ring size	cyclisation yield (%)	deprotection yield (%)
1,0	[3,3,2]	70: 8	n/a
1,1	[3,3,3]	71: 15	73: 84
1,2	[3,3,4]	72: 39	n/a

A route was necessary that would provide reliable synthesis of a range of polyazamacrocycles. The route also needed to be flexible enough to accommodate various types of functionality within the ring. It was clear that it was crucial to find a protecting group that could be removed dependably and under milder conditions. It was also desirable to stay within the Richman-Atkins-type cyclisation of sulfonamides, as it offered the required flexibility in ring size construction.

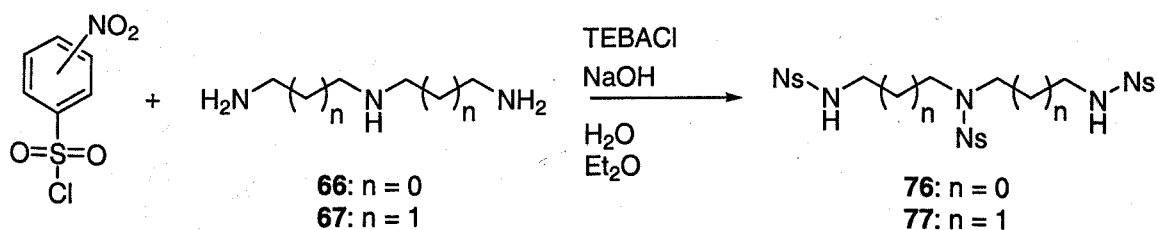
2.2. Alternative protecting group strategies

A number of alternative sulfonamide protecting groups were available. The 2- and 4-nitrobenzenesulfonyl (nosyl, **74**) and (2-trimethylsilyl)ethanesulfonyl (SES, **75**) protecting groups have been used for the synthesis of polyazamacrocycles. Both were attractive: the nosyl group was reported to give good yields for the cyclisation and mild deprotection could be carried out using a thiol;^{152, 153} and the SES group provided high yields in the cyclisation and mild deprotection was accomplished using fluoride.^{151, 192}



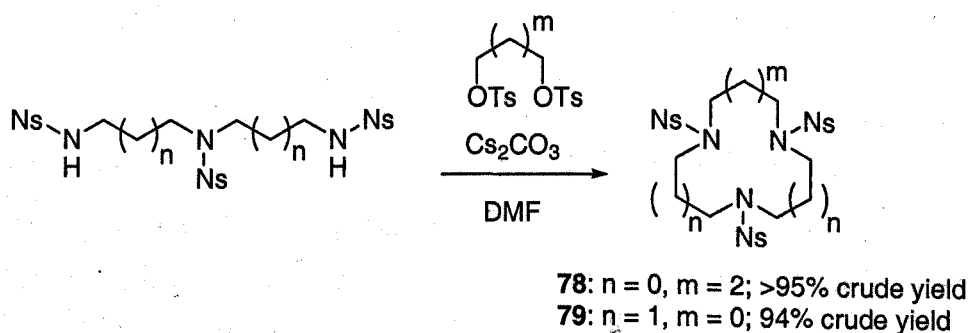
Initially both groups were investigated; however the use of the nosyl group proved to be more difficult than expected. Preliminary attempts at the protection of triamines with 2- or 4-nitrobenzenesulfonyl chloride under phase transfer conditions using TEBACl (Scheme 2.2.1) were complicated by the low solubility of the *N,N'*-bis-nosylated material in diethyl ether and the steric hindrance at the secondary amine. This was particularly a problem in the protection of diethylenetriamine (**66**).

Scheme 2.2.1



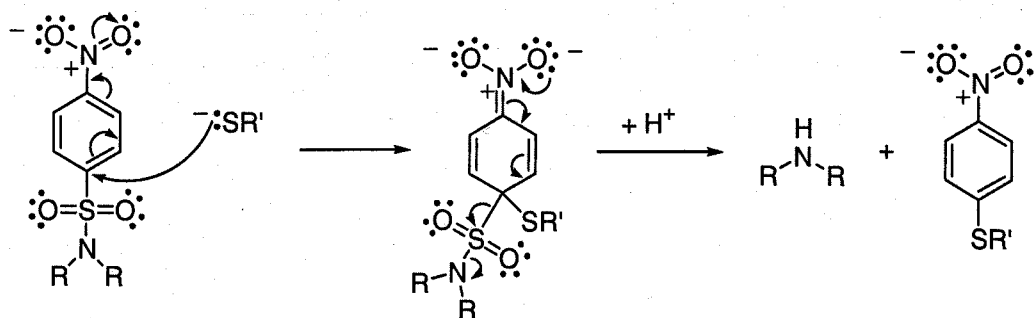
Following the initial protection of the primary amine functionality, some of the bis-protected material precipitated from solution. This resulted in a mixture of bis- and tris-protected triamines that was difficult to separate and gave low yields of the desired tris-nosylated triamine. This primary amine selectivity has been reported previously and with the right conditions can provide an advantage for orthogonal protection.¹⁹³ However, this did not suit the purposes of our project. Changing the solvent to dichloromethane or *N,N*-dimethylformamide reduced the precipitation, but still gave a mixture of products. Column chromatography could be used to achieve ~90% purity but the yield was unsatisfactory (29%).

Scheme 2.2.2

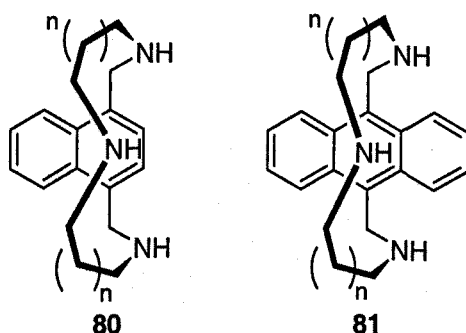


Additionally, the cyclisation and deprotection of nosyl-amides was not straightforward. The cyclisation of two nosylated triamines was attempted with moderate success, giving the products **78** and **79** (Scheme 2.2.2). The crude macrocyclic sulfonamides were not purified, as TLC and ¹H NMR spectra showed complex mixtures although they contained mostly the desired material. Attempts to deprotect the compounds were unsuccessful. The deprotection of nosylamides is reported to occur as in Scheme 2.2.3.¹⁹⁴ The product then needs to be separated from the byproducts either by chromatography or by aqueous extraction.

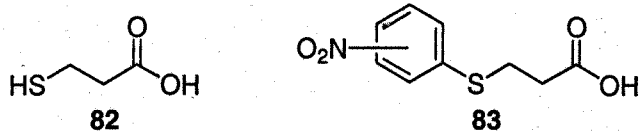
Scheme 2.2.3



A one-pot cyclisation/deprotection strategy for nosylated polyazamacrocycles has been previously reported. However the primary advantage lay in the synthesis of polyaza[n]naphthalenophanes and polyaza[n]anthracenophanes, e.g. **80** and **81**.¹⁵²

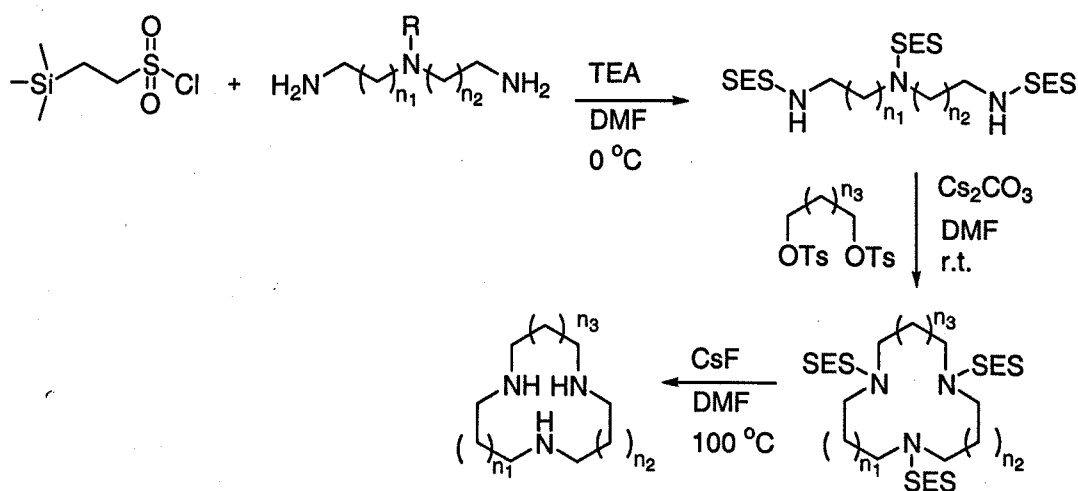


The purification of the deprotected material was not described in detail, but it is likely that the increased hydrophobicity of the cyclophanes allowed them to be purified by column chromatography or by extraction from aqueous solution. This was not possible with the highly water-soluble alkyl triazamacrocycles. Thus it was difficult to separate the free amines from the byproducts of the deprotection. 3-Mercaptopropionic acid (**82**) was used as the thiol, in the hope that the carboxylic acid byproduct **83** could be separated from the triazamacrocycles using acid/base extraction techniques. It was possible to precipitate the bulk of **83** upon acidification of the solution. However, it was too difficult to separate the desired material from the resulting crude mixture. During this time the SES-protecting group was showing promise, so the nosyl route was abandoned.



The method of Hoyer *et al.*¹⁵¹ was used for the synthesis, cyclisation and deprotection of SES-amides according to **Scheme 2.2.4**. 2-(Trimethylsilyl)ethanesulfonyl chloride (SES-Cl, **85**) is not commercially available, so it was synthesised according to the procedure of Weinreb *et al.* from the corresponding sulfonate salt **84** (either purchased from Aldrich or synthesised from vinyltrimethylsilane) as in **Scheme 2.3.1**.¹⁹⁵

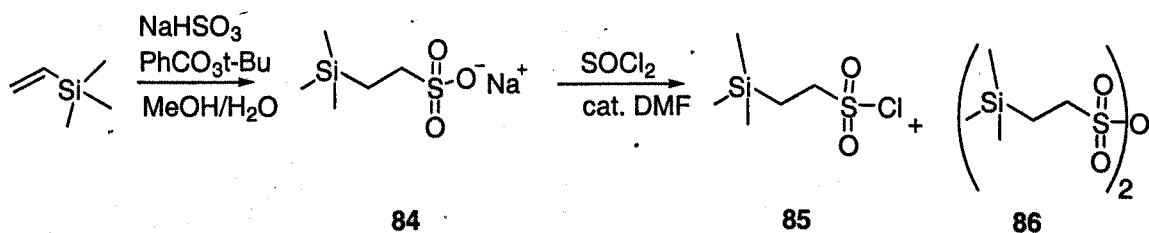
Scheme 2.2.4



2.3. Synthesis of (2-trimethylsilyl)ethanesulfonyl chloride

The formation of the sulfonyl chloride (**Scheme 2.3.1**) was variable. The first attempt gave a high yield of pure material, but subsequent attempts resulted in low conversion and significant amounts of anhydride byproduct **86** (as observed by ¹H and ¹³C NMR spectroscopy). The conditions were kept under strict control: the sulfonate salt was thoroughly dried before use; glassware was oven-dried and argon-cooled; and the thionyl chloride (SOCl₂) was predistilled. However, after multiple attempts the yield of **85** was consistently lower than 30%.

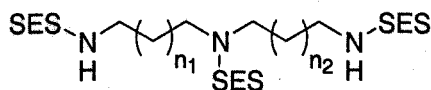
Scheme 2.3.1



The variation of factors such as dryness of **84**, brand of SOCl_2 used and length of reaction time had no consistent effect on yield. Over the course of 30-40 repetitions the only recognisable differences were obtained by ensuring efficient dispersion of **84** during the addition of SOCl_2 (by crushing **84** to a fine powder before use and using twice the amount of SOCl_2). However, even that provided only a marginal increase in reliability of the reaction. The resulting mixture of **85** and **86** required separation by distillation. Even under high vacuum the heat necessary for the distillation caused significant decomposition of **85** to **86** and HCl . Finally it was found that increasing the amount of DMF from 0.04 eq. to 0.4 eq. ensured the production of **85** exclusively. It was then possible to produce pure **85** consistently in high yield (70-86% overall from vinyltrimethylsilane) without the need for distillation. Representative ^1H NMR spectra are shown in **Figs. 2A** and **2B** to illustrate the purity achieved with 0.4 eq. DMF (**2A**), compared with the crude material when only 0.04 eq. DMF was used (**2B**).

2.4. SES-triamines

Practical difficulties were also encountered in the protection of the commercially available triamines (**Scheme 2.2.4**). Again, yields and purities were inconsistent even after repetitions of the same reaction. Reaction times of less than 16 hours resulted in lower yields. Reaction temperatures above 5-10 $^\circ\text{C}$ resulted in a brown odorous byproduct and reduced yield. The best yields were obtained by adding the SES-Cl sufficiently slowly to keep the temperature below 10 $^\circ\text{C}$; monitoring the temperature of the reaction with an internal thermometer; and using an immersion cooler to keep the reaction below 5 $^\circ\text{C}$ while stirring overnight. The compounds **87-89** were obtained in 46, 71 and 87% yield, respectively.



87: $n_{1,2} = 0$

88: $n_{1,2} = 1$

89: $n_1 = 1; n_2 = 2$

In some cases, triamines with the desired carbon bridge lengths were not commercially available. For access to macrocycles with these bridge lengths, a route

was developed from primary sulfonamides and the corresponding haloalkanenitriles to give the bisalkanenitrile sulfonamides. The nitriles could be reduced to the primary amines and subsequently protected as sulfonamides for cyclisation to macrocycles. The initial strategy used nosylsulfonamide **90** (Scheme 2.4.1). The alkylation of the sulfonamide and reduction of the resulting bis-alkanenitrile to the diamine were straightforward, giving the products **91** and **92** in 67 and 78% yields, respectively. However, the nosyl group rendered the diamine **92** difficult to purify and it was not possible to separate the byproduct of nosyl deprotection **83** (as described by Scheme 2.2.3) from the desired triamine **93**.

Scheme 2.4.1

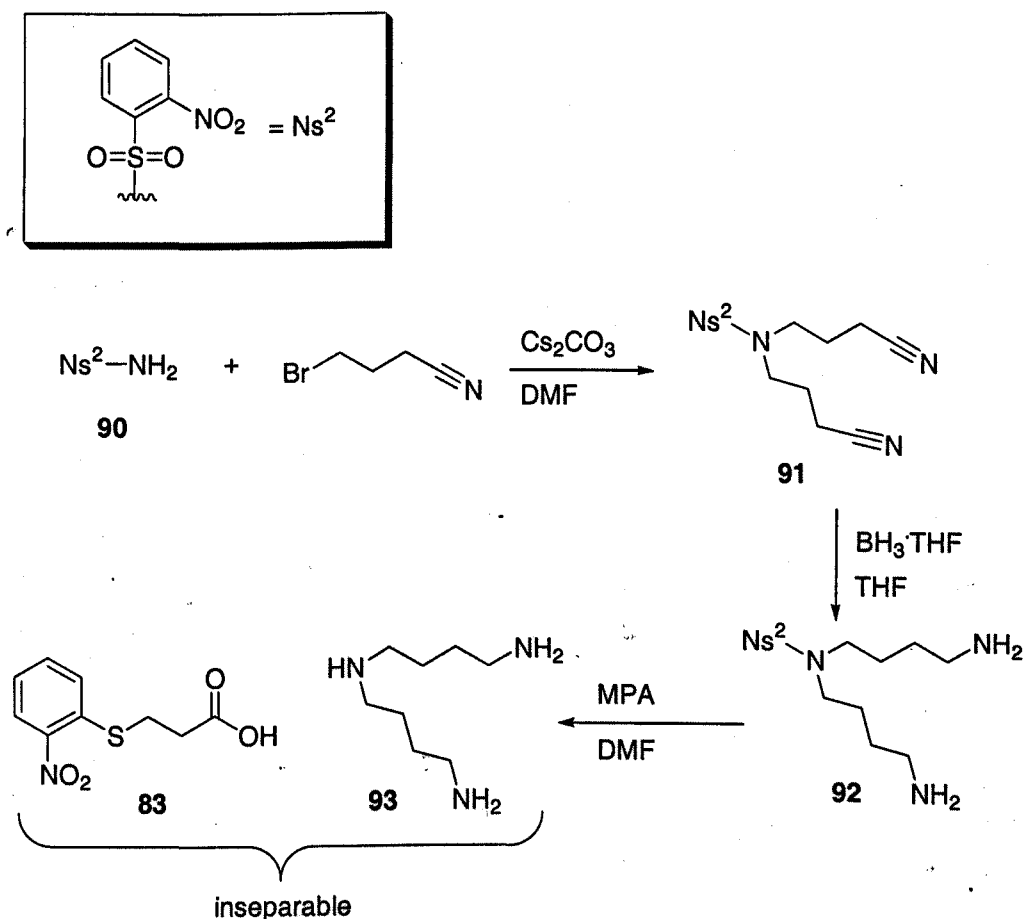


Fig. 2A. SES-CI (crude) when 0.4 eq. DMF was used

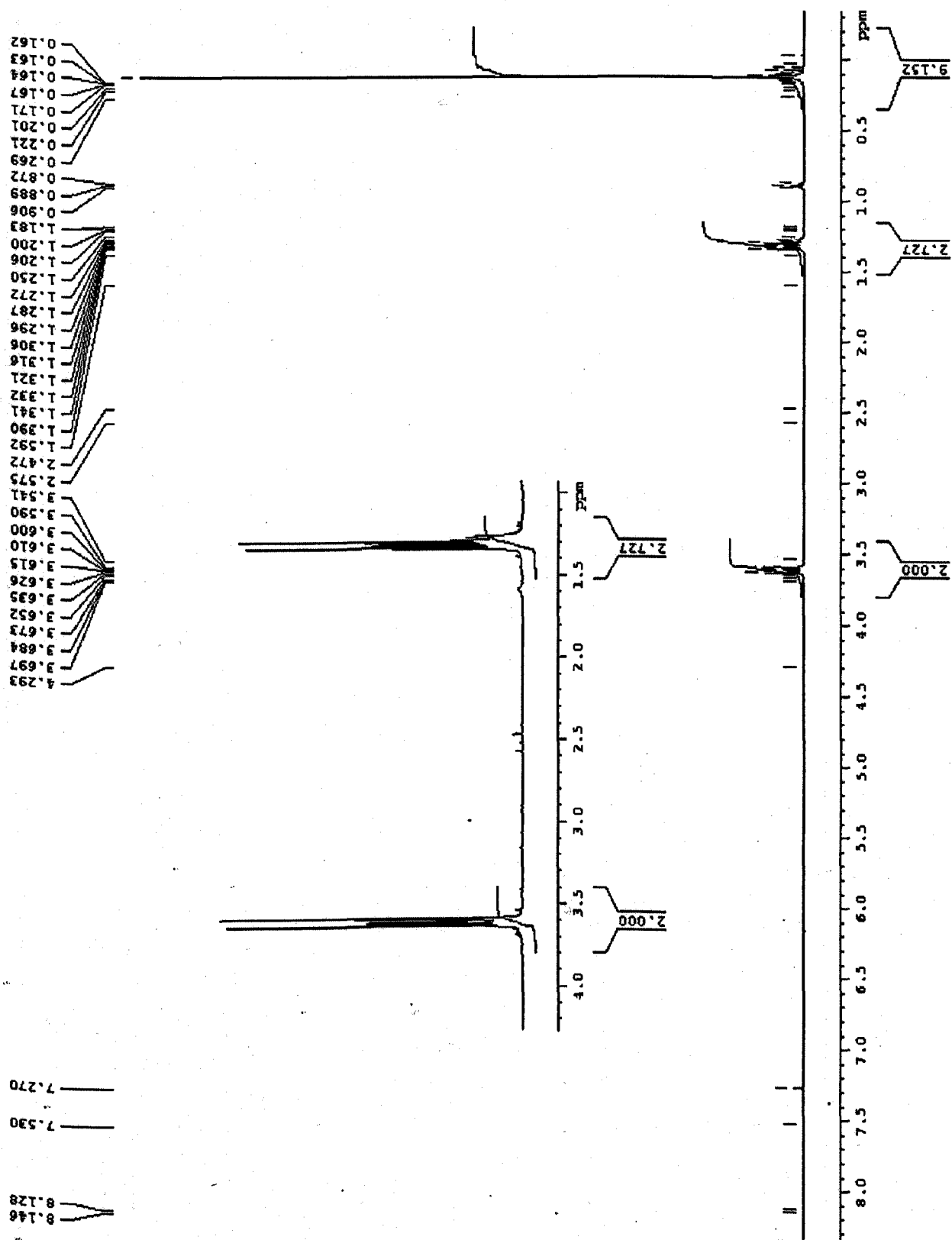
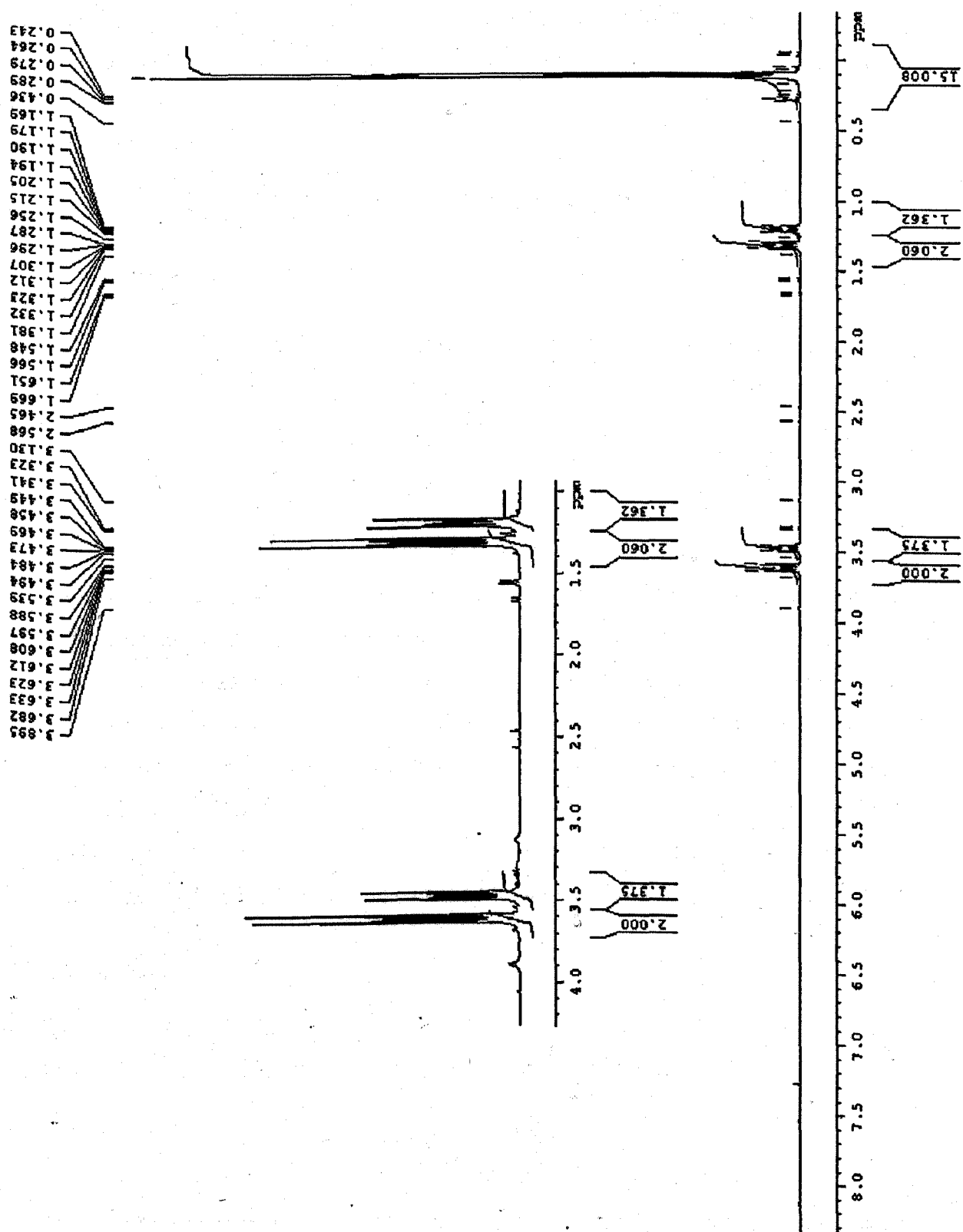
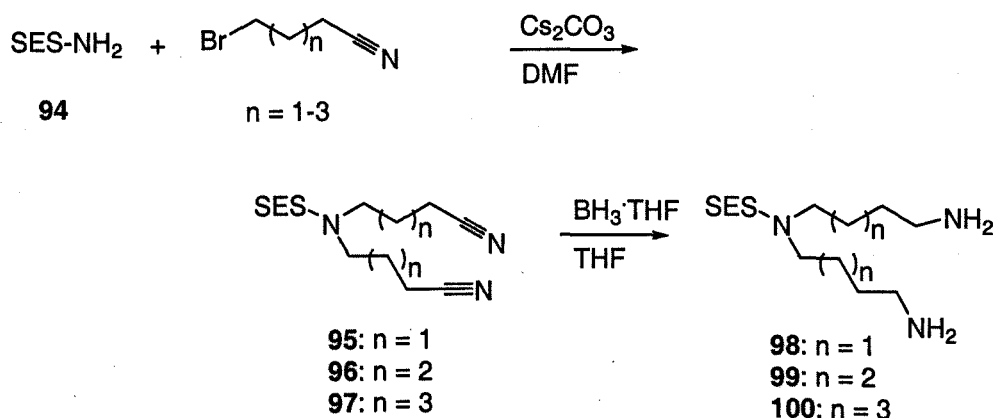


Fig. 2B. Mixture of SES-Cl and SES-anhydride when 0.04 eq. DMF was used



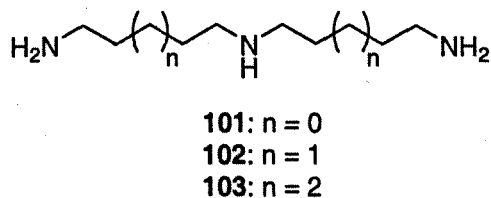
With ease of deprotection in mind, the protecting group was changed to SES (Scheme 2.4.2). **94** was obtained in good yield from SES-Cl and gaseous ammonia (generated by warming stirred conc. aqueous NH_3).

Scheme 2.4.2



The mono-*N*-SES-triamines **98-100** were acquired in good overall yield (~ 70% from **94**) with little or no purification required. The selective protection of the secondary amine provides the opportunity for orthogonal protection of the subsequent triazamacrocycles. Also, the SES group can be removed in good yield (to achieve 50-60% yield overall from **94**), offering better yields than previously published for the synthesis of the biologically interesting triamines **101-103**.^{191, 196, 197} Yields for building triamines are given in Table 2.4.1. The mono-*N*-SES-triamines **98-100** were also tris-protected to give the tris-SES-triamines **104-106**, which were cyclised as in Scheme 2.2.4.

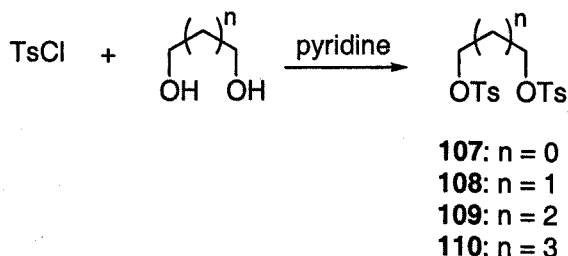
Table 2.4.1



n	R = CN	R = CH ₂ NH ₂	deprotected triamine	over three steps	Tris-SES-triamine
1	95: 96%	98: 96%	101: 84%	77%	104: 52%
2	96: 76%	99: 95%	102: 84%	61%	105: 62%
3	97: 73%	100: 97%	103: 46%	32%	106: 65%

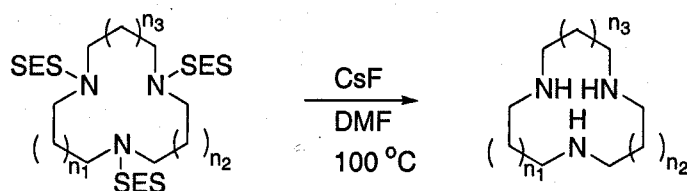
2.5. Cyclisation and deprotection

Scheme 2.5.1



Ditosylate formation (Scheme 2.5.1) was straightforward and high-yielding. The cyclisation (Scheme 2.2.4) generally proceeded smoothly at room temperature. The reaction could be monitored for disappearance of ditosylate by TLC of evaporated aliquots. Little or no oligomerization was observed for the larger ring sizes (e.g. $n > 0$) and the macrocyclic sulfonamides **111-121** could usually be purified by crystallisation from MeOH or 2-PrOH. The only combination of sulfonamide and ditosylate to produce significant quantities of oligomer was **87** and **109**, which gave the dimer **122**. The production of **122** was concentration dependent and could be minimised by increasing the dilution (from 0.08 M to 0.03 M sulfonamide/ditosylate in DMF). The dimerisation was not immediately recognised, as the two compounds co-eluted during column chromatography and the mixture gives a ^1H NMR spectrum that can be rationalised as representing the triaza-[2,2,4] compound **112** (Fig. 2C). The dimer was eventually identified from mass spectrometry and analytically pure material was obtained from multiple columns. The spectroscopic identification of these two compounds is illustrated in Figs. 2D, 2E and 2F. Yields for cyclisation and deprotection are given in Table 2.5.1.

Table 2.5.1



n_1, n_2, n_3	ring size	cyclisation yield (%)	deprotection yield (%)
0,0,1	[2,2,3]	111: 53	123: 55
0,0,2	[2,2,4]	112: 29	124: 52 ¹
1,1,0	[3,3,2]	113: 45	125: 44 ²
1,1,1	[3,3,3]	114: 48	126: 58
1,1,2	[3,3,4]	115: 64	37: 39 ²
1,1,3	[3,3,5]	116: 54	127: 62 ²
2,2,1	[4,4,3]	117: 41	128: 33 ²
1,2,3	[3,4,5]	118: 47	129: 34 ²
2,2,2	[4,4,4]	119: 29	130: 67 ²
3,3,2	[5,5,4]	120: 29	131: 33 ²
4,4,2	[6,6,4]	121: 21	132: 31 ²
(0,0,2) ₂	[2,2,4] ₂ hexaaza	122: 51	133: 28 ²

¹ deprotected using TBAF; reported as apparent yield after distillation relative to TBAOH (deduced from ¹H NMR spectroscopy)

² purified by Kugelrohr distillation

The deprotection of SES-amides proceeded according to Scheme 2.5.2,¹⁹² using caesium fluoride. Although ¹H and ¹³C NMR spectra of aliquots showed when the material was fully deprotected and there was no significant amount of byproduct, only relatively low yields of deprotected material were isolated. No water was used in the workup, which might have reduced recovery of the highly water-soluble amines and the parent macrocycles are not volatile under normal solvent evaporation pressures. Some possible reasons for this lower yield are discussed in the next section.

Scheme 2.5.2

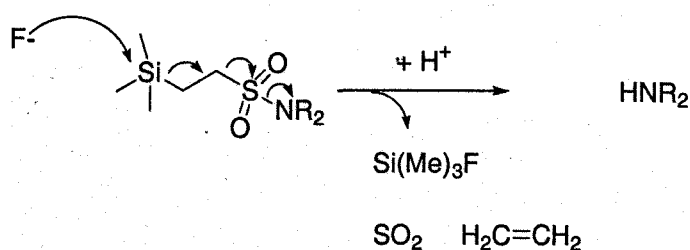


Fig. 2C. Crude SES-[2,2,4] (112 and 122)

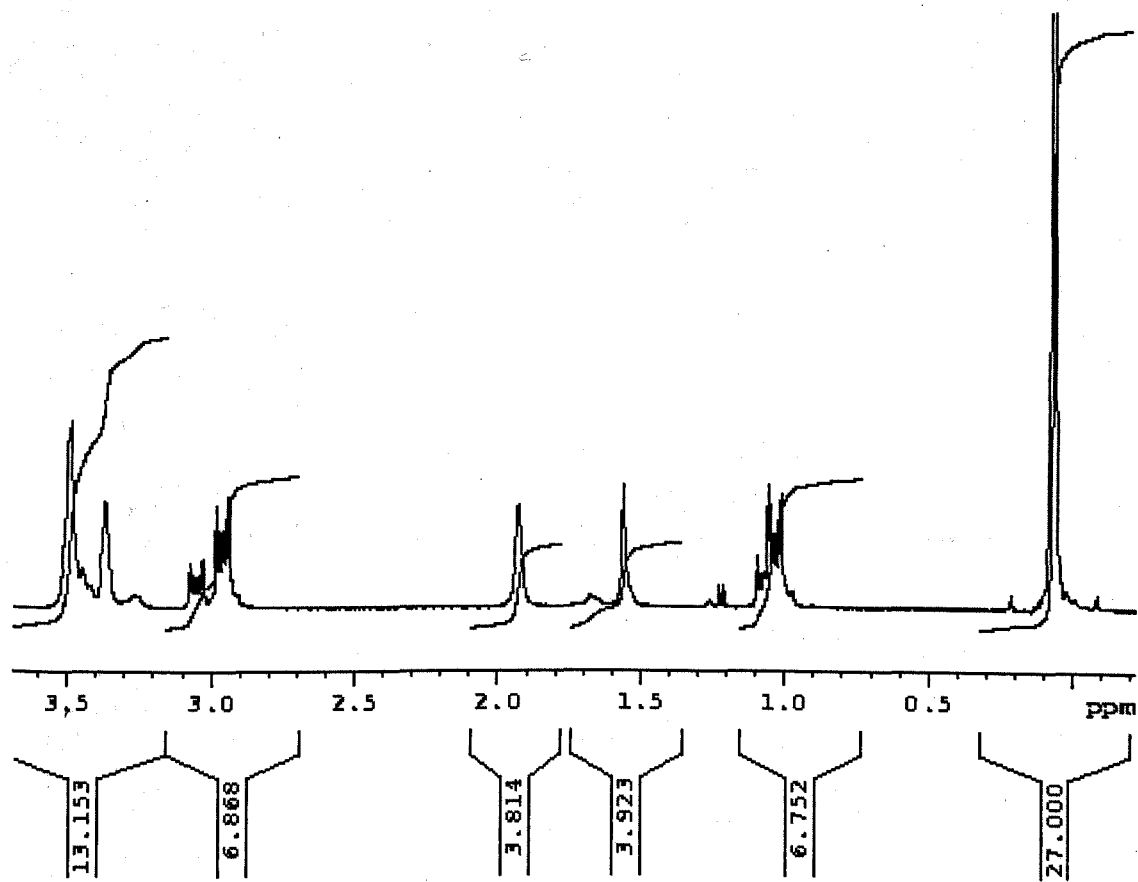


Fig. 2D. ¹H NMR spectra of 122 (top) and 112 (bottom)

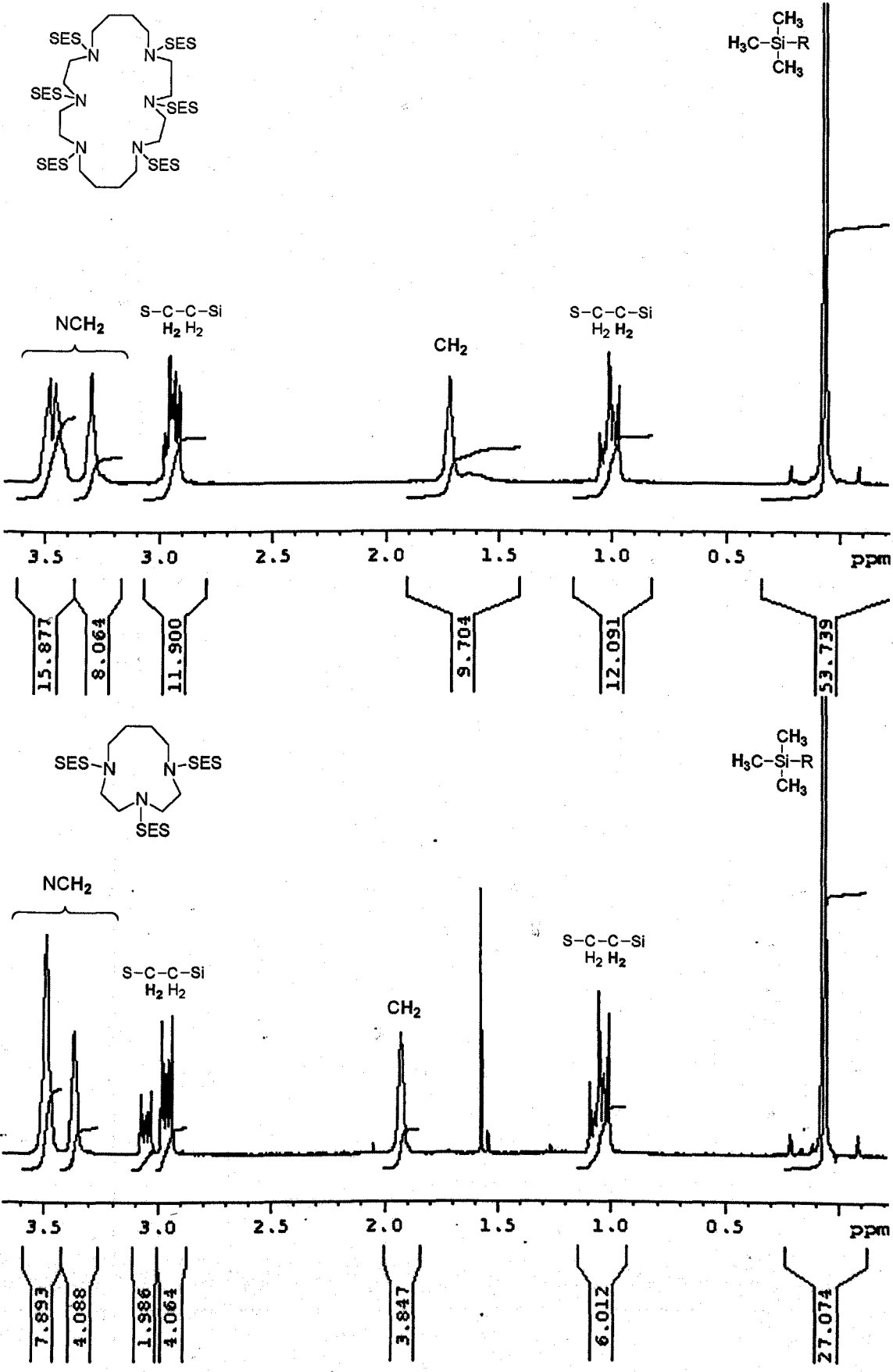


Fig. 2E. ^{13}C NMR spectra of 122 (top) and 112 (bottom)

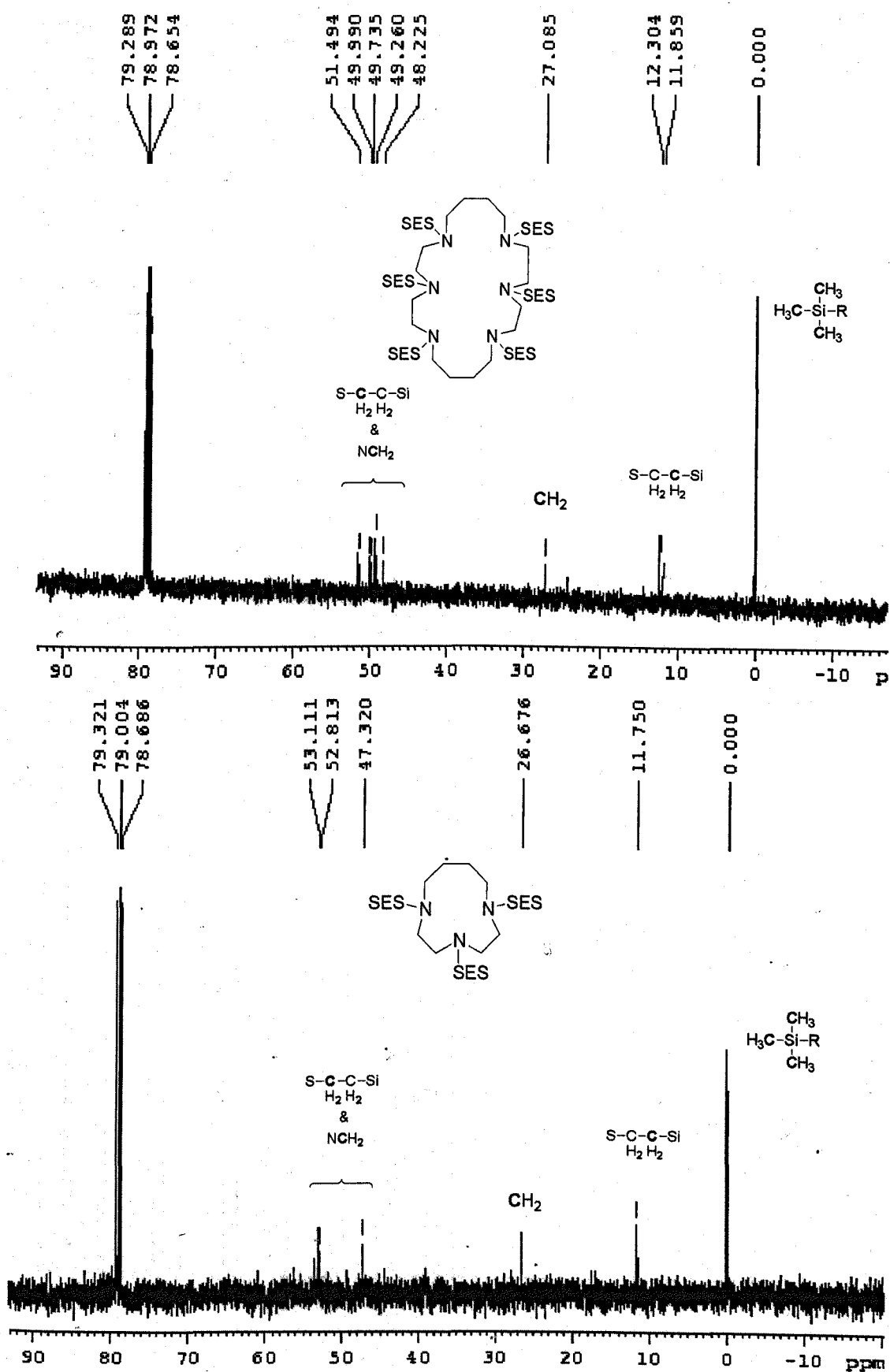
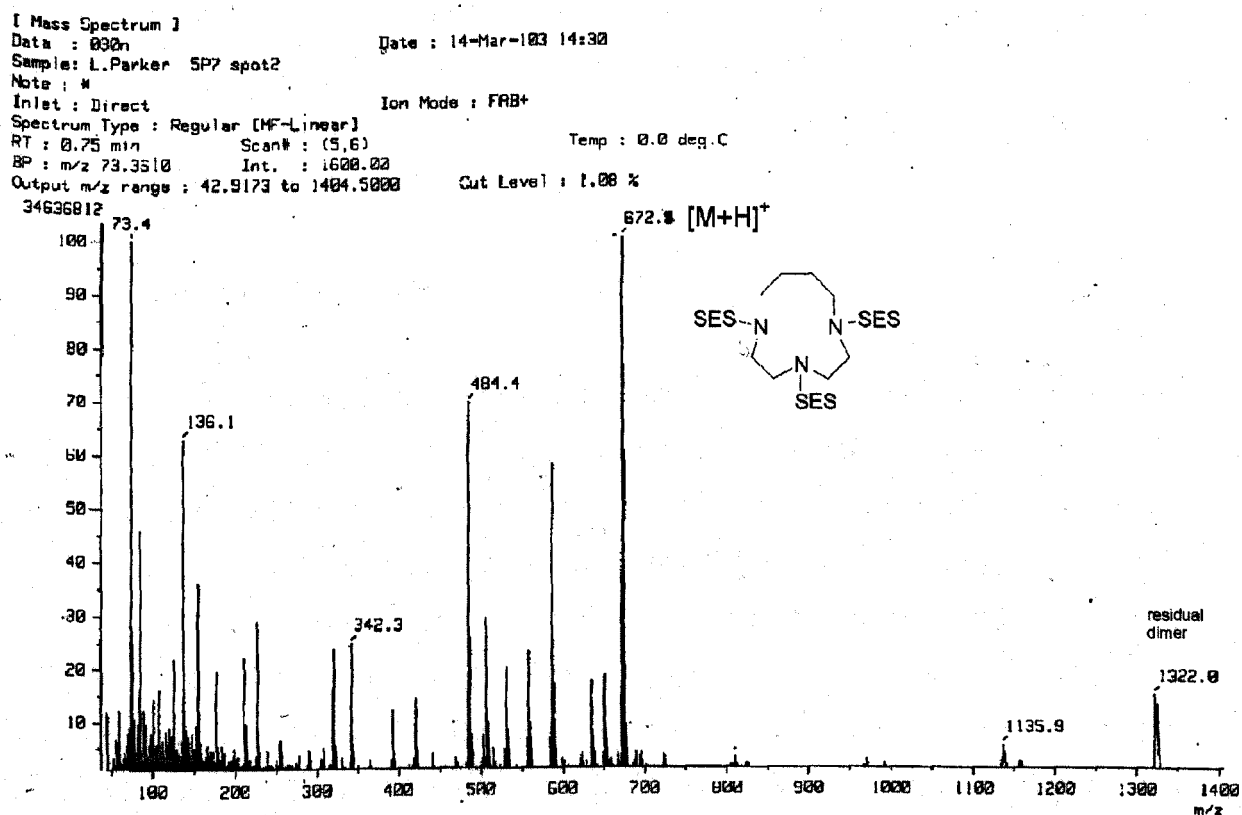
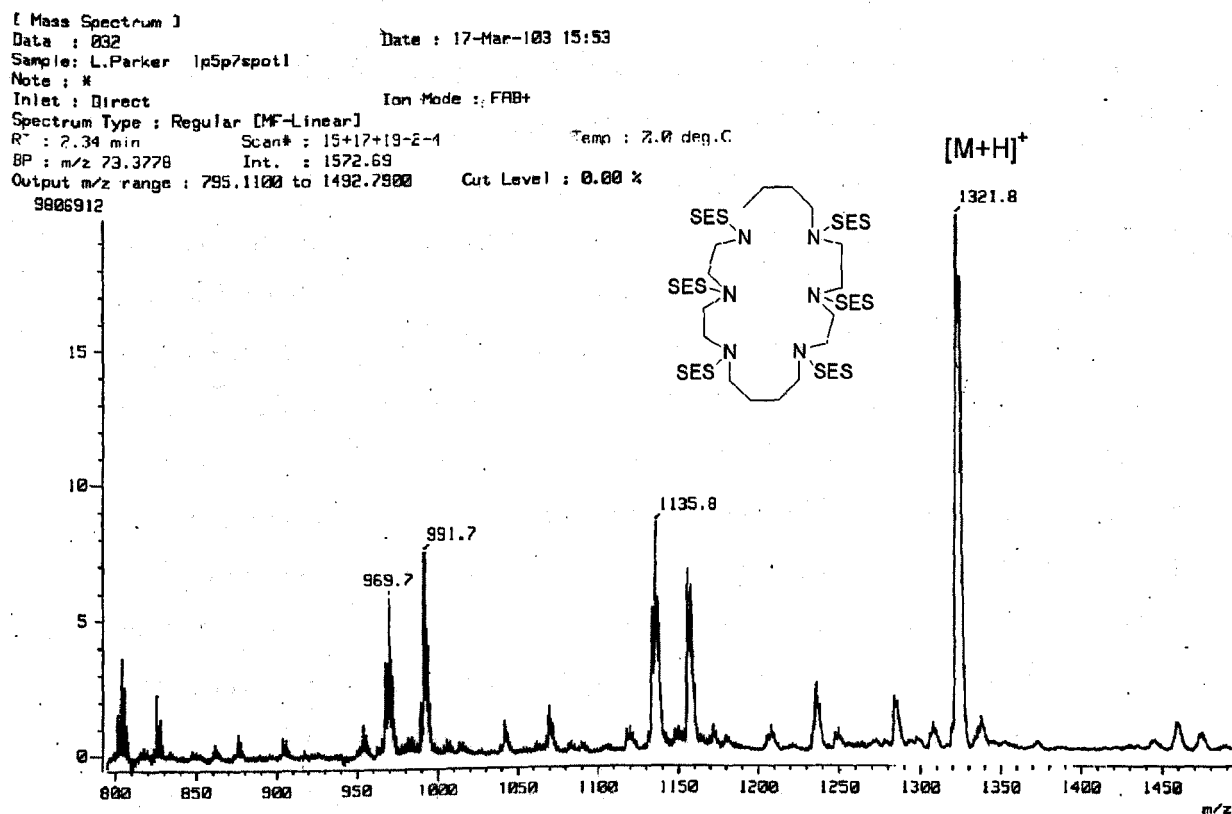


Fig. 2F. Mass spectra of 122 (top) and 112 (bottom)



2.6. Purification of parent macrocycles

Most of the free triazamacrocycles were purified by Kugelrohr distillation. The compounds that were not distilled were produced during an earlier stage of the project and time did not allow their syntheses to be repeated. Consequently, only the distilled macrocycles were successfully converted into mustard drugs. Their high purity facilitated this process. Previous work in the group had encountered difficulties with the purities of the parent macrocycles. The purity can be judged from the definition of the peaks in the ^1H NMR spectra, which are broad and less distinguishable from each other in the crude material (**Fig. 2G**). Upon Kugelrohr distillation, some pure amine was obtained as a clear oil, but a significant amount of yellow oil remained in the original flask. It was not possible to distill this material even at temperatures exceeding $250\text{ }^\circ\text{C}$ and pressures below 0.1 mmHg . ^1H NMR spectroscopy of the yellow material showed it contained mostly the macrocyclic amine. However, slight chemical shift changes indicated that the free amine may have complexed to residual Cs^+ ions (**Fig. 2H**). Small macrocyclic heterocycles are known to chelate to alkali metal ions, e.g. 18-crown-6 forms a strong complex with K^+ . Also, a 'perfect fit' between ion size and macrocycle cavity is not necessary for complexation to occur.¹⁹⁸ Attempts to free the parent amine using EDTA, or forming the HCl salt, were not successful.

2.7. Alternative fluoride sources

To circumvent the problem of metal ion chelation, alternative fluoride sources were investigated. Although tetraalkylammonium fluorides will successfully remove the SES-groups, their byproducts are very difficult to remove from the desired amines. Separation by Kugelrohr distillation was repeatedly unsuccessful. The tetraalkylammonium compounds distilled together with the product. Although they should decompose to their corresponding triamines with heat, this was not seen in practice. Other fluoride sources were unsuccessful at deprotecting the sulfonamides. The results are given in **Table 2.7.1**. The success of the deprotection was assessed by ^1H NMR spectroscopy of evaporated aliquots, looking for disappearance of peaks corresponding to the SES group.

Table 2.7.1

fluoride	solvent	conditions	result
TBAF	THF	reflux	deprotected, but byproducts wouldn't separate
TBAF on alumina	DMF	100 °C	deprotected, but byproducts wouldn't separate
tetraethylammonium fluoride (TEAF)	DMF	100 °C	deprotected, but byproducts wouldn't separate
tetramethylammonium fluoride (TMAF)	DMF	100 °C	incomplete deprotection, byproducts difficult to separate
polymer-supported fluoride (Aldrich)	THF	10-20 eq. reflux 3 days	no reaction
polymer-supported fluoride (Aldrich)	DMF	10-20 eq. 100 °C 5 days	no reaction
ammonium difluoride	DMSO-d6	100 °C	no reaction
ammonium fluoride	DMF	Overnight 100 °C	no reaction
ammonium fluoride	DMF	Microwave 110 °C 15 min	no reaction
KF/ 18-crown-6	DMF	10 eq. 100 °C	some deprotection, but no product isolated from residual 18-crown-6
HF/pyridine	DMF	sonication 35 °C overnight	no reaction
40 % aq. HF	DMF	Sonication 35 °C overnight	no reaction

Fig. 2G. ^1H NMR spectra of distilled (top) and crude (bottom) 37.

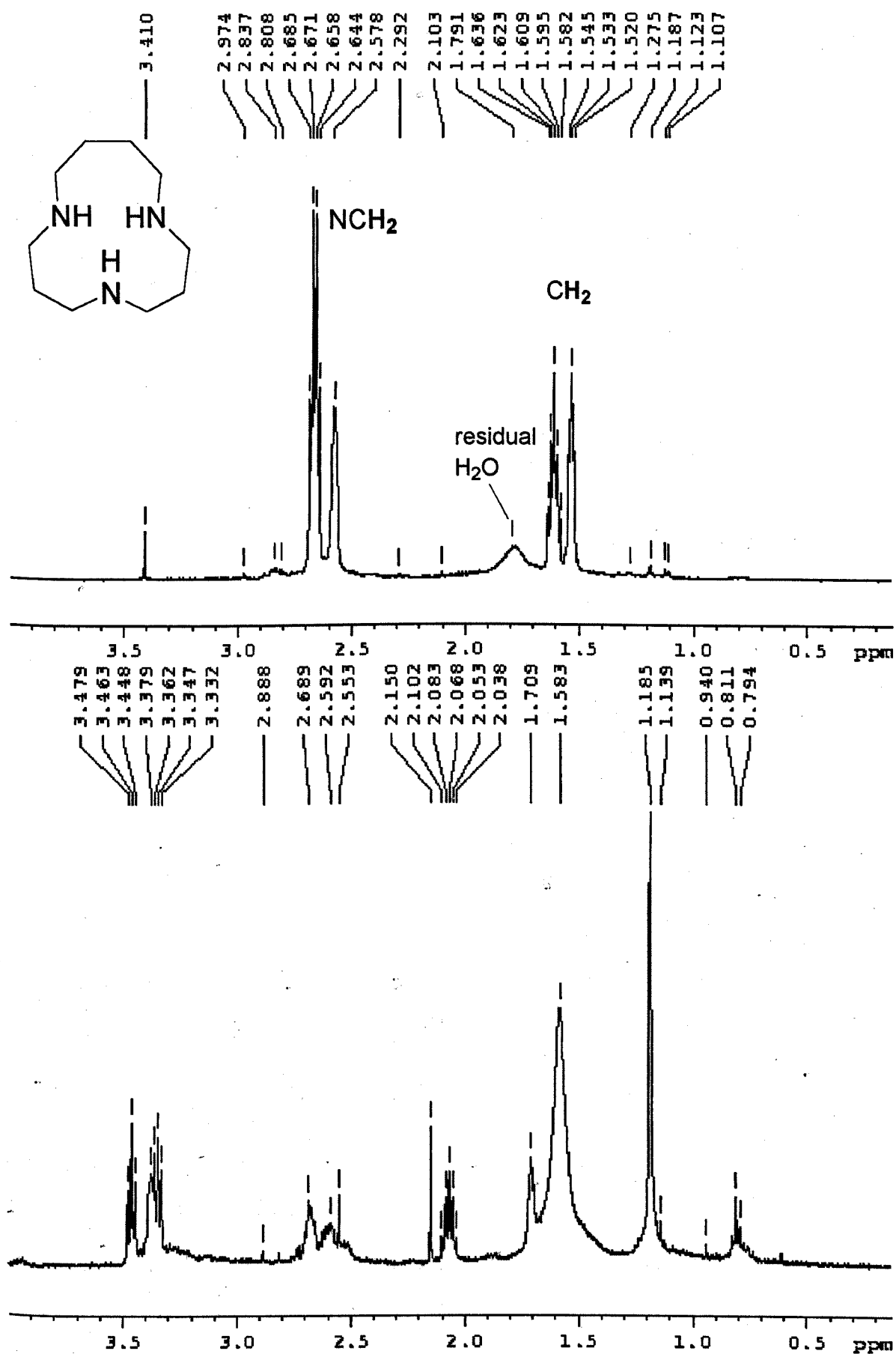
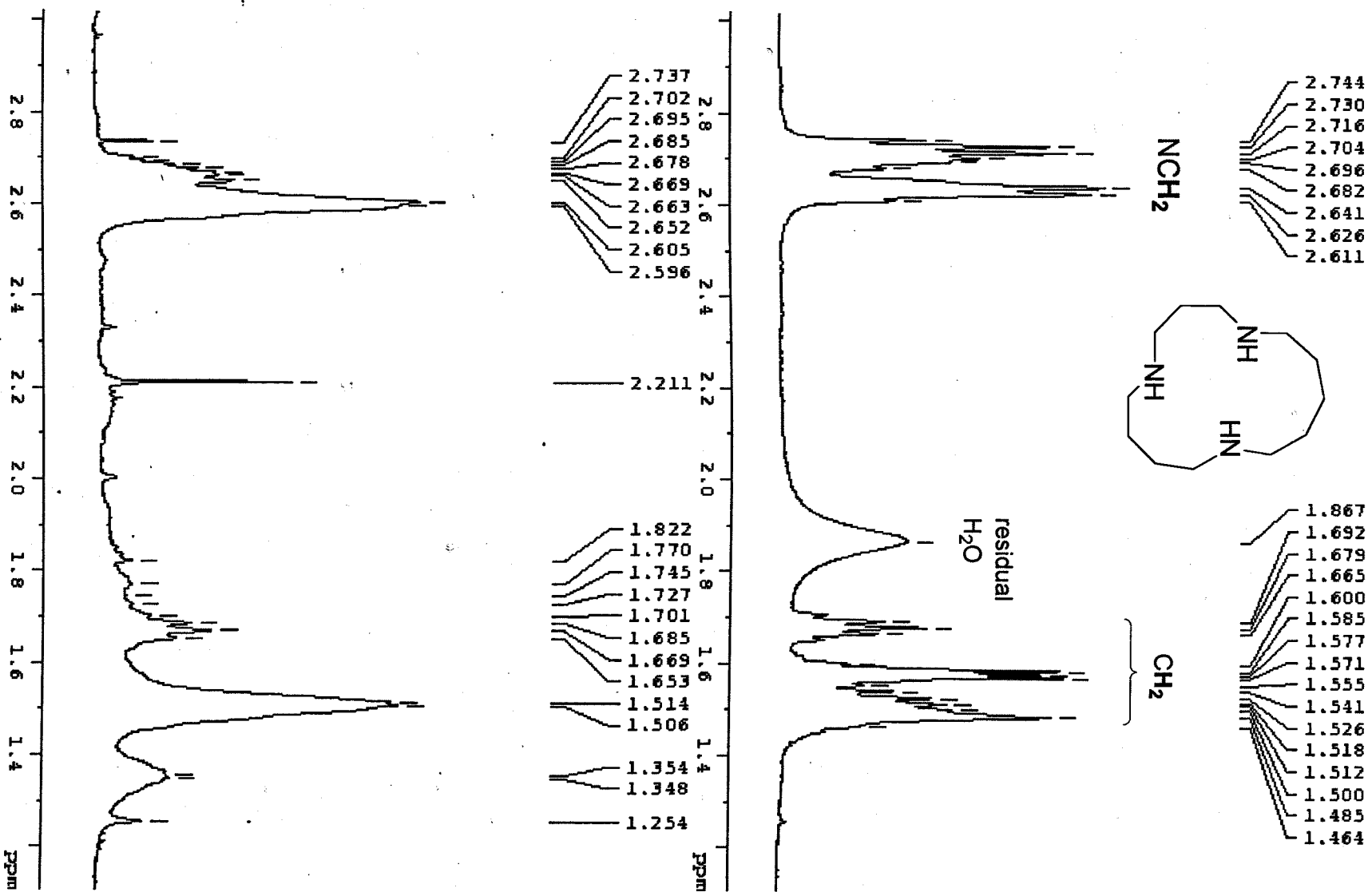
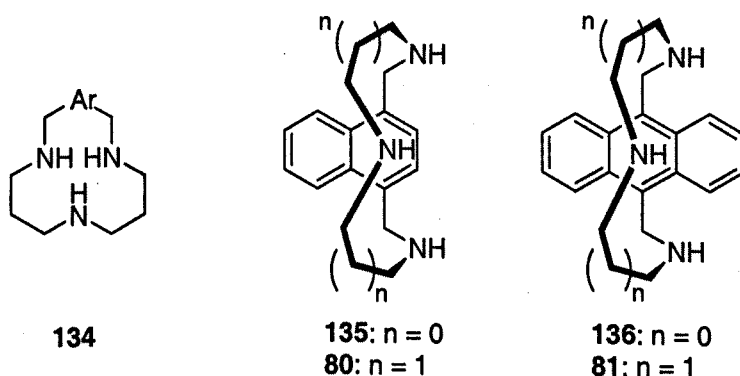


Fig. 2H. ^1H NMR spectra of 129, distilled (top) and residue from distillation (bottom)

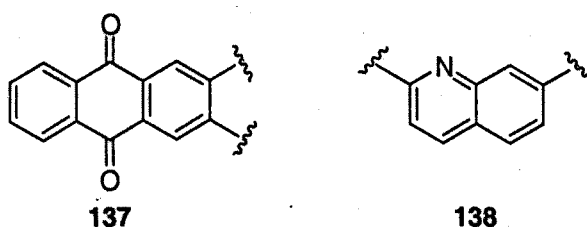


2.8. Synthesis of triazacyclophanes

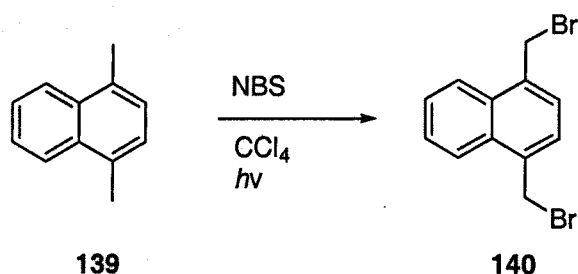
As a secondary synthetic goal, it was desirable to demonstrate the utility of the SES-group for synthesising macrocycles with sensitive functionality. Cyclophanes (e.g. general structure **134**) were good candidates for this, since their benzyl linkages are more susceptible to hydrolysis under the harsh conditions usually employed in the Richman-Atkins synthesis. Indeed, Hoyer *et al.*¹⁵¹ showed that the SES deprotection was mild enough for the synthesis of the (naphthaleno)phanes **135** and **80** and the (anthraceno)phanes **136** and **81**.



Macrocycles with anthraquinone (**137**) and quinoline (**138**) linkers were chosen as targets, as their cyclophanes have not been reported previously. The naphthalene linker was also chosen. All three of these groups have previously exhibited the ability to intercalate with DNA.¹⁹⁹ Mustards with intercalation ability show enhanced cytotoxicity,²⁰⁰ and the addition of aromatic functionality within the ring would increase the lipophilicity of the resulting macrocycles.

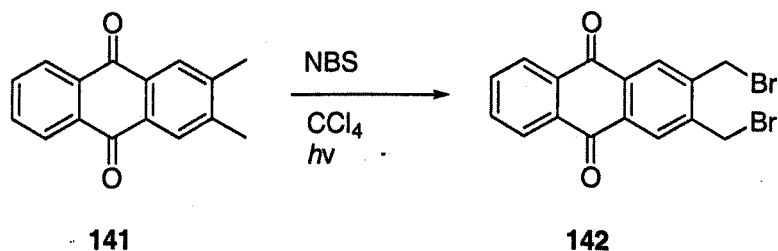


Scheme 2.8.1



Neither the bis(bromomethyl) nor the bis(hydroxymethyl) derivatives of naphthalene, anthraquinone and quinoline are commercially available. It was therefore necessary to synthesise the bis(bromomethyl) compounds from their dimethyl derivatives with *N*-bromosuccinimide in CCl₄.²⁰¹ The regiochemistry of the bromomethyl groups was restricted to the corresponding commercially available dimethyl compounds. 1,4-Bis(bromomethyl)naphthalene **140** was prepared in 53% yield and purified by crystallisation from MeCN/hexane (Scheme 2.8.1). Similarly, 2,3-dimethylantraquinone **141** was reacted to give **142** in 37% yield and was purified by recrystallisation from ethanol (Scheme 2.8.2).

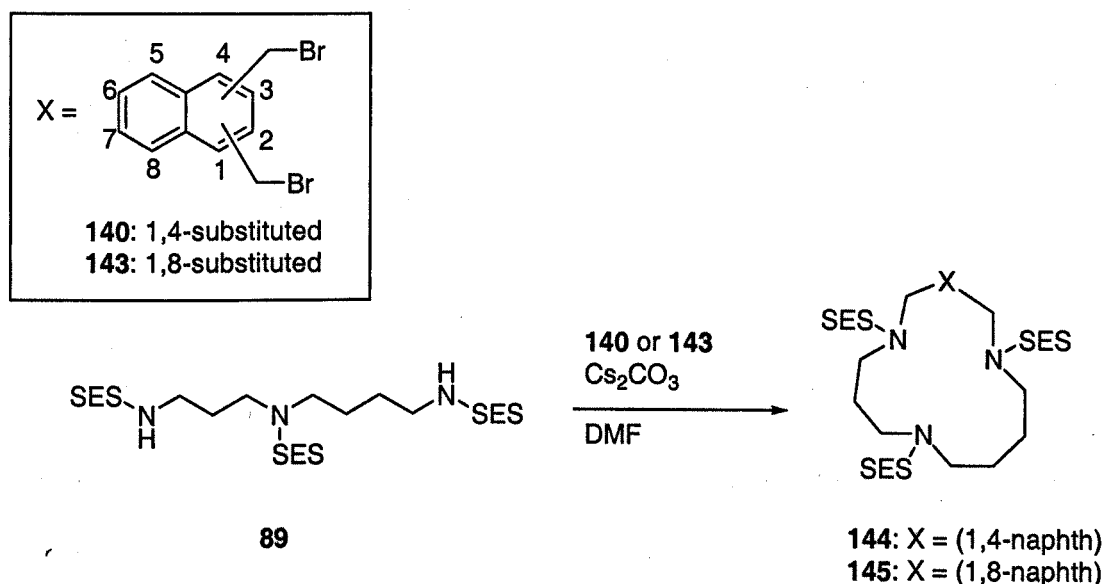
Scheme 2.8.2



Attempts to form the 2,7-bis(bromomethyl)quinoline in this way were unsuccessful due to over-bromination on the aromatic ring, even when only two equivalents of NBS were used. The resulting mixture did not contain a significant amount of the desired material and it could not be separated by column chromatography. Also unfortunately, the preliminary attempt at cyclisation of 2,3-bis(bromomethyl)anthraquinone with tris-SES-spermidine was unsuccessful. It produced a complex mixture that could not be separated by column chromatography. Similar halide substitution reactions with this compound are known,^{202, 203} so it may still be possible to synthesise the macrocycle.

The bis(bromomethyl)naphthalene compounds were cyclised with tris-SES-spermidine according to **Scheme 2.8.3** [the 1,8-bis(bromomethyl)naphthalene was formerly available from Aldrich but has since been discontinued].

Scheme 2.8.3



As would be expected, the yield for the cyclisation of the sterically-hindered ([1,8]naphthaleno)phane **145** was relatively low at only 18%. The deprotection proceeded in variable but sufficient yield (**146** [1,4] and **147** [1,8], respectively, 25% and 93%). However the compounds decompose upon distillation so they cannot be purified in the same way as the alkyltriazamacrocycles.

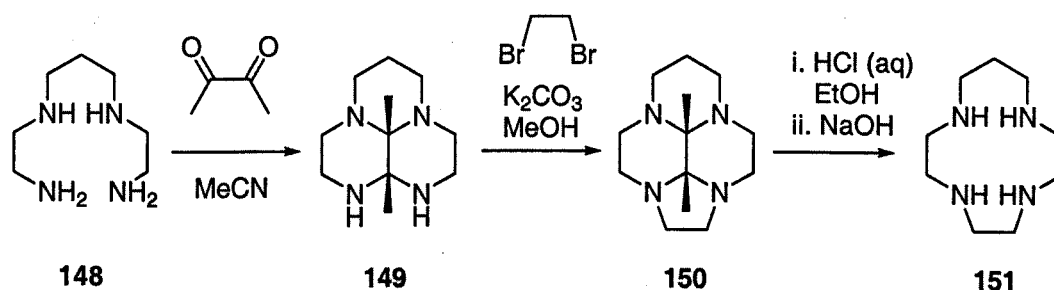
The synthesis of the (naphthaleno)phanes only marginally improves the demonstration of utility of the SES-group (with respect to the article by Hoye *et al.*¹⁵¹). It is likely, however, that further optimisation of the synthesis of additional bis(bromomethyl) aromatic compounds and also of the cyclisation of SES-amides with sensitive linkers is possible. Unfortunately, this strategy was taken up near the end of the project and it was not possible to carry it on.

2.9. Alternative routes to polyazamacrocycles

The use of SES-protecting groups in the modified Richman-Atkins synthesis of polyazamacrocycles is flexible and allows access to a range of compounds for drug

discovery. However, it is not very convenient or cost-efficient. Carbon-template methods were investigated in the interest of finding more efficient routes to polyazamacrocycles. The primary targets were the tetraazamacrocycles that were less efficiently obtained using the SES route. Unfortunately, not all of these attempts met with success.

Scheme 2.9.1

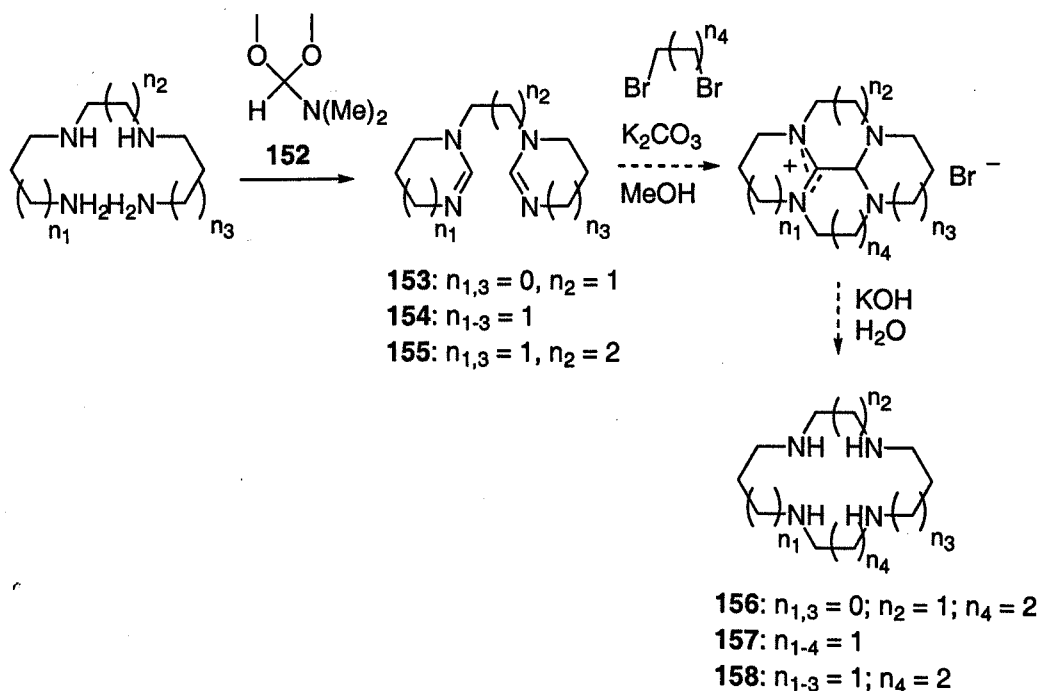


As described in section 1.4.1 of this thesis, the [2,2,2,3] tetraazamacrocycle **151** was synthesised from the aminal-templated linear tetraamine **149** (Scheme 2.9.1). The yields were not as high as reported in the literature (only 12% overall yield of the free base as opposed to 77% reported for the HCl salt¹⁴⁸) but they were sufficient to provide a useful amount of parent macrocycle for the synthesis of the nitrogen mustard derivatives. The low yield was probably due to low purity of the 1,4-butanedione—it may be necessary to distill it before use.

Cyclen (**36**) was prepared in only 8% overall yield from **153** (Scheme 2.9.3) according to the bis-imidazoline diamino-carbene method (Scheme 1.4.1.10, section 1.4.1).¹⁴⁹ Again, the yields were not as good as published (52% overall from triethylenetetraamine) but a sufficient amount of material was produced so the route was not optimised. It was desirable to apply this short method to the synthesis of cyclam and other tetraazamacrocycles from cheap starting amines, e.g. bis(3-aminopropyl)ethane-1,2-diamine (Scheme 2.9.3). Accordingly, **153** and two bis-tetrahydropyrimidines (**154** and **155**) were synthesised by condensing the tetraamines with *N,N*-dimethylformamide dimethyl acetal (**152**). Their cyclisation to tricyclic bromide salts (and subsequent hydrolysis to the free macrocycles **156-158**) was attempted. 1H and ^{13}C NMR spectroscopy of the intermediates, thought to be the crude bromide salts, looked promising. However, only the starting tetraamine was obtained after hydrolysis, with just trace amounts of the macrocycles produced

at best. It was possible that the diaminocarbene insertion was taking place, but that the conformations were unfavourable for the formation of the fourth ring. This route was not pursued further.

Scheme 2.9.3



2.10. Conclusions

Four key synthetic observations are reported in this work. First, we have found that the synthesis of SES-chloride is greatly simplified by using ten times as much DMF catalyst as reported in the literature, resulting in higher yields, and virtually no purification is required. Second, the scale up of macrocycle synthesis using SES-amides is not as simple as it appears in the previous publication. However, it can be used to produce a range of triazamacrocycles, including four novel compounds, for derivatisation and testing as *N*-mustard analogues. Third, although CsF causes problems for the purification and yield of the triazamacrocycles synthesised, it is the best reagent found so far for their deprotection and the products can be effectively purified using Kugelrohr distillation. Finally, linear triamines can also be built from SES-amides in high yield with little purification necessary. All of these results provide practical improvements on what has been reported in the literature. They also offered access to the series of compounds desired initially for

comparison of the cross-linking efficiency of macrocyclic *N*-mustards with different carbon bridge lengths. The successful synthesis of linear triamines and the range of novel triazamacrocycles described here, including the improved synthesis of SES-chloride, has been accepted for publication.²⁰⁴

Chapter 3

3. Synthesis of polyazamacrocyclic nitrogen mustard derivatives

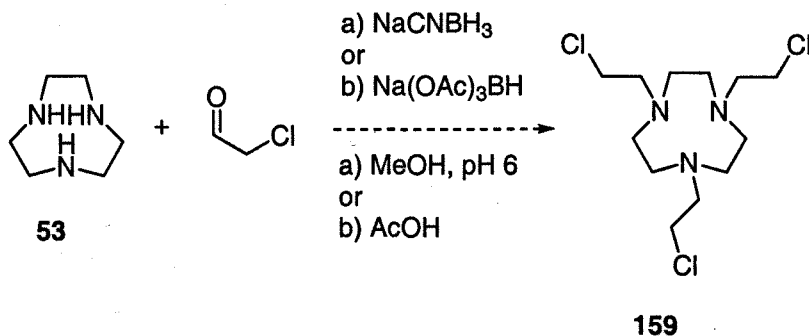
Initially, the formation of the mustard derivatives proved problematic for some of the triazamacrocycles, especially for compounds with unsymmetrical carbon bridge lengths. Attempts at hydroxyethylation in water and ethanol with excess ethylene oxide (as used previously in the group)¹²¹ resulted in polymerisation of the material to give poly(ethyleneglycol)-substituted amines. Using less than a large excess of ethylene oxide gave mixtures of material that was not fully alkylated. Two alternative routes to *N*-(2-chloroethyl) derivatives were investigated, but were not successful. During this investigation, the ethylene oxide alkylation was optimised.

3.1. Unsuccessful routes: reductive alkylation; chloroacetamides

3.1.1. Reductive alkylation

Using 1,4,7-triazacyclononane (ta₉n, **53**) as a model triazamacrocyclic, a one-step reductive alkylation process was investigated for the synthesis of poly-*N*-(2-chloroethyl) derivatives (**Scheme 3.1.1.1**). This type of reductive alkylation has been reported before with linear amines, using NaCNBH₃²⁰⁵ and Na(OAc)₃BH²⁰⁶ as reducing agents. The reaction was carried out using each borohydride. Using an excess of NaCNBH₃ as the reducing agent in methanol/aq. HCl at pH 6 for four days resulted in a mixture of products, as shown by TLC and ¹H NMR spectroscopy. Although this mixture did appear to contain some of the desired tri-substituted product **159**, too many amine impurities were present for purification *via* conversion into an acid salt. The material was too sensitive to aziridinium ion formation and hydrolysis to purify by column chromatography.

Scheme 3.1.1.1



Using $\text{Na(OAc)}_3\text{BH}$ in acetic acid also appeared to give some of the desired product. After 2.75 hours, ^1H NMR spectroscopy showed that most of the tacn was unreacted, but mono-, di- and tri-substituted material were also present. Repeating the reaction and monitoring it by TLC showed that the reaction was still incomplete after three days, but beyond that time side reactions took place that resulted in a complex mixture of products. ^1H NMR spectroscopy of the mixture showed it did not contain a significant amount of the desired material.

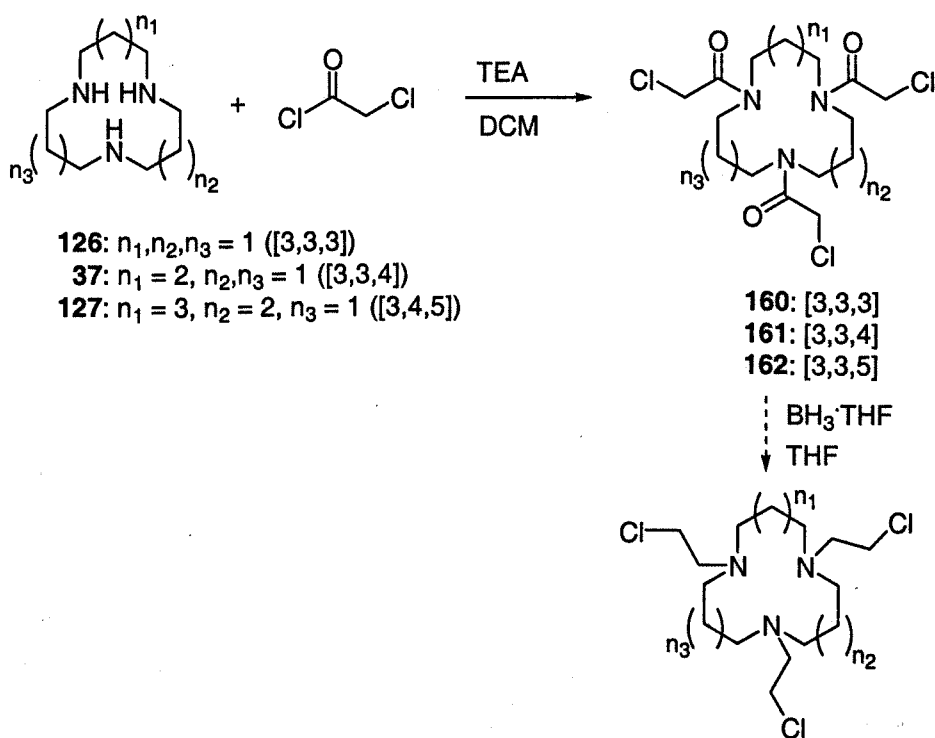
Given the protonation behaviour of triazamacrocycles such as **53**,²⁰⁷ it is probable in solutions of pH 4-6 (as in the above reactions), that the macrocycle is not fully protonated. This could allow the formation of aziridinium ions, resulting in alkylation of residual amines from starting material that was not fully reacted. The observation that the material initially does react to some degree, but over time produces a complex mixture of similar compounds supports this hypothesis. Given the relative simplicity of other routes, the reductive alkylation strategy was abandoned.

3.1.2. Chloroacetamides

Parker *et al.* reported the synthesis of *N*-(2-chloroethyl) macrocycles *via* acylation to their chloroacetamide intermediates.²⁰⁸ Three of the triazamacrocycles (**126**, **37** and **127**) were acylated with chloroacetyl chloride to give the chloroacetamides (Scheme 3.1.2.1), which could be purified by column chromatography. Parker *et al.* used $\text{BH}_3\cdot\text{S}(\text{Me})_2$ to reduce the chloroacetamides.²⁰⁸ Use of $\text{BH}_3\cdot\text{THF}$ gave a mixture of products, some of which appeared to be over-reduced to the *N*-ethyl derivatives. None of the desired *N*-(2-chloroethyl) material

could be isolated from the mixture. During this time, the ethylene oxide alkylation procedure was optimised so this route was also abandoned.

Scheme 3.1.2.1



3.2. Poly-*N*-(2-hydroxyethyl) derivatives

The parent macrocycles were converted into their poly-*N*-(2-hydroxyethyl) derivatives using ethylene oxide.²⁰⁹ The optimum reaction conditions were found to be stirring in ethanol overnight at less than 10 °C, with a large excess of ethylene oxide (Scheme 3.2.1). Details of compounds **163-183** and yields are given in Table 3.3.1. In this way, most of the triazamacrocycles could be successfully tri-substituted (examples of spectroscopic identification for **170** are given in Figs. 3A and 3B). The [3,3,4] and [3,3,5] macrocycles **37** and **127** proved to be particularly difficult to alkylate at all three nitrogens. However, the products of various degrees of alkylation could be separated by Kugelrohr distillation. In one case, the symmetrically di-substituted derivative of the [3,3,5] compound (**167**) was isolated in high purity from the distillations. It was converted into its mustard derivative and included in the testing to compare the effects of di-substituted vs. tri-substituted macrocyclic mustards. The [2,2,2,3] tetraazamacrocycle was also synthesised as

detailed in Section 2.9 and converted into its hydroxyethyl derivative (**184**) in 85% yield.

Fig. 3A. FAB Mass spectrum of **170**

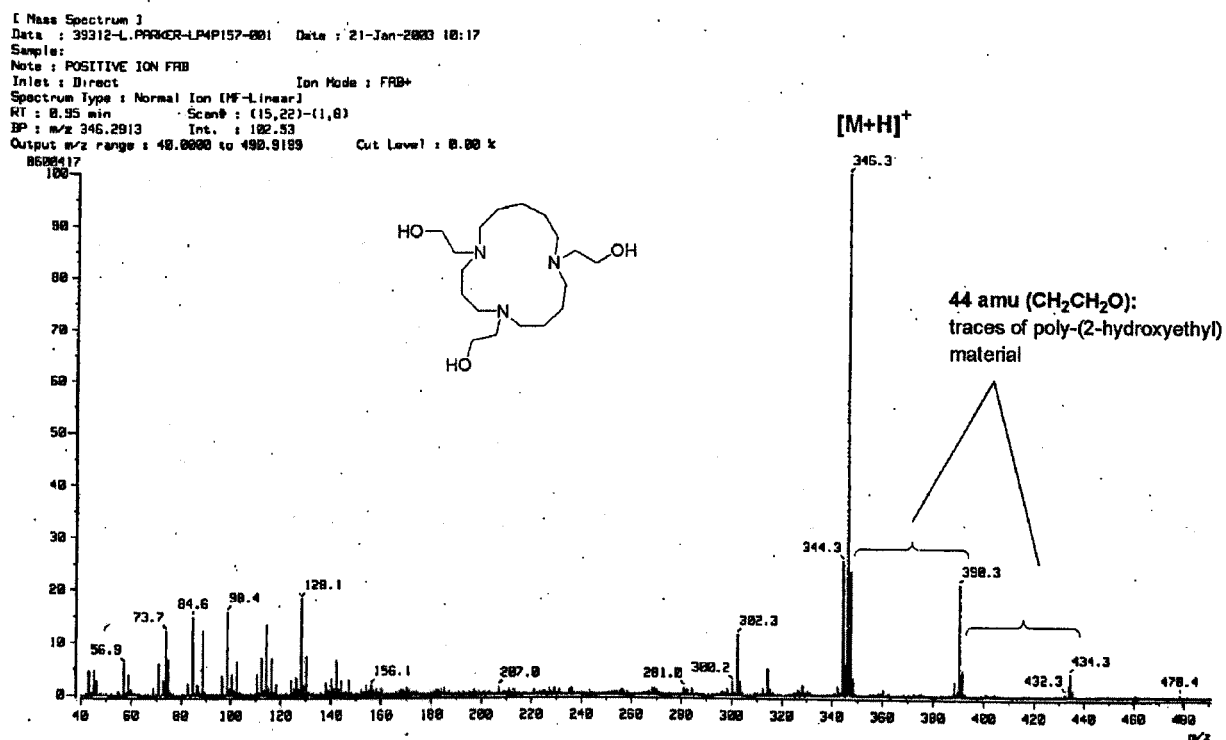
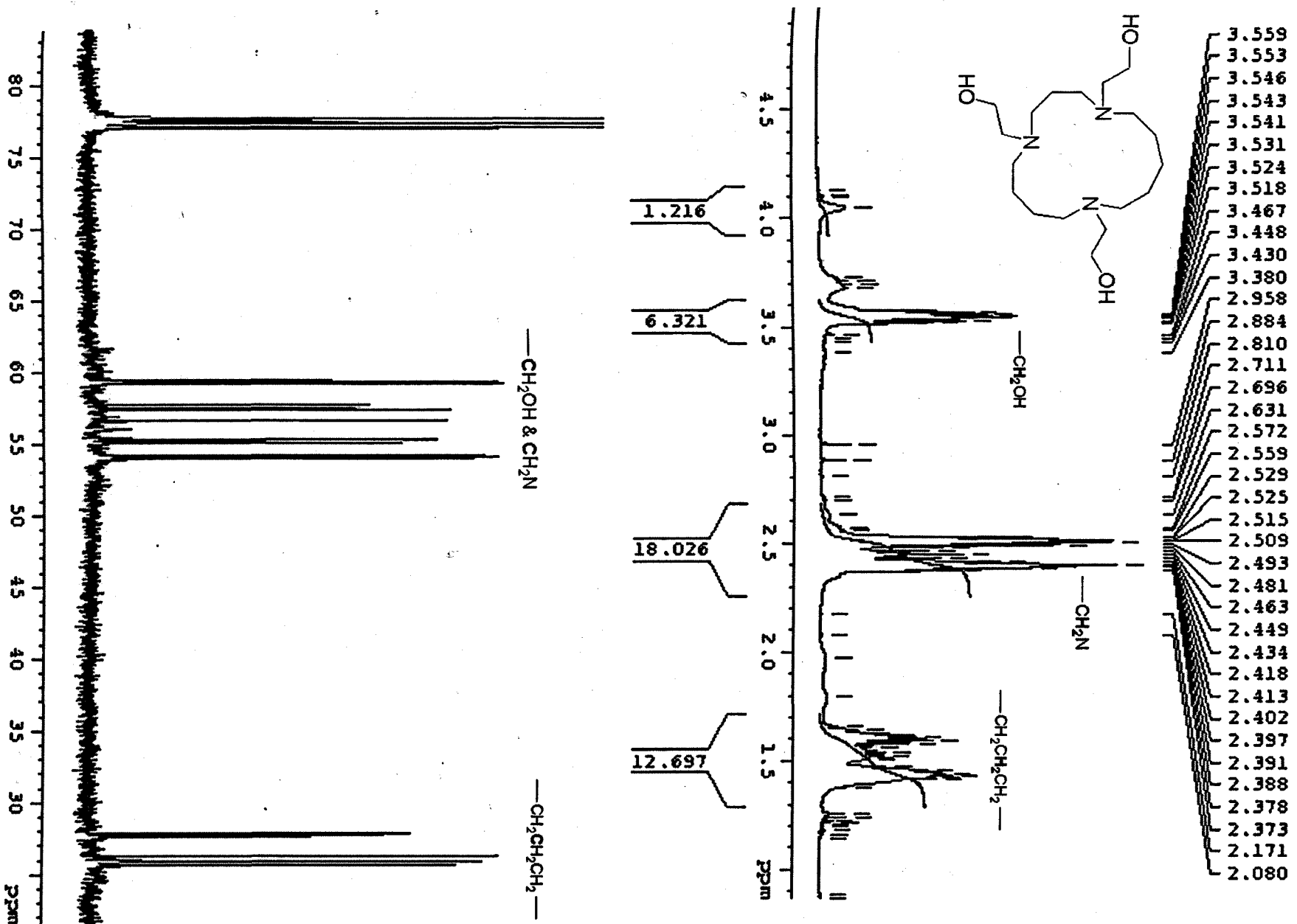
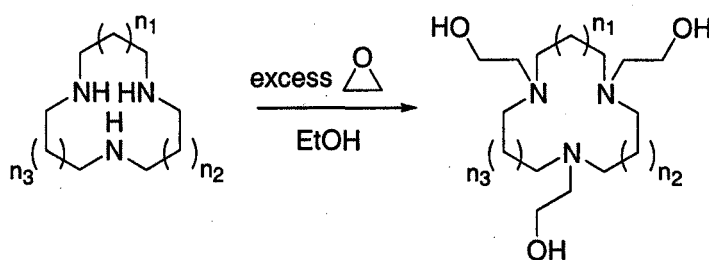


Fig. 3B. ^1H (top) and ^{13}C (bottom) NMR spectra for 170 (calibrated to CHCl_3)



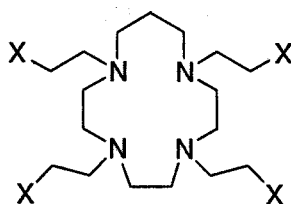
Scheme 3.2.1



3.3. Macrocyclic nitrogen mustard derivatives

The mustard derivatives were formed by heating the poly-*N*-(2-hydroxyethyl) compounds in thionyl chloride overnight (Scheme 3.3.1).²¹⁰ The material was usually isolated without the need for purification, but could be precipitated from methanol with diethyl ether if necessary. The peaks in the ^1H and ^{13}C NMR spectra for these hydrochloride salts were usually broad and sometimes unclear, but the evidence for the presence of each compound could be obtained by mass spectrometry. An example of the characterisation using ^1H NMR and mass spectrometry (for bis-substituted mustard 177) is given in Fig. 3C. Compound details and yields are given in Table 3.3.1.

The macrocyclic nitrogen mustards were tested for their ability to cross-link DNA and for their cytotoxicity against the human chronic myeloid leukaemia cell line K562. The biological test procedures are discussed in Chapter 5. One additional tetraazamacrocyclic mustard was later prepared (185) in quantitative yield, but was not included in the first round of testing.



184: X = OH

185: X = Cl (2HCl salt)

Scheme 3.3.1

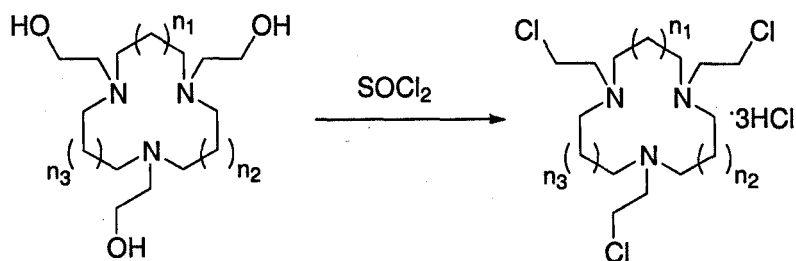


Table 3.3.1

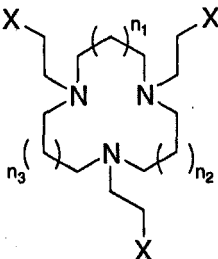
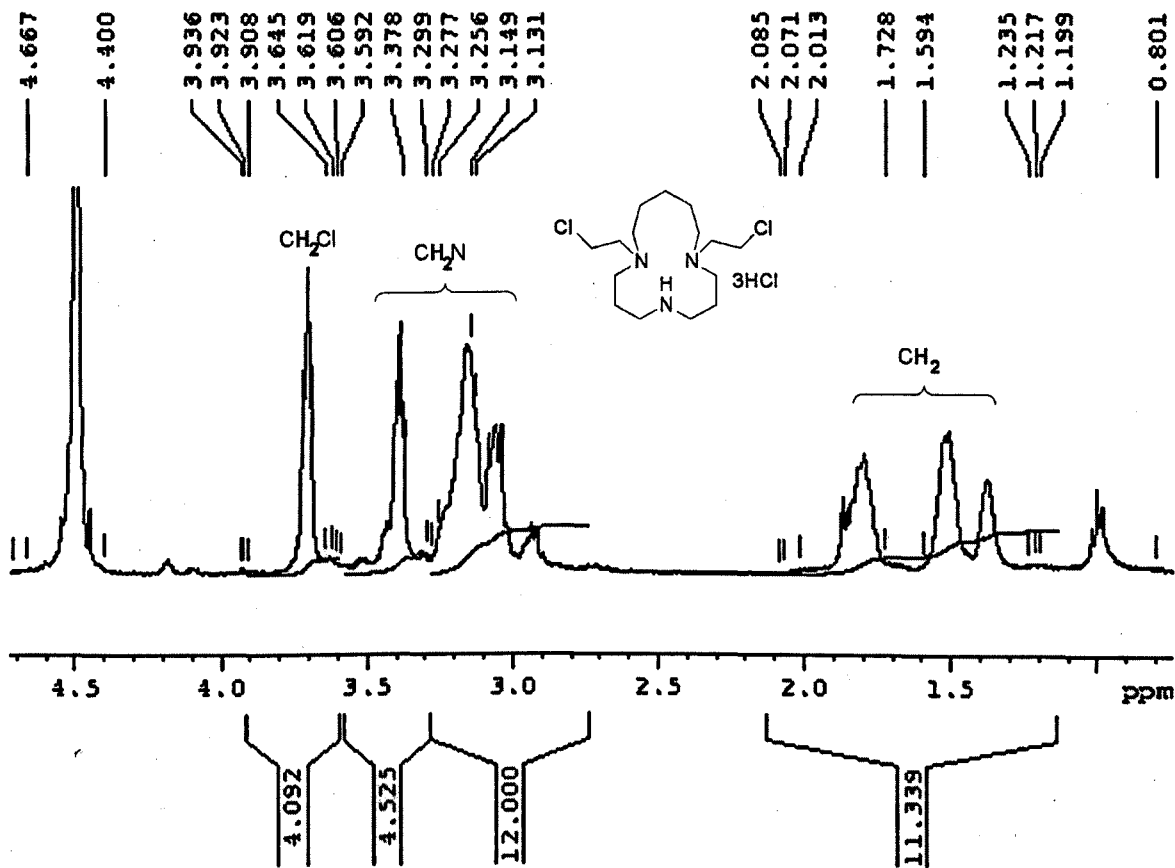
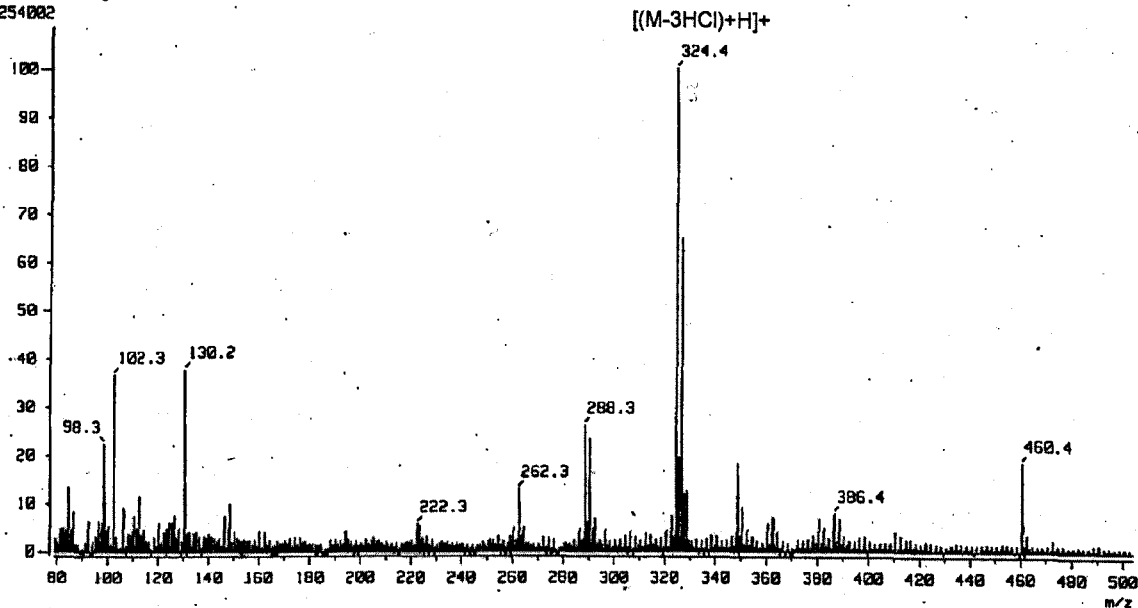
<div style="display: flex; align-items: center; justify-content: center;">  <div style="margin-left: 20px;"> 163-173: X = OH 174-183: X = Cl (HCl salt) </div> </div>			
n_1, n_2, n_3	ring size	yield X = OH (%)	yield X = Cl (%)
0,0,0	[2,2,2]	163: 85	174: 99
0,1,1	[2,3,3]	164: 85	n/a
1,1,1	[3,3,3]	165: 88	175: 61
1,1,2	[3,3,4]	166: 44	176: 89
1,1,3	[3,3,5]	(bis) 167: 13	(bis) 177: 99
1,1,3	[3,3,5]	(tris) 168: 57	(tris) 178: 93
1,2,2	[3,4,4]	169: 68	179: 85
1,2,3	[3,4,5]	170: 96	180: 99
3,3,1	[5,5,4]	171: 99	181: 99
4,4,1	[6,6,4]	172: 99	182: 99
2(1,1,2)	[2,2,4,2,2,4]	173: 74	183: 83

Fig. 3C. Characterisation of bis-substituted [3,3,5] mustard 177. ¹H NMR spectrum (top) and FAB mass spectrum (bottom)



[Mass Spectrum]
Data : 007
Sample: L.Parker 149
Note : #
Inlet : Direct
Spectrum Type : Regular [MF-Linear]
RT : 2.90 min
Scan# : (15,17)-(2,4)
BP : m/z 324.3718
Int. : 739.34
Output m/z range : 78.8271 to 503.7598
Cut Level : 0.00 %
25254002

Date : 27-Feb-1993 09:19
Ion Mode : FRB+
Temp : 8.0 deg.C

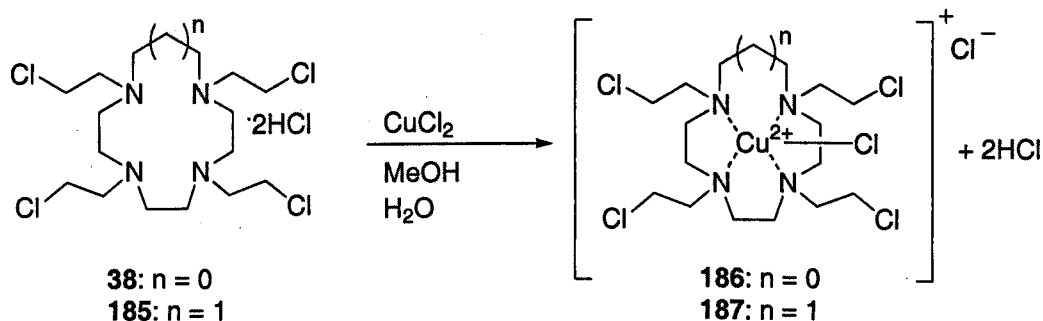


Chapter 4

4. Coordination chemistry of novel polyazamacrocycles

4.1. Synthesis of metal complexes

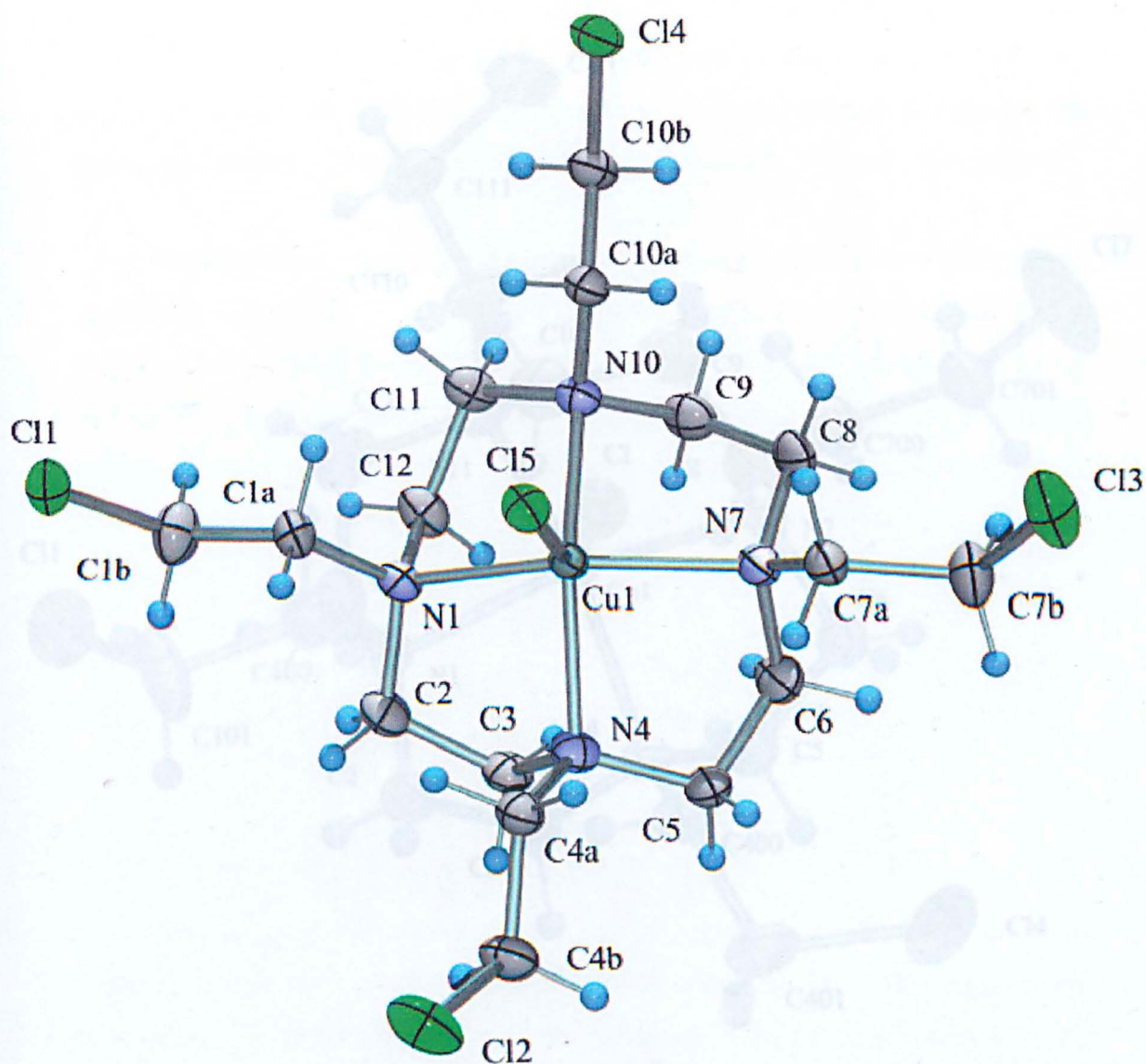
Scheme 4.1.1



The formation of metal complexes of the poly-*N*-(2-chloroethyl) ligands was not always simple, because the typical way to complex an azamacrocycle (from its halide salt) with a metal is to neutralise the salt first then add a solution of a desired metal salt.⁹³⁻⁹⁶ The neutralisation of the mustard ligands is complicated by how easily they can be hydrolysed in water. At neutral or basic pH, aziridinium ion formation and hydrolysis of the 2-chloroethyl functionality causes decomposition of the ligand. Fortunately, the Cu(II) complexes of **38** and **185** (**186** and **187**) could be formed from their hydrochloride salts (Scheme 4.1.1) and precipitated in acceptable yield from the resulting solution. Yields are given in Table 4.1.1 (eight pages on).

186 was crystallised as its tetrafluoroborate salt and analysed by X-ray crystallography. All X-ray crystallography was performed by Louis Farrugia in this department. The crystal structure is illustrated in Fig. 4A. The complex exhibits bowl-shaped conformation and the geometry around the Cu(II) ion is square-pyramidal with the Cu(II) sitting well out of the plane of the four coordinating nitrogen atoms.

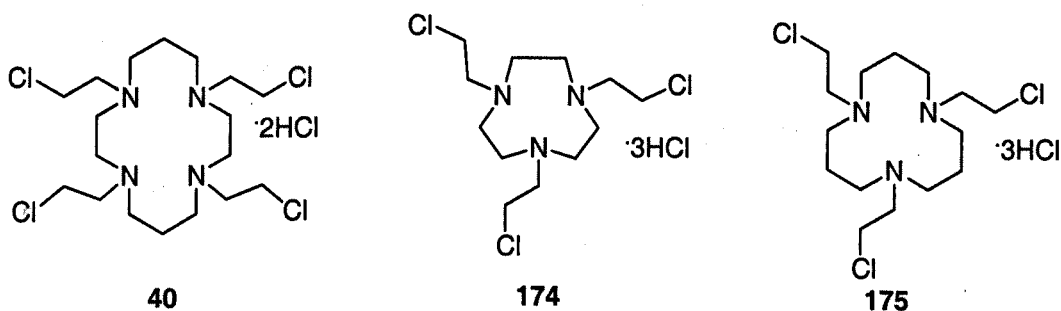
Fig. 4A. X-ray crystal structure of 186.



Bond lengths (Å)		Bond angles (°)	
Cu1-N1	2.099	N1-Cu1-N4	85.11
Cu1-N4	2.060	N1-Cu1-N7	146.0
Cu1-N7	2.062	N4-Cu1-N7	86.51
Cu1-N10	2.065	N4-Cu1-N10	148.95
Cu1-Cl5	2.361(8)	N7-Cu1-N10	87.03
		N10-Cu1-N1	85.33

The complex of homocyclen *N*-mustard [2,2,2,3] (**187**) was crystallised as its hexafluorophosphate salt. The crystal structure and important bond lengths and angles are given in **Fig. 4B**. The Cu(II) ion adopts a similar geometry to that for **186** (square pyramidal), however this complex has Z- (or saddle-) shaped conformation.

Unfortunately, easy complexation from the acid salt was not the case for ligands **40**, **174** or **175**. Initial attempts to complex the hydrochloride salt of **40** with Cu(II) without neutralisation resulted in no complex formation. Neutralising the salt with either 1 M NaOH or triethylamine resulted in swift hydrolytic decomposition and complexation of the resulting 2-hydroxyethyl compound **188** (as indicated by the crystal structure shown in **Fig. 4C** and UV-Vis spectroscopic analysis).



The λ_{max} of the tetra-*N*-(2-hydroxyethyl) compound **188** is significantly higher than that for the tetra-*N*-(2-chloroethyl) complex **190**. This allowed the identification of **188** (using UV-Vis spectroscopy) as the primary complex in the solution from which it crystallised. This was supported by X-ray crystallographic analysis. The crystal structure shows that the 2-chloroethyl substituents have been hydrolysed to 2-hydroxyethyl, either before or after complexation. This phenomenon is discussed further in section 4.2. Here the Cu(II) sits only slightly out of the plane of the four coordinating nitrogen atoms and one of the oxygens coordinates as well to give the complex overall square pyramidal geometry, with the Cl1 atom participating in a non-bonding interaction (**Fig. 4C**).

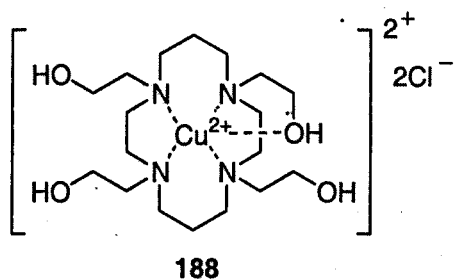
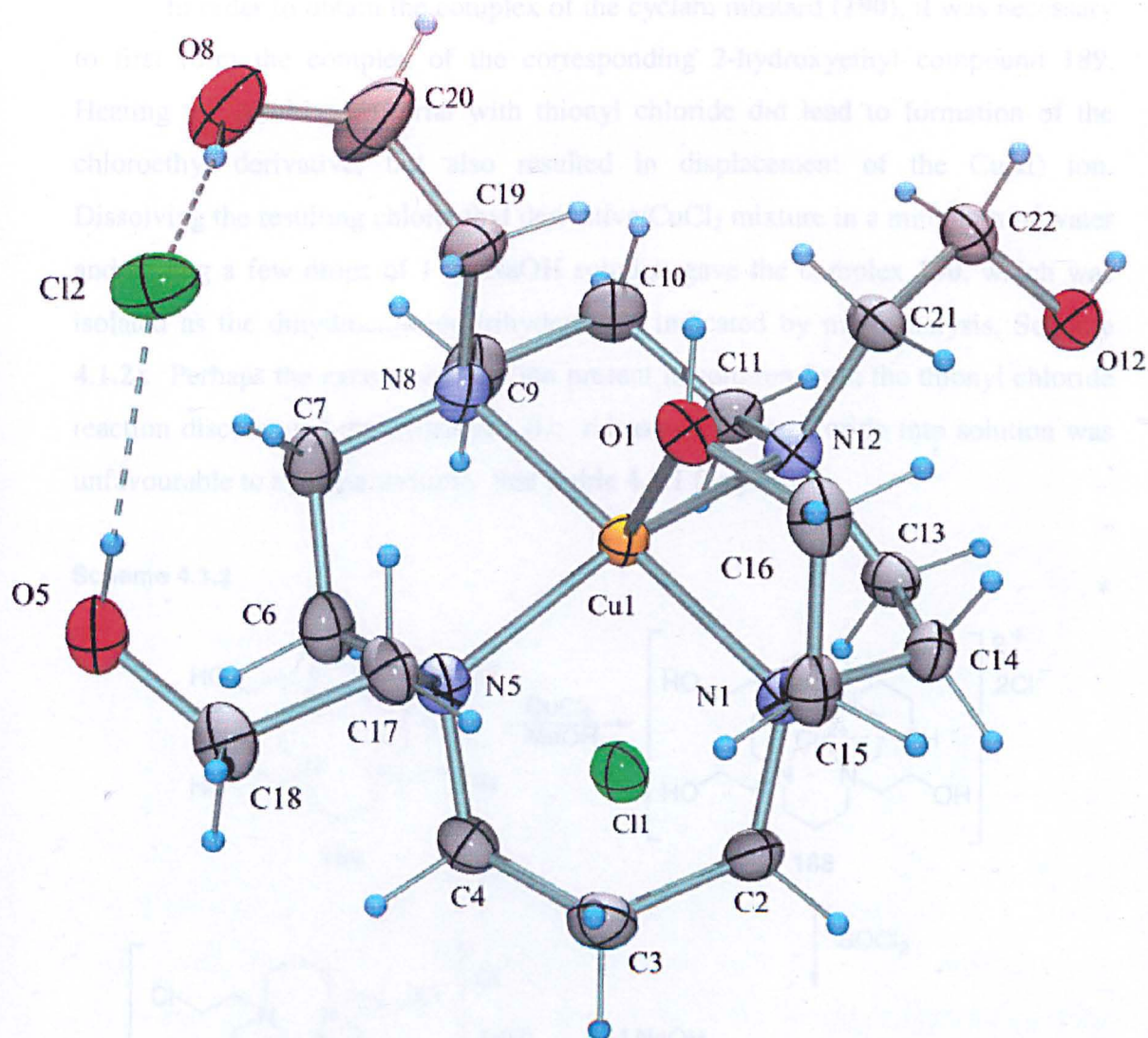


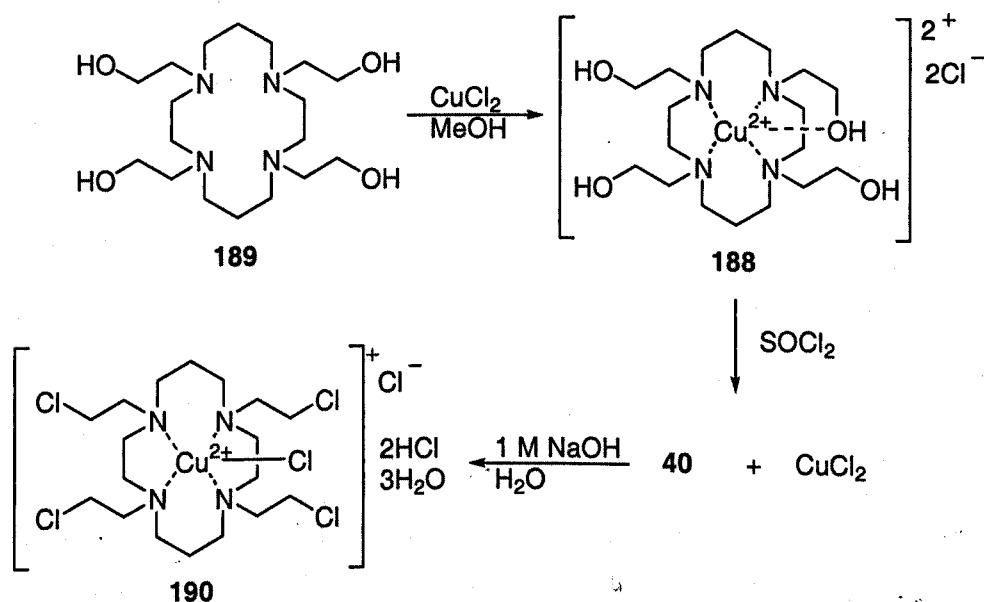
Fig. 4C. X-ray structure of 188.



Bond lengths (Å)		Bond angles (°)	
Cu1-N1	2.070	N1-Cu1-N5	93.83
Cu1-N5	2.080	N1-Cu1-N8	177.11
Cu1-N8	2.086	N5-Cu1-N8	84.68
Cu1-N12	2.102	N5-Cu1-N12	157.6
Cu1-O1	2.275	N8-Cu1-N12	96.68
Cu1-Cl1	4.006	N12-Cu1-N1	85.65

In order to obtain the complex of the cyclam mustard (**190**), it was necessary to first form the complex of the corresponding 2-hydroxyethyl compound **189**. Heating the resulting material with thionyl chloride did lead to formation of the chloroethyl derivative, but also resulted in displacement of the Cu(II) ion. Dissolving the resulting chloroethyl derivative/CuCl₂ mixture in a minimum of water and adding a few drops of 1 M NaOH solution gave the complex **190**, which was isolated as the dihydrochloride trihydrate (as indicated by microanalysis, **Scheme 4.1.2**). Perhaps the excess chloride ion present in solution from the thionyl chloride reaction discouraged the hydrolysis (i.e. release of more chloride into solution was unfavourable to the equilibrium). See **Table 4.1.1** for yield.

Scheme 4.1.2

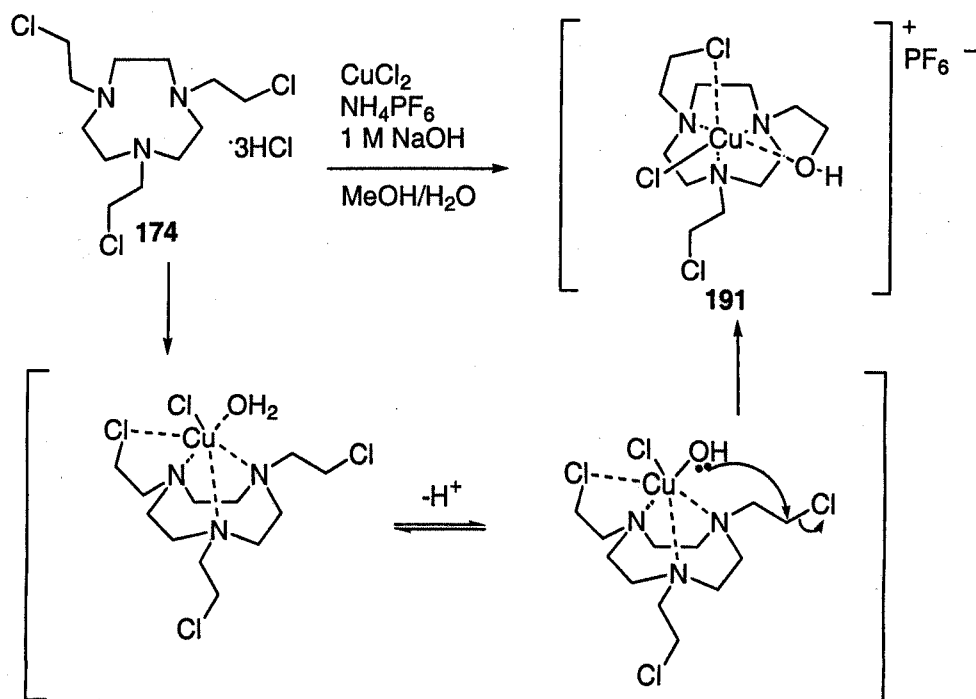


Similarly, the ligands **174** and **175** would not form complexes from their hydrochloride salts. Addition of 1 M NaOH resulted in some complex formation, as apparent from the color change of the solution. However, the complexation of **174** resulted in the mono-*N*-(2-hydroxyethyl) compound **191** [as shown by isolation and X-ray crystallography of the PF₆⁻ salt (**Fig. 4D**)]. A proposed mechanism for this selective hydrolysis is shown in **Scheme 4.1.3**.

The complex **191** adopts distorted octahedral geometry, as evidenced by the elongated bonds for Cu1-Cl11 and Cu1-N4, and the distortion from 90° of the angles

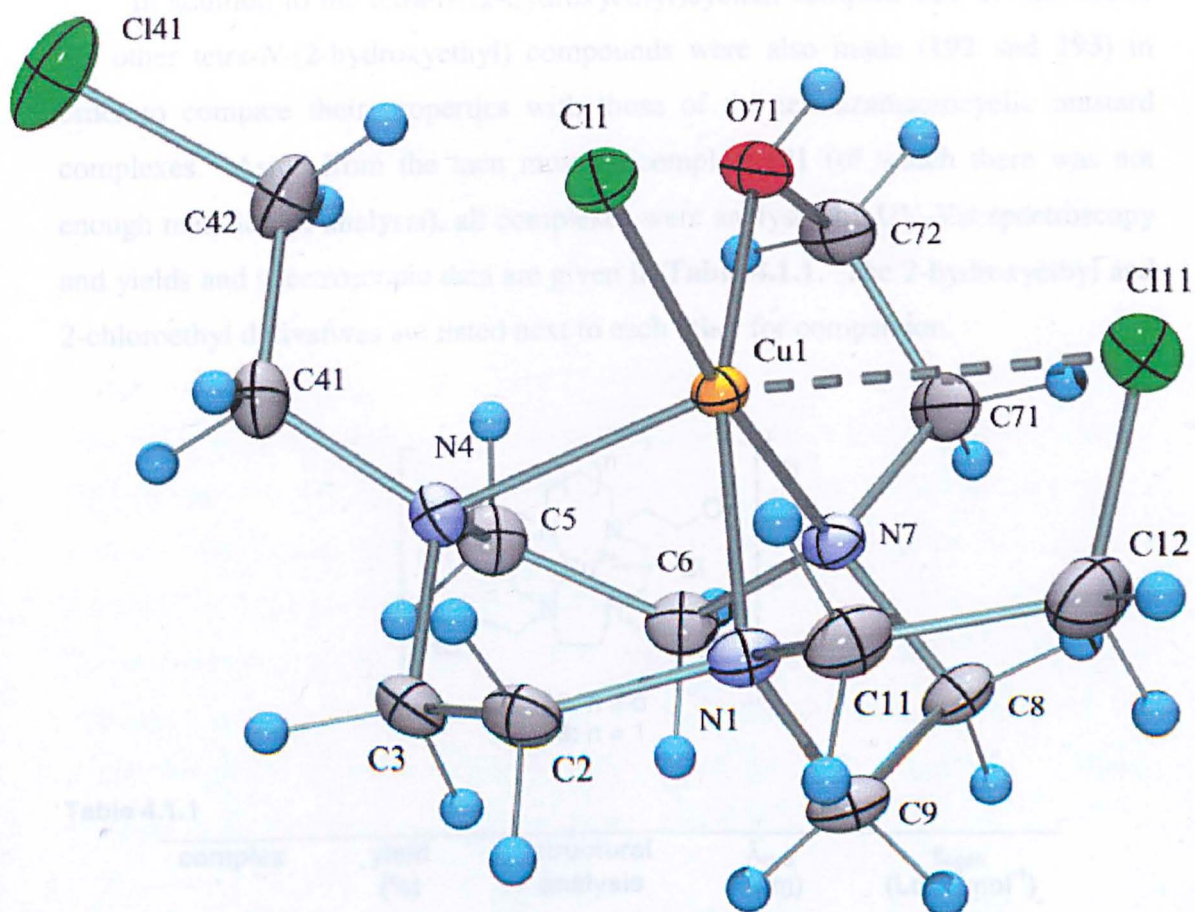
between Cu1 and the coordinating atoms around the central plane (N1, N7, O71 and Cl1, Fig. 4D).

Scheme 4.1.3



Free coordination sites at the metal centre in the complexation of **174** with Cu(II) could allow for the coordination of a water molecule. The Cu(II) acts as a Lewis-acid, allowing the water to be deprotonated at neutral pH and activating it for intramolecular hydrolytic attack on a nearby 2-chloroethyl substituent on N7 (Fig 4D). The resulting 2-hydroxyethyl substituent then occupies the coordination site, preventing further water complexation and hydrolysis. This type of Lewis-acid activation in macrocyclic metal complexes is well known for Cu(II)^{183, 184} and also for Zn(II),¹⁷⁸ and may be an issue for most tridentate complexes of triazamacrocyclic mustards (e.g. also for **175**). Although this is an interesting outcome, it may have an adverse effect on the potency of the parent mustard compound. Also, the yields were unsatisfactory (Table 4.1.1)—in fact no significant amount of the complex of **175** could be isolated or crystallised for X-ray analysis. The complexation of triazamacrocycles is known to be more difficult than for tetraazamacrocycles, as their formation/stability constants are generally lower, which could account for the problem of low yields. Attempts to form the complex of **175** from the 2-hydroxyethyl analogue in a similar manner to Scheme 4.1.2 were unsuccessful.

Fig. 4D. X-ray crystal structure of 191.



Bond lengths (Å)		Bond angles (°)	
Cu1-N1	2.048(7)	N1-Cu1-N4	85.22
Cu1-N4	2.249(0)	N1-Cu1-N7	85.38
Cu1-N7	2.030(5)	N4-Cu1-N7	84.42
Cu1-O(7)1	2.029(9)	N1-Cu1-Cl1	98.06
Cu1-Cl1	2.268(3)	N1-Cu1-O(7)1	166.32
Cu1-Cl11	3.086(1)	N4-Cu1-Cl1	99.92
		N4-Cu1-O(7)1	101.62
		N7-Cu1-Cl1	174.64
		N7-Cu1-O(7)1	83.53

In addition to the tetra-*N*-(2-hydroxyethyl)cyclam complex **188**, complexes of the other tetra-*N*-(2-hydroxyethyl) compounds were also made (**192** and **193**) in order to compare their properties with those of the tetraazamacrocyclic mustard complexes. Aside from the tacn mustard complex **191** (of which there was not enough material for analysis), all complexes were analysed by UV-Vis spectroscopy and yields and spectroscopic data are given in **Table 4.1.1**. The 2-hydroxyethyl and 2-chloroethyl derivatives are listed next to each other for comparison.

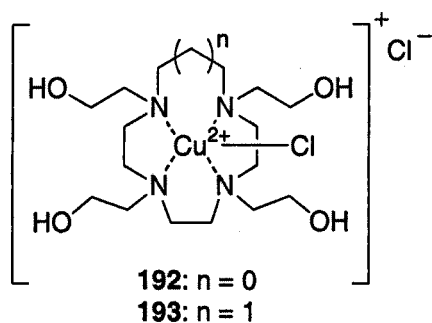


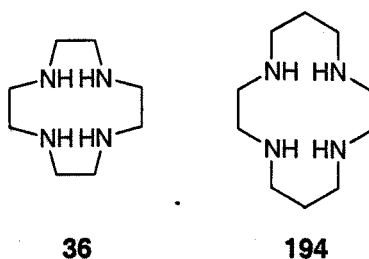
Table 4.1.1

complex	yield (%)	structural analysis	λ_{max} (nm)	ϵ_{coeff} ($\text{Lcm}^{-1}\text{mol}^{-1}$)
192	>99		607	309
186	75	[1:1]	622	515
193	>99		588	315
187	22	[1:1]	599	315
188	>99	[1:1]	636	n.d.
190	23		590	817
191	10	[1:1]	n.d.	n.d.

4.2. Stability of polyazamacrocyclic metal complexes

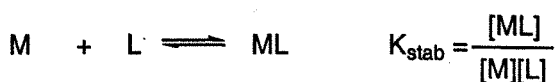
4.2.1. Discussion of stability

Although they are different qualities, the selectivity of a ligand for various metal ions and the stability of the resulting complex can often be correlated.⁹⁷ The 'size-match selectivity' idea is the most popularly accepted theory for stability and selectivity in macrocycle-metal complexation. It holds that macrocycles will favourably bind metal ions whose atomic radii best match their cavity size. Despite the widespread use of this theory, most of the evidence suggests that chelate ring size is much more important in predicting the relative thermodynamic stabilities between macrocycles with different carbon bridge lengths and metal ions of various sizes. The conformation adopted by the ligand (determined by the chelate rings) plays an important role in the preorganisation of the ligand for complexation and can contribute to the thermodynamic stability. The denticity (number of chelating moieties in the molecule) vs. metal ion size is also a factor.



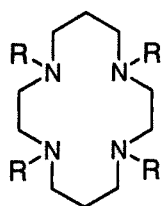
Accordingly, (and as suggested by molecular mechanics calculations),⁹⁸ it is expected that macrocycles complexing to form five-membered chelate rings are less strained when complexing with (and thus 'prefer') bigger metal ions. Macrocycles complexing to form six-membered chelate rings are less strained when complexing with smaller metal ions. Thus, cyclam (**194**), with its two six-membered and two five-membered chelate rings, has a higher stability constant (defined by K_{stab} according to Eq. 4.2.1.1) with Cu(II) than that for cyclen (**36**) which has four five-membered chelate rings (Table 4.2.1.1).

Eq. 4.2.1.1

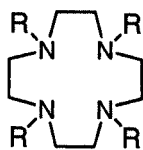


The addition of donor pendant arms such as *N*-(2-hydroxyethyl) to cyclam and cyclen decreases the stabilities of their complexes. The decrease is most pronounced with smaller metal ions, especially Cu(II) (see Table 4.2.1.1). A number of factors contribute to this change. The primary contribution is probably from the higher strain created by the increased steric bulk, as a similar effect is seen with the tetra-*N*-methyl substituted derivatives. It is interesting to note, though, that the decrease in stability for cyclen is less pronounced than for cyclam. Indeed, as the size of the *N*-alkyl group increases, the substituted cyclen Cu(II) complex is eventually more stable than that of the corresponding cyclam complex. This is probably due to the tetrahedral nitrogens being preorganised for coordination to a small ion such as Cu(II).

Table 4.2.1.1⁹⁸



194, 195, 189



36, 196, 197

parent backbone	R = H	R = Me	R = CH ₂ CH ₂ OH
Cyclam[Cu(II)] (log K)	194 (28.09)	195 (18.3)	189 (15.7)
Cyclen[Cu(II)] (log K)	36 (24.8)	196 (18.37)	197 (~19.5)

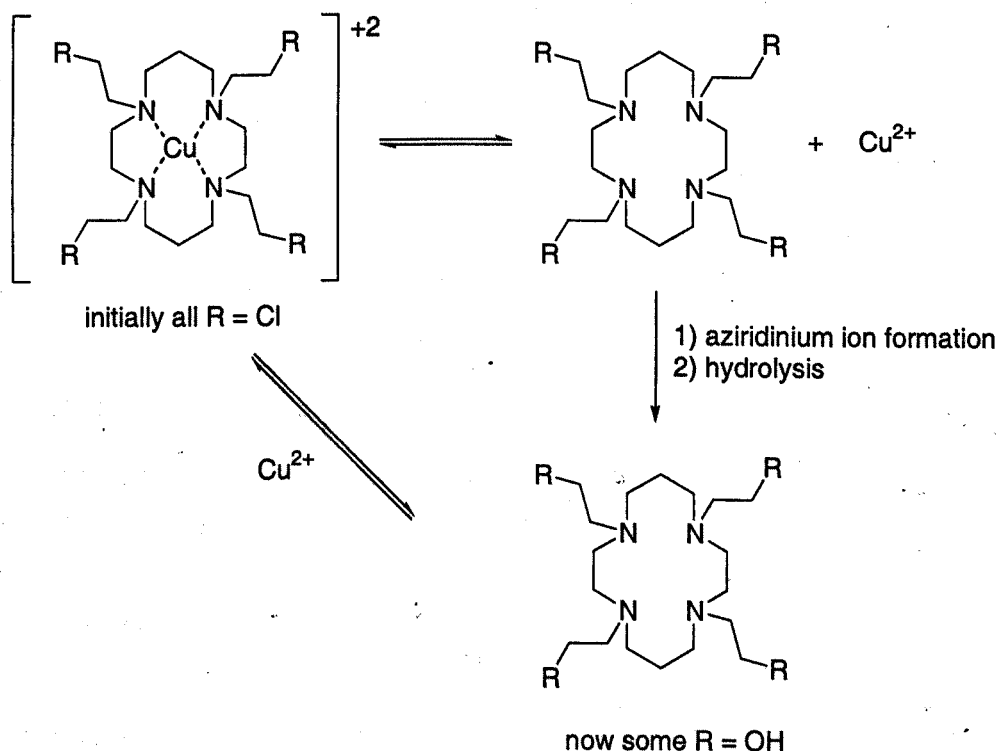
There are a number of reasons why it was not possible to determine stability constants for the ligands reported here. In order to be relevant for comparison to existing data, the stability constants for metal complexes need to be determined under specific conditions with specialised titration equipment, as detailed by Martell and Motekaitis.⁹⁹ However, the facile hydrolysis of these ligands in neutral or basic solution makes it nearly impossible to obtain meaningful titration data. Other methods using UV-Vis spectroscopy, such as competition studies, are unsuitable because they require the protonation constants for the ligand to be known.²¹¹ Protonation constants are also very difficult to determine for the nitrogen mustard ligands, because the ligands decompose under neutral or basic conditions. However,

the stabilities of the novel complexes in relation to each other could be qualitatively estimated from UV-Vis decomposition and cyclic voltammetry data.

4.2.2. 'Aqueous stability' of mustard macrocycle complexes

The mustard ligands are highly susceptible to hydrolysis and decomposition at neutral pH. When complexed with a metal ion, they should only hydrolyse to a significant extent if there is a sufficient concentration of the free ligand present at equilibrium (Scheme 4.2.2.1). Complexes with high thermodynamic stability will only have low concentrations of free ligand and should not decompose in aqueous solution. Complexes with low thermodynamic stability will decompose to their 2-hydroxyethyl analogues.

Scheme 4.2.2.1



In Scheme 4.2.2.1, initially R = Cl. If the complex is less stable, a cycle begins whereby the 2-chloroethyl substituents are successively hydrolysed to R = OH. This may continue until R = OH for all substituents, or it may stop at some point if the intermediate complex is sufficiently stable. The λ_{\max} values for Cu(II) complexes of the 2-hydroxyethyl substituted ligands are sufficiently different from

those of the tetra-*N*-(2-chloroethyl) analogues. Thus the 'decomposition' of each mustard complex can be monitored by UV-Vis spectroscopy, giving qualitative information about the stability of that complex in aqueous solution.

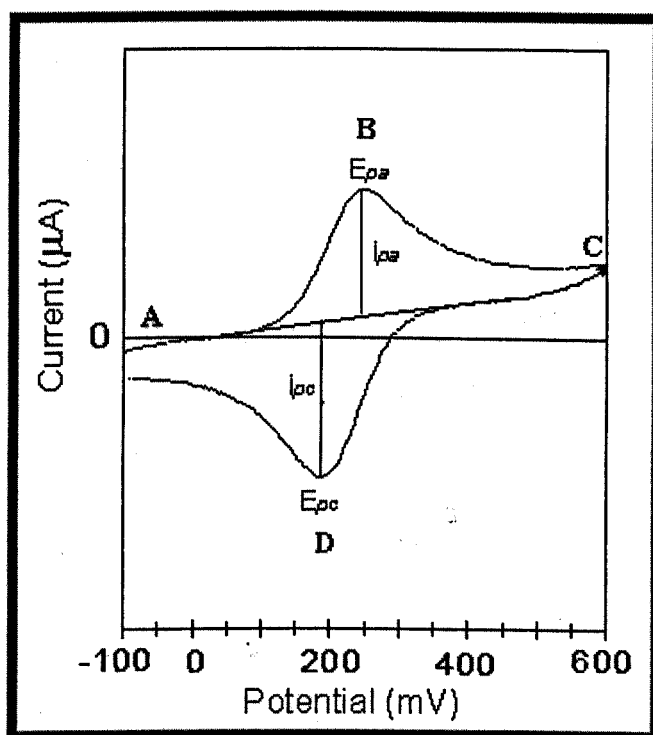
4.2.3. Electrochemistry and complex stability

The electrochemistry of metal complexes in solution can be studied using a variety of techniques, including polarography, cyclic, square wave and differential pulse voltammetry.²¹² Although these techniques can provide valuable information on the viability of biological electron transfer, factors such as metabolism, membrane transport and tissue pH can have unpredictable effects on actual redox behaviour *in vivo*. Therefore it is not possible to correlate the behaviour observed by electroanalytical techniques directly with *in vivo* bioreduction or oxidation. However, reduction potentials measured through these techniques can provide benchmark estimates for the feasibility of bioreduction. It is generally accepted that compounds with reduction potentials between -0.2 and -0.4 V vs. the normal hydrogen electrode (NHE) can be reduced by endogenous reductase enzymes.⁵⁰ However, many compounds with reduction potentials outside this range still exhibit bioreductive activity *in vivo*, suggesting that reductive activation is unpredictable and values obtained in the laboratory should not be used exclusively for screening purposes. Still, electroanalytical techniques can be employed in the interest of characterising the properties of new potentially bioreducible drugs as long as the conditions are reproducible and relevant to biological systems. Here cyclic voltammetry has been used to examine the redox behaviour and estimate the reduction potentials of the mustard complexes under simulated approximations of physiological conditions.

Cyclic voltammetry uses a changing potential in an electrochemical cell to monitor the electron transfer behaviour of the components of the solution studied. The potential is scanned through a range of voltages to a maximum and back again and an electrode measures the current produced in the sample when the compound is oxidised and reduced. The voltage (V or mV) of potential applied is plotted against the observed current density (μA), giving a spectrum representing the reduction and subsequent back oxidation of the species in the solution. The reduction produces a

negative peak (cathodic peak i_{pc} at potential E_{pc}) and the oxidation gives a positive peak (anodic peak i_{pa} at potential E_{pa}). The redox potential ($E_{1/2}$) is the halfway point between those two peaks [$E_{1/2} = (E_{pc} + E_{pa})/2$]. The speed of the potential scan is the 'scan rate.' The shape of the peak illustrates the change in concentration of the reacting species vs. the product near the electrode. The size and appearance of the peaks are a function of the scan rate and the 'reversibility' of the redox reaction, depending on whether the reduced species remains in contact with the measuring electrode within the time scale for reoxidation. Reversible behaviour is characterised by the spectrum shown in Fig. 4E. For a system to be classically reversible, the potential difference between the cathodic and anodic peaks should be less than 60 mV. Greater distances between the peaks indicates a 'quasi-reversible' process.

Fig. 4E. Example of a reversible cyclic voltammogram.²¹³



The speed of the electron transfer reaction also affects the appearance of the cyclic voltammogram. Fast electron transfer generally gives the same peak potentials even with increasing scan rate, resulting in conditions nearer to 'ideal' which can show predictable diffusion and concentration behaviour. Slow electron transfer results in a maximum peak potential shift towards more positive values with increasing scan rate, due to a slower decrease in the concentration of the reduced

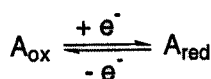
species at the electrode. Metal deposition on the electrode can cause sharp spikes in the current and is usually remedied by thorough polishing of the working electrode. Other spectral abnormalities can occur as a result of adsorption of other solution components onto the electrode, including reactant species, reduction products, or their intermediates.

Irreversible behaviour produces a cathodic peak, but no corresponding equal but opposite anodic peak, implying that the back oxidation does not occur reliably. The oxidation peak for an irreversible reaction may just be smaller than the reduction peak, or it may not appear at all. The cause of the irreversibility is sometimes a chemical change in the reduced species, but can be physical (e.g. due to precipitation of the reduced species from solution).

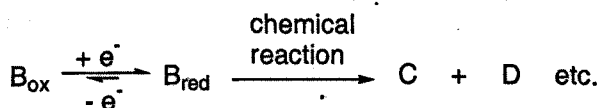
The reversibility of the cyclic voltammogram can give valuable information about the thermodynamic stability of the reduced complex. Thermodynamically stable reduced complexes will remain intact near the electrode until the potential is reversed and they are reoxidised (Scheme 4.2.2.1A). If the reduced complex changes significantly during the sweep time, the redox behaviour will change and thus the voltammogram will show irreversible or quasi-irreversible behaviour. Complexes of lower stability can undergo irreversible chemical change before they are reoxidised (Scheme 4.2.2.1B), resulting in less reliable redox reactions and negative shifts in the E_{pc} with increasing scan rate. However it is sometimes possible to obtain reversible spectra by increasing the scan rate and thus oxidising the compound before decomposition can occur.^{212, 214}

Scheme 4.2.2.1

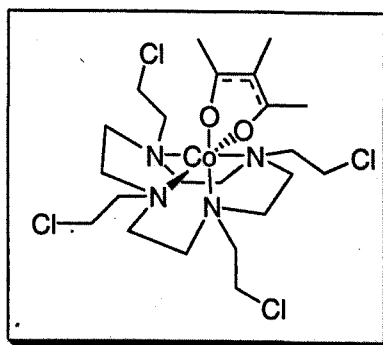
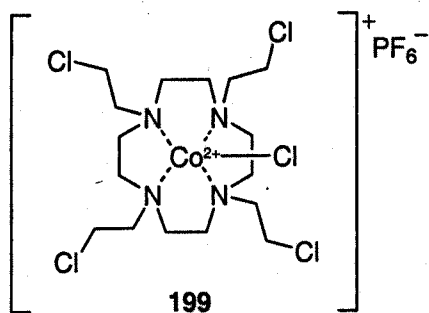
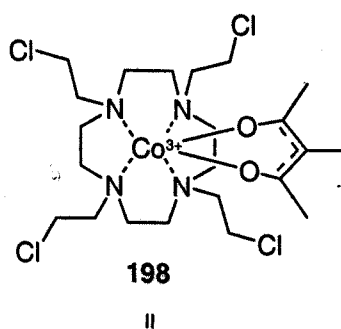
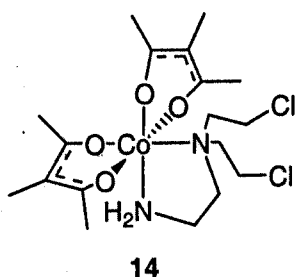
A:



B:



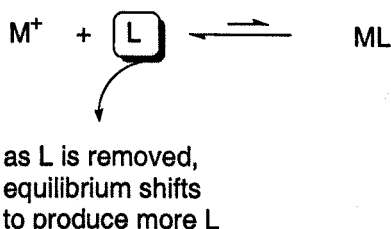
These properties can have implications for the selectivity of bioreductive drugs. For example, the Co(III) complexes like **14**, described previously by Denny and Wilson showed quasi-irreversible redox behaviour.⁷² They also showed fairly high toxicity to oxygenated tumour cells. Denny and Wilson originally proposed that the cytotoxicity of the compounds in the presence of O₂ was probably due to the dissociation of the reduced Co(II) complex before reoxidation to the Co(III) complex could occur.⁷⁵ However, they also reported that the half life of the activity of their complex when incubated in the medium was only a few hours. The complexes lost their aerobic and anaerobic cytotoxicity after short periods of time in aqueous solution. This implies that the complex dissociated in solution and was hydrolysed to the inactive 2-hydroxyethyl analogue even without being reduced by cellular systems. Additionally, the complexes like **14** showed significant cytotoxicity that was independent of the oxygenation of the cell culture. Complexes of this linear 3° amine ligand are much less thermodynamically stable in general compared to complexes of 1° amine as well as linear and macrocyclic 2° amine ligands.²¹⁵ It is possible that the Co(III) metal itself was toxic, but it does appear that there is some other mechanism of activity taking place, e.g. the mustard was available in the uncomplexed form in solution.



Excessive toxicity was observed for the Co(III) complex of our macrocyclic mustard ligand **198** as well, which was formed from the Co(II) complex **199**.²¹⁶ If thermodynamic stability is lower, the equilibrium for the complex formation reaction will lie to the $M^+ + L$ side. That leaves the free ligand available for reaction with nucleophiles before the metal is reduced. Reaction of L with nucleophiles (N) decreases the concentration of L as it forms LN, which in turn means that more free L will be produced by the equilibrium process (**Scheme 4.2.3.1**). So, it seems possible that the low selectivity observed for Co(III) complexes of macrocyclic nitrogen mustards is due to the inherent instability of the oxidised complex itself.

Scheme 4.2.3.1

low stability constant K:

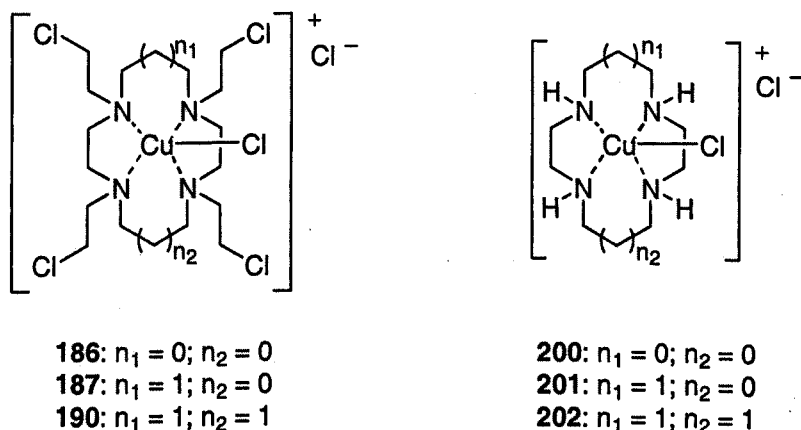


Accordingly, it was desirable to produce mustard complexes that showed sufficient thermodynamic stability to prevent hydrolysis and/or reaction while oxidised. It was also important that the reduced complex should be sufficiently stable to allow time for reoxidation, to ensure that active mustard release would be minimal in aerobic tissue.

The known *in vivo* hypoxia selectivity of Cu(II) bis(thiosemicarbazone) complexes⁷⁶ (e.g. **15**, section 1.2.2) made Cu(II) an attractive candidate for mustard complex formation. More powerfully, empirical evidence from biodistribution studies of radiolabelled Cu(II) complexes of cyclen and cyclam derivatives (e.g. **16**, section 1.2.2) suggests that they are bioreducible. 24 hours after injection with ⁶⁴Cu(II) complexes of a variety of azamacrocyclic complexes, the highest concentration of ⁶⁴Cu was found in the tumour tissue of tumour-bearing Golden Syrian hamsters.⁸¹ The authors suggested that the observance of ⁶⁴Cu in tumours as well as other tissues was due to transchelation with enzymatic cold Cu(II). This should be seen most frequently where the ⁶⁴Cu(II) ion was reduced to the less stable

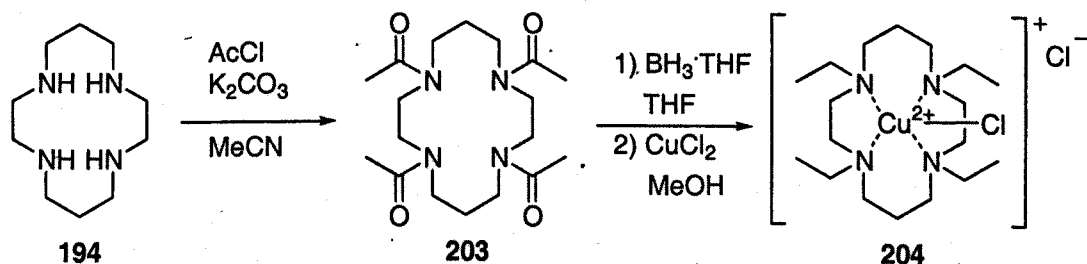
$^{64}\text{Cu(I)}$, as in hypoxic tissue. These data were simply reported as 'good tumour uptake' as compared to uptake by tissues in normal Sprague-Dawley rats, but it can also be interpreted to suggest that bioreductive behaviour will probably be observed for Cu(II) complexes of cyclam and cyclen derivatives.

4.3. Electrochemistry of novel mustard complexes



The novel macrocyclic mustard complexes studied (**186**, **187**, **190** and **191**) showed a marked difference in their aqueous stability and their electrochemical behaviour. The redox potential of each compound was measured with cyclic voltammetry in aqueous phosphate buffer at pH 7.2 with ferrocenecarboxylic acid (FCA) as an internal standard (+533 mV vs. NHE, or +334 mV vs. sat. Ag/AgCl),²¹⁷ using a three-electrode cell with a Pt macrodisc working electrode (2.0 mm), Pt wire counter electrode and either the Ag/AgNO_3 electrode [$E^\circ(\text{vs. Ag/AgNO}_3) = E^\circ + 253$ mV (vs. Ag/AgCl)], or the saturated Ag/AgCl reference electrode [$E^\circ(\text{vs. Ag/AgCl}) = E^\circ - 199$ mV (vs. NHE)].²¹⁸ The potentials were corrected for the published potential of FCA and reported vs. sat. Ag/AgCl . The solutions were degassed with N_2 before analysis, to simulate the hypoxic environment.

Scheme 4.3.1

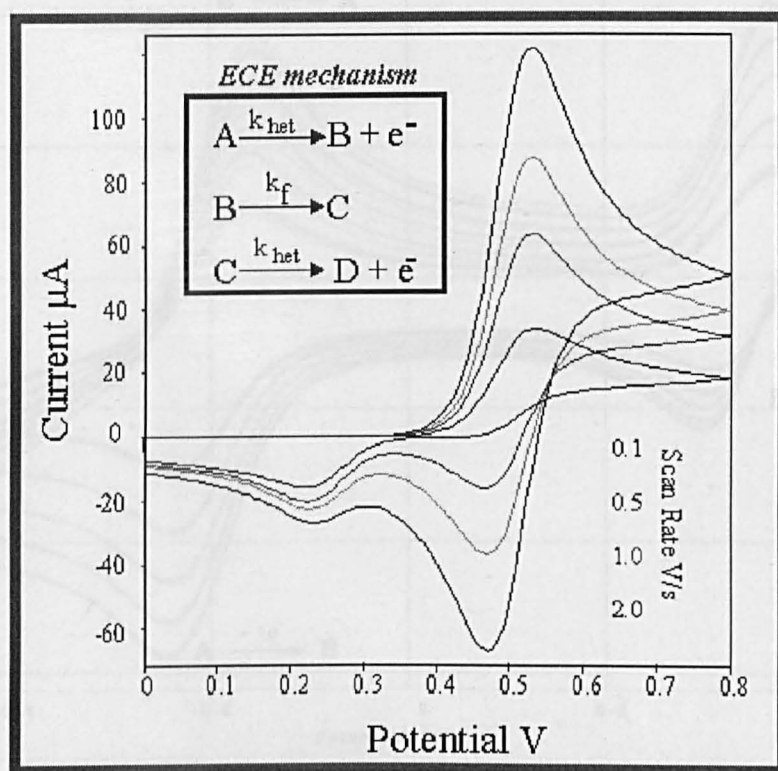


The redox potentials of the parent macrocycle complexes [cyclen[Cu(II)]Cl₂ (200), homocyclen[Cu(II)]Cl₂ (201) and cyclam[Cu(II)]Cl₂ (202)] and the 2-hydroxyethyl analogues (188, 192 and 193) were also measured, in order to compare the reduction potentials with the stability constants. The tetra-*N*-ethyl derivative of cyclam was prepared and complexed as well (204) (as in **Scheme 4.3.1**), in order to investigate if the 2-chlorethyl substituents had an effect on the reduction potential. The tetra-*N*-ethyl derivative of cyclen could not be synthesised in the same way as for cyclam (due to difficulties in fully acylating the compound), so it was not prepared. The two most significant voltammograms, for 186 and 190, are shown in **Figs. 4F** and **4G**. The rest are reproduced in **Appendix 1**. For comparison of the reduction potentials of various complexes to each other, they are listed to at least two significant figures. However due to experimental variation, these values are only accurate to one significant figure when comparing them to data obtained from other published experiments. Results are listed in **Table 4.3.1** (four pages on).

The voltammogram for 190 shown in **Fig. 4G** probably represents either an electrochemical-chemical-electrochemical (ECE) reaction pathway (**Fig. 4H top**), or a electrochemical-chemical (EC) pathway (**Fig 4H bottom**).²¹³ In the ECE pathway, the initial reduction of the mustard complex is followed by a chemical reaction, probably the dissociation and hydrolysis of the ligand. Subsequent complexation of the new ligand with Cu(II) [from Cu(I) that had been reoxidised] in solution results in another electrochemical reaction taking place, giving the additional smaller peaks. The EC pathway would occur if the ligand was dissociating and hydrolysing after the reduction took place, so the reoxidation would be less apparent. This could be the case for many of the other irreversible spectra as well (**Appendix 1**).

Fig. 4F. Cyclic voltammogram for 185.

Fig. 4H. ECE (top) and EC (bottom) voltammograms



solution of 185 (2 mM) in 100 mM phosphate buffer (pH 7.3) with ferrocenecarboxylic acid as internal standard; scan rates from 100–500 mV/s

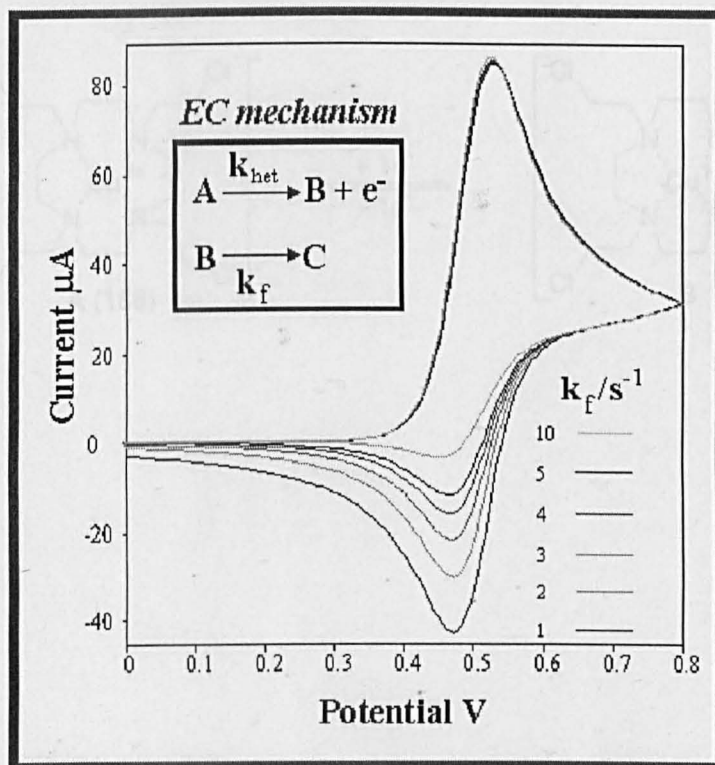
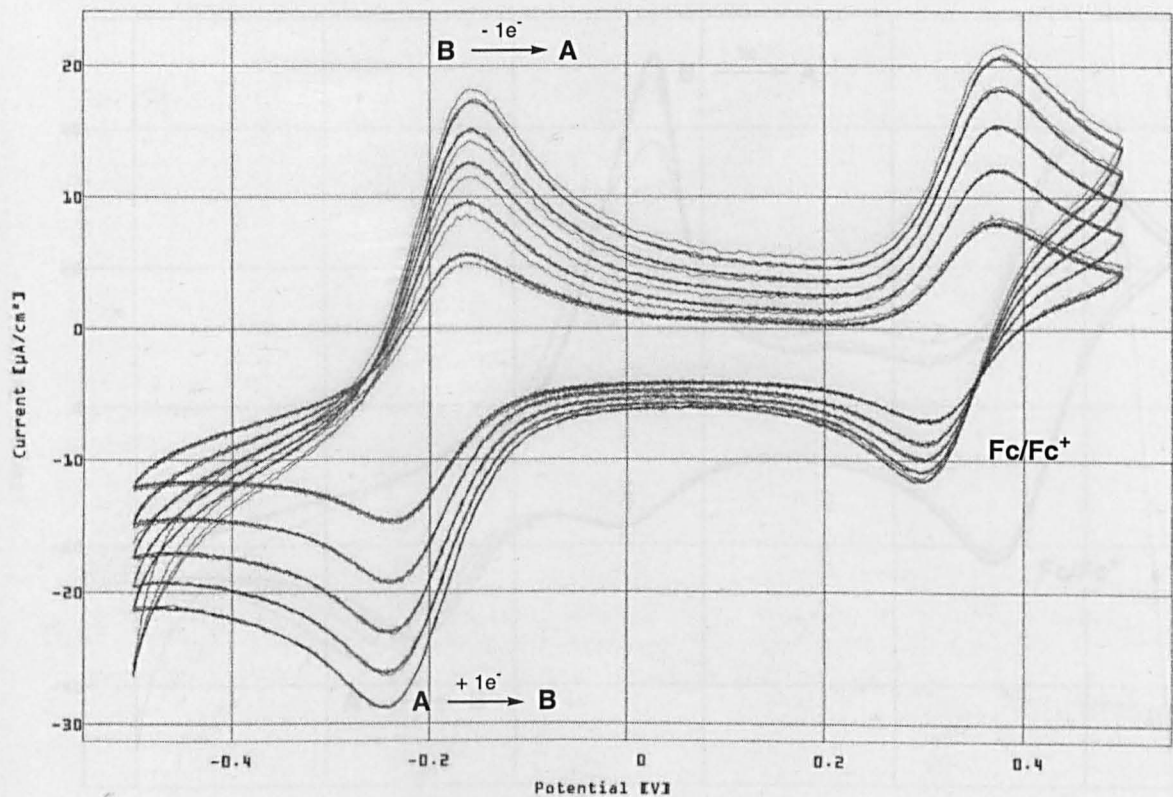


Fig. 4F. Cyclic voltammogram for 186.



solution of 186 (2 mM) in 100 mM phosphate buffer (pH 7.2) with ferrocenecarboxylic acid as internal standard; scan rates from 100-500 mV/s

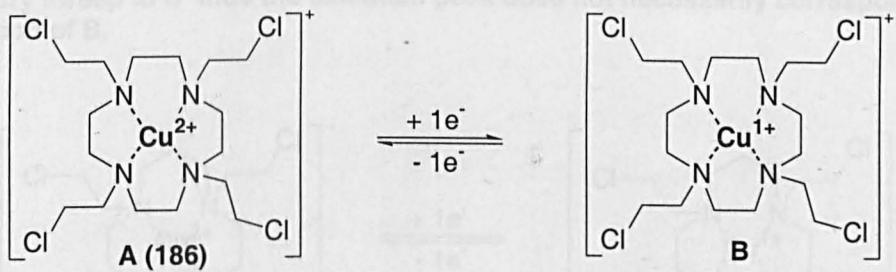
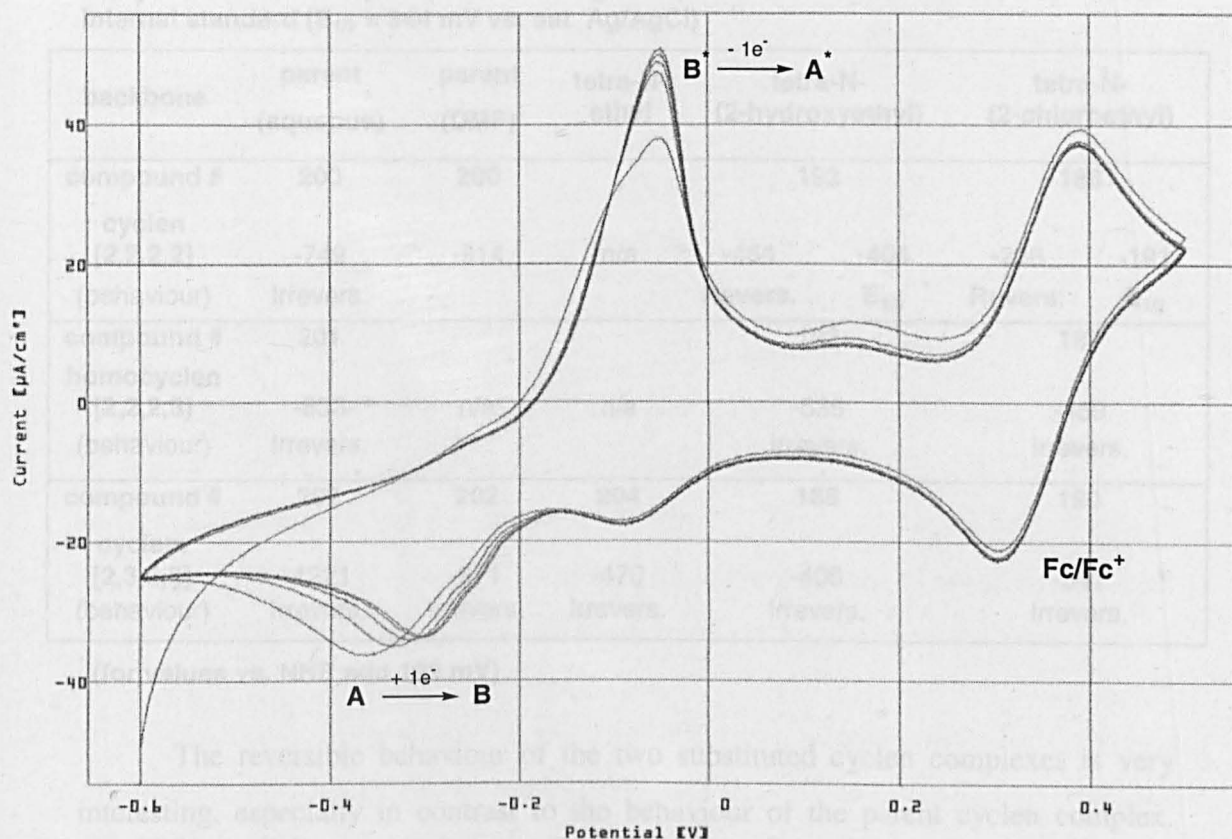


Fig. 4G. Cyclic voltammogram for 190



solution of 190 (1 mM) in 100 mM phosphate buffer (pH 7.2) with ferrocenecarboxylic acid as internal standard; scan rate 100 mV/s

B^* to A^* indicates that the reduced species, B, has changed during the timescale of the voltammetry sweep to B^* thus the oxidation peak does not necessarily correspond to the oxidation of B.

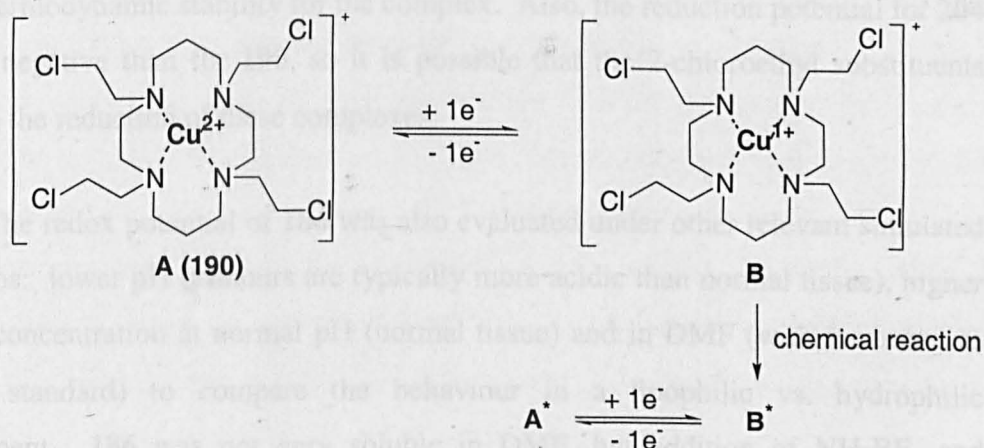


Table 4.3.1. Reduction potentials for main peaks E_{pc} (mV) vs. sat. Ag/AgCl^{*} of Cu(II) complexes in 100 mM phosphate buffer (pH 7.2) unless otherwise stated, with FCA as internal standard ($E_{1/2}$ = 344 mV vs. sat. Ag/AgCl)

backbone	parent (aqueous)	parent (DMF)	tetra-N- ethyl	tetra-N- (2-hydroxyethyl)		tetra-N- (2-chloroethyl)	
compound #	200	200		192		186	
cyclen [2,2,2,2] (behaviour)	-749 Irrevers.	-914	n/a	-464 Revers.	-404 $E_{1/2}$	-236 Revers.	-191 $E_{1/2}$
compound #	201			193		187	
homocyclen [2,2,2,3] (behaviour)	-833 Irrevers.	n/a	n/a	-536 Irrevers.		-459 Irrevers.	
compound #	202	202	204	188		190	
cyclam [2,3,2,3] (behaviour)	-1221 Irrevers.	-971 Irrevers.	-470 Irrevers.	-406 Irrevers.		-341 Irrevers.	

^{*} (for values vs. NHE add 199 mV)

The reversible behaviour of the two substituted cyclen complexes is very interesting, especially in contrast to the behaviour of the parent cyclen complex. Reversibility implies sufficient stability of the reduced complex, so **186** and **192** seem to be more stable when reduced than the rest of the complexes studied. Additionally, however, higher chelate ring strain is characterised by a more negative redox potential.²¹⁹ The more negative reduction potential observed for **192** suggests that its chelate rings are more strained—a property that would normally result in lower thermodynamic stability for the complex. Also, the reduction potential for **204** is more negative than for **190**, so it is possible that the 2-chloroethyl substituents facilitate the reduction of these complexes.

The redox potential of **186** was also evaluated under other relevant simulated conditions: lower pH (tumours are typically more acidic than normal tissue), higher oxygen concentration at normal pH (normal tissue) and in DMF (with ferrocene as internal standard) to compare the behaviour in a lipophilic vs. hydrophilic environment. **186** was not very soluble in DMF, but addition of NH_4BF_4 and sonication for 20 minutes allowed the preparation of a 1.0 mM solution. Aside from analysis of **190** at lower pH, these additional tests were not performed with other compounds due to lack of material. The results are listed in **Table 4.3.2**.

Table 4.3.2. E_{pc} (vs. sat. Ag/AgCl) under alternative conditions

compound	N ₂ , pH 7.2, aq. phosphate buffer	N ₂ , pH 4.9, aq. phosphate buffer	O ₂ , pH 7.2, aq. phosphate buffer	N ₂ , DMF
186	-236 mV	-270 mV	-303 mV	E_{pc} : -963 mV
(behaviour)	Reversible	Reversible	Reversible	Irreversible
190	E_{pc} : -341	E_{pc} : -349 mV		
(behaviour)	Irreversible	Irreversible		

* (for values vs. NHE add 199 mV)

Again, the difference in $E_{1/2}$ for **186** under oxic vs. hypoxic conditions appears to be significant (comparison of the voltammograms shown in **Fig. 4I**). The reduction potential difference observed (70-80 mV) can lead to a 10-fold change in the reduction rate.⁵⁰ The slower reduction rate in the presence of oxygen might well play a part in the selective release of the cytotoxin under hypoxic conditions.

Another point of interest is the large difference between the redox behaviour of **186** in DMF vs. phosphate buffer. The redox reaction is no longer reversible (**Fig. 4J**). There appear to be two reduction peaks (although one is more likely to correspond to **186** and the other perhaps to another component of the solution). Denny and Wilson⁷² measured the reduction potentials of their bio-reducible Co(III) complexes in dichloromethane (as their complexes were not soluble in aqueous solution) and also saw irreversible reductions. The redox behaviour observed for **186** in DMF corresponds better to the behaviour seen by Denny and Wilson. It appears that reduction potentials measured in non-protic solvents don't compare easily with those measured in aqueous solution. Without knowing the precise mechanism for enzymatic reduction of these complexes (and thus whether the reduction takes place in the aqueous or the lipophilic membrane environment), it is difficult to know which potential is more relevant to the activity. However, aqueous systems provide better information about the thermodynamic stabilities of the oxidised (Cu[II]) and reduced (Cu[I]) complexes and so are more useful in predicting hypoxia selectivity (discussed further in Chapter 5).

Fig. 4I. Oxic vs. hypoxic voltammograms for 186 in 100 mM phosphate buffer, pH 7.2

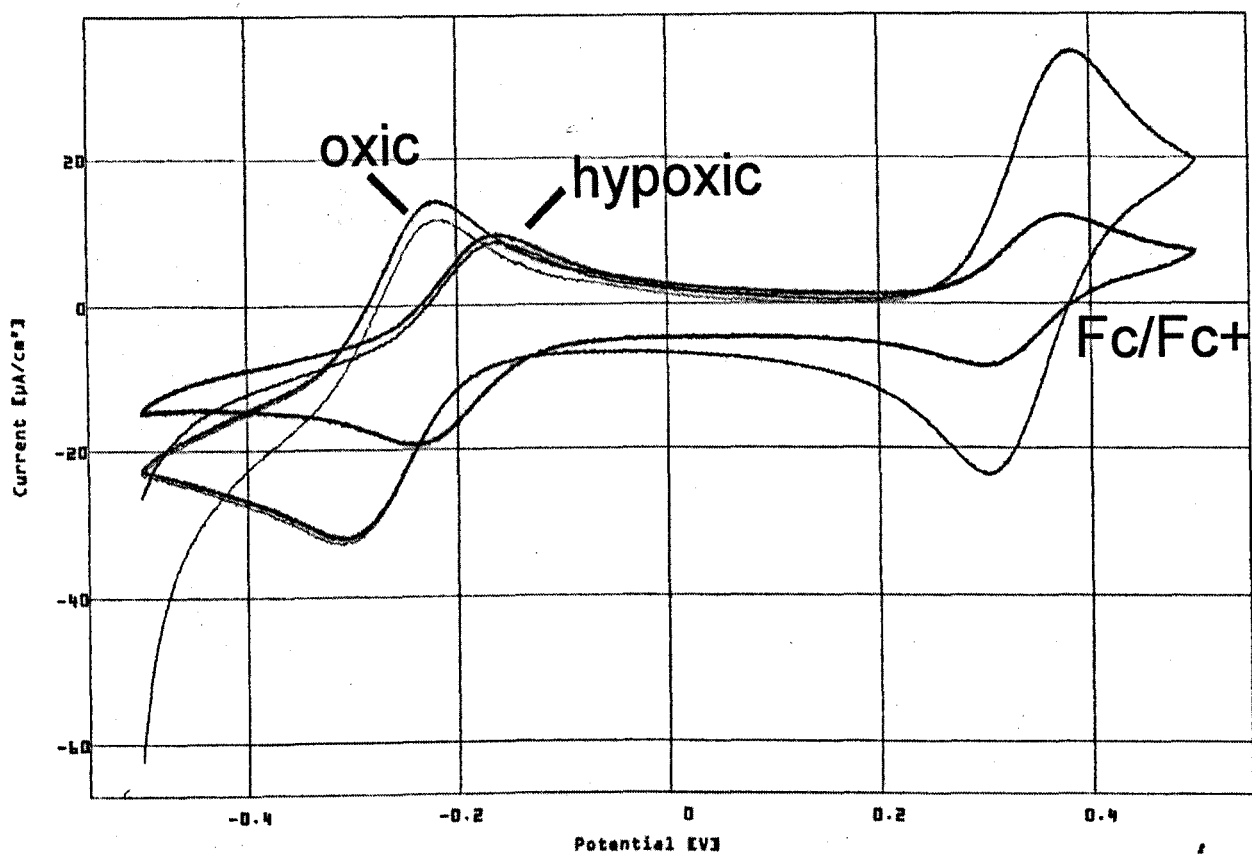
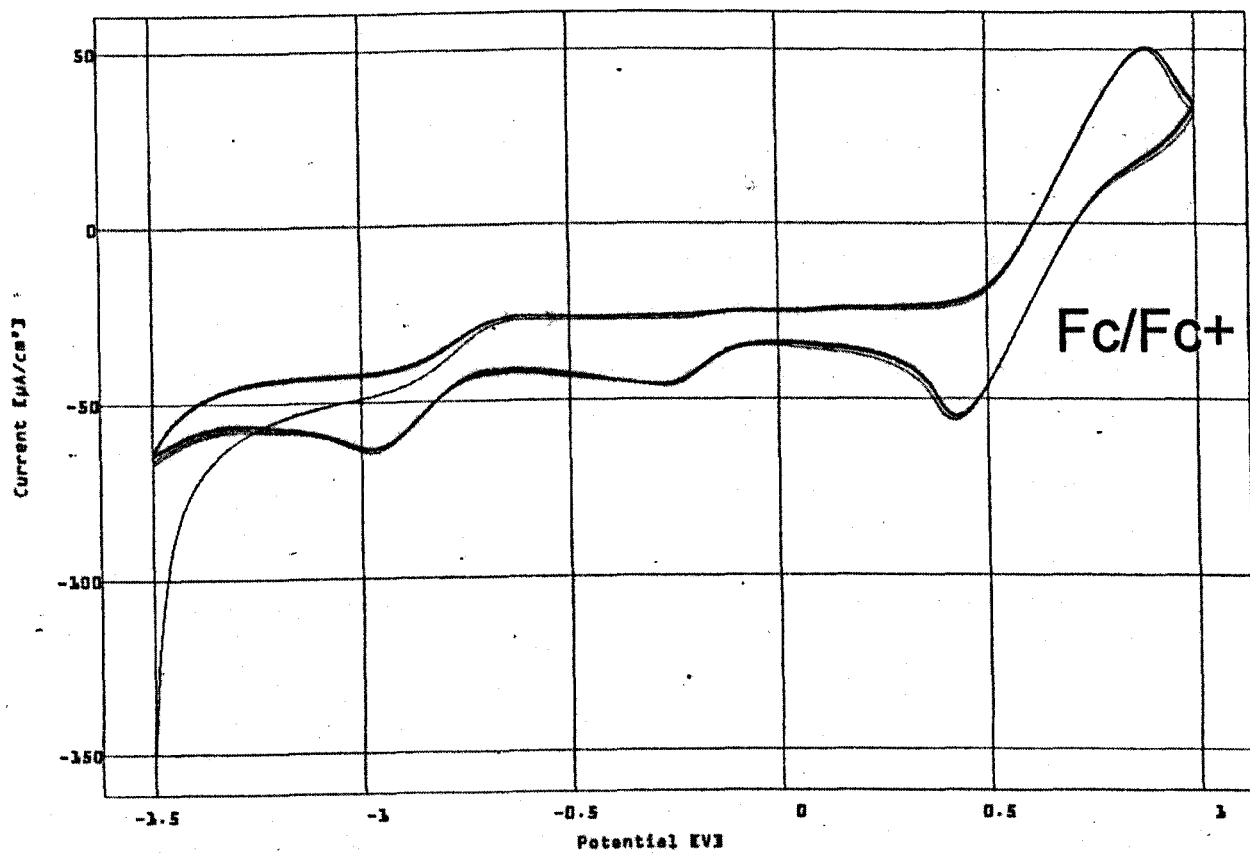


Fig. 4J. Voltammogram for 186 in DMF (1.0 mM, 100 mM TBABF₄).



4.4. Aqueous stability of novel complexes

The aqueous stability was assessed by observing the hydrolysis from the tetra-*N*-(2-chloroethyl) complex (**186**, **187** and **190**) to a poly-*N*-(2-hydroxyethyl) complex (**Scheme 4.2.2.1**). The reaction was monitored by UV-Vis spectroscopy, with the λ_{max} known for each complex, watching for a shift towards the λ_{max} for the tetra-*N*-(2-hydroxyethyl) complex. The λ_{max} values were sufficiently different so that the hydrolysis could be effectively observed. The aqueous stability is defined here as $t_{1/2}(\delta)$: the time necessary for a λ_{max} shift of half the difference between those for their mustard and poly-(2-hydroxyethyl) derivatives. If the complex is thermodynamically stable, no change in λ_{max} should be seen even after the material is left for extended periods of time in aqueous solution. If it is not thermodynamically stable, it should go through the series of reactions shown in **Scheme 4.2.2.1**.

Table 4.4.1

complex	186	187	190
$t_{1/2}(\delta)$	> 14 days	> 7 days	~ 24 hours

Values for $t_{1/2}(\delta)$ for three of the mustard complexes are given in **Table 4.4.1**. **186** and **187** exhibited no significant change in λ_{max} (622 nm and 599 nm respectively) after long periods of time at concentrations of 1-5 mM in 100 mM aqueous phosphate buffer at pH 7.2 (see **Fig. 4K** for **186** and **4L** for **187**). Additionally, **186** retained its potency against *Trypanosoma brucei* even after three weeks as a 2 mM solution in water (this is discussed further in Chapter 5). A 1 mM solution of the cyclam-based mustard complex **190** in 100 mM aqueous phosphate buffer at pH 7.2, however, showed a marked shift in its λ_{max} after just 48 h (from 636 nm to 624 nm) (**Fig. 4M**). This indicated the ligand was decomposing and the resulting 2-hydroxyethyl substituted cyclam was then complexing with Cu(II) (**Scheme 4.2.2.1**). Although it was not possible to quantify the extent of hydrolysis of **190**, it was clear that the complex was not stable under aqueous conditions.

Fig. 4K. $t_{1/2}(\delta)$ analysis (UV-Vis spectroscopy) for 186.

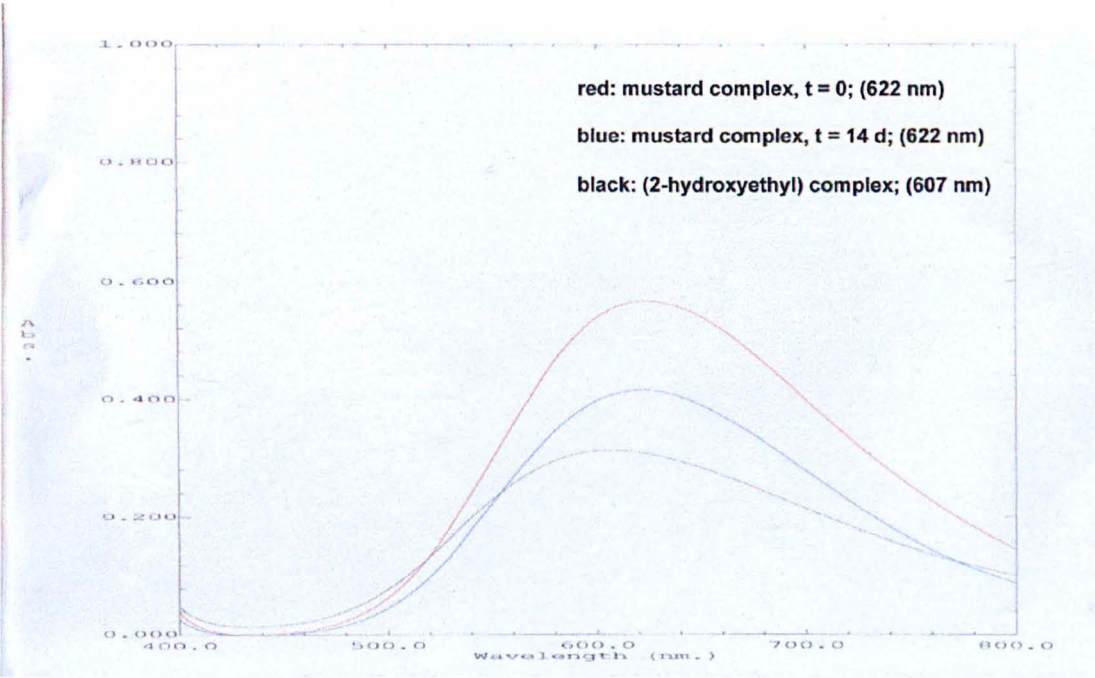


Fig. 4L. $t_{1/2}(\delta)$ analysis (UV-Vis spectroscopy) for 187.

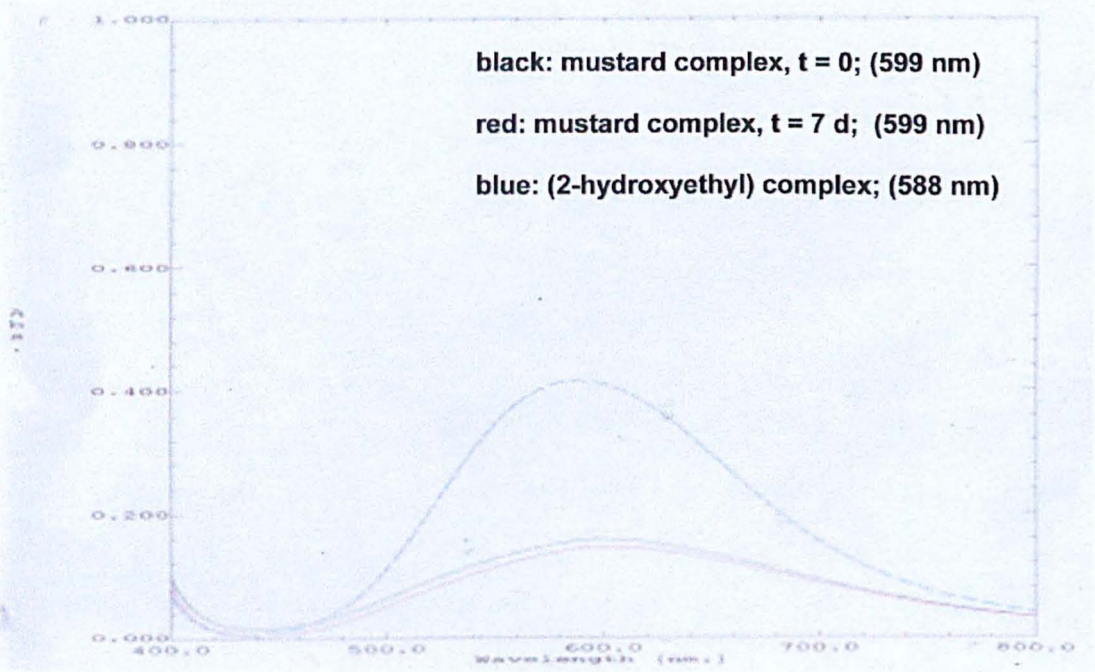
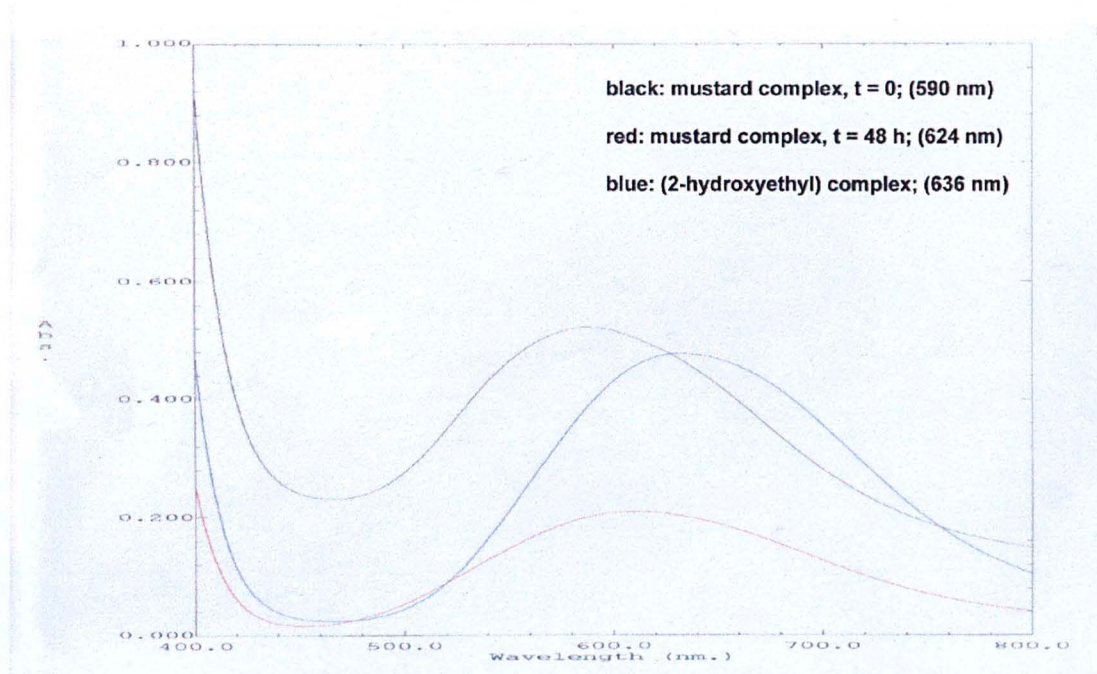


Fig. 4M. $t_{1/2}(\delta)$ analysis (UV-Vis spectroscopy) for 190.



4.5. Additional complexation

4.5.1. Co(II) complex of cyclen mustard

The Co(II) complex **199** was formed easily and crystallised as the PF_6^- salt. The crystal structure is given in **Fig. 4N** and the chelate rings formed are similar in conformation to those in the Cu(II) complex. The Co(II) ion exhibits square pyramidal geometry and, as for the Cu(II) complex, the cobalt sits well out of the plane created by the four coordinating nitrogen atoms. This complex is much more soluble in organic solvents e.g. acetonitrile or methanol than in water; in fact it does not dissolve significantly in 100 mM phosphate buffer at pH 7.2. Oxidation of the Co(II) to Co(III) was attempted but only starting material **199** was obtained. Alternative methods involving oxidation of the cobalt prior to complexation were also attempted, but the product could not be isolated. Due to the difficulties encountered with bio-reducible cobalt complex formation and the relative success with Cu(II) complexation, cobalt complexes were not pursued further.

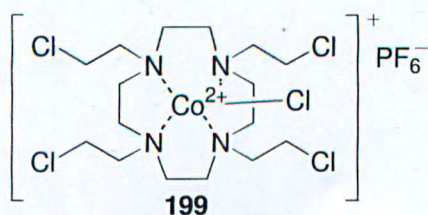
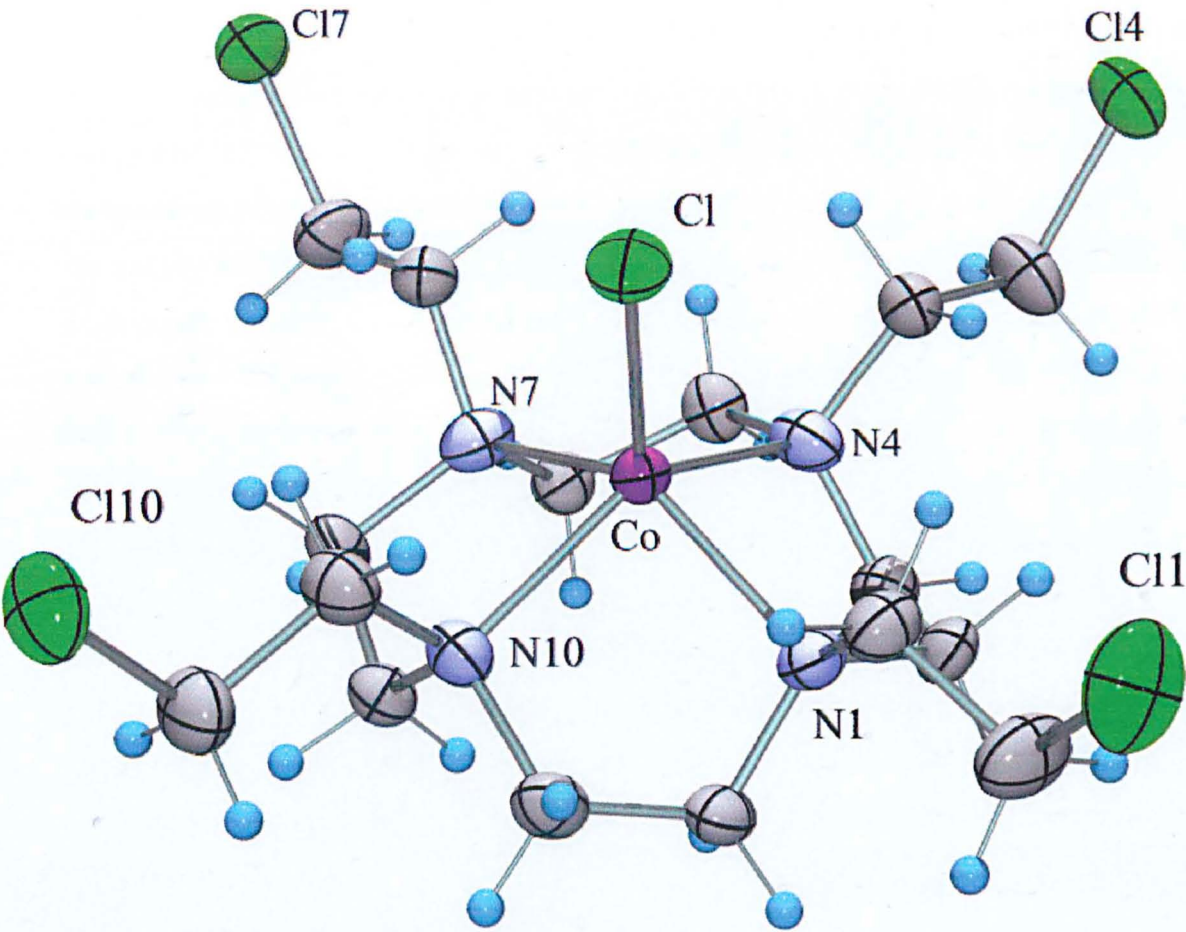


Fig. 4N. Co(II) complex of cyclen mustard (199).

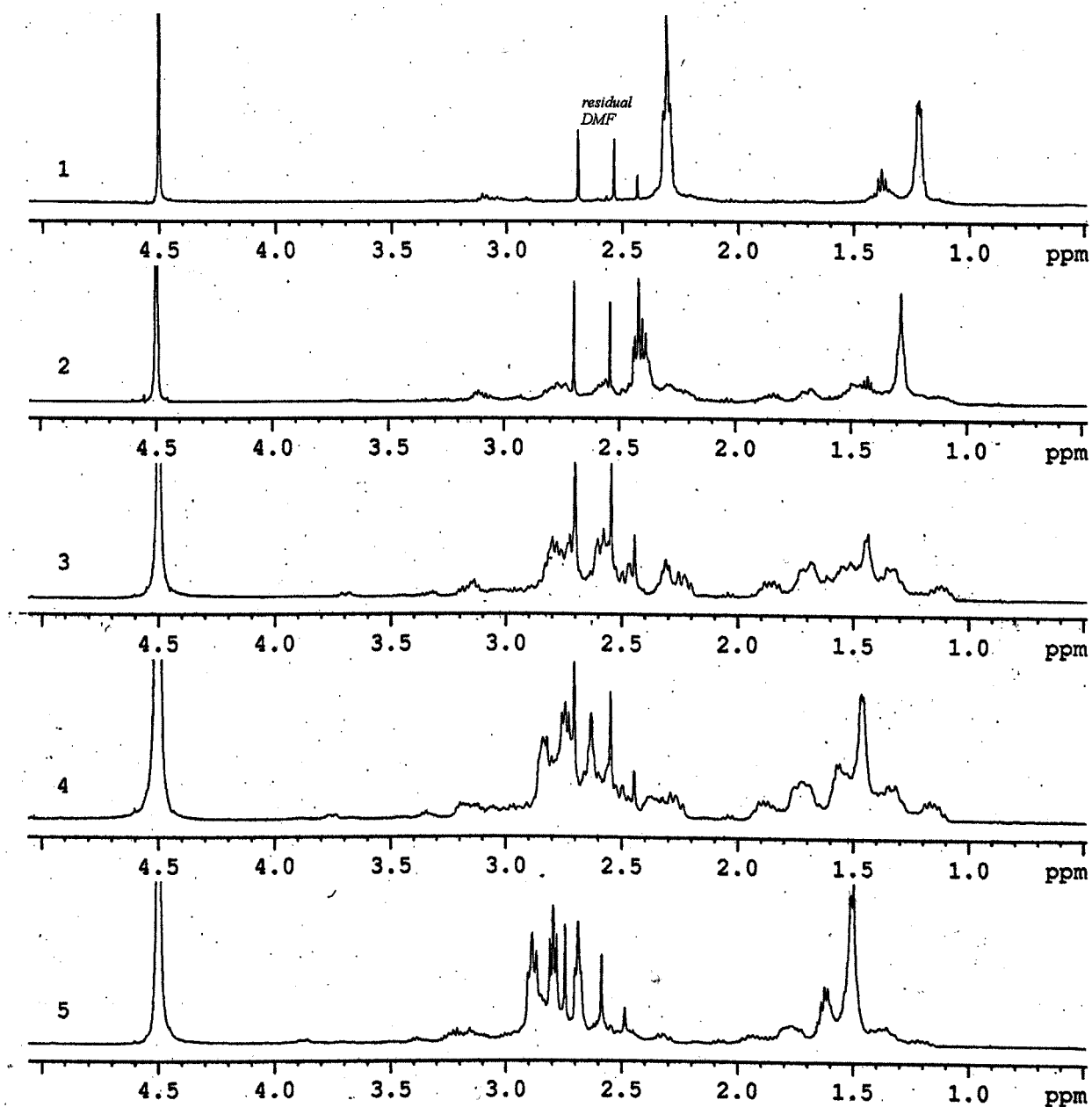


	Bond lengths (Å)	(Cu(II) complex)		Bond angles (°)	(Cu(II) complex)
Co-N1	2.1503	(2.099)	N1-Co-N4	83.90	(85.11)
Co-N4	2.1426	(2.060)	N1-Co-N7	139.01	(146.0)
Co-N7	2.1565	(2.062)	N4-Co-N7	83.02	(86.51)
Co-N10	2.1515	(2.065)	N4-Co-N10	139.70	(148.95)
Co-Cl	2.2490	(2.3618)	N7-Co-N10	82.15	(87.03)
			N10-Co-N1	83.22	(85.33)

4.5.2. Complexation of novel parent triazamacrocycles

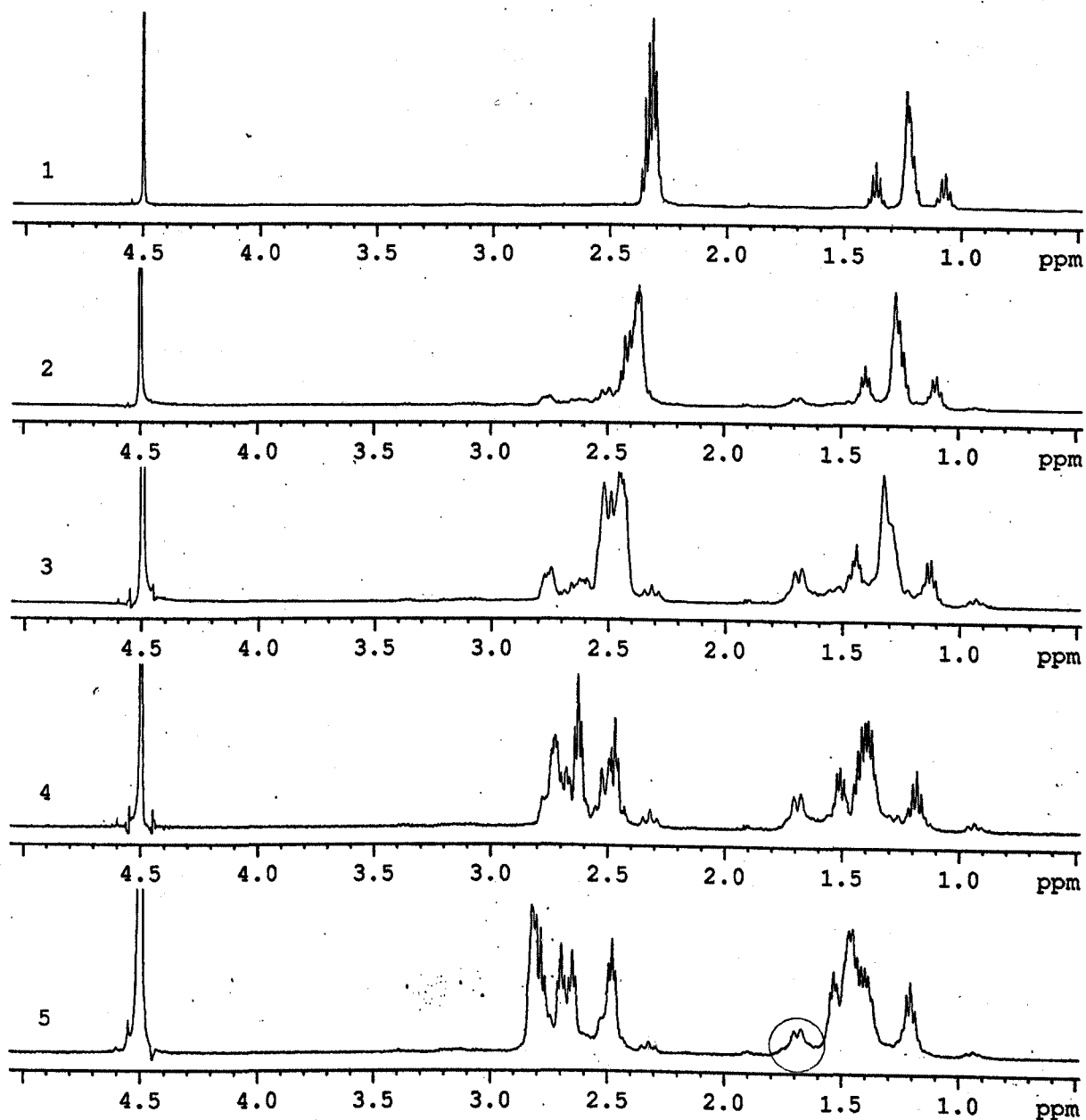
Attempts were made to prepare and crystallise complexes of the [4,4,3] (**128**) and [3,4,5] (**129**) novel triazamacrocycles with $\text{Cu}(\text{NO}_3)_2$. Initially very small yields of crystals did form in the complexation reaction solutions, but they were not of X-ray quality and attempts to recrystallise the materials resulted in decomposition to a deep green solution from which no crystallisation would occur, even upon evaporation to dryness. The color change [from bright blue $\text{Cu}(\text{NO}_3)_2$ solution to a dark green solution of the ligand with the $\text{Cu}(\text{II})$ salt] indicated that some kind of coordination was taking place. Since X-ray crystallography was proving problematic, NMR spectroscopic studies of the complexations were undertaken using $\text{Zn}(\text{II})$, since it does not have an effect on the acquisition of interpretable NMR spectra. Compounds **128** and **129** were titrated with a solution of ZnBr_2 and monitored by ^1H NMR spectroscopy with the addition of increasing amounts of the ZnBr_2 solution. The degree of formation of the 1:1 complex could be observed at each step, as shown in **Figs. 4O** and **4P**. For both **128** and **129**, the changes in chemical shift induced in all of the signals corresponding to $\text{CH}_2\text{-N}$ indicated that all three of the amine groups of each macrocycle were complexing to the $\text{Zn}(\text{II})$. The structures of the complexes were analysed by 2-dimensional NMR spectroscopy (COSY, HMQC, HMBC) and the structural assignments are suggested in the experimental section for this chapter (refer to **Appendix 2** for 2-dimensional NMR spectra). The circled peak in the final complex of **129** (**Fig. 4O**) may correspond to a coordinated water molecule (supported by the lack of HMQC and HMBC correlations for that proton peak). Titration of this complex with base would provide some insight into the pK_a of this bound water, however this was beyond the scope of the present studies. Initial attempts to crystallise these complexes were unsuccessful, but changing the crystallisation conditions (e.g. solvent system, counter ion, etc.) may allow for the production of X-ray quality crystals and structural characterisation.

Fig. 40. Titration of 128 with Zn(II)



	1	2	3	4	5
Eq. Zn(II) added	0	0.25	0.50	0.75	1.0

Fig. 4P. Titration of 129 with Zn(II)



	1	2	3	4	5
Eq. Zn(II) added	0	0.25	0.50	0.75	1.0

4.6. Conclusions

As suggested in the literature, it was found that azamacrocycles generally form thermodynamically stable Cu(II) complexes. The substituted cyclen-based mustard ligand gave the most stable complex, which was advantageous for its biological activity. The thermodynamic stability of the oxidised [Cu(II)] and reduced [Cu(I)] complexes could be assessed using cyclic voltammetry and UV-Vis spectroscopy and reversible redox behaviour and high thermodynamic stability were found to correlate positively with the desired biological activity. The reduction potential for the hypoxia selective complex was less negative than the so-called 'ideal range,' but the activity and selectivity were still better than previously published for this type of bio-reducible prodrug (discussed Chapter 5).

Chapter 5

5. Biological testing and results

5.1. DNA-crosslinking and cytotoxicity of uncomplexed mustards

The novel nitrogen mustards 174-183 (see Table 3.3.1 for structures) were assessed for their cytotoxicity and DNA cross-linking efficiency by Prof. John Hartley at University College London. The results are listed in Table 5.1.1. The cytotoxicities were determined against the human chronic myeloid leukemia cell line K562 using the MTT cell proliferation assay after a one hour exposure to each drug. For the cross-linking assays, the drugs were each reacted with linearised plasmid DNA for 2 h, after which the DNA was precipitated and incubated with strand separation buffer. Gel electrophoresis was performed against single-stranded and double-stranded DNA as controls, resulting in the cross-linked DNA migrating with the double-stranded control. The percent double-stranded DNA in each band was determined from densitometry of autoradiographed images of the gels. The cross-linking activity is expressed as XL₅₀: the concentration of drug which resulted in 50% cross-linked DNA.

Table 5.1.1

Compound [ring size]	174 [2,2,2]	175 [3,3,3]	176 [3,3,4]	177 [3,3,5]- bis	178 [3,3,5]- tris	179 [3,4,4]	180 [3,4,5]	181 [5,5,4]	182 [6,6,4]	183 [2,2,4] ₂
IC ₅₀ ^a (μM)	10.5 ± 0.9	6 ± 2	25 ± 14	6.25 ± 1	25 ± 12	>100	21 ± 7	>100	35	100
XL ₅₀ (μM)	0.060	0.090	0.045	0.010	0.035	n.d. ^b	n.d. ^b	0.035	0.100	>0.300
# of atoms in ring	9	12	13	14	14	14	14	17	20	22

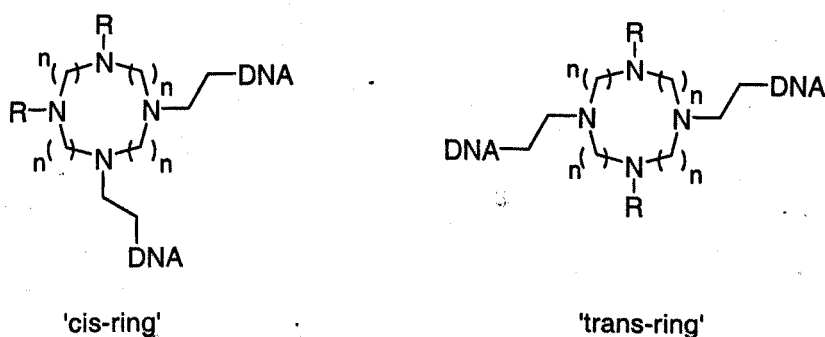
^aagainst human chronic myeloid leukaemia cell line K562; ^bunable to acquire meaningful cross-linking data

The cytotoxicities vary widely, and don't show an obvious relationship to the cross-linking efficiency. This is probably due to hydrolytic decomposition of the

mustard drugs in cell growth medium, but could also result from differences in uptake of the drugs. It is possible that the hydrolysis was not as rapid under the conditions required for the cross-linking reaction. With the exception of the hexaaxamacrocyclic mustard, all of the compounds are remarkably potent DNA cross-linking agents, with XL_{50} activities in the nanomolar range. Particularly notable is the increased cross-linking efficiency in the bis-substituted mustard **177** as opposed to the tris-substituted compound **178**. It is likely that the free secondary amine in **177** exists in its protonated form at physiological pH, thus the improvement may arise from the increased possibility for electrostatic interaction of **177** with DNA.

Otherwise, it is difficult to see a clear structure-activity relationship for the cross-linking activities of this series of drugs. It seems roughly that 9 to 17-membered rings are all capable of highly efficient cross-linking, but ring sizes greater than 17 are too large. This agrees with previous cross-linking data from the group, with XL_{50} values (inferred) falling between 10 and 100 nM for macrocyclic mustards with 12-15-membered rings.

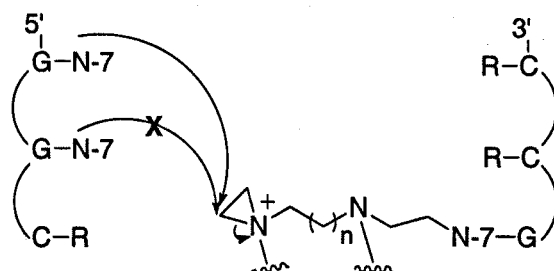
Fig. 5A



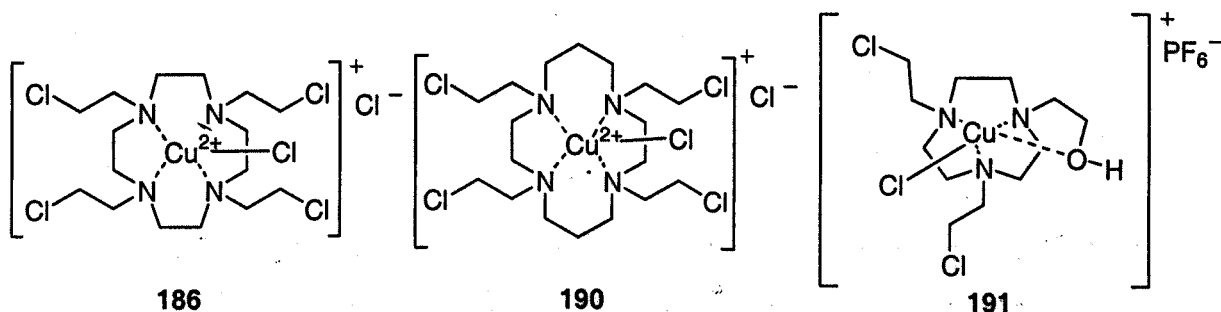
It is not possible to determine which bifunctional cross-links are being formed from the tetra-substituted mustards—i.e. between 'cis-' or 'trans-ring' alkylating substituents (Fig. 5A). Bifunctional *N*-mustard drugs usually form 'diagonal' cross-links between non-adjacent guanines (5'-GNC-3'/3'-CNG-5'), rather than forming the 5'-GC-3'/3'-CG-5' cross-link (Fig. 5B). This is thought to be due to distortion of the classical B-DNA structure induced by the initial alkylation to the mono-functional adduct.²²⁰ All of the parent ring structures are quite flexible, so it is probable that nearly all the possible cross-links are being formed. Without

detailed molecular modelling of these compounds in aqueous solution, it is difficult to estimate the diameters of the different rings and between alkylating moieties. Thus it is not possible at this time to compare the actual distances with the cross-linking efficiency.

Fig. 5B



5.2. Hypoxia selectivity of Cu(II) complexes of selected macrocyclic mustards



Results for the testing of **186**, **190** and **191** as bio-reducible prodrugs were very exciting. They were tested *in vitro*, by Prof. Ian Stratford's group at the University of Manchester, under aerobic and anaerobic conditions against the lung-derived tumour cell line A549 using the MTT cell proliferation assay. The cytotoxicities of the complexes under aerobic and hypoxic conditions supported the prediction that redox reversibility would give hypoxia selective release of the *N*-mustard. The water solubility of the complexes (up to at least 10 mM) made their testing and possible use as pharmaceuticals much more practical than for the previous Co(III) complexes. **186** is one of the best hypoxia selective cytotoxins that has been tested on the cell line used in this study, the lung-derived A549. The results

of the testing are given in **Table 5.2.1**. The cytotoxicities of the free ligands (against K562) and the reduction potentials for the complexes are included for comparison.

Table 5.2.1

Parent macro-cycle	Free ligand	IC ₅₀ ^a (μM)	Cu(II) complex	T _{1/2} (δ) (days)	E _{1/2} (rev) or E _{pc} ^(b)	Cell kill (μM) ^c		HCR ^d	ACR ^e
						IC ₅₀ (air)	IC ₅₀ (N ₂)		
Cyclen	38	22	186	>14	-37 (rev)	53.35 ± 9.71	2.18 ± 0.25	24	-
Cyclam	40	7.5	190	1	-142 (irrev)	10.10 ± 1.29	51.28 ± 10.58	-	5
Tacn	174	10.5	191	n.d.	-240 (irrev)	8.44 ± 0.68	15.87 ± 0.85	-	2

^a against human chronic myeloid leukaemia cell line K562; ^b mV (vs. NHE); ^c against human lung tumour cell line A549; ^d HCR is the hypoxic cytotoxicity ratio: IC₅₀ (air) / IC₅₀ (N₂); ^e ACR is the aerobic cytotoxicity ratio: IC₅₀ (N₂) / IC₅₀ (air)

186 was 24 times more active under hypoxic conditions, indicating that it targets slow-growing hypoxic cells selectively *in vitro* through reduction of the complex and release of the mustard (probably *via* cytochrome p450 or a similar 1 e⁻ reductase). Its aerobic toxicity was approximately ten times less than that previously reported for the most promising Co(III) complex of a linear mustard, SN24771 (14).⁷² So the complexation of this mustard to Cu(II) as a bio reducible prodrug also provided the advantage of potent delivery of the cytotoxin.

190 and 191 showed no evidence of deactivation *via* complexation. They exhibited typical characteristics of classical nitrogen mustard drugs. Their IC₅₀ values under aerobic conditions were similar to those for their free ligands and they even showed some degree of aerobic selectivity, common behaviour in drugs which target fast growing oxic cells. This supported the observations from UV-Vis analysis that suggested the stability of the oxidized complex was very important for deactivation of the mustard ligand. It is likely that these complexes (190 and 191) exist significantly as their free ligands in solution, making bio reduction less relevant as a mechanism for activation. They could also be activated *via* a different bio reduction pathway, e.g. by NQO1 (which is oxygen-independent). However, it is clear that in essence, these compounds have no selectivity for hypoxia and are not good prodrugs. As discussed in Chapter 4, polyazamacrocyclic metal complex

stabilities can vary widely depending on the metal ion, parent ring size and the conformation of the chelate rings formed.^{98, 124, 215} The biological evidence given here shows that these properties are critical to the behaviour of metal complexes as prodrugs.

Two new key observations have been made in this work regarding the characteristics that are necessary in the design of hypoxia selective, metal-complexed *N*-mustard prodrugs. Firstly, the thermodynamic stability of the oxidised complex must be sufficient to render the complex robust in aqueous solution. Secondly, reversible redox behaviour suggests optimum stability of the reduced complex for avoiding undesirable release of the cytotoxin under oxic conditions. Also, previous applications of macrocyclic Cu(II) complexes for targeting hypoxic tissue have used the ligands as vectors for radioactive copper.⁸¹ Here, we have used the copper as a delivery agent for the cytotoxic ligand. This new strategy could provide a significant therapeutic advantage in the fields of alkylating agent therapeutics and selective targeting of hypoxic tissue.

5.3. Anti-parasitic activity of polyazamacrocycles and selected Cu(II) complexes

Anti-parasitic activity of polyazamacrocycles has not been published previously. We were interested in assessing the activity of these polyamine analogues against parasites, which are known to be sensitive to disruption of their polyamine metabolism and transport. A series of polyazamacrocycles was tested by Dr. Michael Barrett (University of Glasgow) against *Leishmania mexicana* and *Trypanosoma brucei*. This included some tetraazamacrocyclic *N*-(2-hydroxyethyl)-substituted derivatives [e.g. 1,4,7,10-tetra(2-hydroxyethyl)cyclen (**197**)] and three of the novel triazamacrocycles reported in this thesis (**128**, **129** and **146**). Cultures of the two parasites in logarithmic phase were treated with serial concentrations of the drugs and incubated at 37 °C for five days. IC₅₀ values for the activity against *L. mexicana* were determined from the acid-phosphatase activity assay. Survival of the parasite was measured from the extent of bis-*p*-nitrophenylphosphate hydrolysis by acid-phosphatase in live cells, giving yellow *p*-nitrophenolate ion which could be

measured using UV-Vis spectroscopy. IC_{50} values for the activity against *T. brucei* were determined from the alamar blue cell staining assay.²²¹ Living parasites convert the alamar blue dye into a colourless form, thus the level of surviving parasites can be determined from the concentration of alamar blue left in the culture after incubation at 37 °C for 24 h (measured by UV-Vis spectroscopy). The results are listed in **Table 5.3.1**.

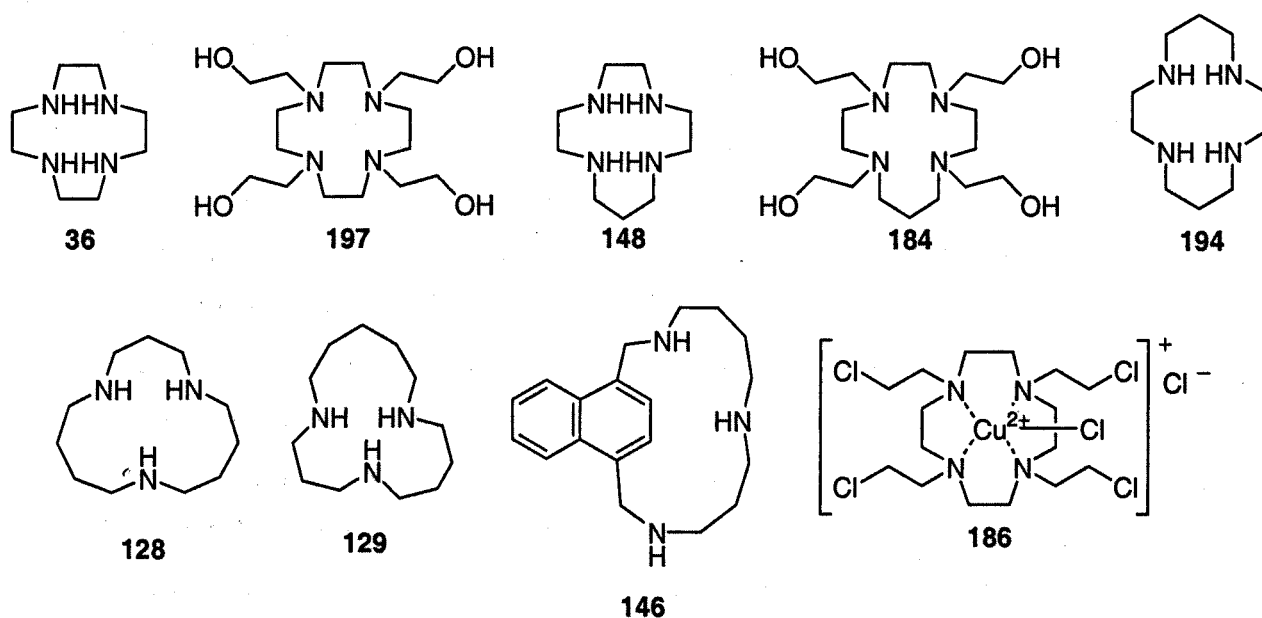


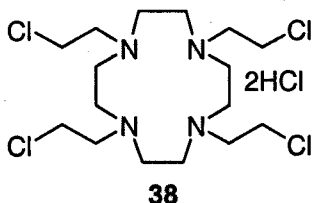
Table 5.3.1. Screening for anti-parasitic activity of polyazamacrocycles

compound	IC_{50} (μ M) <i>L. mexicana</i>	IC_{50} (μ M) <i>T. brucei</i>
36	>3,000	75
197	no effect	no effect
148	120	430
184	90	no effect
194	135	600
128	150	no effect
129	250	no effect
146	65	45
186	52	5

It is difficult to determine any trends in the activities from these results. However it is clear that the activity profiles of polyazamacrocycles in the two parasites are quite different. Cyclen (36) was moderately active against *T. brucei*, yet virtually inactive in *L. mexicana*. The opposite was true for the unsubstituted

novel triazamacrocycles **128** [3,4,4] and **129** [3,4,5], as well as for the *N*-(2-hydroxyethyl)-substituted [2,2,2,3] tetraazamacrocycle **184**. These differences could suggest that *L. mexicana* and *T. brucei* use different pathways in the uptake of polyazamacrocycles, or that they have variable sensitivity to transition metal sequestration by chelating drugs. The only compound which gave similar activity in the two parasites was the novel naphthyl-bridged triazamacrocycle **146** [3,4,(1,4-naphth)]. This was probably due to its greater lipophilicity, which would increase its cell membrane permeability.

The high potency and interesting activity difference for the cyclen mustard complex **186** prompted further investigation. Trypanosomatid parasites, including *L. mexicana* and *T. brucei*, are known to have increased levels of reductase as a protection against oxidative stress imposed as a defence strategy by their host organisms.^{222, 223} Trypanothione reductase (TRYR) is their primary reductase enzyme, similar to glutathione reductase but specific to these types of parasites.²²² It seemed possible that the nitrogen mustard was being selectively released in *T. brucei* through reduction of the Cu(II) to Cu(I), in a similar manner to the selective release in hypoxic tumour cells (Section 5.2). Alternatively, if the organisms were merely sensitive to copper or copper complexes, other ligands complexed to copper should show similar cytotoxicity. To probe the mechanism of the cytotoxicity, the Cu(II) complex of the inactive ligand **197** (**192**) was tested again on *T. brucei* alongside the mustard complex **186**, as well as the free ligands for both. A previously prepared solution of **186** (three weeks old) which had been stored under refrigeration was also included, in order to assess whether the mustard complex would retain its activity after storage in aqueous solution. Results are given in Table 5.3.2.



Compound	197	192	38	186 ^a	186 ^b
IC ₅₀ (μM)	>600	>450	21	4.3	4.5

Like its corresponding ligand **197**, the Cu(II) complex **192** was essentially inactive at concentrations below 200 µg/ml. This supported the theory that the toxicity arose from the mustard being released due to bioreduction of the Cu(II), rather than some general Cu(II) toxicity. The mustard complex was approximately 100 times more active than its corresponding ligand, which showed that complexation seemed to be protecting the mustard from being deactivated by bioreduction to **197** in the aqueous test medium. Also, the complex retained its activity for a reasonably long storage in aqueous solution. This agreed with the lack of λ_{max} shift observed for this complex by UV-Vis spectroscopy after extended storage in water (Chapter 4), further supporting the qualitative determination of the high thermodynamic stability of this complex.

Given the encouraging results for trypanosomes and leishmania, the activity of the cyclen mustard complex was also assessed against malaria parasites. Due to

the short time frame remaining for the project, we decided to perform *in vivo* tests first in order to obtain some qualitative information about the toxicology of these mustard prodrugs. The susceptibility of malaria parasites to oxidative stress and bio reducible drugs has been documented.²²⁵⁻²²⁷ In the light of the apparent bio reductive activation in trypanosomes, it seemed plausible that this complex would also be reduced by malarial reductases (of which glutathione reductase dominates). Given the structural differences between human and malarial glutathione reductase (the latter of which has a much larger active site),²²⁸ it was hoped that malaria parasites would be more sensitive to cytotoxins released through bio reduction than their host organism. At this time we are still waiting for the results of the *in vivo* antimalarial testing.

5.4. Conclusions

The series of polyazamacrocyclic nitrogen mustards described here generally showed potent DNA cross-linking activity, but the cytotoxicities were variable. Polyazamacrocycles were found to have variable but generally low activity *in vitro* against two parasites, *L. mexicana* and *T. brucei*. The cyclen mustard Cu(II) complex showed interesting biological activity in a number of areas. It was somewhat selective for *T. brucei* over *L. mexicana*, which may have been due to bio reductive activation in the reductase-rich trypanosomes. Most importantly, this complex was found to be an effective bio reducible cytotoxin in tumour cells *in vitro*. This is the first example of a macrocyclic *N*-mustard complex that shows hypoxia selectivity and provides an exciting lead into the further development of this new strategy for bio reducible prodrug design.

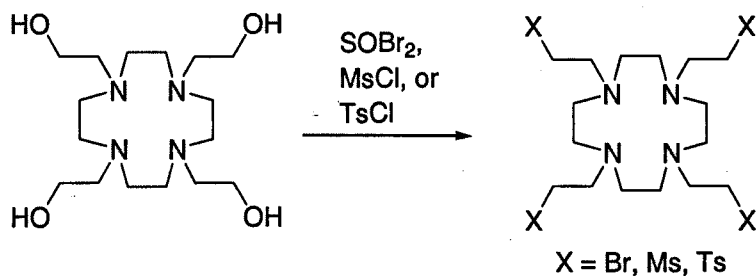
5.5. Future Work

It would be useful to investigate further the utility of the SES-protecting group for the synthesis of azamacrocycles. The heterocycle cyclophane synthesis discussed in this thesis could be optimised and expanded to include other heterocycles and sensitive functionality. Also, it is important to find an alternative deprotection and purification route in order to improve the yields of the parent macrocycles. One possibility is to use TBAF or TEAF to remove the SES-group and to separate the byproducts from the macrocycle using ion-exchange chromatography. This would require some method development, but could provide far better yields of material.

It would also be interesting to produce more macrocyclic polyamine analogues for anti-parasitic testing. Analogues with increased lipophilicity and/or polyamine tags¹⁶⁸ should show better uptake into parasites and thus perhaps better activity. Another area that could be explored further is the mechanism of uptake and cytotoxicity of the macrocycles tested in *L. mexicana* and *T. brucei*. Given the difference in the profiles of activity seen for polyazamacrocycles in the two parasites, it would be useful to investigate whether they are acting as unnatural polyamine analogues or by some other pathway.

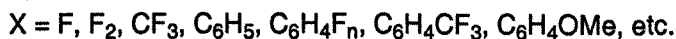
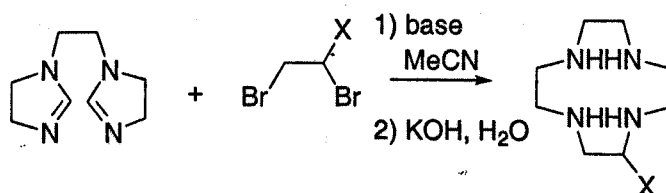
Most importantly, there is extensive opportunity for the development of macrocyclic *N*-mustard complexes as bioreducible prodrugs. The first aim is to produce a series of analogues of **186**, looking to find compounds with more negative reduction potentials in order to obtain increased hypoxia selectivity (as reported for Cu-ATSM derivatives by Maurer *et al.*).⁷⁷ This can be achieved by increasing the electron-withdrawing character of the ligand.⁷⁷ There are a number of structural features which should impart this effect. The simplest variation would be to alter the leaving group of the mustard (e.g. from Cl to Br, mesylate, or tosylate, **Scheme 5.5.1**) Given the trend observed in the reduction potentials of cyclen-based Cu(II) complexes (**Table 4.3.1**), this should have an effect on the electron transfer to and from Cu(II) and therefore the reduction potential.

Scheme 5.5.1



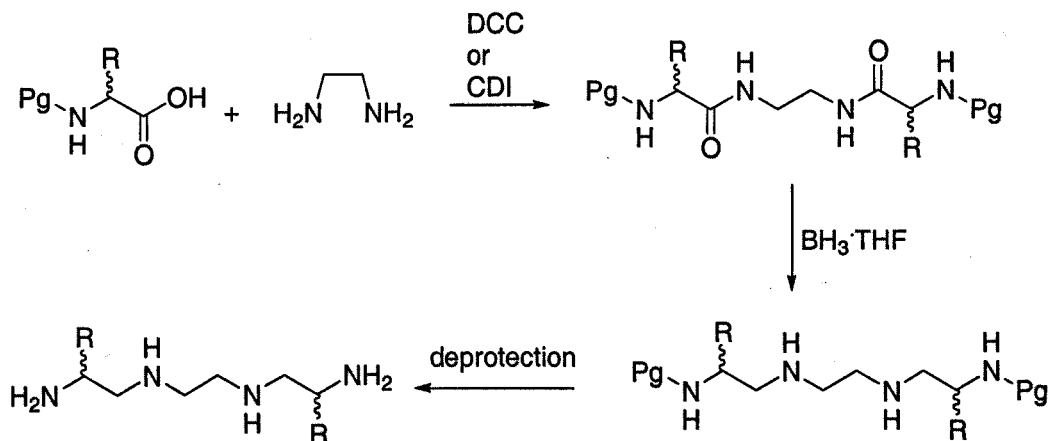
Another possibility is to substitute the parent cyclen-based ring with functionality that will change its electronic character. Although not trivial, there are a few possible routes to synthesise these analogues. The bisimidazoline route (Scheme 1.4.1.10, section 1.4) is a cheap and straightforward option and various substituted dibromoalkanes or diol ditosylates could be used (e.g. Scheme 5.5.2). The dibromoalkanes or ditosylates could either be purchased (if commercially available) or synthesised from alkenyl or styryl precursors.^{229, 230} The main drawback of this approach is the susceptibility of the dibromoalkanes etc. to elimination.^{231, 232} However with the right choice of base this problem might be overcome.

Scheme 5.5.2



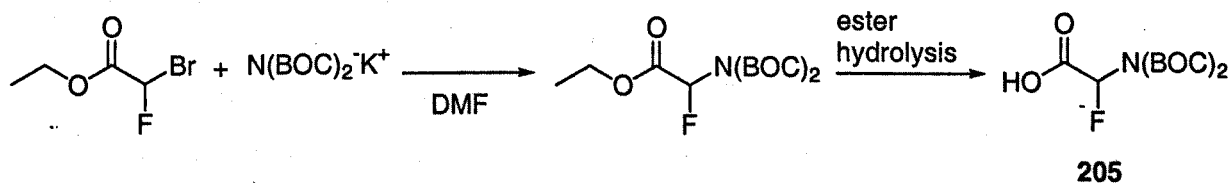
Another novel route to substituted cyclen-based macrocycles could involve coupling *N*-protected amino acids to ethane-1,2-diamine with dicyclohexylcarbodiimide (DCC) or 1,1-carbonyldiimidazole (CDI), followed by reduction of the resulting diamide to the tetraamine (Scheme 5.5.3).

Scheme 5.5.3



These tetraamines could then be cyclised as in **Scheme 5.5.2**, or *via* normal Richman-Atkins cyclisation after conversion into the sulfonamides. Fluorine substituents could be incorporated through the use of protected fluoroglycine (**205**) (synthesised as in **Scheme 5.5.4** using the potassium salt of bis-BOC-protected ammonia^{233,234}). C-Fluorinated amides are known to be stable to reduction using lithium aluminium hydride²³⁵ and borane.²³⁶⁻²³⁸ An advantage of building tetraamines from amino acids is that the stereochemistry of the substituents could be more easily controlled. Another advantage of this route is that it may circumvent any problems with elimination of substituted dibromoalkanes etc. Using lysine as the amino acid would allow for the preparation of polyamine-tagged macrocycles (**Scheme 5.5.5**), which should be able to utilise the polyamine transport system for entrance into cells,¹⁶⁸ which might improve the targeting of the mustard complexes.

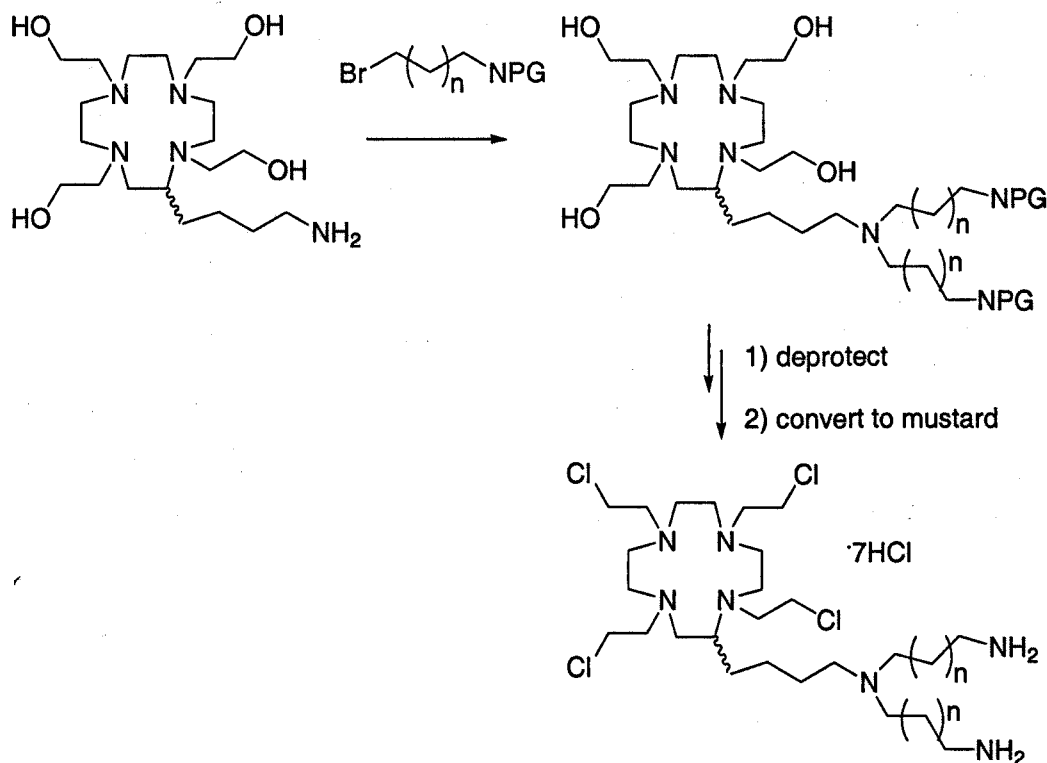
Scheme 5.5.4.



Cyclen analogues synthesised by these routes could be converted into their mustard derivatives and complexed to Cu(II). Mustards substituted with linear polyamine functionality should still complex to Cu(II) preferentially with the macrocyclic hydrochloride salt over the linear triamine salt. The reduction potentials and thermodynamic stabilities of the oxidised (Cu[II]) and reduced (Cu[I])

complexes could be assessed using UV-Vis spectroscopy and cyclic voltammetry (as in Chapter 4). This should provide improved selectivity for the bioreduction of the complex and release of the cytotoxin.

Scheme 5.5.5



Eventually it will be important to understand the biodistribution of these complexes. This can be accomplished by complexing the ligand to a radioactive copper ion, e.g. ⁶⁴Cu(II) or ⁶⁷Cu(II) and tracking the levels of radioactivity in different tissues over time. Indeed, if accumulation of radioactive copper is seen in tumour tissue (as for similar ligands),⁸¹ this strategy might also provide a two-pronged attack against tumours: targeted radiotherapy and release of cytotoxin.

Cu(II) complexes of the analogues described above would be assessed for hypoxia selectivity by Prof. Stratford's group. The best candidates from *in vitro* testing against a range of tumour cell lines would be selected for *in vivo* studies by the Stratford group. It should be possible to progress rapidly towards more selective compounds and a better understanding of these drugs. The results presented in this thesis should stimulate the discovery and development of new hypoxia selective cytotoxins that are useful in the treatment of cancer.

Chapter 6

6. Experimental Section

All experiments were carried out under an atmosphere of N₂ or Ar. Glassware was oven-dried and N₂ cooled. Chemicals were purchased from Aldrich Chemical Company (Gillingham, Dorset, UK) or Lancaster Synthesis Ltd (Morecambe, Lancs, UK) and used without further purification. DMF and ethanol were dried by 3 times sequential drying over 3 Å molecular sieves.²³⁹ 'Wet DMF' refers to DMF that was used as purchased and not dried. Melting points were measured with a Gallenkamp apparatus and are uncorrected. ¹H and ¹³C NMR spectra were recorded on a Bruker DPX 400 spectrometer, with chemical shift values reported in on the δ scale (TMS = 0) relative to residual chloroform ($\delta_{\text{H}} = 7.27$ or $\delta_{\text{C}} = 77.2$) as internal standards unless otherwise stated. Coupling constants (*J*) are reported in Hertz (Hz). Mass spectrometry was performed on a JEOL JMS-700 spectrometer and infrared spectra obtained *via* solution phase (in CDCl₃) IR using an FT-IR spectrophotometer.

6.1. Experimental to Chapter 2

General procedures 2a-l

- a) Formation of diol tosylates:²⁴⁰ *p*-Toluenesulfonyl chloride (1.5 eq., 2.3 M) was dissolved in dry pyridine and held below 0 °C. A solution of the diol (1 eq, 6 M) in dry pyridine was added slowly dropwise while stirring. After 4 h, the mixture was poured into water and the resulting precipitate filtered and washed well with water. It was dried by suction and recrystallized from hot ethanol.
- b) Formation of mesitylenesulfonamides:²⁴⁰ The triamine (1 eq., 1 M) was dissolved in 10% aqueous NaOH solution. A solution of mesitylenesulfonyl chloride (3 eq., 1 M) in diethyl ether was added very slowly dropwise and the mixture stirred extremely vigorously overnight. Methanol was added to

the resulting coagulated precipitate and it was filtered, washed with methanol and dried under vacuum.

c) Richman-Atkins cyclisation of Mts-protected sulfonamides:²⁴⁰ The sulfonamide (1 eq., 0.02 M) was dissolved in dry DMF. NaH (3 eq., 60% suspension in oil) was added, causing fizzing. After stirring for 1 hour, a solution of the diol ditosylate (1 eq., 0.2 M in dry DMF) was added dropwise. The mixture was heated to 100 °C while stirring overnight. The solvent was concentrated *in vacuo* to approximately 10% of its original volume and dripped into 20 times its volume of ice water while stirring. The resulting cream coloured precipitate was filtered, washed well with water and purified by column chromatography (99:1 CHCl₃-MeOH, alumina) or recrystallization.

d) Deprotection of mesitylenesulfonamide-macrocycles (*adapted from Reddy et al.*):¹⁷⁰

1) **Attempted deprotection:** The protected macrocycle (1 eq., 0.09 M) was dissolved in dichloromethane. A solution of phenol (40 eq., 2 M in 30% HBr/AcOH) was added and the mixture stirred very vigorously at reflux for 7 – 9 d. The solution was cooled to r.t., distilled water was added and the mixture extracted with dichloromethane (3 x 50 ml) to remove phenol, some of the acid and unreacted starting material. The dichloromethane was removed *via* rotary evaporation, the residue was taken up in acetone and left in the freezer to crystallize the unreacted sulfonamide. The aqueous layer of the extraction was concentrated to dryness *via* rotary evaporation at ~ 1.0 mm Hg (achieved with a vacuum pump). The resulting crude hydrobromide salt of the polyazamacrocycle was taken up in a minimum of distilled water, basified to above pH 12 with NaOH and extracted with dichloromethane (3 x 50 ml). The organic layer was dried with MgSO₄, filtered and the solvent removed *via* rotary evaporator to give an oil which contained the desired macrocycle plus impurities. Column chromatography was attempted

using 80:20 CHCl_3 -MeOH as eluent on alumina, but no product was isolated.

- 2) Reaction conditions were as above, except that benzyltriethylammonium chloride (0.02 eq.) was also added to the initial reaction mixture and the solution heated at reflux for 14 days followed by 14 days of standing at room temperature. By the end of this period, crystals had formed in the solution, which were filtered off and shown by ^1H NMR spectroscopy to be the HBr salt of the product. The filtrate was worked up as above, but the crude HBr salt from the aqueous layer was washed in hot ethanol and isolated instead of being converted into the free base.
- e) Synthesis of 2-(trimethylsilyl)ethanesulfonic acid, sodium salt (adapted from Weinreb *et al.*):¹⁹⁵ Vinyltrimethylsilane (28 ml, 1 eq.) was combined in a 250 ml round-bottom flask, equipped with a two-neck adaptor, reflux condenser and thermometer, with 70 ml MeOH and t-butyl peroxybenzoate (0.02 eq.). A solution of 36.1 g sodium bisulfite in 70 ml distilled water was added and the suspension stirred and heated to 50 °C for 48-72 h (monitoring the internal temperature). Upon completion, the suspension was transferred to a 1 L flask and the solvent removed by rotary evaporation, adding 50 mL of MeOH twice to assist the removal of residual water. The resulting white solid was taken up in 200 ml MeOH and stirred for 10 min, after which it was filtered through a pad of Celite. The filter cake was removed from the Celite and stirred again with an additional 200 ml of MeOH for 10 min. The process was repeated once more, for a total of 3 washes of the solid. All the filtrates were combined in a tared 500 ml round bottom flask and rotary evaporated. The solid product was dried on the rotary evaporator with a water bath temperature of 60-80 °C for 4 hours.
- f) Synthesis of 2-(trimethylsilyl)ethanesulfonyl chloride (adapted from Weinreb *et al.*):¹⁹⁵ The sulfonate salt (1 eq.), was crushed to a fine powder in a round bottom flask equipped with stir bar, oil bubbler and pressure-equalizing addition funnel and cooled to 0 °C with an ice water bath. Thionyl chloride (16 eq.) was added dropwise *via* the addition funnel,

causing evolution of SO_2 . After all the thionyl chloride was added, catalytic DMF (0.4 eq.) was added slowly *via* syringe. The solution was allowed to come to room temperature and stirred overnight. The excess thionyl chloride was removed by rotary evaporation and the resulting slurry diluted twice with hexane and the hexane evaporated. The slurry was washed well with 200 ml hexane and filtered through a pad of Celite, thoroughly washing through with more hexane. The filtrate was concentrated under reduced pressure to yield the pure product. No further purification was necessary.

- g) Formation of primary sulfonamides from sulfonyl chlorides: The sulfonyl chloride was pre-cooled in an ice-water bath. A solution of concentrated NH_3 (0.88) was added dropwise with stirring. The resulting suspension was held at reflux for 2 h. After cooling to room temperature, water was added to assist precipitation of the product, which was filtered off under suction and washed with water. The resulting crystalline solid was dried under vacuum at 100°C .
- h) Alkylation of primary sulfonamides and cyclisation of SES-protected sulfonamides:¹⁵¹ The sulfonamide was dissolved in dry DMF (1 eq., 0.05 M in DMF) in a 3-neck round bottom flask fitted with a pressure equalizing addition funnel. Caesium carbonate (3 eq.) was added and the mixture stirred. For the alkylation of primary sulfonamides, the alkyl bromide was added *via* syringe. For the cyclisations, the diol ditosylate was dissolved in dry DMF (1 eq., 0.18 M in DMF) and added *via* syringe. The suspension was stirred for 3 – 4 d. The reaction was monitored by TLC (20:1 CH_2Cl_2 -EtOAc, silica) of evaporated aliquots, watching for disappearance of starting material. Upon completion, the solvent was thoroughly removed *in vacuo*, the residue taken up in CH_2Cl_2 and washed with 25 ml distilled water and 25 ml brine. The organic layer was dried with Na_2SO_4 and rotary evaporated to give the crude product. The material was purified by flash chromatography (for tris-SES-sulfonamides: 20:1 CH_2Cl_2 -EtOAc, silica; for nitriles and alcohols: as specified).

- i) Reduction of nitriles:²⁴¹ The nitrile was dissolved in dry THF in a 3-necked round-bottom flask with reflux condenser. BH_3 -THF complex (8 eq., 1 M in THF) was added *via* syringe. The solution was held at reflux for 2 h. Upon cooling to room temperature, the excess borane was carefully quenched with 6 M HCl (5-10 ml). The solution was basified to pH 13-14 with NaOH pellets, extracted with CH_2Cl_2 (3 x 75 ml), dried with Na_2SO_4 , filtered and rotary evaporated to give the pure amine.
- j) Formation of SES-sulfonamides (*Hoye et al.*):¹⁵¹ The triamine in dry DMF (1 eq., 0.7 M in DMF) was combined with triethylamine (5 eq.) in a round bottom flask with a septum and brought to 0 °C. The sulfonyl chloride in dry DMF (4 eq., 3 M in DMF) was added *via* pressure-equalizing addition funnel. The mixture was stirred overnight at 0 °C. The solvent was thoroughly removed *in vacuo* and the residue taken up in distilled water and extracted with dichloromethane (3 x 50 ml). The organic extracts were combined, dried with Na_2SO_4 and concentrated under reduced pressure to give the crude product. The material was purified either by recrystallization in methanol or 2-propanol, or by flash chromatography (9:1 CH_2Cl_2 -EtOAc, silica), giving the product as a white solid.
- k) Deprotection of macrocyclic 2-(trimethylsilyl)ethanesulfonamides:¹⁵¹ The macrocyclic sulfonamide was dissolved in dry DMF (1 eq., 0.05 M in DMF) in a round bottom flask fitted with a reflux condenser and oil bubbler. Caesium fluoride was added (20 eq.) and the mixture held at 95 °C while stirring overnight. The solvent was thoroughly removed *in vacuo*, the white solid residue taken up in CHCl_3 and filtered through Celite with CH_2Cl_2 . The filtrate was concentrated to give the products as oils or waxy solids, which were purified by Kugelrohr distillation.
- l) Synthesis of bisbromomethyl aromatic compounds:²⁰¹ The dimethyl aromatic compound (1 eq.) and *N*-bromosuccinimide (NBS) (4 eq.) were dissolved in CCl_4 . The solution was exposed to UV radiation while stirring. The reaction was monitored by TLC (9:1 DCM/EtOAc) for disappearance of the dimethyl compound. Upon completion, DCM was added (50 ml) to

dissolve all solids and the solvent was evaporated. The residue was purified by recrystallisation to give the bisbromomethyl compound.

Experimental details

6.1.1. Diol ditosylate formation



107

1,2-Ethanediol ditosylate (107)

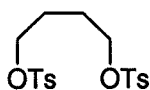
Using 1,2-ethanediol (3.50 g, 56.1 mmol), **107** was prepared according to general procedure **2a** as white crystals (17.2 g, 90% yield). m.p. 121.3-123.7 °C (lit. m.p. 123-125 °C); NMR spectroscopy agreed with literature values.²⁴⁰ δ_{H} (CDCl_3) 2.47 (6 H, s, ArCH_3), 4.19 (4 H, s, TsOCH_2), 7.34-7.76 (8 H, m (AA'BB'), ArH); δ_{C} 22.1 (CH_3), 67.1 (CH_2), 128.4 and 130.4 (CH), 132.7 and 145.7 (C)



108

1,3-Propanediol ditosylate (108)

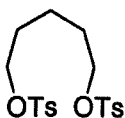
Using 1,3-propanediol (5.00 g, 65.7 mmol), **108** was prepared according to general procedure **2a** as white crystals (18.3 g, 79% yield). m.p. 90.4-92.8 °C (lit. m.p. 91-93 °C); NMR spectroscopy agreed with literature values.²⁴⁰ δ_{H} (CDCl_3) 2.01 (2 H, quintet, J 5.6, CH_2), 2.47 (6 H, s, ArCH_3), 4.07 (4 H, t, J 6.0, TsOCH_2), 7.35-7.77 (8 H, m (AA'BB'), ArH); δ_{C} 22.1 (CH_3), 29.1 (CH_2), 66.2 (TsOCH_2), 128.3 and 130.4 (CH), 133.0 and 145.5 (C)



109

1,4-Butanediol ditosylate (**109**)

Using 1,4-butanediol (3.50 g, 38.8 mmol), **109** was prepared according to general procedure **2a** as white crystals (10.28 g, 66% yield). m.p. 79.7-80.6 °C (lit. m.p. 80-81 °C); NMR spectroscopy agreed with literature values.²⁴² δ_{H} (CDCl_3) 1.70 (4 H, broad s, CH_2), 2.46 (6 H, s, ArCH_3), 3.99 (4 H, broad s, TsOCH_2), 7.34-7.78 (8 H, m (AA'BB'), ArH); δ_{C} 22.1 (CH_3), 25.4 and 69.8 (CH_2), 128.2 and 130.3 (CH), 133.3 and 145.3 (C)

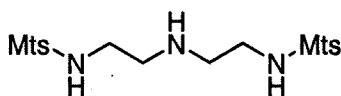


110

1,5-Pentanediol ditosylate (**110**)

Using 1,5-pentanediol (6.84 g, 65.7 mmol), **110** was prepared according to general procedure **2a** as white crystals (22.5 g, 90% yield). m.p. 73.9-75.0 °C; NMR spectroscopy agreed with literature values.²⁴³ δ_{H} (CDCl_3) 1.26-1.39 (2H, m), 1.57-1.64 (4H, m), 2.46 (6H, s), 3.96-3.99 (4H, m), 7.34-7.78 (8H, aa'bb'); δ_{C} (CDCl_3) 22.0 (CH_3), 21.9, 28.6 and 70.4 (CH_2), 128.2 and 130.3 (ArCH), 133.4 and 145.2 (ArC).

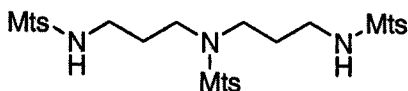
6.1.2. Mesitylenesulfonamides



68

1,7-Bis(mesitylenesulfonyl)triazasheptane (68)

According to general procedure **2b**, using **66** (10.0 g, 96.9 mmol), **68** was isolated as a white powder (10.4 g, 23% yield). m.p. 108.9-111.3 °C; ν_{\max} (CDCl₃ solution cell) 1160, 1322, 1560, 1604, 2855, 2984, 3310, 3406 cm⁻¹; δ_{H} (CDCl₃) 2.30 (6 H, s, CH₂NHSO₂C₆H₂-o-(CH₃)₂-p-CH₃), 2.63 (12 H, s, CH₂NHSO₂C₆H₂-o-(CH₃)₂-p-CH₃), 2.65 (4 H, t, J 5.2, (CH₂)₂NH), 2.94 (4 H, m, Mts-NHCH₂), 6.96 (4 H, s, CH₂NHSO₂C₆H₂(CH₃)₃); δ_{C} 21.3 (p-CH₃), 23.3 (m-CH₃), 42.2 (HNCH₂), 48.2 (Mts-NHCH₂), 132.4 (CH), 133.7, 139.5 and 142.6 (C); m/z (CI⁺ mode isobutane) 468.2 ([M+H]⁺, 38%), 255.2 (100), 119.2 (45). Found: [M+H]⁺ 468.1988. C₂₂H₃₄O₄N₂S₂ requires 468.1991.



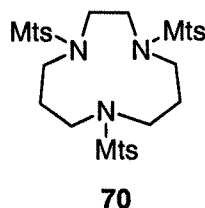
70

1,5,9-Tris(mesitylenesulfonyl)triazanonane (69)

According to general procedure **2b**, using **67** (10.0 g, 76.2 mmol), **69** was isolated as a white powder (47.7 g, 92 % yield). m.p. 121.3-124.3 °C; ν_{\max} (CDCl₃ solution cell) 1154, 1213, 1320, 1604, 2508, 2898, 2984, 3390 cm⁻¹; δ_{H} (CDCl₃) 1.61 (4 H, quintet, J 6.4, NHCH₂CH₂CH₂N), 2.29 (3H, s, (CH₂)₂NSO₂C₆H₂-o-(CH₃)₂-p-CH₃), 2.30 (6 H, s, CH₂NHSO₂C₆H₂-o-(CH₃)₂-p-CH₃), 2.54 (6 H, s, (CH₂)₂NSO₂C₆H₂-o-(CH₃)₂-p-CH₃), 2.59 (12 H, s, CH₂NHSO₂C₆H₂-o-(CH₃)₂-p-CH₃), 2.80 (4 H, broad q, J 5.6, NHCH₂CH₂), 3.19 (4 H, t, J 6.8, CH₂CH₂NR), 4.77 (2 H, broad t, NHCH₂), 6.93 (2 H, s, (CH₂)₂NSO₂C₆H₂(CH₃)₃), 6.95 (4 H, s, CH₂NHSO₂C₆H₂(CH₃)₃); δ_{C} 21.3 (p-CH₃), 23.3 (m-CH₃), 28.0 (CH₂), 39.7 (Mts-NCH₂), 43.3 (Mts-NHCH₂), 132.4 and 132.6 (CH), 139.3, 140.4, 142.5 and 143.4 (C); m/z (CI⁺ mode isobutane)

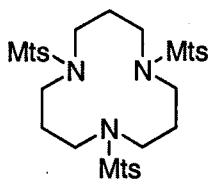
678.2 ($[M+H]^+$, 15%), 494.2 (42), 439.2 (10), 283.2 (31), 269.2 (20), 183.1 (19), 119.2 (100), 105.1 (36). Found: $[M+H]^+$ 678.2714. $C_{33}H_{48}O_6N_3S_3$ requires 678.2705.

6.1.3. Cyclisation of mesitylenesulfonamides



1,4,8-Tris(mesitylenesulfonyl)-1,4,8-triazacycloundecane (70)

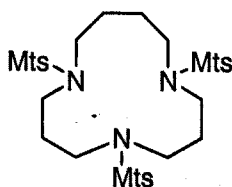
Using **69** (3.60 g, 5.31 mmol) and **107** (1.82 g, 5.31 mmol), **70** was prepared according to general procedure **2c** and purified by column chromatography as a white foamy solid (0.282 g, 7.5% yield). ν_{\max} ($CDCl_3$ solution cell) 1158, 1311, 1605, 1645, 2896, 2975 cm^{-1} ; δ_H ($CDCl_3$) 1.97 (4 H, quintet, J 6.4, $MtsNCH_2CH_2$), 2.30 (3 H, s, $(CH_2)_3N(SO_2C_6H_2-o-(CH_3)_2-p-CH_3)(CH_2)_3$), 2.32 (6 H, s, $(CH_2)_3N(SO_2C_6H_2-o-(CH_3)_2-p-CH_3)(CH_2)_2$), 2.50 (6 H, s, $(CH_2)_3N(SO_2C_6H_2-o-(CH_3)_2-p-CH_3)(CH_2)_3$), 2.58 (12 H, s, $(CH_2)_3N(SO_2C_6H_2-o-(CH_3)_2-p-CH_3)(CH_2)_2$), 3.19-3.28 (8 H, m, $MtsNCH_2CH_2CH_2$), 3.47 (4 H, s, $MtsNCH_2$), 6.94 (2 H, s, $(CH_2)_3N(SO_2C_6H_2-o-(CH_3)_2-p-CH_3)(CH_2)_3$), 6.97 (4 H, s, $(CH_2)_3N(SO_2C_6H_2-o-(CH_3)_2-p-CH_3)(CH_2)_2$); δ_C 21.3, 23.3 and 23.8 (CH_3), 24.9, 42.6, 47.5 and 49.4 (CH_2), 132.4 and 132.7 (CH), 139.6, 140.7, 143.1 and 144.3 (C); m/z (FAB+ mode) 704.4 ($[M+H]^+$, 100%), 521.4 (20), 520.4 (62), 338.3 (26), 336.3 (12), 226.1 (13), 183.1 (19), 119.2 (98). Found: $[M+H]^+$ 704.2862. $C_{35}H_{50}O_6N_3S_3$ requires 704.2862. Microanalysis results: 59.71% C, 7.18% H, 5.79% N. Theoretical: 59.71% C, 7.02% H, 5.97% N.



71

1,5,9-Tris(mesitylenesulfonyl)-1,5,9-triazacyclododecane (71)

Using **69** (6.10 g, 9.00 mmol) and **108** (3.17 g, 9.00 mmol), **71** was prepared according to general procedure **2c** and purified by column chromatography as a white foamy solid (0.983 g, 15% yield). m.p. 206.4-208.9 °C; ν_{\max} (CDCl₃ solution cell) 1154, 1213, 1315, 2898, 2973 cm⁻¹; δ_{H} (CDCl₃) 1.98 (6 H, quintet, J 6.8, [CH₂]₂CH₂), 2.31 (9 H, s, SO₂C₆H₂-o-(CH₃)₂-p-CH₃), 2.58 (18 H, s, SO₂C₆H₂-o-(CH₃)₂-p-CH₃), 3.24 (12 H, t, J 6.8, MtsNCH₂), 6.95 (6 H, s, SO₂C₆H₂-o-(CH₃)₂-p-CH₃); δ_{C} 21.2 and 23.4 (CH₃), 26.2 and 44.5 (CH₂), 132.5 (CH), 140.6 and 143.1 (C); m/z (FAB+ mode) 718.4 ([M+H]⁺, 19%), 534.4 (11), 307.1 (31), 289.1 (12). Found: [M+H]⁺ 718.3016. C₃₆H₅₂O₆N₃S₃ requires 718.3018. Microanalysis results: 60.04% C, 7.14% H, 5.75% N. Theoretical: 60.22% C, 7.16% H, 5.85% N.



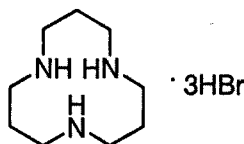
72

1,5,9-Tris(mesitylenesulfonyl)-1,5,9-triazacyclotridecane (72)

Using **69** (4.07 g, 6.00 mmol) and **109** (2.39 g, 6.00 mmol), **72** was prepared according to general procedure **2c** and purified by recrystallization from EtOAc as white crystals (1.7 g, 39% yield). m.p. 211.3-213.1 °C; ν_{\max} (CDCl₃ solution cell) 1152, 1310, 1565, 1610, 1732, 2861, 2985 cm⁻¹; δ_{H} (CDCl₃) 1.79-1.88 (8 H, m, CH₂CH₂N), 2.299 and 2.306 (3 H and 6 H, s, NC₆H₂-o-(CH₃)₂-p-CH₃), 2.55 and 2.57 (6 H and 12 H, s, NC₆H₂-o-(CH₃)₂-p-CH₃), 3.12 (4 H, t, J 5.9, NCH₂CH₂), 3.23 (8 H, m, NCH₂CH₂CH₂N), 6.93 and 6.96 (2 H and 4 H, s, NC₆H₂-o-(CH₃)₂-p-CH₃); δ_{C} 21.3 (p-CH₃), 23.2 and 23.5 (m-CH₃), 27.1 and 28.6 (CH₂), 43.3, 47.9 and 49.6

(NCH₂), 132.4 and 132.6 (CH), 132.8, 133.1, 140.4, 140.6, 142.8, 143.0 (C); Microanalysis results: 60.47% C, 7.27% H, 5.64% N. Theoretical: 60.71% C, 7.30% H, 5.74% N.

6.1.4. Deprotection of mesitylenesulfonamides

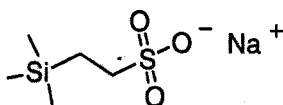


73

1,5,9-Triazacyclododecane trihydrobromide (**73**)

Using **71** (0.500 g, 0.696 mmoles), **73** was prepared according to general procedure **2d-2** as a peach powder (0.256 g, 89% yield); NMR spectroscopy agreed with literature values.²⁴⁴ δ_{H} (D₂O) 2.16 (6 H, quintet, J 6.8, (NCH₂)₂CH₂), 3.28 (12 H, t, J 6.8, NCH₂); δ_{C} (D₂O/DMSO) 20.5 (CH₂), 42.3 (NCH₂).

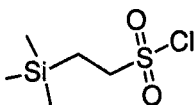
6.1.5. Synthesis of SES-chloride



84

2-(Trimethylsilyl)ethanesulfonic acid, sodium salt (**84**)

Using vinyltrimethylsilane (28 ml, 181 mmol), **84** was prepared according to general procedure **2e** as a white solid (32.0 g, 86% yield); NMR spectroscopy agreed with literature values.¹⁹⁵ δ_{H} (DMSO); 0.00 (9H, s), 0.83-0.88 (2H, m), 2.36-2.41 (2H, m); δ_{C} (DMSO) 0.00 (CH₃), 13.6 and 48.2 (CH₂).

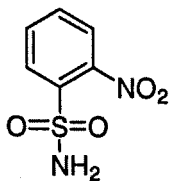


85

2-(Trimethylsilyl)ethanesulfonyl chloride (85)

Using **84** (30.8 g, 151 mmol), **85** was prepared according to general procedure **2f** as a clear oil (25.7 g, 85% yield). TLC (1:1 Pet. Ether-EtOAc, silica) rf. 0.80; NMR spectroscopy agreed with literature values.¹⁹⁵ δ_{H} (CDCl_3) 0.12 (9 H, s, $\text{Si}(\text{CH}_3)_3$), 1.30-1.34 (2 H, m, SiCH_2), 3.59-3.64 (2 H, m, SO_2CH_2); -1.61 (SiCH_3), 12.4 (SiCH_2), 63.8 (SO_2CH_2).

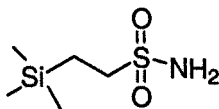
6.1.6. Building triamines from sulfonamides



90

2-Nitrobenzenesulfonamide (90)

Using 2-nitrobenzenesulfonyl chloride (10.0 g, 45.1 mmol) and conc. NH_3 (100 ml), **90** was prepared according to general procedure **2g** and recrystallized from EtOH to give light yellow crystals (5.3 g, 58% yield). Melting point agreed with literature value.²⁴⁵ m.p. 190-193 °C (lit. 190-191 °C); δ_{H} (DMSO) 7.83-7.96 (6 H, m, ArH and NH_2); δ_{C} (DMSO) 124.6, 129.2, 133.0 and 133.8 (CH), 136.1 and 147.5 (C).

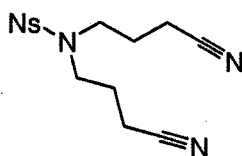


94

(2-Trimethylsilyl)ethanesulfonamide (94)

Ammonia gas, produced by gentle warming (30-40 °C) of 8M aqueous ammonia solution, was bubbled through a stirred solution of **85** (11.0 g, 55 mmol) in

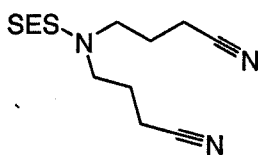
dichloromethane (100 ml) at 0 °C. After 2 h the reaction mixture was filtered, washed with water, dried (MgSO₄) and concentrated to give **94** as a cream crystalline solid (8.73 g, 88% yield) m.p. 85-88 °C; IR: ν_{\max} (Golden Gate) 1147, 1271, 1327, 1547, 2900 and 2952 cm⁻¹; δ_{H} (CDCl₃) 0.08 (9 H, s, Si(CH₃)₃), 1.08-1.12 (2 H, m, SiCH₂), 3.03-3.08 (2 H, m, SO₂CH₂) and 4.59 (2 H, bs, NH₂); δ_{C} (CDCl₃) -1.60 (SiCH₃), 11.3 (SiCH₂) and 52.0 (SO₂CH₂); m/z (FAB+ mode) 352.5 ([M+H]⁺ 100%), 226.2 (7), 169.2 (3), 84.6 (24), 73.7 (95). Found [M+H]⁺ 352.2452, C₁₅H₃₈O₂N₃SiS requires 352.2454.



91

N-(2-Nitrobenzenesulfonyl)-bis-(3-cyanopropyl)amine (**91**)

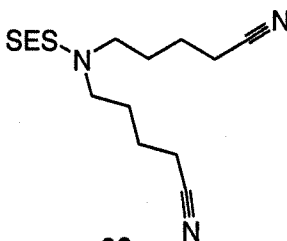
Using **90** (5.00 g, 24.7 mmol) and 4-bromobutyronitrile (7.32 g, 49.5 mmol), **91** was prepared according to general procedure **2h** and recrystallized from MeOH to give yellow crystals (5.6 g, 67% yield); m.p. 85-86 °C; ν_{\max} (CDCl₃ solution cell) 1126, 1165, 1217, 1371, 1468, 1547, 2401, 2902, 2947 and 3020 cm⁻¹; δ_{H} (CDCl₃) 1.93-2.00 (4 H, quintet, J = 7.2, CH₂), 2.40-2.44 (4 H, t, J = 7.1, CH₂CN), 3.42-3.46 (4 H, t, J = 7.4, NCH₂), 7.66-8.10 (4 H, m, ArH); δ_{C} (CDCl₃) 14.9, 24.8 and 46.9 (CH₂), 124.9, 131.7, 132.6 and 134.7 (ArCH), 118.9 and 148.4 (ArC); m/z (CI+ mode isobutane) 363.2 (5%), 337.2 ([M+H]⁺, 100), 307.2 (32), 290.3 (18), 288.3 (3), 276.1 (2), 240.1 (2), 208.2 (2), 181.2 (4), 152.2 (68), 150.1 (28), 124.1 (4), 97.1 (4) and 69.1 (5); Found [M+H]⁺ 337.0971, C₁₄H₁₇O₄N₄S requires 337.0971.



95

N-(2-(Trimethylsilyl)ethanesulfonyl)-bis-(3-cyanopropyl)amine (**95**)

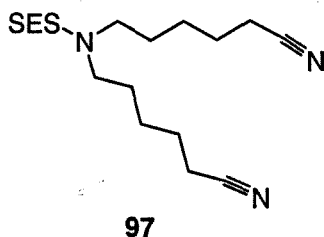
Using **94** (2.00 g, 11.0 mmol) and 4-bromobutyronitrile (3.27 g, 22.1 mmol), **95** was prepared according to general procedure **2h** (no purification necessary) as a beige oil (3.35 g, 96% yield); IR: ν_{max} (Golden Gate) 1138, 1167, 1250, 1327, 1421, 1460, 1672, 2247 and 2953 cm^{-1} ; δ_{H} (CDCl_3) 0.07 (9 H, s, $\text{Si}(\text{CH}_3)_3$), 0.98-1.04 (2 H, m, SiCH_2), 1.95-2.03 (4 H, quintet, $J = 7.2$, CH_2), 2.44-2.48 (4 H, t, $J = 7.0$, CH_2CN), 2.84-2.96 (2 H, m, SO_2CH_2), 3.32-3.36 (4 H, t, $J = 7.1$, NCH_2); m/z (FAB+ mode) 338.1 ($[\text{M}+\text{Na}]^+$, 100%), 271.1 (10), 73.8 (30); Found $[\text{M}+\text{Na}]^+$ 338.1334, $\text{C}_{13}\text{H}_{25}\text{O}_2\text{N}_3\text{SiNa}$ requires 338.5017.



96

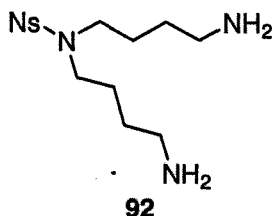
N-(2-(Trimethylsilyl)ethanesulfonyl)-bis-(4-cyanobutyl)amine (**96**)

Using **94** (1.5 g, 8.27 mmol) and 5-bromovaleronitrile (2.68 g, 16.54 mmol), **96** was prepared according to general procedure **2h** and purified by column chromatography (EtOAc, silica) to give a yellow oil (2.16 g, 76% yield); r.f. = 0.64 (EtOAc); IR: ν_{max} (Golden Gate) 1140, 1167, 1250, 1329, 2249 and 2952 cm^{-1} ; ^1H NMR: δ_{H} (CDCl_3) 0.06 (9 H, s), 0.97-1.01 (2 H, m), 1.68-1.81 (8 H, m), 2.42-2.45 (4 H, t, $J = 6.6$), 2.85-2.90 (2 H, m), 3.24-3.28 (4 H, t, $J = 6.8$); ^{13}C NMR: δ_{C} (CDCl_3) -1.6, 10.7, 17.1, 22.6, 47.8, 48.0, 119.6; MS: m/z (CI+ mode) 344.3 ($[\text{M}+\text{H}]^+$, 35%), 316.2 (9), 280.3 (2), 252.2 (30), 226.2 (4), 211.2 (3), 180.2 (2), 138.2 (1), 111.1 (1), 73.1 (3), 57.1 (100); Found $[\text{M}+\text{H}]^+$ 344.1827, $\text{C}_{15}\text{H}_{30}\text{O}_2\text{N}_3\text{Si}$ requires 344.1828.



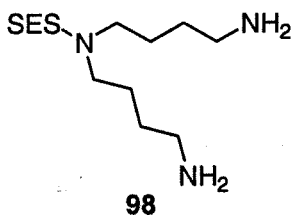
***N*-[(2-Trimethylsilyl)ethanesulfonyl]-bis-(cyanopentyl)amine (**97**)**

Using **94** (1.5 g, 8.27 mmol) and 6-bromocapronitrile (2.91 g, 16.5 mmol), **97** was prepared according to general procedure **2h** purified by column chromatography (EtOAc, silica) to give a yellow oil (2.26 g, 73% yield); r.f. = 0.61 (EtOAc); IR: ν_{max} (Golden Gate) 1139, 1250, 1327 and 2951 cm^{-1} ; ^1H NMR: δ_{H} (CDCl_3) 0.06 (9 H, s), 0.97-1.02 (2 H, m), 1.45-1.53 (4 H, m), 1.61-1.74 (8 H, m), 2.35-2.39 (4 H, t, $J = 7.0$), 2.84-2.88 (2 H, m), 3.19-3.22 (4 H, t, $J = 7.5$); ^{13}C NMR: δ_{C} (CDCl_3) -1.6, 10.7, 17.5, 25.3, 26.1, 29.0, 48.2, 48.3, 119.85; MS: m/z (FAB+ mode) 372.4 ($[\text{M}+\text{H}]^+$ 12%), 280.4 (92), 226.2 (12), 197.2 (12), 149.1 (28), 73.7 (100), 56.0 (9). Found $[\text{M}+\text{H}]^+$ 372.2153, $\text{C}_{17}\text{H}_{34}\text{O}_2\text{N}_3\text{SiS}$ requires 372.2141.



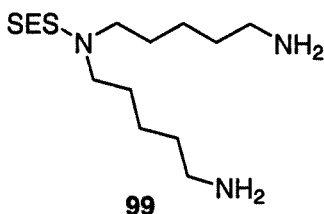
***N*-(2-Nitrobenzenesulfonyl)-bis-(3-aminopropyl)amine (**92**)**

Using **91** (1.00 g, 2.97 mmol), **92** was prepared according to general procedure **2i** as an orange oil (0.70 g, 70% yield); δ_{H} (CDCl_3) 1.37-1.44 (4 H, m, CH_2), 1.51-1.64 (4 H, m, CH_2), 2.66-2.69 (4 H, t, $J = 7.0$, Ns-NCH_2), 3.28-3.32 (4 H, t, $J = 7.8$, NCH_2), 7.60-8.03 (4 H, m, ArH).



6-[(2-Trimethylsilyl)ethanesulfonyl]-1,6,11-triazaundecane (98)

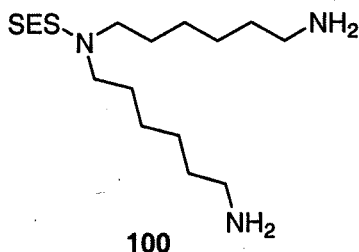
Using **95** (3.28 g, 10.4 mmol), **98** was prepared according to general procedure **2i** as a clear oil (3.24 g, 96% yield); IR: ν_{\max} (Golden Gate) 1136, 1165, 1215, 1252, 1323, 1458, 1560, 2341, 2360 and 2943 cm^{-1} ; δ_{H} (CDCl_3) 0.06 (9 H, s, $\text{Si}(\text{CH}_3)_3$), 0.98-1.04 (2 H, m, SiCH_2), 1.42-1.49 (4 H, m, CH_2), 1.60-1.68 (4 H, m, CH_2), 2.71-2.73 (4 H, t, $J = 7.0$, SES-NCH_2), 3.20-3.24 (4 H, t, $J = 7.7$, NCH_2); δ_{C} (CDCl_3) -1.6 (SiCH_3), 10.7 (SiCH_2), 26.9, 31.1, 42.1, 48.4 and 48.9 (CH_2); m/z (FAB+ mode) 324.2 ($[\text{M}+\text{H}]^+$, 50%), 253.1 (10), 226.1 (5), 136.1 (6), 101.4 (5), 73.8 (100) and 70.9 (23);



Found $[\text{M}+\text{H}]^+$ 324.2147, $\text{C}_{13}\text{H}_{34}\text{O}_2\text{N}_3\text{SiS}$ requires 324.2141.

7-[(2-Trimethylsilyl)ethanesulfonyl]-1,7,13-triazatridecane (99)

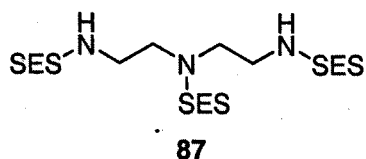
Using **96** (2.10 g, 6.11 mmol), **99** was prepared according to general procedure **2i** as a clear oil (2.05 g, 95% yield); IR: ν_{\max} (Golden Gate) 1167, 1248, 1327, 1560, 2862 and 2927 cm^{-1} ; ^1H NMR: δ_{H} (CDCl_3) 0.06 (9H, s), 0.98-1.02 (2H, m), 1.24-1.51 (12 H, m), 1.56-1.64 (4 H, quintet, $J = 7.3$), 2.68-2.72 (4 H, t, $J = 7.0$), 2.83-2.88 (2 H, m), 3.18-3.22 (4 H, t, $J = 7.6$); ^{13}C NMR: δ_{C} (CDCl_3) -1.7, 10.7, 24.3, 29.3, 33.6, 42.3, 48.1, 48.3; MS: m/z (FAB+ mode) 352.5 ($[\text{M}+\text{H}]^+$ 100%), 226.2 (7), 169.2 (3), 84.6 (24), 73.7 (95). Found $[\text{M}+\text{H}]^+$ 352.2452, $\text{C}_{15}\text{H}_{38}\text{O}_2\text{N}_3\text{SiS}$ requires 352.2454.



8-[(2-Trimethylsilyl)ethanesulfonyl]-1,8,15-triazapentadecane (**100**)

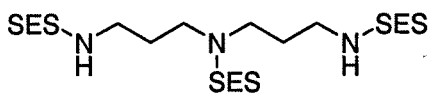
Using **97** (2.24 g, 6.03 mmol), **100** was prepared according to general procedure **2i** as a clear oil (2.22 g, 97% yield); IR: ν_{\max} (Golden Gate) 1165, 1250, 1325, 1464, 1572, 2856 and 2929 cm^{-1} ; ^1H NMR: δ_{H} (CDCl_3) 0.04 (9 H, s), 0.97-1.01 (2 H, m), 1.21-1.48 (16 H, m), 1.54-1.61 (4 H, quintet, $J = 7.4$), 2.68 (4H, t, $J = 6.9$), 2.82-2.86 (2 H, m), 3.18 (4 H, t, $J = 6.7$); ^{13}C NMR: δ_{C} (CDCl_3) -1.6, 10.7, 26.9, 26.9, 29.4, 33.9, 42.3, 48.1, 48.3; MS: m/z (FAB+ mode) 380.5 ($[\text{M}+\text{H}]^+$ 72%), 288.4 (3), 226.2 (4), 185.3 (4), 98.5 (16), 73.7 (100). Found $[\text{M}+\text{H}]^+$ 380.2773, $\text{C}_{17}\text{H}_{42}\text{O}_2\text{N}_3\text{SiS}$ requires 380.2767.

6.1.7. SES-amide synthesis



1,4,7-Tris[(2-trimethylsilyl)ethanesulfonyl]-1,4,7-triazaheptane (**87**)

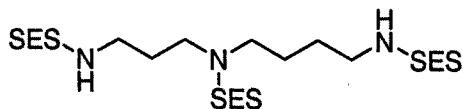
Using **66** (1.5 g, 14.5 mmol) and **85** (10.2 g, 50.9 mmol), **87** was prepared according to general procedure **2j** and purified by column chromatography to give a cream solid (4.03 g, 46% yield); ^1H and ^{13}C NMR data agreed with literature values.¹⁵¹ δ_{H} (CDCl_3) 0.06 (27 H, s, $\text{Si}(\text{CH}_3)_3$), 1.00-1.05 (6 H, m, SiCH_2), 2.96-3.05 (6 H, m, SO_2CH_2), 3.34-3.38 (4 H, q, J 6.0, NHCH_2), 3.44-3.46 (4 H, t, J 5.6, $\text{N}(\text{CH}_2)_2$), 5.09 (2 H, broad s, NH); δ_{C} -1.59 (CH_3), 10.4 and 10.8 (SiCH_2), 43.0 (NCH_2), 47.8 and 49.4 (SO_2CH_2), 50.8 (NHCH_2)



88

1,5,9-Tris[(2-trimethylsilyl)ethanesulfonyl]-1,5,9-triazanonane (88)

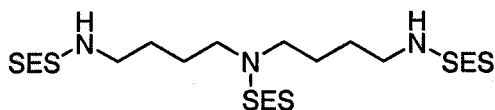
Using **67** (0.820 g, 6.23 mmol) and **85** (5.00 g, 24.9 mmol), **88** was prepared according to general procedure **2j** and purified by column chromatography to give a white waxy solid (2.77 g, 71% yield); m.p. 100.2-101.5 °C (lit. 106.5-107.5 °C¹⁵¹); ¹H and ¹³C NMR and IR data agreed with literature values.¹⁵¹ ν_{\max} (CDCl₃ solution cell) 1340, 1166, 1213, 1253, 1330, 1711, 2897, 2978, 3398 cm⁻¹; δ_{H} (CDCl₃) 0.07 (27 H, s, Si(CH₃)₃), 0.97-1.04 (6 H, m, SiCH₂), 1.85 (4 H, quintet, J 8.0, (CH₂)₂CH₂), 2.89-2.96 (6 H, m, SO₂CH₂), 3.21 (4 H, broad q, J 7.9, CH₂NH), 3.36 (4 H, t, J 8.0, CH₂N), 4.94 (2 H, t, J 8.0, NH); δ_{C} -1.58 (SiCH₃), 10.6 and 10.9 (SiCH₂), 32.7 (CH₂), 41.9 (NCH₂), 48.7 and 48.9 (SO₂CH₂), 50.8 (NHCH₂).



89

1,5,10-Tris[(2-trimethylsilyl)ethanesulfonyl]-1,5,10-triazadecane (89)

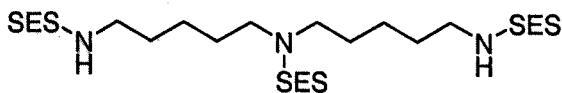
Using **59** (2.60 g, 36.1 mmol) and **85** (14.5 g, 72.2 mmol), **89** was prepared according to general procedure **2j** and recrystallised from methanol/water (~1:2) to give a cream powder (10.0 g, 87% yield); m.p. 104-106 °C; ν_{\max} (CDCl₃ solution cell) 1142, 1169, 1254, 1327, 1383, 1468, 2900, 2956, 3294 and 3394 cm⁻¹; δ_{H} (CDCl₃) 0.06 (27 H, s, SiCH₃), 0.98-1.04 (6 H, m, SiCH₂), 1.57-1.64 (2 H, quintet, J = 6.8, CH₂), 1.69-1.76 (2 H, quintet, J = 6.8, CH₂), 1.82-1.88 (2 H, quintet, J = 6.0, CH₂), 2.87-2.96 (6 H, m, SO₂CH₂), 3.12-3.37 (8 H, m, NCH₂), 4.63-4.66 (1 H, t, J = 6.4, NH) and 5.15-5.18 (1 H, t, J = 6.8, NH); δ_{C} (CDCl₃) -1.60 (SiCH₃), 10.9 (SiCH₂), 26.5, 27.7, 30.6, 40.3, 43.0, 46.1, 47.7 and 49.0 (CH₂); *m/z* (FAB+ mode NaI) 660.1 ([M+Na]⁺, 100 %), 494.2 (11.5), 330.2 (6.5), 273.1 (7), 147.1 (5), 73.8 (98) and 60.0 (8); Found [M+Na]⁺ 660.2457, C₂₂H₅₅O₆N₃Si₃S₃Na requires 660.2459.



104

1,6,11-Tris[(2-trimethylsilyl)ethanesulfonyl]-1,6,11-triazaundecane (**104**)

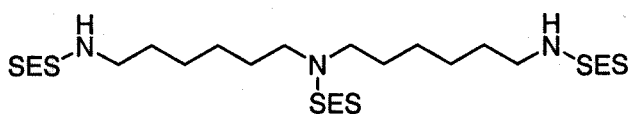
Using **98** (1.27 g, 3.97 mmol) in DMF (10 ml) and **85** (2.00 g, 9.94 mmol), **104** was prepared according to general procedure **2j** and purified by column chromatography to give a white solid (1.33 g, 52% yield); m.p. 145.5-146.8 °C; IR: ν_{\max} (Golden Gate) 1036, 1072, 1109, 1130, 1171, 1244, 1267, 1284, 1311, 1421, 2954 and 3278 cm^{-1} ; ^1H NMR: δ_{H} (CDCl_3) 0.07 (27 H, s), 0.98-1.03 (6 H, m), 1.60-1.67 (4 H, m), 1.74-1.80 (4 H, m), 2.86-2.97 (6 H, m), 3.14-3.20 (4 H, q, $J = 6.2$), 3.23-3.27 (4 H, t, $J = 7.2$), 4.93-4.96 (2 H, t, $J = 6.2$); ^{13}C NMR: δ_{C} (CDCl_3) -1.6, 10.5, 10.9, 26.5, 27.6, 43.0, 47.6, 48.7, 49.2; MS: m/z (FAB+ mode NaI) 674.1 ($[\text{M}+\text{Na}]^+$, 56 %), 560.2 (13), 486.1 (10), 305.1 (22), 136.0 (9), 73.3 (100); Found $[\text{M}+\text{Na}]^+$ 674.2609, $\text{C}_{23}\text{H}_{57}\text{O}_6\text{N}_3\text{Si}_3\text{S}_3\text{Na}$ requires 674.2615.



105

1,7,13-Tris[(2-trimethylsilyl)ethanesulfonyl]-1,7,13-triazatridecane (**105**)

Using **99** (2.00 g, 5.69 mmol) and **85** (2.86 g, 14.2 mmol), **105** was prepared according to general procedure **2j** and recrystallised from isopropanol/water (~2:1) to give a cream solid (2.42 g, 62% yield); m.p. 95-99 °C; IR: ν_{\max} (Golden Gate) 1171, 1246, 1315 and 2951 cm^{-1} ; ^1H NMR: δ_{H} (CDCl_3) 0.05 (9 H, s), 0.06 (18 H, s), 0.97-1.03 (6 H, m), 1.39-1.45 (4 H, m), 1.57-1.67 (8 H, m), 2.84-2.88 (2 H, m), 2.91-2.95 (4 H, m), 3.12 (4 H, q, $J = 6.6$), 3.20 (4 H, t, $J = 7.4$), 4.49 (2 H, t, $J = 6.1$); ^{13}C NMR: δ_{C} (CDCl_3) -1.6, 10.7, 11.0, 23.8, 29.0, 30.3, 43.4, 48.0, 48.4, 49.0, 138.4; MS: m/z (FAB+ mode NaI) 702.6 ($[\text{M}+\text{Na}]^+$ 38%), 664.5 (5), 616.6 (6), 588.6 (18), 516.5 (22), 514.5 (18), 333.4 (18), 279.3 (9), 215.2 (8), 136.1 (20), 73.4 (99); Found $[\text{M}+\text{Na}]^+$ 702.2898, $\text{C}_{25}\text{H}_{61}\text{N}_3\text{O}_6\text{Si}_3\text{S}_3\text{Na}$ requires 702.2928.

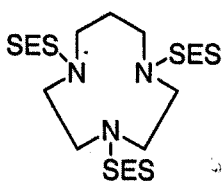


106

1,8,15-Tris[(2-trimethylsilyl)ethanesulfonyl]-1,8,15-triazapentadecane (106)

Using **100** (2.20 g, 5.79 mmol) and **85** (3.02 g, 15.0 mmol), **106** was prepared according to general procedure **2j** and purified by column chromatography to give white crystals (2.67 g, 65%); m.p. 89-91 °C; IR: ν_{\max} (Golden Gate) 1173, 1246, 1284, 1313, 1460, 2856 and 2929 cm^{-1} ; ^1H NMR: δ_{H} (CDCl_3) 0.05 (9 H, s), 0.06 (18 H, s), 0.97-1.03 (6 H, m), 1.35-1.44 (8 H, m), 1.54-1.63 (8 H, m), 2.83-2.88 (2 H, m), 2.91-2.95 (4 H, m), 3.11 (4 H, q, $J = 6.7$), 3.19 (4 H, t, $J = 7.5$), 4.50 (2 H, t, $J = 6.1$); ^{13}C NMR: δ_{C} (CDCl_3) -1.6, 1.4, 10.7, 11.0, 26.3, 29.3, 30.7, 43.5, 48.1, 48.3, 49.0; MS: m/z (FAB+ mode NaI) 730.7 ($[\text{M}+\text{Na}]^+$ 12%), 616.7 (4), 542.5 (3), 293.3 (1), 226.2 (1), 147.1 (2), 73.3 (100), 44.1 (12); Found $[\text{M}+\text{Na}]^+$ 730.3224, $\text{C}_{27}\text{H}_{65}\text{N}_3\text{O}_6\text{Si}_3\text{S}_3\text{Na}$ requires 730.3241.

6.1.8. Cyclisation of SES-amides

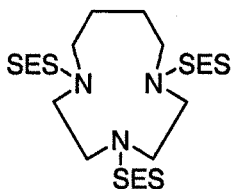


111

1,4,7-Tris[(2-trimethylsilyl)ethanesulfonyl]-1,4,7-triazacyclodecane (111)

Using **87** (0.650 g, 1.09 mmol) and **108** (0.380 g, 1.09 mmol) in DMF (20 ml), **111** was prepared according to general procedure **2h** and purified by column chromatography to give a white solid (0.334 g, 53% yield); mp = 82.1-84.5 °C; ν_{\max} (Golden Gate) 1068, 1136, 1167, 1248, 1325, 1454 and 2952 cm^{-1} ; δ_{H} (CDCl_3) 0.07 (27 H, s, $\text{Si}(\text{CH}_3)_3$), 1.02-1.06 (6 H, m, SiCH_2), 1.67 (2 H, m, NCH_2CH_2), 2.95-3.00 (6 H, m, SO_2CH_2), 3.31-3.54 (12 H, m, NCH_2); δ_{C} -1.61 (SiCH_3), 9.97 and 10.2 (SiCH_2), 30.7 (CH_2), 45.9 and 46.4 (SO_2CH_2), 48.2, 52.4 and 52.7 (NCH_2); m/z (EI+

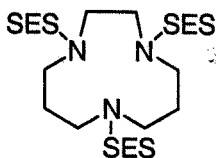
mode) 620.3 ($[M-CH_3]^+$, 6%), 470.3 (45), 406.3 (10), 378.3 (10), 350.3 (7), 212.2 (10), 140.2 (13), 73.1 (100); Found $[M-CH_3]^+$ 620.2170, $C_{21}H_{50}N_3O_6S_3Si_3$ requires 621.0990.



112

1,4,7-Tris[(2-trimethylsilyl)ethanesulfonyl]-1,4,7-triazacycloundecane (112)

Using **87** (0.570 g, 0.954 mmol) and **109** (0.380 g, 0.954 mmol), **112** was prepared according to general procedure **2h** and purified by column chromatography to give a cream solid (0.176 g, 28% yield); m.p. 193-195 °C (dec.); ν_{\max} (Golden Gate) 978, 1009, 1136, 1167, 1248, 1325, 1367, 1417, 1464 and 2952 cm^{-1} ; δ_H ($CDCl_3$) 0.07 (27 H, s, $Si(CH_3)_3$), 0.975-1.10 (6 H, m, $SiCH_2$), 1.93 (4 H, broad m, NCH_2CH_2), 2.91-3.08 (6 H, m, SO_2CH_2), 3.30-3.49 (12 H, m, NCH_2); δ_C -1.60 ($SiCH_3$), 10.2 ($SiCH_2$), 25.1 (CH_2), 45.7 (SO_2CH_2), 50.2, 51.5 and 53.8 (NCH_2); m/z (FAB+ mode NaI) 1322.0 ($[2M+Na]^+$, 13%), 672.3 ($[M+Na]^+$, 100%), 484.4 (68), 342.3 (23), 136.1 (63), 73.4 (98); Found $[M+Na]^+$ 672.2478, $C_{23}H_{55}N_3O_6Si_3S_3Na$ requires 672.2459.

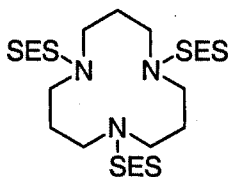


113

1,5,9-Tris[(2-trimethylsilyl)ethanesulfonyl]-1,5,9-triazacycloundecane (113)

Using **88** (0.98 g, 1.57 mmol) and **107** (0.54 g, 1.57 mmol), **113** was prepared according to general procedure **2h** and recrystallised from MeOH to give a cream solid (0.43 g, 45% yield); m.p. 181.4-184.6 °C; ν_{\max} (Golden Gate) 1016, 1134, 1164, 1248, 1325, 1417, 1454 and 2952 cm^{-1} ; δ_H ($CDCl_3$) 0.07 (27 H, s, $Si(CH_3)_3$), 0.98-1.04 (6 H, m, $SiCH_2$), 2.02-2.05 (4 H, m, NCH_2CH_2), 2.85-2.97 (6 H, m, SO_2CH_2), 3.19-3.49 (12 H, m, NCH_2); δ_C ($CDCl_3$) -1.61, 10.1, 10.4, 26.1, 44.3, 45.4, 46.7,

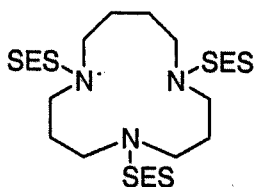
49.2, 52.6; m/z (FAB+ mode NaI) 1321.8 ($[2M+Na]^+$, 20%), 672.3 ($[M+Na]^+$, 100%), 586.5 (37), 484.4 (37), 136.1 (60), 73.4 (37); Found $[M+Na]^+$ 672.2478, $C_{23}H_{55}N_3O_6Si_3S_3Na$ requires 672.2459.



114

1,5,9-Tris[(2-trimethylsilyl)ethanesulfonyl]-1,5,9-triazacyclododecane (114)

Using **88** (2.00 g, 3.20 mmol) and **108** (1.23 g, 3.20 mmol) in DMF (40 ml), **114** was prepared according to general procedure **2h** and purified by column chromatography to give a white solid (1.03 g, 48% yield); m.p. 176.3-178.2 °C (lit. 177.6-178.7 °C¹⁵¹); 1H and ^{13}C NMR data agreed with literature values;¹⁵¹ δ_H ($CDCl_3$) 0.07 (27 H, s, $Si(CH_3)_3$), 0.98-1.03 (6 H, m, $SiCH_2$), 2.01-2.06 (6 H, m, NCH_2CH_2), 2.85-2.90 (6 H, m, $SiCH_2$), 3.37-3.41 (12 H, m, NCH_2); δ_C -1.73 ($SiCH_3$), 10.4 ($SiCH_2$), 28.4 (CH_2), 45.8 (NCH_2), 46.5 (SO_2CH_2).

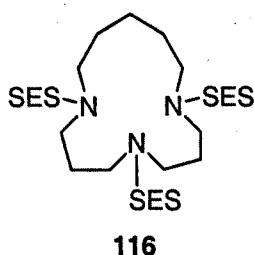


115

1,5,9-Tris[(2-trimethylsilyl)ethanesulfonyl]-1,5,9-triazacyclotridecane (115)

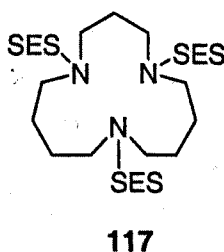
Using **88** (2.00 g, 3.13 mmol) and **109** (1.20 g, 3.13 mmol) in DMF (40 ml), **115** was prepared according to general procedure **2h** and recrystallised from MeOH to give a white solid (1.38 g, 64% yield); m.p. 189.4-191.8 °C; ν_{max} (Golden Gate) 1018, 1064, 1107, 1130, 1167, 1215, 1248, 1325, 1358, 1450, 1466 and 2952 cm^{-1} ; δ_H ($CDCl_3$) 0.05-0.06 (27 H, 2s, $Si(CH_3)_3$), 0.98-1.01 (6 H, m, CH_2CH_2Si), 1.84 (4 H, broad s, CH_2CH_2NSES), 1.95 (4 H, m, $CH_2(CH_2NSES)_2$), 2.83-2.89 (6 H, m, SO_2CH_2), 3.32-3.35 (8 H, m, $CH_2(SESNCH_2)_2$), 3.45-3.48 (4 H, m, $SESNCH_2CH_2$);

δ_C (ref. $\text{CHCl}_3 = 79.0$) 0.00 and 0.048 (CH_3Si), 12.1 and 12.3 (CH_2Si), 30.1 and 30.7 (SO_2CH_2), 45.5, 47.7, 49.8, 51.4 and 53.6 (CH_2); m/z (FAB+ mode) 678.3 ($[\text{M}+\text{H}]^+$, 9%), 614.4 (10%), 512.3 (25%), 348.3 (12%), 210.1 (9.5%); Found: $[\text{M}+\text{H}]^+$ 678.2955, $\text{C}_{25}\text{H}_{60}\text{O}_6\text{N}_3\text{Si}_3\text{S}_3$ requires 678.2952.



1,5,9-Tris[(2-trimethylsilyl)ethanesulfonyl]-1,5,9-triazacyclotetradecane (116)

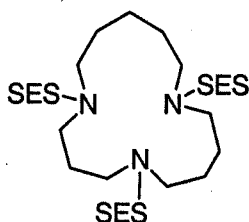
Using **88** (2.00 g, 3.20 mmol) and **110** (1.32 g, 3.20 mmol) in DMF (40 ml), **116** was prepared according to general procedure **2h** and purified by column chromatography to give a white solid (1.21 g, 54% yield); m.p. 175.0-177.3 °C; ν_{max} (CDCl_3 solution cell) 1142, 1167, 1254, 1333, 1381, 1464, 2866, 2902 and 2956 cm^{-1} ; δ_H (CDCl_3) 0.06 (27 H, s, SiCH_3), 0.96-1.04 (6 H, m, SiCH_2), 1.57-1.64 (2 H, m, CH_2), 1.67-1.72 (4 H, m, CH_2), 1.90-1.97 (4 H, m, CH_2), 2.84-2.89 (6 H, m, SO_2CH_2), 3.23-3.40 (12 H, m, NCH_2); δ_C (CDCl_3) -1.6 (SiCH_3), 10.4 and 10.6 (SiCH_2), 23.7, 29.4, 31.0, 45.8, 46.9, 48.5, 48.7 and 50.7 (CH_2); m/z (FAB+ mode NaI) 714.1 ($[\text{M}+\text{Na}]^+$, 15%), 548.2 (4), 526.2 (4), 362.2 (3), 360.2 (2.9), 268.2 (1), 210.1 (5), 98.5 (5) and 73.8 (100); Found $[\text{M}+\text{Na}]^+$ 714.2930, $\text{C}_{26}\text{H}_{61}\text{O}_6\text{N}_3\text{Si}_3\text{S}_3\text{Na}$ requires 714.2928.



1,5,10-Tris[(2-trimethylsilyl)ethanesulfonyl]-1,5,10-triazacyclotetradecane (117)

Using **89** (2.00 g, 3.13 mmol) and **109** (1.25 g, 3.13 mmol) in DMF (40 ml), **117** was prepared according to general procedure **2h** and purified by column chromatography to give a white solid (0.90 g, 41% yield); m.p. 145.0-147.6 °C; ν_{max} (CDCl_3 solution

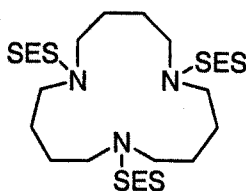
cell) 1142, 1167, 1254, 1333, 1379, 1460, 2866, 2922 and 2956 cm^{-1} ; δ_{H} (CDCl_3) 0.05 (27 H, s, SiCH_3), 0.97-1.03 (6 H, m, SiCH_2), 1.76 (8 H, bs, CH_2), 1.99-2.05 (2 H, m, CH_2), 1.90-1.97 (4 H, m, CH_2), 2.83-2.88 (6 H, m, SO_2CH_2), 3.20-3.30 (12 H, m, NCH_2); δ_{C} (CDCl_3) -1.6 (SiCH_3), 10.37 and 10.42 (SiCH_2), 27.5, 27.6, 32.8, 45.9, 49.0, 50.4 and 51.6 (CH_2); m/z (FAB+ mode NaI) 714.1 ($[\text{M}+\text{Na}]^+$, 27%), 548.2 (6), 362.2 (5), 360.2 (4), 305.2 (1), 210.1 (5), 142.1 (2), 84.5 (10), 73.8 (100) and 59.9 (5); Found $[\text{M}+\text{Na}]^+$ 714.2926, $\text{C}_{26}\text{H}_{61}\text{O}_6\text{N}_3\text{Si}_3\text{S}_3\text{Na}$ requires 714.2928.



118

1,5,10-Tris[(2-trimethylsilyl)ethanesulfonyl]-1,5,10-triazacyclopentadecane (118)

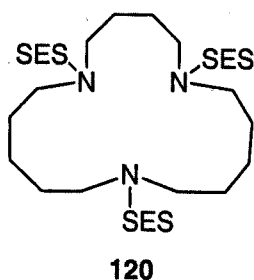
Using **89** (5.00 g, 7.82 mmol) and **110** (3.23 g, 7.82 mmol), **118** was prepared according to general procedure **2h** and purified by column chromatography to give a white glassy solid (2.41 g, 47% yield); m.p. 95.2-97.5 $^{\circ}\text{C}$; ν_{max} (CDCl_3 solution cell) 1140, 1167, 1254, 1333, 1377, 1464, 2868, 2902 and 2956 cm^{-1} ; δ_{H} (CDCl_3) 0.06 (27 H, s, SiCH_3), 0.96-1.03 (6 H, m, SiCH_2), 1.55-1.65 (10 H, m, CH_2), 1.94-1.98 (2 H, m, CH_2), 2.84-2.89 (6 H, m, SO_2CH_2), 3.20-3.34 (12 H, m, NCH_2); m/z (FAB+ mode NaI) 728.1 ($[\text{M}+\text{Na}]^+$, 93%), 654.1 (1.5), 562.2 (17), 540.2 (4), 490.2 (1), 420.2 (1), 398.2 (11), 376.2 (2.5), 341.2 (1), 210.1 (5), 177.2 (1.5), 84.7 (6.5) and 73.8 (100); Found $[\text{M}+\text{Na}]^+$ 728.3083, $\text{C}_{27}\text{H}_{63}\text{O}_6\text{N}_3\text{Si}_3\text{S}_3\text{Na}$ requires 728.3085.



119

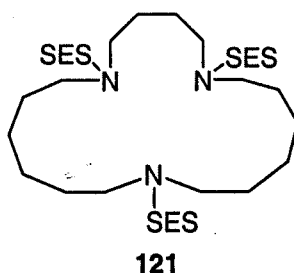
1,6,11-Tris[(2-trimethylsilyl)ethanesulfonyl]-1,6,11-triazacyclopentadecane (119)

Using **104** (0.940 g, 1.45 mmol) and **109** (0.580 g, 1.45 mmol), **119** was prepared according to general procedure **2h** and purified by column chromatography to give a white solid (0.294 g, 29% yield). m.p. 133.2-135.0 °C; ν_{\max} (Golden Gate) 1045, 1105, 1134, 1167, 1211, 1248, 1325, 1376, 1417, 1456, 2952 and 3020 cm^{-1} ; δ_{H} (CDCl_3) -0.07 (27 H, s, $\text{Si}(\text{CH}_3)_3$), 0.80-0.93 (6 H, m, SiCH_2), 1.58 (12 H, broad s, CH_2), 2.66-2.81 (6 H, m, SO_2CH_2), 3.11 (12 H, broad s, NCH_2); δ_{C} (CDCl_3) -1.59 (SiCH_3), 10.5, 27.3, 46.2 and 50.1 (CH_2). m/z (FAB+ mode NaI) 728.3 ($[\text{M}+\text{Na}]^+$, 70%), 690.2 (13), 642.3 (15), 540.3 (60), 476.3 (6), 376.2 (42), 374.2 (27), 210.0 (31), 142.1 (10); Found $[\text{M}+\text{Na}]^+$ 728.3054, $\text{C}_{27}\text{H}_{63}\text{O}_6\text{N}_3\text{Si}_3\text{S}_3\text{Na}$ requires 728.3084.



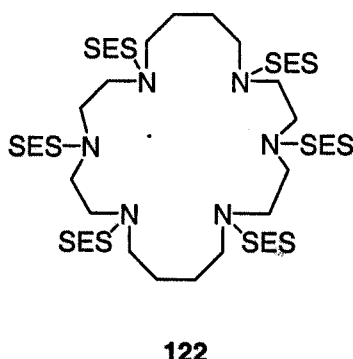
1,6,12-Tris[(2-trimethylsilyl)ethanesulfonyl]-1,6,12-triazacycloheptadecane (120)

Using **105** (1.80 g, 2.64 mmol) and **109** (0.97 g, 2.64 mmol), **120** was prepared according to general procedure **2h** and purified by column chromatography to give a white solid (0.56 g, 29% yield); m.p. 120-124°C; IR: ν_{\max} (Golden Gate) 1136, 1165, 1250, 1327 and 2951 cm^{-1} ; ^1H NMR: δ_{H} (CDCl_3) 0.05 (27 H, s), 0.97-1.02 (6 H, m), 1.40-1.47 (4 H, m), 1.59-1.69 (12 H, m), 2.84-2.88 (6 H, m), 3.18-3.24 (12 H, m); ^{13}C NMR: δ_{C} (CDCl_3) -1.6, 1.4, 10.6, 10.7, 23.6, 27.6, 29.4, 30.1, 47.3, 47.7, 48.6, 49.6, 49.7; MS: m/z (FAB+ mode) 734.8 ($[\text{M}+\text{H}]^+$ 2%), 718.7 (2), 670.8 (4), 614.7 (4), 568.6 (6), 404.5 (6), 402.5 (4), 210.2 (6), 147.1 (3), 73.7 (100); Found $[\text{M}+\text{H}]^+$ 734.3541, $\text{C}_{29}\text{H}_{68}\text{O}_6\text{N}_3\text{Si}_3\text{S}_3$ requires 734.3578.



1,6,13-Tris[(2-trimethylsilyl)ethanesulfonyl]-1,6,13-triazacyclononadecane (121)

Using **106** (2.60 g, 3.66 mmol) and **109** (1.34 g, 3.66 mmol), **121** was prepared according to general procedure **2h** and purified by column chromatography to give a white solid (0.59 g, 21% yield); m.p. 129-134°C; IR: ν_{\max} (Golden Gate) 1167, 1248, 1327, 2860 and 2929 cm^{-1} ; ^1H NMR: δ_{H} (CDCl_3) 0.05 (27 H, s), 0.97-1.01 (6 H, m), 1.37-1.44 (8 H, m), 1.62-1.68 (12 H, m), 2.83-2.88 (6 H, m), 3.16-3.23 (12 H, m); ^{13}C NMR: δ_{C} (CDCl_3) -1.6, 1.3, 10.5, 26.3, 26.3, 27.1, 29.7, 29.9, 46.7, 46.9, 49.3, 49.9, 50.0; MS: m/z (FAB+ mode) 762.8 ($[\text{M}+\text{H}]^+$ 2%), 746.8 (3), 698.8 (7), 642.7 (6), 596.7 (17), 432.6 (13), 430.6 (11), 210.2 (6), 147.1 (3) 73.7 (100); Found $[\text{M}+\text{H}]^+$ 762.3885, $\text{C}_{15}\text{H}_{30}\text{O}_2\text{N}_3\text{SiS}$ requires 762.3891.

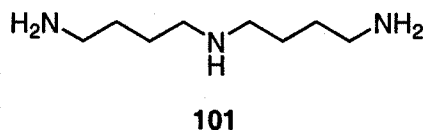


1,5,9,12,17,20-Hexa[(2-trimethylsilyl)ethanesulfonyl]-1,5,9,12,17,20-hexaazacyclodocosane (122)

Using **87** (2.00 g, 3.35 mmol) and **109** (1.30 g, 3.35 mmol) in DMF (40 ml), **122** was prepared general procedure **2h** and washed with boiling 2-PrOH (50 ml) for 2 h to give a cream solid (1.12 g, 51% yield); m.p. 218.1-221.2 °C; ν_{\max} (Golden Gate) 989, 1136, 1167, 1248, 1335, 1456 and 2954 cm^{-1} ; δ_{H} (CDCl_3) 0.07 (54 H, s), 0.97-1.05 (12 H, m), 1.72 (8 H, broad s), 2.91-2.98 (12 H, m), 3.30 (8 H, broad m), 3.46-3.80 (16 H, broad m); δ_{C} (CDCl_3) -1.60, 10.2, 10.7, 25.5, 46.6, 47.7, 48.1, 48.4, 49.9; m/z

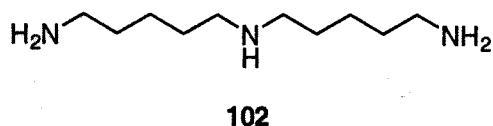
(FAB+ mode NaI) 1322.51 ($[M+Na]^+$, 20%), 1157.8 (6), 1135.8 (8), 991.7 (7) and 969.7 (6); Found $[M+Na]^+$ 1322.5068, $C_{46}H_{111}N_6O_{12}Si_6S_6Na$ requires 1322.5098.

6.1.9. Deprotection of SES-amides



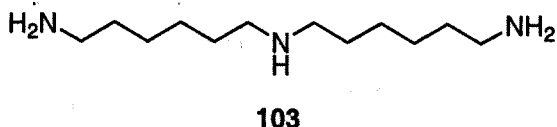
1,6,11-triazaundecane (**101**)

Using **98** (3.24 g, 10.0 mmol), **101** was prepared according to general procedure **2k** to give a beige oil (1.34 g, 84%); 1H and ^{13}C NMR spectra agreed with literature values.¹⁹⁶ δ_H ($CDCl_3$) 1.39-1.52 (8H, m), 2.57 (4H, t, $J = 6.9$), 2.66 (4H, t, $J = 6.7$); δ_C ($CDCl_3$) 27.8, 31.8, 42.4, 50.1.



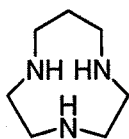
1,7,13-triazatridecane (**102**)

Using **99** (0.200 g, 0.569 mmol), **102** was prepared to give an oil (0.089 g, 84% yield); 1H and ^{13}C NMR spectra agreed with literature values.¹⁶⁹ δ_H ($CDCl_3$) 1.34-1.61 (10H, m), 2.62 (4H, t, $J = 7.2$), 2.71 (4H, t, $J = 6.9$); δ_C ($CDCl_3$) 25.1, 30.4, 34.1, 42.5, 50.4.



1,8,15-triazapentadecane (**103**)

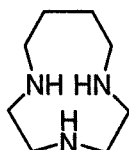
Using **100** (1.45 g, 3.82 mmol), **103** was prepared according to general procedure **2k** to give an oil (0.38 g, 46% yield); 1H and ^{13}C NMR spectra agreed with literature values.¹⁹⁷ δ_H ($CDCl_3$) 1.33-1.55 (12H, m), 2.60 (4H, t, $J = 7.2$), 2.69 (4H, t, $J = 6.9$); δ_C ($CDCl_3$) 27.2, 27.7, 30.6, 34.2, 42.5, 50.4.



123

1,4,7-Triazacyclodecane (123)

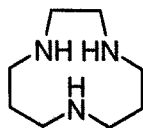
Using **111** (0.731 g, 1.15 mmol), **123** was prepared according to general procedure **2k** as an orange oil (0.090 g, 55% yield); ^1H and ^{13}C NMR spectra were consistent with values reported for the trihydrochloride salt;²⁰⁷ δ_{H} (CDCl_3) 1.55-1.60 (2 H, m), 2.52-2.83 (12 H, m); δ_{C} (CDCl_3) 26.8, 47.0, 48.3, 49.4.



124

1,4,7-Triazacycloundecane (124)

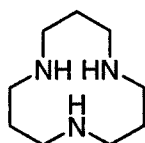
Using **112** (0.111 g, 0.170 mmol), **124** was prepared according to general procedure **2k** (using TBAF in place of CsF) and not isolated from byproduct (0.014 g, 52% yield); ^1H and ^{13}C NMR spectra were consistent with values reported for the trihydrochloride salt;^{246]} δ_{H} (CDCl_3) 1.82-1.88 (4H, m), 2.55-2.90 (12H, m); δ_{C} (CDCl_3) 26.5, 27.2, 46.8, 48.5 and 49.8.



125

1,5,9-Triazacycloundecane (125)

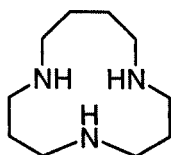
Using **113** (0.960 g, 1.47 mmol), **125** was prepared according to general procedure **2k** and purified by Kugelrohr distillation (0.035 mmHg/191 °C) to give a clear oil (0.102 g, 44% yield). ^1H and ^{13}C NMR spectra were consistent with values reported for the trihydrochloride salt;²⁴⁷ δ_{H} (CDCl_3) 1.78-1.84 (4 H, quintet, $J = 5.2$), 2.71 (4 H, s), 2.79-3.00 (8 H, broad m); δ_{C} (CDCl_3) 24.2, 46.8, 48.3, 48.5.



126

1,5,9-Triazacyclododecane (**126**)

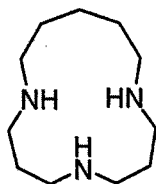
Using **114** (0.788 g, 1.18 mmol), **126** was prepared according to general procedure **2k** as an orange oil (0.117 g, 58% yield); ^1H and ^{13}C NMR spectra agreed with literature values.¹⁵¹ δ_{H} (CDCl_3) 1.81-1.87 (6 H, quintet, J 5.3), 2.87-3.0 (12 H, t, J 5.4); δ_{C} (CDCl_3) 26.2 (CH_2), 49.1 (NCH_2).



37

1,5,9-Triazacyclotridecane (**37**)

Using **115** (0.670 g, 0.992 mmol), **37** was prepared according to general procedure **2k** and purified by Kugelrohr distillation (1.0 mmHg/144°C) to give a pale yellow oil (0.073 g, 39 % yield). ^1H and ^{13}C NMR spectra were consistent with values reported for the trihydrochloride salt;¹⁵⁹ ν_{max} (CDCl_3 solution cell) 2203, 2422, 2711, 2846, 2924 cm^{-1} ; δ_{H} (CDCl_3) 1.80-1.87 (8 H, m, NCH_2CH_2), 2.77-2.78 (4 H, m, NCH_2CH_2), 2.80-2.89 (8 H, m, $\text{NCH}_2\text{CH}_2\text{CH}_2\text{N}$); δ_{C} 26.9 and 27.6 (CH_2), 49.2, 51.1 and 50.5 (NCH_2).

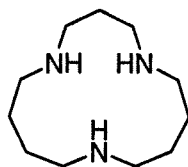


127

1,5,9-Triazacyclotetradecane (**127**)

Using **116** (1.21 g, 1.75 mmol), **127** was prepared according to general procedure **2k** and purified by Kugelrohr distillation (0.035 mmHg/171 °C) to give a clear oil

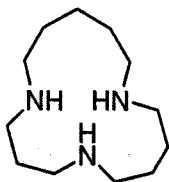
(0.216 g, 62% yield); ^1H and ^{13}C NMR spectra were consistent with values reported for the trihydrobromide salt;²⁴⁸ ν_{max} (CDCl_3 solution cell) 1383, 1473, 1645, 1672, 2856 and 2933; δ_{H} (CDCl_3) 1.43-1.57 (8 H, m, CH_2), 1.67-1.73 (2 H, m, CH_2), 2.65-2.73 (12 H, m, NCH_2); δ_{C} (CDCl_3) 20.9, 25.7, 28.5, 47.2, 47.5 and 49.2 (CH_2); m/z (EI+ mode) 199.2 ($[\text{M}]^+$, 18%), 198.2 (3), 170.2 (2), 155.1 (5), 141.1 (6), 112.11 (15), 98.1 (48), 82.9 (100), 70.1 (28) and 47.0 (30); Found $[\text{M}]^+$ 199.2049, $\text{C}_{11}\text{H}_{25}\text{N}_3$ requires 199.2048.



128

1,5,10-Triazacyclotetradecane (128)

Using **117** (0.897 g, 1.28 mmol), **128** was prepared according to general procedure **2k** and purified by Kugelrohr distillation (0.1 mmHg/170 °C) to give a pale yellow oil (0.084 g, 33% yield); ν_{max} (CDCl_3 solution cell) 1383, 1470, 1560, 1643, 1672, 2902 and 2983; δ_{H} (CDCl_3) 1.55-1.64 (8 H, m, CH_2), 1.68-1.74 (2 H, m, CH_2), 2.64-2.74 (12 H, m, NCH_2); δ_{C} (CDCl_3) 25.2, 25.9, 46.2, 48.2 and 49.1 (CH_2); m/z (EI+ mode) 199.2 ($[\text{M}]^+$, 19%), 182.2 (3), 154.1 (5), 141.1 (7), 112.1 (15), 98.1 (26), 84.0 (100), 63.0 (51) and 44.1 (23); Found $[\text{M}]^+$ 199.2047, $\text{C}_{11}\text{H}_{25}\text{N}_3$ requires 199.2048.

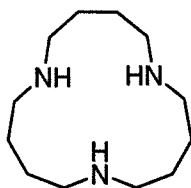


129

1,5,10-Triazacyclopentadecane (129)

Using **118** (0.898 g, 1.27 mmol), **129** was prepared according to general procedure **2k** and purified by Kugelrohr distillation (0.1 mmHg/170 °C) to give a pale yellow oil (0.093 g, 34% yield); ν_{max} (CDCl_3 solution cell) 1383, 1470, 1560, 1645, 1672, 2854, 2933 and 2983; δ_{H} (CDCl_3) 1.49-1.60 (10 H, m, CH_2), 1.64-1.70 (2 H, m,

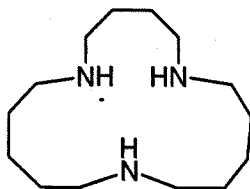
CH₂), 2.61-2.74 (12 H, m, NCH₂); δ_C (CDCl₃) 23.9, 27.2, 27.9, 28.1, 28.6, 28.8, 47.9, 48.3, 48.6, 49.7 and 50.2 (CH₂); m/z (EI+ mode) 213.2 ([M]⁺, 19%), 196.2 (3), 183.2 (3), 155.2 (6), 141.1 (6), 126.1 (13), 98.1 (53), 84.0 (100), 82.9 (48), 70.1 (36) and 47.0 (34); Found [M]⁺ 213.2206, C₁₂H₂₇N₃ requires 213.2205.



130

1,6,11-Triazacyclopentadecane (**130**)

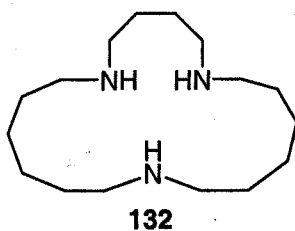
Using **119** (0.294 g, 0.416 mmol), **130** was prepared and purified by Kugelrohr distillation (0.05 mmHg/160 °C) to give a pale tan oil (0.060 g, 67% yield); ¹H NMR: δ_H (CDCl₃) 1.59 (12 H, broad s), 2.68 (12 H, broad s); ¹³C NMR: δ_C (CDCl₃) 27.3, 48.7; MS: m/z (FAB+ mode) 214.2 ([M+H]⁺, 100%), 212.2 (11), 126.1 (12), 84.6 (7), 73.7 (10), 48.0 (6); Found [M+H]⁺ 214.2285, C₁₂H₂₈N₃ requires 214.2283.



131

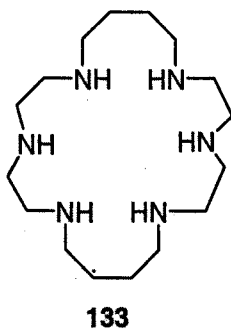
1,6,12-Triazacycloheptadecane (**131**)

Using **120** (0.50 g, 0.681 mmol), **131** was prepared according to general procedure **2k** and purified by Kugelrohr distillation (0.05 mmHg/150 °C) to give a clear oil (0.054 g, 33% yield); ¹H NMR: δ_H (CDCl₃) 1.35-1.59 (19 H, m), 2.62-2.66 (12 H, m); ¹³C NMR: δ_C (CDCl₃) 24.7, 27.7, 29.1, 29.3, 48.7, 49.0, 49.1; MS: m/z (EI+ mode) 241.3 ([M+H]⁺, 14%), 225.3 (2), 200.3 (3), 183.2 (4), 155.2 (11), 140.2 (22), 112.2 (21), 84.1 (100), 70.1 (34), 44.1 (23); Found [M+H]⁺ 241.2520, C₁₄H₃₁N₃ requires 241.2518.



1,6,13-Triazacyclononadecane (132)

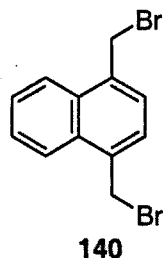
Using **121** (0.49 g, 0.643 mmol), **132** was prepared according to general procedure **2k** and purified by Kugelrohr distillation (0.05 mmHg/165 °C) to give a clear oil (0.054 g, 31% yield); ^1H NMR: δ_{H} (CDCl_3) 1.38-1.58 (23 H, m), 2.62-2.68 (12 H, m); ^{13}C NMR: δ_{C} (CDCl_3) 26.5, 26.7, 27.7, 29.4, 29.6, 28.7, 49.0, 49.4; MS: m/z (EI+ mode) 269.4 ($[\text{M}+\text{H}]^+$, 43%), 237.3 (5), 225.3 (6), 211.3 (14), 169.2 (25), 154.2 (23), 126.2 (33), 112.2 (97), 84.1 (100), 70.1 (57), 55.1 (44); Found $[\text{M}+\text{H}]^+$ 241.2520, $\text{C}_{14}\text{H}_{31}\text{N}_3$ requires 241.2518.



1,5,9,12,17,20-Hexaazacyclodocosane (133)

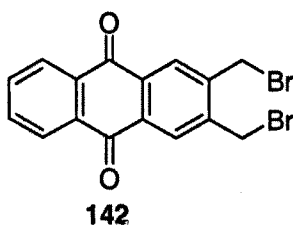
Using **122** (1.35 g, 1.03 mmol), **133** was prepared according to general procedure **2k** and purified by Kugelrohr distillation (0.035 mmHg/220 °C) to give a pale yellow solid (0.092 g, 28% yield); ^1H and ^{13}C NMR spectra were consistent with values reported for the hexahydrochloride salt;²⁴⁹ δ_{H} (CDCl_3) 1.54-1.56 (8 H, m), 1.67 (6 H, broad s), 2.63 (8 H, broad s), 2.67-2.75 (16 H, m); δ_{C} (CDCl_3) 28.5, 49.1, 49.6, 50.1.

6.1.10. Synthesis of cyclophanes



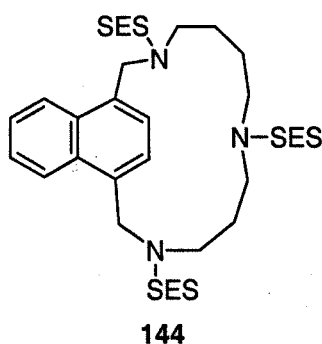
1,4-Bis(bromomethyl)naphthalene (**140**)

Using 1,4-dimethylnaphthalene (1.00 g, 6.40 mmol) and NBS (4.6 g, 25.6 mmol), **140** was prepared in 3 h according to general procedure **2l** and recrystallised from MeCN/hexane (~1:2) to give yellow crystals (0.593 g, 30% yield); ^1H and ^{13}C NMR spectra agreed with literature values;²⁵⁰ δ_{H} (CDCl_3) 4.95 (4H, s, CH_2Br), 7.50 (2H, s, ArH), 7.66-7.70 (2H, m, ArH), 8.20-8.24 (2H, m, ArH); δ_{C} (CDCl_3) 31.4 (CH_2), 125.0, 127.3, 127.6 (ArCH), 132.3, 135.3 (ArC).



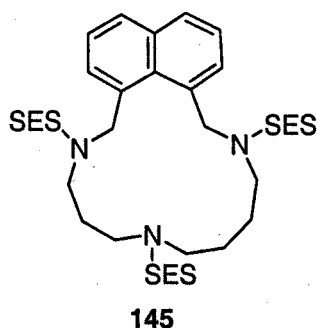
2,3-Bis(bromomethyl)anthraquinone (**142**)

Using 2,3-dimethylantraquinone (0.50 g, 2.1 mmol) and NBS (1.51 g, 8.47 mmol), **142** was prepared overnight according to general procedure **2l** and recrystallised from EtOH to give a yellow solid (0.224 g, 37% yield); ^1H and ^{13}C NMR spectra agreed with literature values;²⁵¹ δ_{H} (CDCl_3) 4.77 (4H, s, CH_2Br), 7.82-7.85 (2H, m, ArH), 8.32-8.34 (4H, m, ArH); δ_{C} (CDCl_3) 28.2 (CH_2), 127.4, 130.0, 134.5, (ArCH), 133.4, 133.7, 142.8 (ArC), 182.2 (CO).



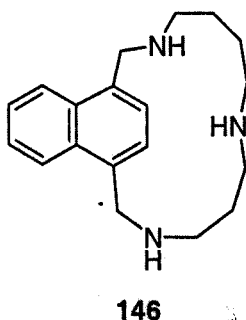
**1,5,10-Tris[(2-trimethylsilyl)ethanesulfonyl]-1,5,10-triaza(1,4)naphthalenophane
(144)**

Using **140** (0.593 g, 1.89 mmol) and **89** (1.21 g, 1.89 mmol), **144** was prepared according to general procedure **2h** and recrystallised from 2-propanol to give a cream solid (0.795 g, 53% yield); δ_{H} (CDCl_3) 0.00 (9H, s, CH_3Si), 0.13 (18H, s, CH_3Si), 0.69-0.87 (6H, m), 1.14-1.21 (4H, m), 1.27-1.36 (2H, m), 2.14-2.27 (2H, m), 2.51-2.69 (4H, m), 2.92-3.13 (6H, m), 3.24-3.41 (2H, m), 4.10-4.13 (1H, d, $J = 13.2$), 4.20-4.17 (1H, d, $J = 13.2$), 5.45-5.48 (1H, d, $J = 13.2$), 5.53-5.56 (1H, d, $J = 13.2$), 7.47-7.53 (2H, m), 7.65-7.70 (2H, m), 8.49-8.63 (2H, m); δ_{C} (CDCl_3) -1.6 and -1.5 (CH_3), 10.5, 10.6, 25.7, 26.2, 28.2, 30.9, 45.9, 46.1, 46.8, 46.9, 47.5, 48.6, 48.7, 53.1, 53.9 and 64.8 (CH_2), 125.4, 125.7, 127.6, 127.8, 128.4 and 128.7 (ArCH), 132.7, 132.9, 133.8 and 134.1 (ArC); m/z (FAB+ mode/NOBA) 790.7 ($[\text{M}+\text{H}]^+$, 6%), 726.7 (13), 698.7 (11), 624.6 (32), 560.6 (4), 458.5 (7), 252.3 (5), 226.2 (16), 141.1 (11) and 73.7 (100). Found $[\text{M}+\text{H}]^+$ 790.3272, $\text{C}_{34}\text{H}_{64}\text{N}_3\text{O}_6\text{S}_3\text{Si}_3$ requires 790.3265.



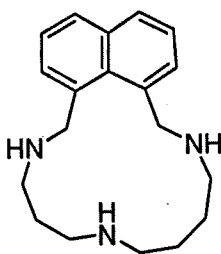
1,5,10-Tris[(2-trimethylsilyl)ethanesulfonyl]-1,5,10-triaza(1,8)naphthalenophane (145)

Using 1,8-bisbromomethylnaphthalene (0.50 g, 1.59 mmol) and **89** (1.02 g, 1.59 mmol), **145** was prepared according to general procedure **2h** and purified by column chromatography to give a white foamy solid (0.23 g, 18% yield); δ_{H} (CDCl_3) 0.06 (9H, s), 0.14 (18H, s), 0.76-0.81 (2H, m), 1.13-1.29 (8H, m), 2.59-2.63 (2H, m), 2.91-2.97 (4H, m), 3.05-3.15 (4H, m), 3.39-3.45 (4H, m), 7.44-7.53 (2H, m), 7.69-7.90 (4H, m).



1,5,10-Triaza(1,4)naphthalenophane (146)

Using **144** (0.795 g, 1.00 mmol), **146** was prepared according to general procedure **2k** to give a clear oil (0.074 g, 25% yield); δ_{H} (CDCl_3) 0.68-1.02 (4H, m), 1.15-1.34 (2H, m), 1.38-1.51 (2H, m), 1.64-1.78 (1H, m), 1.91-2.04 (1H, m), 2.12-2.27 (2H, m), 2.42-2.85 (5H, m), 3.70-3.91 (2H, m), 4.68-4.87 (2H, m), 7.32-7.67 (4H, m), 8.20-8.33 (2H, m); δ_{C} (CDCl_3) 26.1, 28.0, 29.1, 43.9, 45.7, 47.3, 48.0, 50.9 and 51.7 (CH_2), 124.7, 124.8, 125.9, 125.93, 126.6 and 126.9 (ArCH), 132.4, 132.5, 136.3 and 137.2 (ArC); m/z (FAB+ mode) 298.3 ($[\text{M}+\text{H}]^+$, 96%), 280.3 (5), 254.3 (4), 224.2 (8), 196.2 (5), 168.1 (8), 155.1 (19), 141.1 (12), 98.4 (11), 73.7 (29), 70.8 (17), 45.1 (8); Found $[\text{M}+\text{H}]^+$ 298.2222, $\text{C}_{19}\text{H}_{28}\text{N}_3$ requires 298.2283.

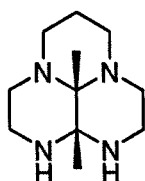


147

1,5,10-Triaza(1,8)naphthalenophane (**147**)

Using **145** (0.233 g, 0.294 mmol), **147** was prepared according to general procedure **2k** to give a lt. brown oil (0.082 g, 93% yield); δ_{H} (CDCl_3) 1.52-1.76 (9H, m), 2.70-2.73 (4H, m), 2.89-2.96 (4H, m), 4.23 (2H, s), 4.63 (2H, s).

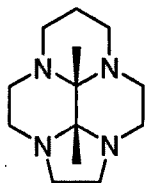
6.1.11. Carbon template routes



149

9a,9b-Dimethyl-octahydro-1,3a,6a,9-tetraaza-phenalene (**149**)

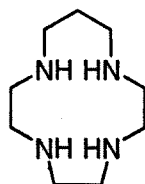
N,N'-Bis(2-aminoethyl)-1,3-propanediamine (1.00 g, 6.24 mmol) was dissolved in dry MeCN (12.5 ml) and cooled to 0 °C on an ice bath. A solution of butanedione (0.540 g, 6.24 mmol) in MeCN (12.5 ml) was dripped in slowly and the mixture stirred for 2 h. The solvent was removed by rotary evaporation and the resulting residue recrystallised from hexane to give **149** as white crystals (0.94 g, 69% yield); m.p. = 98-100 °C (lit. 110 °C); ^1H and ^{13}C NMR spectra agreed with literature values;¹⁴⁸ δ_{H} (CDCl_3) 1.16-1.21 (1H, m), 1.33 (3H, s), 1.41 (3H, s), 2.21-2.63 (7H, m), 2.72-2.77 (1H, m), 2.91-2.94 (1H, m), 3.13-3.35 (3H, m), 3.58-3.63 (1H, m); δ_{C} (CDCl_3) 10.8 and 23.7 (CH_3), 18.4, 39.3, 42.1, 45.8, 46.7, 49.1 and 51.3 (CH_2), 68.2 and 73.4 (C).



150

9b,9c-Dimethyl-decahydro-2a,4a,7a,9a-tetraaza-cyclopenta[cd]phenalene (**150**)

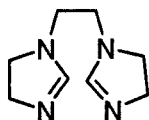
149 (0.940 g, 4.33 mmol) was dissolved in MeCN (43 ml) with K_2CO_3 (6.00 g, 43.2 mmol). 1,2-Dibromoethane (1.22 g, 6.49 mmol) was added *via* syringe and the mixture stirred at room temperature for 6 h. The solution was filtered, the solvent evaporated and the residue was purified by column chromatography (99:1 $CHCl_3$ /MeOH, neutral alumina) to give **150** as a yellow oil (0.47 g, 44% yield); 1H and ^{13}C NMR spectra agreed with literature values;¹⁴⁸ δ_H ($CDCl_3$) 1.15 (3H, s), 1.17-1.20 (1H, m), 1.40 (3H, s), 2.31-2.82 (11H, m), 2.92-2.96 (2H, m), 3.19-3.30 (3H, m), 3.63-3.74 (1H, m); δ_C ($CDCl_3$) 12.06 and 13.1 (CH_3), 18.7, 45.0, 46.1, 46.4, 46.8, 48.6, 50.0 and 50.6 (CH_2), 72.6 and 78.4 (C).



151

1,4,7,10-Tetraazacyclotridecane (**151**)

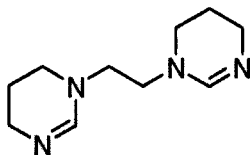
150 (0.467 g, 1.92 mmol) was combined with 10% aqueous HCl (40 ml) in EtOH (20 ml) and stirred at reflux for 2 days. The solvent was evaporated and the residue basified to pH 14 with NaOH. Toluene was added and the water removed using Dean-Stark apparatus. The toluene was evaporated and the residue recrystallised from hexane to give **151** as beige crystals (0.146 g, 39% yield); 1H and ^{13}C NMR spectra agreed with literature values;²⁵² δ_H ($CDCl_3$) 1.67-1.76 (2H, m), 2.67-2.85 (16H, m); δ_C ($CDCl_3$) 25.6, 44.3, 44.6, 45.8 and 46.9.



153

1,1-Ethylenedi-2-imidazoline (**153**)

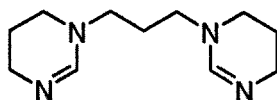
152 (8.15 g, 68.3 mmol) was added to triethylenetetraamine (5.00 g, 34.2 mmol) and the mixture was refluxed for 1 h. Excess solvent (MeOH, $\text{NH}(\text{Me})_2$) was removed *in vacuo* and the residue recrystallised from THF to give **153** as white hygroscopic crystals (2.43 g, 43% yield); ^1H and ^{13}C NMR spectra agreed with literature values,¹⁴⁹ δ_{H} (CDCl_3) 3.20-3.25 (8H, m), 3.80-3.85 (4H, m), 6.78-6.79 (2H, m); δ_{C} (CDCl_3) 47.1, 49.0 and 55.2 (CH_2), 157.4 (CH_3).



154

1,1-Ethylenedi-2-(1,4,5,6-tetrahydro-pyrimidine) (**154**)

152 (20.5 g, 172 mmol) was added to *N,N'*-Bis(3-aminopropyl)-1,2-ethanediamine (15.0 g, 86.1 mmol) and the mixture was refluxed for 1 h. Excess solvent (MeOH, $\text{NH}(\text{Me})_2$) was removed *in vacuo* to give **154** as a white hygroscopic solid (16.7 g, 99.9% yield); ^1H and ^{13}C NMR spectra agreed with literature values;²⁵³ δ_{H} (CDCl_3) 1.77-1.83 (4H, m), 3.11-3.15 (8H, m), 3.24-3.26 (4H, m), 6.89 (2H, s); δ_{C} (CDCl_3) 21.4, 42.6, 44.3 and 51.5 (CH_2), 149.8 (CH).

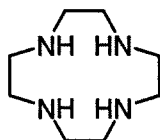


152

1,1-Propylenedi-3-(1,4,5,6-tetrahydro-pyrimidine) (**155**)

152 (0.640 g, 5.32 mmol) was added to *N,N'*-Bis(3-aminopropyl)-1,3-propanediamine (0.500 g, 2.66 mmol) and the mixture was refluxed for 1 h. Excess

solvent (MeOH, $\text{NH}(\text{Me})_2$) was removed *in vacuo* to give **155** as a clear oil which was distilled using Kugelrohr apparatus (212 °C/0.2 mmHg) (0.44 g, 78% yield); ^1H and ^{13}C NMR spectra agreed with literature values;²⁵³ δ_{H} (CDCl_3) 1.70-1.87 (6H, m), 3.05-3.14 (6H, m), 3.23-3.35 (4H, m), 3.45 (2H, s), 6.95 (2H, s); δ_{C} (CDCl_3) 21.5, 27.2, 43.3, 44.0 and 50.4 (CH_2), 150.2 (CH).



36

1,4,7,10-Tetraazacyclododecane (cyclen) (**36**)

The templated bromide salt (2.79 g, 10.2 mmol) was dissolved in water (10 ml) and dripped into a refluxing solution of KOH (3.19 g, 81.7 mmol) in water (10 ml). The solution was refluxed for 1 h, then filtered and concentrated until a white solid began to precipitate. This was filtered and the filtrate concentrated further, precipitating more white solid. The solids were combined (0.513 g, 29% yield); ^1H and ^{13}C NMR spectra agreed with literature values;¹⁴⁹ δ_{H} (CDCl_3) 2.59 (16H, s); δ_{C} (CDCl_3) 46.1.

6.2. Experimental to Chapter 3

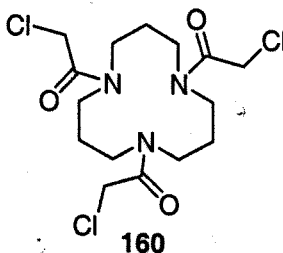
General procedures 3a-c

- a) Acylation of polyazamacrocycles:²⁵⁴ The polyazamacrocycle (either the free base or as an acid salt) was dissolved (or suspended) in dry DCM and cooled to 0 °C on an ice bath. Triethylamine (4 eq. for free bases, 8 eq. for salts) was added *via* syringe and the mixture stirred until dissolved. Chloroacetyl chloride was added *via* syringe and the solution stirred for 20 min. The ice bath was removed and the solution stirred at room temperature overnight. The solution was washed with water (2 x 25 ml), the organic layer dried with Na_2SO_4 , filtered and rotary evaporated to an oil. The crude amide was purified by column chromatography (97:3 CH_2Cl_2 -MeOH, silica).

- b) *N*-Hydroxyethylation of macrocyclic polyamines:²⁰⁹ The macrocyclic polyamine free base (1 eq.) was dissolved in EtOH (1 ml/mg) in a round bottom flask fitted with a cold finger, was cooled to ~ 5 °C with a cryocooler. Ethylene oxide (approximately 10 drops) was dripped in by condensing on the cold finger. The mixture was stirred and held at 5 °C overnight, after which the solvent was removed by rotary evaporation. The residue was typically pure, but could be purified by Kugelrohr distillation if necessary.
- c) Conversion to chloroethyl derivative:²¹⁰ The hydroxyethyl macrocyclic polyamine was stirred with thionyl chloride as reagent and solvent while heating to ~50 °C overnight. The excess thionyl chloride was removed *in vacuo* leaving the trishydrochloride salt, which was usually sufficiently pure for analysis and testing. If necessary, the salt could be recrystallized in methanol or 2-propanol.

Experimental details

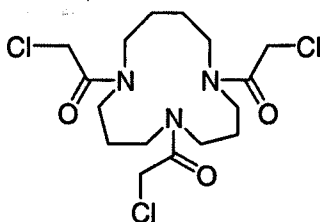
6.2.1. Chloroacetamides



1,5,9-Tris-chloroacetyl-1,5,9-triazacyclododecane (**160**)

Using 1,5,9-triazacyclododecane trihydrobromide (0.100 g, 0.242 mmol), **160** was prepared according to general procedure **3a** to give a tan oil (0.034 g, 35% yield); δ_{H} (CDCl_3) 2.10 (6 H, broad s, CH_2), 3.52-3.54 (12 H, broad m, NCH_2), 4.10 (6 H, s, CH_2Cl); δ_{C} (CDCl_3) (rotamers present) 28.3, 41.4, 45.2 and 47.2 (CH_2), 170.0 and 172.1 (CO); m/z (EI+ mode) 364 ($[\text{M}-\text{Cl}]^+$, 7%), 350 (100), 322 (83), 286 (15), 267 (11), 231 (7), 217 (18), 203 (24), 189 (14), 162 (13), 160 (30), 134 (69), 124 (15),

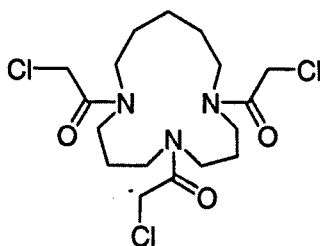
112 (20), 91 (34), 70 (100), 56 (76), 44 (55); Found $[M-Cl]^+$ 364.1193, $C_{15}H_{24}O_3N_3Cl_2$ requires 364.1195.



161

1,6,10-Tris-chloroacetyl-1,6,10-triazacyclotridecane (161)

Using **37** (0.112 g, 0.602 mmol), **161** was prepared according to general procedure **3a** to give a tan oil (0.046 g, 18% yield); δ_H ($CDCl_3$) 1.78 (4 H, broad s, CH_2), 1.96-2.04 (4 H, broad m, CH_2), 3.38-3.56 (12 H, m, NCH_2), 4.05-4.12 (6 H, m, CH_2Cl); δ_C ($CDCl_3$) (rotamers present) 27.2, 28.2, 29.7, 41.4, 41.7, 44.6, 46.3, 47.5, 48.2, 48.6 and 50.8 (CH_2), 167.3, 167.8, 168.6 and 169.4 (CO).



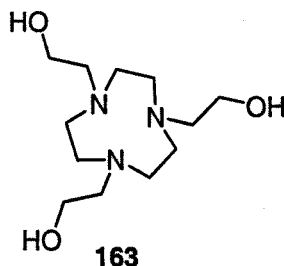
162

1,7,11-Tris-chloroacetyl-1,7,11-triazacyclotetradecane (162)

Using **127** (HCl salt, 0.128 g, 0.418 mmol), **162** was prepared according to general procedure **3a** to give a tan oil (0.042 g, 23% yield); δ_H ($CDCl_3$) 1.47 (2 H, broad s, CH_2), 1.72-1.75 (4 H, broad m, CH_2), 1.92-1.99 (4 H, broad m, CH_2), 3.32-3.47 (12 H, m, NCH_2), 4.07-4.09 (6 H, m, CH_2Cl); δ_C ($CDCl_3$) (rotamers present) 23.0, 23.8, 26.9, 27.5, 27.5, 28.4, 28.6, 28.9, 29.5, 29.9, 30.5, 41.6, 41.7, 45.2, 45.6, 45.9, 46.6, 48.1, 48.6, 49.1, 49.2, 49.4, 50.0 and 50.2 (CH_2), 167.6, 167.7 (CO); m/z (FAB+ mode) 430.1 ($[M+H]^+$, 98%, $[^{37}Cl]$), 428.1 ($[M+H]^+$, 100, $[^{35}Cl]$), 350.1 (12), 316.2 (2), 295.1 (5), 134.1 (5), 98.5 (10) and 56.1 (10); Found $[M+H]^+$ 428.1277,

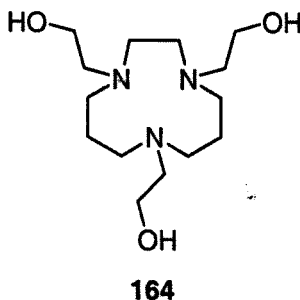
$C_{17}H_{29}O_3N_3^{35}Cl_3$ requires 428.1275; Found $[M+H]^+$ 430.1269, $C_{17}H_{29}O_3N_3^{37}Cl_3$ requires 430.1247.

6.2.2. Hydroxyethyl derivatives



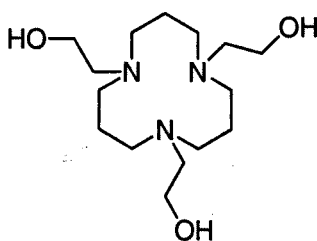
1,4,7-Tris(2-hydroxyethyl)-1,4,7-triazacyclononane (**163**)

Using 1,4,7-triazacyclononane (0.050 g, 0.387 mmol) and ethylene oxide (1 ml), **163** was prepared according to general procedure **3b** to give a clear oil (0.086 g, 85% yield); 1H and ^{13}C NMR spectra agreed with literature values;²⁵⁵ δ_H ($CDCl_3$) 2.63 (12 H, s), 2.75-2.77 (6 H, t, J 5.1), 3.58-3.61 (6 H, t, J 5.1,); δ_C 53.3, 59.8 and 60.4 (CH_2).



1,5,9-Tris(2-hydroxyethyl)-1,5,9-triazacycloundecane (**164**)

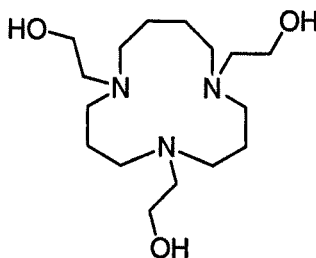
Using **125** (0.039 g, 0.25 mmol), **164** was prepared according to general procedure **3b** as a light yellow oil (0.044 g, 65% yield); ν_{max} ($CDCl_3$ solution cell) 1423, 1475, 2401, 2812, 2954 and 3683; δ_H ($CDCl_3$) 1.65 (4H, bs), 2.35-2.60 (18H, m), 3.50-3.69 (6H, m); δ_C ($CDCl_3$) 24.9, 52.8, 54.6, 55.4, 59.4, 70.9, 72.8; m/z (FAB+ mode) 290.3 ($[M+H]^+$, 100%), 288.3 (9), 246.3 (2), 227.2 (2), 203.2 (1), 166.2 (4), 154.1 (50), 136.1 (33), 107.4 (10), 88.6 (12), 73.8 (9) and 56.1 (6); Found $[M+H]^+$ 290.2443, $C_{14}H_{32}O_3N_3$ requires 290.2444.



165

1,5,9-Tris(2-hydroxyethyl)-1,5,9-triazacyclododecane (165)

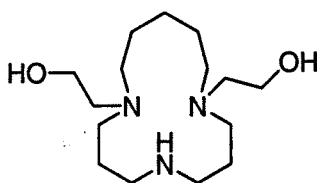
Using 1,5,9-triazacyclododecane (0.050 g, 0.29 mmol), **165** was prepared according to general procedure **3b** as a clear oil (0.079 g, 88% yield); δ_{H} (CDCl_3) 1.74 (6H, quintet, $J = 6.0$), 2.35-2.65 (12H, m), 3.63-3.66 (6H, m); δ_{C} (CDCl_3) 24.1, 51.0, 56.0, 58.7.



166

1,5,9-Tris(2-hydroxyethyl)-1,5,9-triazacyclotridecane (166)

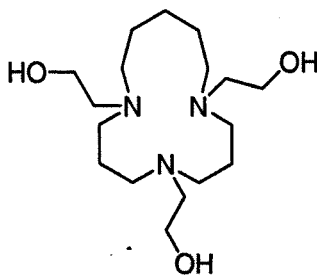
Using **37** (0.040 g, 0.22 mmol), **166** was prepared according to general procedure **3b** and purified by Kugelrohr distillation to give a clear oil (0.030 g, 44% yield); δ_{H} (CDCl_3) 1.62-1.65 (4H, m), 1.67-1.71 (4H, m), 2.49-2.58 (18H, m), 3.59-3.63 (6H, m); δ_{C} (CDCl_3) 23.6, 24.3, 51.7, 52.7, 53.3, 55.1, 56.4, 57.7, 57.9.



167

1,9-Bis(2-hydroxyethyl)-1,5,9-triazacyclotetradecane (167)

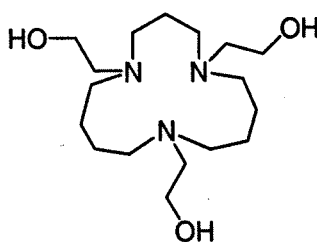
Using **127** (0.075 g, 0.38 mmol), **167** was isolated from an attempted preparation of **168** according to general procedure **3b** and purified by Kugelrohr distillation to give a clear oil (0.014 g, 13% yield); δ_{H} (CDCl_3) 1.40-1.57 (6H, m), 1.76 (4H, quintet, $J = 5.6$), 2.42-2.64 (12H, m), 2.65-2.71 (4H, m), 3.60-3.64 (4H, m); δ_{C} (CDCl_3) 23.1, 25.4, 26.7, 49.1, 51.3, 54.1, 56.8, 60.4; m/z (FAB+ mode) 288.2 ($[\text{M}+\text{H}]^+$, 100%), 286.2 (10), 128.1 (5), 98.4 (7), 73.7 (17); Found $[\text{M}+\text{H}]^+$ 288.2653, $\text{C}_{15}\text{H}_{34}\text{O}_2\text{N}_3$ requires 288.2651



168

1,5,9-Tris(2-hydroxyethyl)-1,5,9-triazacyclotetradecane (168)

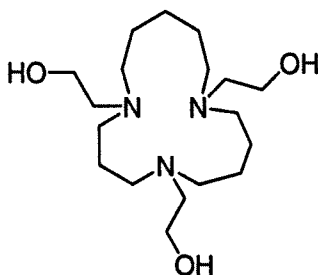
Using **127** (0.060 g, 0.30 mmol), **168** was prepared according to general procedure **3b** as a clear oil (0.057 g, 57% yield); δ_{H} (CDCl_3) 1.55-1.78 (10H, m), 2.42-2.71 (18H, m), 3.54-3.67 (6H, m); δ_{C} (CDCl_3) 23.2, 24.5, 25.1, 25.5, 26.3, 49.1, 51.0, 52.2, 52.5, 53.3, 53.4, 56.4, 56.7, 57.5, 58.9, 59.1 and 59.7; m/z (CI+ mode/isobutane) 388.4 (10%), 349.2 (33), 332.3 ($[\text{M}+\text{H}]^+$, 43), 288.3 (100), 279.2 (22), 270.3 (10), 244.3 (6), 195.2 (4), 151.2 (7), 107.1 (8), 91.1 (4). Found $[\text{M}+\text{H}]^+$ 332.2907, $\text{C}_{17}\text{H}_{38}\text{N}_3\text{O}_3$ requires 332.2913.



169

1,5,10-Tris(2-hydroxyethyl)-1,5,10-triazacyclotetradecane (169)

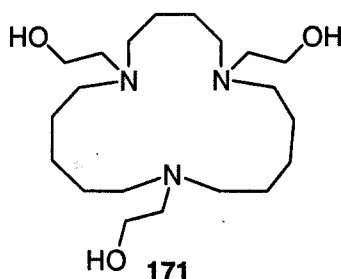
Using **128** (0.041 g, 0.21 mmol), **169** was prepared according to general procedure **3b** as a clear oil (0.046 g, 68% yield); δ_{H} (D_2O) 1.38-1.89 (10H, m), 2.36-2.59 (18H, m), 3.44-3.58 (6H, m); δ_{C} ($\text{D}_2\text{O} + \text{CD}_3\text{OD}$) 21.3, 27.2, 27.8, 55.4, 56.8, 57.0, 57.4, 59.7, 60.8 and 63.6; m/z (CI+ mode/isobutene) 388.4 (20%), 332.3 ($[\text{M}+\text{H}]^+$, 100), 330.3 (10), 288.3 (7). Found $[\text{M}+\text{H}]^+$ 332.2909, $\text{C}_{17}\text{H}_{38}\text{N}_3\text{O}_3$ requires 332.2913.



170

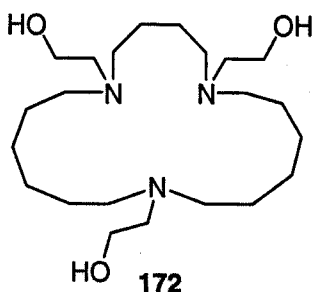
1,5,10-Tris(2-hydroxyethyl)-1,5,10-triazacyclopentadecane (170)

Using **129** (0.040 g, 0.19 mmol), **170** was prepared according to general procedure **3b** as a clear oil (0.063 g, 96% yield); δ_{H} (CDCl_3) 1.35-1.66 (12H, m), 2.37-2.57 (18H, m), 3.53-3.57 (6H, m); δ_{C} (CDCl_3) 25.7, 26.0, 27.7, 27.9, 53.9, 54.1, 54.2, 55.1, 55.4, 56.0, 56.6, 57.5, 57.8, 59.3, 59.4; m/z (FAB+ mode) 346.3 ($[\text{M}+\text{H}]^+$, 100%), 344.3 (20), 302.3 (10), 128.1 (15), 98.4 (14), 84.6 (13), 73.7 (11), 56.9 (6); Found $[\text{M}+\text{H}]^+$ 346.3072, $\text{C}_{18}\text{H}_{40}\text{O}_3\text{N}_3$ requires 346.3070



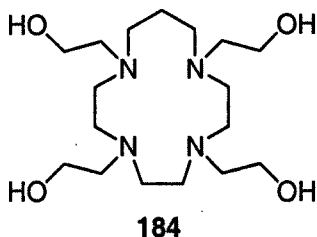
1,6,12-Tris(2-hydroxyethyl)-1,6,12-triazacyclopentadecane (171)

Using **131** (0.040 g, 0.17 mmol), **171** was prepared according to general procedure **3b** as a clear oil (0.061 g, >99% yield); δ_{H} (CDCl_3) 1.32-1.49 (16H, m), 2.28-2.48 (18H, m), 3.45-3.48 (6H, m); δ_{C} (CDCl_3) 25.6, 26.5, 27.8, 28.0, 54.3, 54.4, 54.6, 56.4, 58.4, 58.9 and 59.0 (CH_2); m/z (FAB+ mode/NOBA) 374.6 ($[\text{M}+\text{H}]^+$, 40%), 372.6 (12), 327.2 (5), 281.2 (4), 207.1 (7), 147.1 (14), 98.5 (9), 73.7 (100), 44.1 (8); Found $[\text{M}+\text{H}]^+$ 374.3378, $\text{C}_{20}\text{H}_{44}\text{N}_3\text{O}_3$ requires 374.3383.



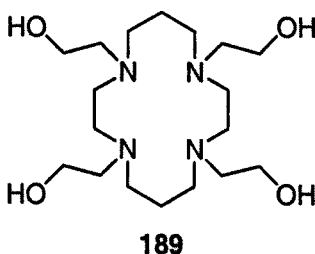
1,6,13-Tris(2-hydroxyethyl)-1,6,13-triazacyclononadecane (172)

Using **132** (0.040 g, 0.15 mmol), **172** was prepared according to general procedure **3b** as a clear oil (0.060 g, >99% yield); δ_{H} (CDCl_3) 1.26-1.51 (20H, m), 2.42-2.61 (18H, m), 3.49-3.55 (6H, m); δ_{C} (CDCl_3) 25.8, 27.1, 27.2, 27.5, 27.6, 53.8, 54.1, 54.3, 56.7, 56.9, 58.6, 58.7 and 77.5 (CH_2); m/z (EI+ mode) 401.7 ($[\text{M}+\text{H}]^+$, 7%), 371.6 (84), 370.6 (83), 324.6 (29), 323.6 (28), 255.4 (14), 225.4 (15), 170.3 (16), 142.2 (38), 112.2 (96), 84.1 (100), 55.1 (100); Found $[\text{M}+\text{H}]^+$ 401.3616, $\text{C}_{22}\text{H}_{47}\text{N}_3\text{O}_3$ requires 401.3617.



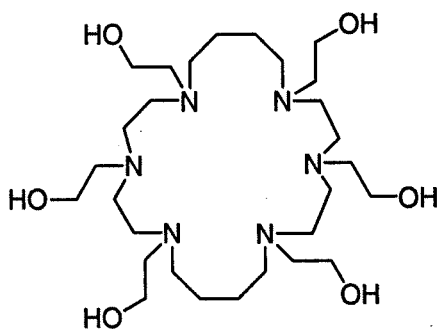
1,4,7,10-Tetra(2-hydroxyethyl)-1,4,7,10-tetraazacyclotridecane (184)

Using **148** (0.080 g, 0.41 mmol), **184** was prepared according to general procedure **3b** as a clear oil that crystallised upon standing to a waxy solid (0.130 g, 85% yield); δ_{H} (CDCl_3) 1.66-1.73 (2H, m), 2.44-2.73 (24H, m), 3.59-3.65 (8H, m); δ_{C} (CDCl_3) 25.9, 52.0, 52.4, 53.5, 54.6, 57.1, 57.5, 59.6 and 59.8.



1,4,8,11-Tetra(2-hydroxyethyl)-1,4,8,11-tetraazacyclotetradecane (189)

Using 1,4,8,11-tetraazacyclotetradecane (0.200 g, 0.998 mmol), **189** was prepared according to general procedure **3b** and recrystallised from $\text{CHCl}_3/\text{Et}_2\text{O}$ (~1:4) to give white crystals (0.190 g, 51% yield); ^1H and ^{13}C NMR spectra and m.p. agreed with literature values;²⁰⁹ δ_{H} (CDCl_3) 1.51-1.76 (4H, m), 2.24-2.59 (24H, m), 3.44-3.56 (8H, m); δ_{C} (CDCl_3) 25.4, 49.3, 52.1, 55.8 and 59.5 (CH_2).

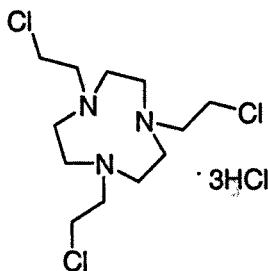


173

1,5,9,12,17,20-Hexa(2-hydroxyethyl)-1,5,9,12,17,20-hexaazacyclodocosane (**173**)

Using **133** (0.040 g, 0.13 mmol), **173** was prepared according to general procedure **3b** to give a clear oil (0.055 g, 74% yield); δ_{H} (CDCl_3) 1.47-1.56 (8H, m), 2.45-2.67 (36H, m), 3.54-3.60 (12H, m); δ_{C} (CDCl_3) 25.3, 52.1, 52.5, 55.3, 56.3, 57.6, 59.5, 59.7; m/z (FAB+ mode) 579.5 ($[\text{M}+\text{H}]^+$, 37%), 535.4 (35), 491.4 (17), 393.3 (10), 322.2 (13), 290.2 (8), 171.1 (22), 114.2 (80), 84.6 (100), 73.7 (87); Found $[\text{M}+\text{H}]^+$ 579.4817, $\text{C}_{28}\text{H}_{63}\text{O}_6\text{N}_6$ requires 579.4809.

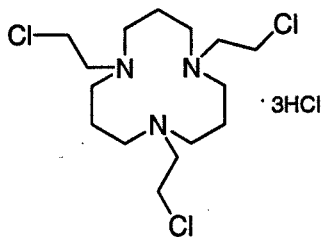
6.2.3. Synthesis of chloroethyl derivatives



174

1,4,7-Tris(2-chloroethyl)-1,4,7-triazacyclononane trihydrochloride (**174**)

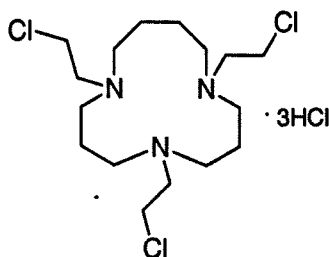
Using **163** (0.086 g, 0.329 mmol) and thionyl chloride (2 ml), **174** was prepared according to general procedure **3c** to give a cream hygroscopic solid (0.138 g, 99% yield); δ_{H} ($\text{DMSO}-d_6$) 2.94 (6H, broad s), 3.20 (6H, broad s), 3.39 (6H, broad s); δ_{C} ($\text{DMSO}-d_6$) 40.5 (ClCH_2), 49.3 (NH^+CH_2), 56.5 ($\text{NH}^+\text{CH}_2\text{CH}_2\text{Cl}$); m/z (FAB+, glycerol) 316.1 ($[(\text{M}-3\text{HCl})+\text{H}]^+$, 100%), 197.1 (5%), 147.0 (8), 106.3 (20), 70.8 (4), 57.0 (4); Found $[(\text{M}-3\text{HCl})+\text{H}]^+$ 316.1106, $\text{C}_{12}\text{H}_{24}\text{N}_3^{35}\text{Cl}_3$ requires 316.1114.



175

1,5,9-Tris-(2-chloroethyl)-1,5,9-triazacyclododecane trihydrochloride (175)

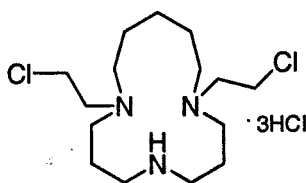
Using **165** (0.032 g, 0.11 mmol), **175** was prepared according to general procedure **3c** as a cream solid (0.030 g, 61% yield); δ_{H} (D_2O) 1.90-1.93 (6H, m), 3.04-3.07 (12H, m), 3.16-3.19 (6H, m), 3.62-3.65 (6H, m); δ_{C} (D_2O , ref. to internal MeOH = 38.0) 18.2, 38.7, 48.9 and 55.5; m/z (FAB+, glycerol) 358.1 $[(\text{M}-3\text{HCl})+\text{H}]^+$, 100%), 340.2 (13), 324.2 (6), 296.1 (4), 232.1 (4), 132.0 (13), 106.3 (33), 84.6 (12), 70.8 (11), 58.9 (7); Found $[(\text{M}-3\text{HCl})+\text{H}]^+$ 360.1553, $\text{C}_{15}\text{H}_{31}\text{N}_3^{35}\text{Cl}_2^{37}\text{Cl}$ requires 360.1556.



176

1,5,9-Tris(2-chloroethyl)-1,5,9-triazacyclotridecane trihydrochloride (176)

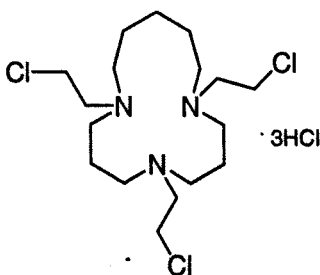
Using **166** (0.030g, 0.094 mmol), **176** was prepared according to general procedure **3c** as a yellow foamy solid (0.041 g, 89% yield); δ_{H} (D_2O) 1.85-1.98 (4H, m), 2.13-2.19 (4H, m), 3.33-3.61 (18H, m), 3.91-3.98 (6H, m); δ_{C} (D_2O) 17.7, 20.4, 37.8, 38.0, 48.8, 49.4, 49.7, 51.4, 56.7, 56.8, 56.9; m/z (FAB+, NOBA) 372.3 $[(\text{M}-3\text{HCl})+\text{H}]^+$, 12%), 357.3 (5), 310.3 (10), 238.3 (5), 169.1 (54), 85.6 (100), 84.6 (15), 66.8 (5); Found $[(\text{M}-3\text{HCl})+\text{H}]^+$ 372.1738, $\text{C}_{16}\text{H}_{33}\text{N}_3^{35}\text{Cl}_3$ requires 372.1740.



177

1,9-Bis(2-chloroethyl)-1,5,9-triazacyclotetradecane trihydrochloride (177)

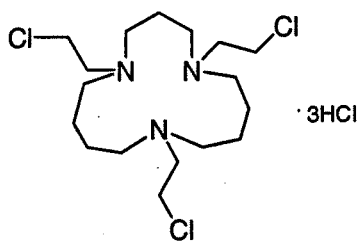
Using **167** (0.014 g, 0.042 mmol), **177** was prepared according to general procedure **3c** as a yellow foamy solid (0.022 g, >99% yield); δ_{H} (D_2O) 1.59 (2H, broad m), 1.73 (4H, broad m), 2.01-2.09 (4H, broad m), 3.26-3.38 (12H, m), 3.59-3.64 (4H, m), 3.91-3.94 (4H, m); δ_{C} (D_2O) 16.9, 18.5, 20.2, 37.8, 40.1, 47.3, 49.6, 55.9; m/z (FAB+) 324.4 ($[(\text{M}-3\text{HCl})+\text{H}]^+$, 100%), 288.3, (22), 262.3 (11), 222.3 (4), 130.2 (38), 102.3 (36), 98.3 (22); Found $[(\text{M}-3\text{HCl})+\text{H}]^+$ 324.1970, $\text{C}_{17}\text{H}_{35}\text{N}_3^{35}\text{Cl}_3$ requires 324.1973.



178

1,5,9-Tris(2-chloroethyl)-1,5,9-triazacyclotetradecane trihydrochloride (178)

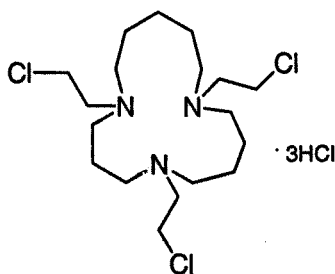
Using **168** (0.057 g, 0.17 mmol), **178** was prepared according to general procedure **3c** as a yellow foamy solid (0.079 g, 93% yield); δ_{H} (D_2O) 1.28 (2H, broad m), 1.43-1.44 (4H, broad m), 1.74-1.75 (4H, broad m); δ_{C} (D_2O , [ref. CD_3OD δ 48.4]) 19.9, 20.6, 35.2, 37.0, 37.7, 50.4, 52.0, 56.2; m/z (FAB+) 386.3 ($[(\text{M}-3\text{HCl})+\text{H}]^+$, 63%), 352.4 (10), 324.3 (100), 288.3 (21), 262.3 (20), 210.3 (12), 167.2 (5), 106.2 (35); Found $[(\text{M}-3\text{HCl})+\text{H}]^+$ 386.1902, $\text{C}_{17}\text{H}_{35}\text{N}_3^{35}\text{Cl}_3$ requires 386.1897.



179

1,5,10-Tris(2-chloroethyl)-1,5,10-triazacyclotetradecane trihydrochloride (179)

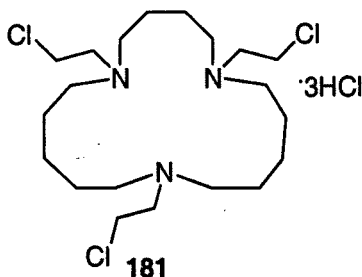
Using **169** (0.040 g, 0.12 mmol), **179** was prepared according to general procedure **3c** as a tan foamy solid (0.051 g, 85% yield); δ_{H} (D_2O) 1.51-1.98 (10H, broad m), 3.05-3.22 (12H, broad m), 3.30-3.39 (6H, m), 3.58-3.67 (6H, m); δ_{C} (D_2O , [ref. CD_3OD δ 48.4]) 19.9, 20.6, 35.2, 37.0, 37.6, 37.7, 50.4, 52.0, 56.2, 56.3; m/z (FAB+) 387.2 ($[(\text{M}-3\text{HCl})+\text{H}]^+$, 18%), 326.2 (6), 289.2 (4), 240.0 (4), 191.1 (28), 135.0 (25), 97.4 (100), 96.4 (93), 77.6 (44), 56.0 (32); Found $[(\text{M}-3\text{HCl})+\text{H}]^+$ 386.1903; $\text{C}_{17}\text{H}_{35}\text{N}_3^{35}\text{Cl}_3$ requires 386.1896.



180

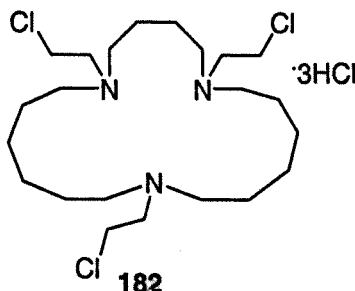
1,5,10-Tris(2-chloroethyl)-1,5,10-triazacyclopentadecane trihydrochloride (180)

Using **170** (0.053 g, 0.15 mmol), **180** was prepared according to general procedure **3c** as a yellow foamy solid (0.079 g, >99% yield); δ_{H} (D_2O) 1.42-1.99 (10H, broad m), 2.05-2.25 (2H, broad m), 3.20-3.53 (12H, broad m), 3.58-3.67 (6H, m), 3.87-3.94 (6H, m); δ_{C} (D_2O) 20.6, 21.2, 21.6, 21.8, 35.3, 37.6, 37.8, 48.5, 50.9, 51.3, 52.2, 56.0, 56.2, 56.4; ; m/z (FAB+) 401.2 ($[(\text{M}-3\text{HCl})+\text{H}]^+$, 48%), 400.2 (13), 367.2 (11), 340.2 (8), 303.2 (5), 190.1 (35), 189.1 (23), 146.0 (22), 96.4 (100), 95.4 (53), 77.6 (33), 56.0 (19); Found $[(\text{M}-3\text{HCl})+\text{H}]^+$ 402.2221; $\text{C}_{18}\text{H}_{39}\text{N}_3^{35}\text{Cl}_3$ requires 402.2210.



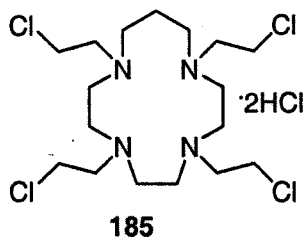
1,6,12-Tris(2-chloroethyl)-1,6,12-triazacyclopentadecane trihydrochloride (181)

Using **171** (0.055 g, 0.15 mmol), **181** was prepared according to general procedure **3c** as a yellow solid (0.080 g, >99% yield); δ_{H} (D_2O) 1.42-1.54 (4H, broad m), 1.71-1.90 (12H, broad m), 3.15-3.98 (24H, broad m); δ_{C} (D_2O) 20.6, 21.3, 22.0, 22.3, 51.6, 52.0, 52.5, 52.7, 53.1, 54.8, 55.1; m/z (FAB+ mode) 428.5 ($[(\text{M}-3\text{HCl})+\text{H}]^+$, 100%) 394.5 (43), 392.5 (25), 366.4 (18), 253.2 (19), 202.2 (22), 148.2 (52), 98.3 (95); Found $[(\text{M}-3\text{HCl})+\text{H}]^+$ 428.2360, $\text{C}_{20}\text{H}_{41}\text{N}_3\text{Cl}_3$ requires 428.2366.



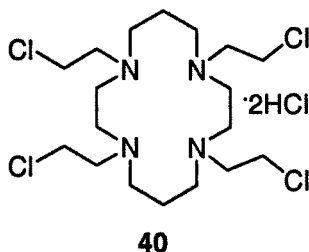
1,6,13-Tris(2-chloroethyl)-1,6,13-triazacyclononadecane trihydrochloride (182)

Using **172** (0.048 g, 0.12 mmol), **182** was prepared according to general procedure **3c** as a yellow solid (0.068g, >99% yield); δ_{H} (D_2O) 1.33-1.57 (8H, broad s), 1.61-1.87 (12H, broad m), 3.12-3.98 (24H, m); δ_{C} (D_2O) 20.3, 21.4, 21.6, 22.2, 22.6, 51.5, 51.9, 52.3, 52.5, 53.3, 55.0, 55.2; m/z (FAB+ mode) 456.6 ($[(\text{M}-3\text{HCl})+\text{H}]^+$, 100%), 359.5 (10), 329.5 (9), 271.3 (8), 216.3 (15), 190.2 (35), 112.3 (32), 96.5 (100), 56.0 (90); Found $[(\text{M}-3\text{HCl})+\text{H}]^+$ 456.2680, $\text{C}_{22}\text{H}_{45}\text{N}_3\text{Cl}_3$ requires 456.2679.



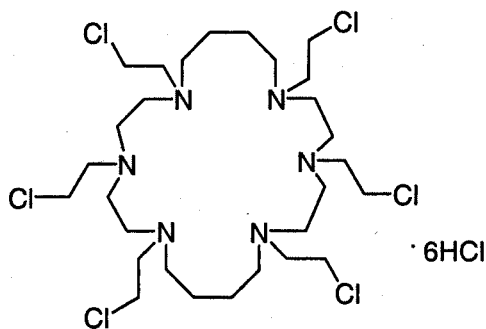
1,4,7,10-Tetra(2-chloroethyl)-1,4,7,10-tetraazacyclotridecane dihydrochloride (**185**)

Using **184** (0.044 g, 0.12 mmol), **185** was prepared according to general procedure **3c** as a yellow solid (0.062 g, 99.9% yield); δ_{H} (DMSO- d_6) 2.10-2.20 (2H, broad s), 2.90-3.43 (24H, broad m), 3.95-4.00 (8H, m); δ_{C} (CDCl₃) 15.5, 49.4, 49.7, 51.1, 54.2, 54.8, 55.7, 56.8, and 65.3.



1,4,8,11-Tetra(2-chloroethyl)-1,4,8,11-tetraazacyclotetradecane dihydrochloride (**40**)

Using **197** (0.188 g, 0.499 mmol), **40** was prepared according to general procedure **3c** to give a cream solid (0.258 g, 98% yield); ^1H and ^{13}C NMR spectra agreed with literature values;²⁵⁶ δ_{H} (D₂O) 1.92-2.18 (4H, m), 3.13-3.37 (16H, m), 3.72-3.79 (16H, m); δ_{C} (D₂O) 17.5, 43.5, 47.9, 56.1 and 57.9 (CH₂).



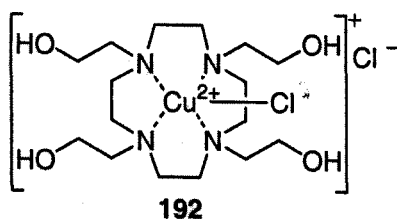
183

1,5,9,12,17,20-Hexa(2-chloroethyl)-1,5,9,12,17,20-hexaazacyclodocosane hexahydrochloride (**183**)

Using **173** (0.055 g, 0.095 mmol), **183** was prepared according to general procedure **3c** to give a tan powder (0.071 g, 83% yield); δ_{H} (D_2O) 1.82-1.95 (8H, broad m), 2.94-3.97 (48H, broad m); δ_{C} (D_2O) 20.5, 20.6, 37.8, 48.8, 53.1, 55.2, 55.6, 56.0.

6.3. Experimental to Chapter 4

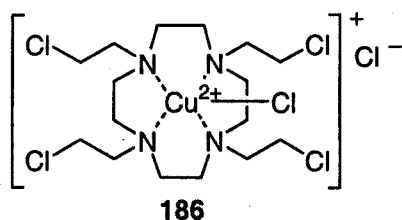
6.3.1. Formation of Cu(II) complexes



192

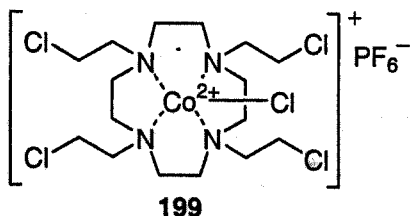
1,4,7,10-Tetra(2-hydroxyethyl)-1,4,7,10-tetraazacyclododecane[Cu(II)]Cl₂ (**192**)

192 was formed from **197** (100 mg, 0.29 mmol) and anhydrous CuCl₂ (39 mg, 0.29 mmol) in methanol (4 ml). The solution was warmed to ~50 °C for 10 minutes. The deep blue-colored solution was evaporated to give **192** as a blue powder (121 mg, 87% yield).



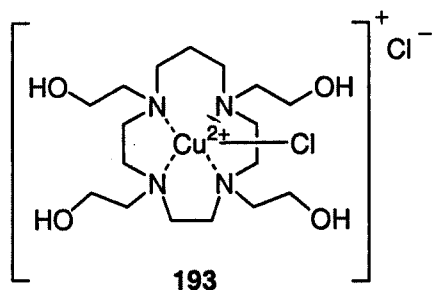
1,4,7,10-Tetra(2-chloroethyl)-1,4,7,10-tetraazacyclododecane[Cu(II)]Cl₂ (186)

186 was formed from the hydrochloride salt of **38** (754 mg, 1.52 mmol) and anhydrous CuCl₂ (205 mg, 1.52 mmol) in methanol/water (30 ml, 5:1). The solution was warmed to ~50 °C for 10 minutes. The deep blue-colored complex precipitated upon cooling the solution and was filtered and dried with suction to give **186** as a blue powder (716 mg, 75% yield). *m/z* (FAB+ mode, glycerol) 520.3 (12%), 485.3 ([*(M-2Cl)+H*]⁺, 100%) 483.3 (57), 421.3 (7), 419.3 (3), 185.1 (14), 147.1 (6), 93.5 (79), 75.7 (37), 57.9 (27); Found [*(M-2Cl)+H*]⁺ 485.0650, C₁₆H₃₂N₄³⁵Cl₃³⁷ClCu requires 485.0651. The material was crystallized as its tetrafluoroborate salt by adding excess NH₄BF₄ to a hot, saturated solution of the chloride in water. The crystals were analysed by X-ray crystallography to confirm the structure (shown in Fig. 4A).



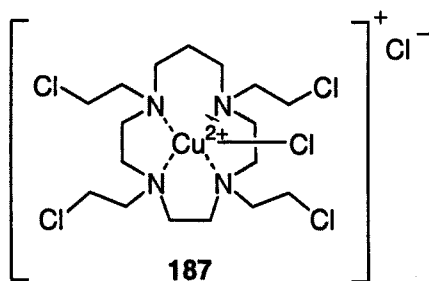
1,4,7,10-Tetra(2-chloroethyl)-1,4,7,10-tetraazacyclododecane[Co(II)]Cl₂ (199)

199 (synthesised by Stephen Lacy) was dissolved in MeCN/H₂O (10 ml, 1:1). Excess NH₄PF₆ was added and the solution left open to the air. Slow evaporation of the MeCN gave long needle-like purple crystals that were of sufficient quality for X-ray analysis. The crystal structure is given in Fig. 4N. *m/z* (FAB+ mode, glycerol) 516.3 ([*(M-PF₆)+H*]⁺, 43%), 514.3 (29), 480.3 (4), 355.3 (4), 263.2 (6), 235.1 (5), 171.1 (63), 157.1 (60), 79.6 (100), 46.1 (7). Found [*(M-PF₆)+H*]⁺ 516.0380, C₁₆H₃₂N₄³⁵Cl₄³⁷ClCu requires 516.0373.



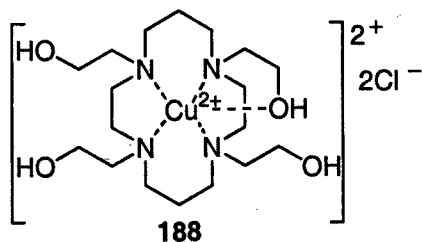
1,4,7,10-Tetra(2-hydroxyethyl)-1,4,7,10-tetraazacyclotridecane[Cu(II)]Cl₂ (193**)**

193 was formed from **184** (45 mg, 0.12 mmol) and anhydrous CuCl₂ (16 mg, 0.12 mmol) in methanol (3 ml). The solution was warmed to ~50 °C for 10 minutes. The deep blue-violet-coloured solution was evaporated to give **187** as a foamy blue-purple solid (61 mg, >99% yield).



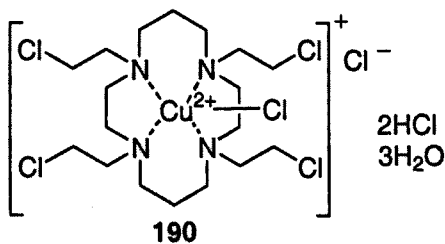
1,4,7,10-Tetra(2-chloroethyl)-1,4,7,10-tetraazacyclotridecane[Cu(II)]Cl₂ (187**)**

187 was formed from the hydrochloride salt of **185** (34 mg, 0.065 mmol) and anhydrous CuCl₂ (9 mg, 0.065 mmol) in methanol/water (3 ml, 5:1). The solution was warmed to ~50 °C for 10 minutes. The bright green-coloured complex precipitated upon cooling the solution and was filtered and dried with suction to give **187** as a light green powder (8 mg, 22% yield). *m/z* (FAB+, glycerol) 499.3 ([*(M-2Cl)+H*]⁺, 95%) 437.3 (40), 373.3 (12), 294.3 (5), 247.1 (4), 202.2 (18), 175.1 (5), 120.2 (7), 110.3 (48), 70.8 (8), 43.2 (3); Found [*(M-2Cl)+H*]⁺ 499.0982, C₁₇H₃₆N₄³⁵Cl₄Cu requires 499.0990. The material was crystallized as its hexafluorophosphate salt by adding excess NH₄PF₆ to a hot, saturated solution of the chloride in water. The resulting precipitate was redissolved by heating in the supernatant and the solution was left to crystallise. Blue-green crystals of X-ray quality grew from the solution after 5 d. The crystals were analysed by X-ray crystallography to confirm the structure (shown in Fig. 4B).



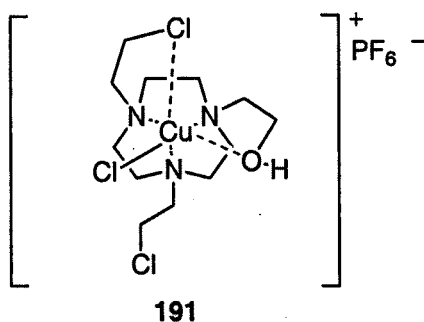
1,4,8,11-Tetra(2-hydroxyethyl)-1,4,8,11-tetraazacyclotetradecane[Cu(II)]Cl₂ (**188**)

188 was formed from **197** (50 mg, 0.13 mmol) and anhydrous CuCl₂ (18 mg, 0.13 mmol) in methanol (2 ml). The solution was warmed to ~50 °C for 10 minutes. The blue-coloured solution was evaporated to give **188** as a bright blue solid (68 mg, >99% yield). λ_{max} = 636 nm (phosphate buffer pH 7.2) [lit. λ_{max} = 630 nm (EtOH)].^{257]}



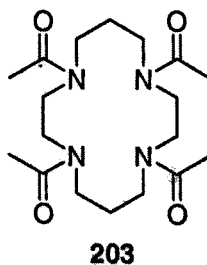
1,4,8,11-Tetra(2-chloroethyl)-1,4,8,11-tetraazacyclotetradecane[Cu(II)]Cl₂ (**190**)

40 required neutralization in order to effect complexation. A solution of **40** (159 mg, 0.256 mmol) and CuCl₂ (36 mg, 0.26 mmol) in H₂O (5 ml) was neutralized with 1 M aq. NaOH (15 drops), causing a color change to deep blue-violet. The solvent was removed *in vacuo* to give **190** as a bright green solid, which was washed with H₂O (10 ml) and filtered (23 mg, 14% yield). MS: *m/z* (FAB+, glycerol) 513.3 ([$(\text{M}-2\text{Cl})+\text{H}$]⁺, 11%), 511.3 (6), 451.4 (23), 449.4 (20), 387.4 (9), 369.3 (6), 277.2 (15), 185.1 (100), 106.3 (16), 75.7 (67), 57.9 (77). Found [$(\text{M}-2\text{Cl})+\text{H}$]⁺ 513.0969. C₁₈H₃₆N₄³⁵Cl₃³⁷ClCu requires 513.0965. Attempts to crystallize **190**, regardless of counter-ion, resulted in hydrolysis of the ligand to the Cu(II) complex of **188** (indicated by crystal structure shown in Fig. 4C). Microanalysis results: 31.86% C, 5.30% H, 8.29% N, 39.47% Cl. Theoretical: C₁₉H₃₉N₄Cl₆Cu(2HCl)(3H₂O) requires 31.40% C, 6.52% H, 7.70% N, 39.03% Cl.



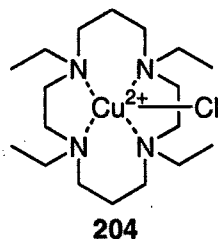
1,4-Bis(2-chloroethyl)-7-(2-hydroxyethyl)-1,4,7-triazacyclononane[Cu(II)]Cl₂ (**191**)

191 was formed from the hydrochloride salt of **174** (115 mg, 0.270 mmol), neutralised with 5 drops 1 M aq. NaOH and anhydrous CuCl₂ (36 mg, 0.270 mmol) in methanol/water (8 ml, 5:1). The solvent was removed *in vacuo* to give a green glassy solid which was taken up in H₂O (5 ml). Excess NH₄PF₆ was added and the solvent evaporated until dark blue-green crystals formed, which were suitable for X-ray crystallography (15 mg, 10% yield). The crystal structure is given in **Fig. 4D**. *m/z* (FAB+, glycerol) 362.3 ([*(M-Cl)PF₆*]+H]⁺, 64%), 326.3 (6), 277.4 (13), 262.3 (4), 185.2 (100), 93.5 (74), 75.7 (14), 58.0 (4), 46.1 (3). Found [*(M-Cl)PF₆*]+H]⁺ 362.0648, C₁₂H₂₅N₃O³⁵Cl³⁷ClCu requires 362.0647.



1,4,8,11-Tetraacetyl-1,4,8,11-tetraazacyclotetradecane (**203**)

1,4,8,11-Tetraazacyclotetradecane (0.100 g, 0.499 mmol) was dissolved in dry MeCN (10 ml) with potassium carbonate (0.69 g, 4.99 mmol) and cooled to 0 °C with an ice bath. Acetyl chloride (0.31 g, 3.99 mmol) was added dropwise and the mixture was allowed to come to room temperature and stirred overnight. The solid was filtered off and the filtrate evaporated to give a clear oil which was washed with hot EtOAc to give **203** as a white solid (0.150 g, 82% yield); δ_H (CDCl₃) 1.91-2.01 (4H, m), 2.12 (6H, s), 2.18 (6H, s), 3.41-3.63 (16H, m); δ_C (CDCl₃) 21.6 and 22.0 (CH₃), 29.0, 45.8, 47.6, 48.7, 49.1 (CH₂), 171.6 and 172.2 (CO).



1,4,8,12-Tetraethyl-1,4,8,12-tetraazacyclotetradecane[Cu(II)]Cl₂ (**204**)

203 (0.156 g, 0.423 mmol) was dissolved in dry THF (20 ml) and treated with 1.0 M BH₃·THF solution in THF (6.8 ml). The solution was refluxed for 2h then cooled and carefully quenched with methanol (30 ml) 6 M aq. HCl (15 ml). The solution was concentrated to ~ 10 ml *via* rotary evaporation, basified to pH 14 with NaOH pellets and extracted with DCM (10 x 30 ml). The combined organic layers were dried with Na₂SO₄, filtered and evaporated to give a clear oil (0.047g, 36% yield), which was taken up in MeOH (10 ml). CuCl₂ was added (0.020 g, 0.15 mmol) and the resulting blue-violet solution evaporated to give **204** as a purple solid.

6.3.2. X-ray crystallography

Details of data collection procedures and structure refinement are given in **Table 6.4.1**. CIF data can be accessed online at <http://www.chem.gla.ac.uk/~louis/data/> (**186**: LJF089; **188**: LJF096; **191**: LJF100; **199**: LJF101; **187**: LJF102). Single crystals of suitable size were attached to glass fibres using acrylic resin and mounted on a goniometer head in a general position. Data were collected on an Enraf-Nonius KappaCCD diffractometer, running under Nonius Collect software and using graphite monochromated X-radiation ($\lambda=0.71073$ Å). All data sets were collected at a temperature of 150K using an Oxford Instruments Cryostream. Typically scan angles of 1-2° were used, with integration times of 50-100 s per image. Precise unit cell dimensions were determined by post-refinement of the setting angles of a large proportion of the data set. The frame images were integrated using Denzo(SMN)²⁵⁸ and the resultant raw intensity files processed using a locally modified version of DENZOX.²⁵⁹ Absorption corrections, either by gaussian quadrature,²⁶⁰ based on the measured crystal faces, or by a semi-empirical correction²⁶¹ were applied to all data sets. Data were then sorted and merged using SORTAV.²⁶² Structures were

solved either by Patterson interpretation (DIRDIF-99)²⁶³ or by direct methods (SIR92).²⁶⁴ All structures except **191** showed disorder in the macrocyclic ring system, with the major component having ~ 80-90% occupancy and all structures showed some disorder in their respective Cl⁻, BF₄⁻ or PF₆⁻ anions. For the major component only, all non-H atoms were allowed anisotropic thermal motion. Aliphatic C-H hydrogen atoms were included at calculated positions, with C-H = 0.96 Å and were refined with a riding model and with U_{iso} set to 1.2 times that of the attached C-atom. Refinement with SHELXL97-2²⁶⁵ using full-matrix least-squares on F^2 and all the unique data. Neutral atom scattering factors, coefficients of anomalous dispersion and absorption coefficients were obtained from published work.²⁶⁶ The absolute configuration for structure **199** was confirmed by the refinement of the Flack absolute structure parameter, which refined to zero within error. Calculations using PLATON²⁶⁷ indicated that there were no voids in the lattice capable of containing solvent molecules. Thermal ellipsoid plots were obtained using the program ORTEP-3 for Windows.²⁶⁸ All calculations were carried out using the WinGX package²⁶⁹ of crystallographic programs.

6.3.3. UV-Vis spectroscopy

6.3.3.1. Characterisation: λ_{max} and ϵ_{coeff}

The λ_{max} and ϵ_{coeff} were evaluated by measuring the absorbance of various concentrations of the complex in aqueous solution in a quartz cuvette (3 ml) with a 1 cm path length (l). The extinction coefficient was determined from Beers' Law ($A = \epsilon cl$). Absorbances (A) vs. concentrations (c) for various dilutions were plotted, giving slope = ϵ_{coeff} . The λ_{max} was taken as the average of the wavelengths at which the absorbance was greatest for each concentration.

6.3.3.2. Aqueous stability of complexes

A solution of the complex (1.0 mM) in 100 mM aqueous phosphate buffer, pH 7.2, was allowed to stand for the required period of time. The λ_{max} of the solution was monitored by UV-Vis spectroscopy, watching for a shift towards the λ_{max} known for the 2-hydroxyethyl complex. The time required for a λ_{max} shift of

half the difference between those for the two complexes was defined as $t_{1/2}(\delta)$. Solutions were monitored for a maximum of two weeks.

6.3.4. Cyclic voltammetry

The redox potential of each compound was measured with cyclic voltammetry using a PGZ301 Dynamic-EIS VoltaLab potentiostat. The analysis was performed on freshly prepared solutions of the complexes (1.0 mM) in aqueous phosphate buffer (100 mM) at pH 7.2, with ferrocenecarboxylic acid (FCA) as an internal standard (+533 mV vs. NHE, or +334 mV vs. sat. Ag/AgCl),²¹⁷ using a three-electrode cell with a Pt macrodisc working electrode (2.0 mm), Pt wire counter electrode and either the Ag/AgNO₃ electrode [$E^\circ(\text{vs. Ag/AgNO}_3) = E^\circ + 253 \text{ mV (vs. Ag/AgCl)}$], or the saturated Ag/AgCl reference electrode. The potentials were corrected for the published potential of FCA and reported vs. NHE (correction factor: $E^\circ [\text{vs. NHE}] = E^\circ [\text{vs. Ag/AgCl}] + 199 \text{ mV}$). The solutions were degassed with N₂ for at least ten minutes before analysis, to simulate the hypoxic environment.

Table 6.4.1. Experimental crystallography details

Compound number	186	188	191
Compound formula	C ₁₆ H ₃₂ BCl ₅ CuF ₄ N ₄	C ₁₈ H ₄₀ Cl ₂ CuN ₄ O ₄	C ₁₂ H ₂₅ Cl ₃ CuF ₆ N ₃ OP
Compound color	blue	blue	blue
<i>M_r</i>	608.06	510.98	542.21
Space group	<i>P</i> 2 ₁ / <i>c</i>	<i>P</i> 2 ₁ / <i>n</i>	<i>P</i> 2 ₁ / <i>c</i>
Crystal system	Monoclinic	Monoclinic	Monoclinic
<i>a</i> /Å	15.0036(2)	15.4336(4)	8.0906(2)
<i>b</i> /Å	8.3325(1)	9.3240(3)	18.3838(4)
<i>c</i> /Å	20.3516(3)	15.7847(5)	13.7631(3)
β/deg	104.162(1)	103.472(1)	93.519(1)
<i>V</i> /Å ³	2466.98(6)	2208.96(12)	2043.21(8)
<i>Z</i>	4	4	4
<i>D_{calc}</i> /g cm ⁻³	1.637	1.536	1.763
<i>F</i> (000)	1244	1084	1100
μ(Mo-Kα)/mm ⁻¹	1.470	1.263	1.601
Crystal size/mm	0.30×0.12×0.09	0.25×0.15×0.15	0.44×0.38×0.30
Transmission coefficients (range)	0.882 - 0.672	0.709 - 0.645	0.644 - 0.490
θ range/deg	2.06 - 27.52	1.26 - 27.55	1.85 - 30.01
No. of data measured	41179	25122	31765
No. of unique data	5651	5024	5945
<i>R_{int}</i>	0.0517	0.0498	0.0350
No. of data in refinement	5651	5024	5945
No. of refined parameters	364	362	270
Final <i>R</i> [<i>I</i> > 2σ ¹⁺] (all data)	0.0296	0.0478	0.0322
<i>R_w</i> ² [<i>I</i> > 2σ ¹⁺] (all data)	0.0435	0.0702	0.0389
Flack parameter	n/a	n/a	n/a
Goodness of fit <i>S</i>	1.039	1.082	1.034
Largest residuals / eÅ ⁻³	0.418, -0.341	0.497, -0.643,	0.723, -0.518
Max shift/esd in last cycle	0.001	0.566	0.009

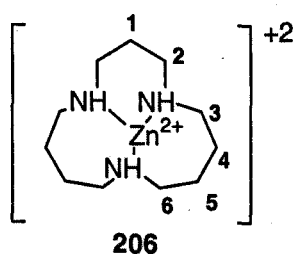
cont. next page

Compound number	199	187
Compound formula	C ₁₆ H ₃₂ Cl ₅ CoF ₆ N ₄ P	C ₁₇ H ₃₄ Cl ₅ CuF ₆ N ₄ P
Compound color	purple	blue
<i>M_r</i>	661.61	680.24
Space group	<i>P</i> 2 ₁ 2 ₁ 2 ₁	<i>P</i> 2 ₁ /c
Crystal system	Orthorhombic	Monoclinic
<i>a</i> /Å	8.8203(1)	12.1978(3)
<i>b</i> /Å	14.1553(2)	17.1387(5)
<i>c</i> /Å	21.0638(4)	13.3259(3)
β/deg	90	107.033(2)
<i>V</i> /Å ³	2629.90(7)	2663.64(12)
<i>Z</i>	4	4
<i>D_{calc}</i> /g cm ⁻³	1.671	1.696
<i>F</i> (000)	1348	1388
μ(Mo-Kα)/mm ⁻¹	1.278	1.439
Crystal size/mm	0.47×0.13×0.11	0.50×0.30×0.15
Transmission coefficients (range)	0.894 - 0.745	0.802 - 0.618
θ range/deg	2.41 - 27.51	1.75 - 30.08
No. of data measured	19793	46816
No. of unique data	5999	7760
<i>R_{int}</i>	0.0382	0.0403
No. of data in refinement	5999	7760
No. of refined parameters	362	463
Final <i>R</i> [<i>I</i> > 2σ ¹⁺] (all data)	0.0279	0.0553
<i>R_w</i> ² [<i>I</i> > 2σ ¹⁺] (all data)	0.0347	0.0720
Flack parameter	0.002(10)	n/a
Goodness of fit <i>S</i>	1.026	1.004
Largest residuals / eÅ ⁻³	0.243, -0.272	1.658, -1.025
Max shift/esd in last cycle	0.001	0.056

$R = \sum (|F_o| - |F_c|) / \sum (F_o)$; $R_w = \{\sum (w(F_o - F_c)^2) / \sum (w(F_o)^2)\}^{1/2}$; $R_w^2 = \{\sum (w(F_o^2 - F_c^2)^2) / \sum (w(F_o^2)^2)\}^{1/2}$; $R_o = \sum [\sigma(F_o^2)] / \sum [F_o^2]$; $R_{int} = \sum \{n/(n-1)\}^{1/2} |F_o^2 - F_o^2(\text{mean})| / \sum F_o^2$
 (summation is carried out only where more than one symmetry equivalent is averaged)

6.3.5. Complexation of novel triazamacrocycles

The triazamacrocycle was dissolved in D₂O in an NMR tube. A solution of ZnBr₂ in D₂O (100 mM) was added in four portions stepwise, providing 0.25 eq., 0.50 eq., 0.75 eq. and 1.0 eq. ZnBr₂ respectively. After the addition of each portion, the tube was shaken vigorously and analysed by ¹H NMR spectroscopy. After a total of 1.0 eq. ZnBr₂ had been added, the resulting complex was analysed by 2-dimensional NMR correlation spectra (COSY, HMQC and HMBC) to determine the extent of complexation and the structure of the ligand complex.

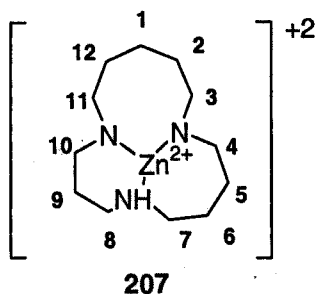


1,5,10-Triazacyclotetradecane[Zn(II)]Br₂ (**206**)

128 (0.013 g, 0.0163 mmol) was dissolved in D₂O (0.50 ml) and titrated as described above. The structure was analysed *in situ* and the complexed product was not isolated. See Appendix 2 for spectra.

Characterisation of 206

assign.	¹ H shift (ppm) (Integ., multip.)	¹³ C shift (ppm)
1	1.78-1.86 (2H, m)	24.3
2	2.96-3.02 (4H, m)	47.7
3	2.86-2.92 (4H, m)	42.5
4	1.66-1.75 (8H, m)	19.9
5	"	22.8
6	3.05-3.12 (4H, m)	45.9



1,5,10-Triazacyclopentadecane[Zn(II)]Br₂ (207)

129 (0.013 g, 0.0163 mmol) was dissolved in D₂O (0.50 ml) and titrated as described above. The structure was analysed *in situ* and the complexed product was not isolated. See **Appendix 2** for spectra.

Characterisation of 207

assign.	¹ H shift (ppm) (integ., multip.)	¹³ C shift (ppm)
1	1.40-1.49 (2H, m)	22.9
2	1.58-1.74 (8H, m)	24.1
3	2.98-3.08 (6H, m)	45.9
4	2.67-2.74 (2H, m)	47.7
5	See 2	25.4
6	See 2	25.5
7	2.90-2.95 (2H, m)	46.6
8	See 3	48.7
9	1.74-1.80 (2H, m)	23.3
10	2.85-2.90 (2H, m)	48.4
11	See 3	43.3
12	3.05-3.12 (4H, m)	See 2

6.4. Experimental to Chapter 5

6.4.1. Anti-cancer testing

6.4.1.1. Cytotoxicity of free mustard ligands (Prof. Hartley)

The cytotoxic effects of the free ligands studied were measured against the human chronic myeloid leukaemia cell line K562. Cells were maintained as a suspension in RPMI 1640 medium supplemented with 10% foetal calf serum (FCS) and 2 mM glutamine (Gln) at 37 °C in a humidified atmosphere containing 5% CO₂/ 95% air. The IC₅₀ values of the series of analogues following a 1 hour exposure to drug were determined using the MTT assay²⁷⁰ as has been previously described.²⁷¹ This is based on the ability of viable tumor cells to convert a yellow tetrazolium salt (3-(4,5-dimethylthiazol-2-yl)-2,5-diphenyl-2*H*-tetrazolium bromide, MTT) into mauve formazan crystals.

6.4.1.2. Cytotoxicity and hypoxia-selectivity of complexes (Prof. Stratford)

The toxicities of the complexes were determined using the MTT proliferation assay.²⁷² All media, plates and other plastic material were placed into the anoxic incubator for at least 24 h prior to the hypoxic experiments. The lung-derived tumor cell line, A549, was exposed to each of the three drugs for 24 h under aerobic or hypoxic conditions. After 24 h exposure, the drug was removed and fresh media instilled into each well. After 96 h incubation at 37 °C, the MTT proliferation assay was performed. The IC₅₀ results were expressed as the mean of at least three different experiments (\pm SEM). HCR is the hypoxic cytotoxicity ratio [IC₅₀ (air) / IC₅₀ (N₂)] and ACR is the aerobic cytotoxicity ratio [IC₅₀ (N₂) / IC₅₀ (air)].

6.4.2. Anti-parasitic testing

6.4.2.1. Cytotoxicity against *Leishmania mexicana* (Dr. Barrett)

Serial dilutions of the drugs (starting at 200 $\mu\text{g/mL}$) in a 96-well plate were incubated at 37 °C with a culture of *L. mexicana* in the logarithmic phase for 5 d. The IC_{50} values were determined using the acid phosphatase assay, which assesses the level of active (live) phosphatase enzyme present in the culture. *p*-Nitrophenylphosphate (40 mg/mL), NaOAc (1.0 M, pH 5.5) and Triton X-100 (1%) were added to the plates and the culture incubated at 37 °C for 1 h. The level of phosphatase activity was determined using UV-Vis spectroscopy (to detect *p*-nitrophenolate ion at 405 nm).

6.4.2.2. Cytotoxicity against *Trypanosoma brucei* (Dr. Barrett)

Serial dilutions of the drugs (starting at 200 $\mu\text{g/mL}$) in a 96-well plate were incubated at 37 °C with a culture of *T. brucei* for 36 h. All experiments were performed in duplicate. The cytotoxicities were determined using the alamar blue assay,²²¹ which measures the ability of viable parasite cells to convert a blue dye to a colorless compound. The cultures were incubated at 37 °C with the dye for a further 24h. IC_{50} values were determined from UV-Vis spectroscopy, detecting dead cells by the concentration of alamar blue dye left in solution.

References

1. Cancer Research U.K., *CancerStats reports*,
<http://www.cancerresearchuk.org/aboutcancer/statistics/cancerstatsreport/>
2. P. C. Nowell, *Science*, 1976, **194**, 23.
3. D. Hanahan and R. A. Weinberg, *Cell*, 2000, **100**, 57.
4. K. W. Kinzler and B. Vogelstein, *Science*, 1998, **280**, 1036.
5. N. A. Thornberry and Y. Lazebnik, *Science*, 1998, **281**, 1312.
6. W. E. Wright, O. M. Pereirasmith and J. W. Shay, *Molecular and Cellular Biology*, 1989, **9**, 3088.
7. K. J. Kim, B. Li, J. Winer, M. Armanini, N. Gillett, H. S. Phillips and N. Ferrara, *Nature*, 1993, **362**, 841.
8. M. B. Sporn, *Lancet*, 1996, **347**, 1377.
9. F. T. Boyle and G. F. Costello, *Chemical Society Reviews*, 1998, **27**, 251.
10. O. B. Eden, J. S. Lilleyman, S. Richards, M. P. Shaw and J. Peto, *British Journal of Haematology*, 1991, **78**, 187.
11. C. D. Runowicz, P. H. Wiernik, A. I. Einzig, G. L. Goldberg and S. B. Horwitz, *Cancer*, 1993, **71**, 1591.
12. A. Grothey and H. J. Schmoll, *Current Opinion in Oncology*, 2001, **13**, 275.
13. R. C. F. Leonard, *British Journal of Cancer*, 2001, **84**, 1437.
14. R. A. Gatenby, H. B. Kessler, J. S. Rosenblum, L. R. Coia, P. J. Moldofsky, W. H. Hartz and G. J. Broder, *International Journal of Radiation Oncology Biology Physics*, 1988, **14**, 831.
15. P. Vaupel, K. Schlenger, C. Knoop and M. Hockel, *Cancer Research*, 1991, **51**, 3316.
16. M. Hockel, K. Schlenger, C. Knoop and P. Vaupel, *Cancer Research*, 1991, **51**, 6098.
17. W. A. Denny, *European Journal of Medicinal Chemistry*, 2001, **36**, 577.
18. S. M. Evans, S. M. Hahn, D. P. Magarelli and C. J. Koch, *American Journal of Clinical Oncology-Cancer Clinical Trials*, 2001, **24**, 467.
19. J. L. Yu, J. W. Rak, P. Carmeliet, A. Nagy, R. S. Kerbel and B. L. Coomber, *American Journal of Pathology*, 2001, **158**, 1325.
20. J. E. Moulder and S. Rockwell, *International Journal of Radiation Oncology Biology Physics*, 1984, **10**, 695.
21. S. Walenta, M. Wetterling, M. Lehrke, G. Schwickert, K. Sundfor, E. K. Rofstad and W. Mueller-Klieser, *Cancer Research*, 2000, **60**, 916.
22. S. Walenta, T. V. Chau, T. Schroeder, H. A. Lehr, L. A. Kunz-Schughart, A. Fuerst and W. Mueller-Klieser, *Journal of Cancer Research and Clinical Oncology*, 2003, **129**, 321.
23. S. Walenta, S. Snyder, Z. A. Haroon, R. D. Braun, K. Amin, D. Brizel, W. Mueller-Klieser, B. Chance and M. W. Dewhirst, *International Journal of Radiation Oncology Biology Physics*, 2001, **51**, 840.
24. R. A. Cairns, R. Khokha and R. P. Hill, *Current Molecular Medicine*, 2003, **3**, 659.
25. R. D. Braun, J. L. Lanzen, S. A. Snyder and M. W. Dewhirst, *American Journal of Physiology-Heart and Circulatory Physiology*, 2001, **280**, H2533.
26. J. D. Chapman, A. J. Franko and J. Sharplin, *British Journal of Cancer*, 1981, **43**, 546.
27. J. D. Chapman, K. Baer and J. Lee, *Cancer Research*, 1983, **43**, 1523.

28. B. M. Garrecht and J. D. Chapman, *British Journal of Radiology*, 1983, **56**, 745.
29. J. S. Lewis, T. L. Sharp, R. Laforest, Y. Fujibayashi and M. J. Welch, *Journal of Nuclear Medicine*, 2001, **42**, 655.
30. B. G. Wouters, S. A. Weppeler, M. Koritzinsky, W. Landuyt, S. Nuyts, J. Theys, R. K. Chiu and P. Lambin, *European Journal of Cancer*, 2002, **38**, 240.
31. H. Cortes-Funes, *Drugs of Today*, 2002, **38**, 11.
32. M. T. Canning, L. M. Postovit, S. H. Clarke and C. H. Graham, *Experimental Cell Research*, 2001, **267**, 88.
33. S. Chakraborti, M. Mandal, S. Das, A. Mandal and T. Chakraborti, *Molecular and Cellular Biochemistry*, 2003, **253**, 269.
34. M. Egeblad and Z. Werb, *Nature Reviews Cancer*, 2002, **2**, 161.
35. G. E. Lash, T. E. Fitzpatrick and C. H. Graham, *Biochemical and Biophysical Research Communications*, 2001, **287**, 622.
36. E. A. O'toole, M. P. Marinkovich, C. L. Peavey, M. R. Amieva, H. Furthmayr, T. A. Mustoe and D. T. Woodley, *Journal of Clinical Investigation*, 1997, **100**, 2881.
37. A. V. Patterson, K. J. Williams, R. L. Cowen, M. Jaffar, B. A. Telfer, M. Saunders, R. Airley, D. Honess, A. J. Van Der Kogel, C. R. Wolf and I. J. Stratford, *Gene Therapy*, 2002, **9**, 946.
38. M. Jaffar, K. J. Williams and I. J. Stratford, *Advanced Drug Delivery Reviews*, 2001, **53**, 217.
39. N. C. Denko, L. A. Fontana, K. M. Hudson, P. D. Sutphin, S. Raychaudhuri, R. Altman and A. J. Giaccia, *Oncogene*, 2003, **22**, 5907.
40. D. Vordermark and J. M. Brown, *International Journal of Radiation Oncology Biology Physics*, 2003, **56**, 1184.
41. N. Goda, H. E. Ryan, B. Khadivi, W. McNulty, R. C. Rickert and R. S. Johnson, *Molecular and Cellular Biology*, 2003, **23**, 359.
42. C. E. Dann, R. K. Bruick and J. Deisenhofer, *Proceedings of the National Academy of Sciences of the United States of America*, 2002, **99**, 15351.
43. F. Yu, S. B. White, Q. Zhao and F. S. Lee, *Proceedings of the National Academy of Sciences of the United States of America*, 2001, **98**, 9630.
44. S. Dai, M. L. Huang, C. Y. Hsu and K. S. C. Chao, *International Journal of Radiation Oncology Biology Physics*, 2003, **55**, 1027.
45. X. Sun, J. R. Kanwar, E. Leung, K. Lehnert, D. Wang and G. W. Krissansen, *Gene Therapy*, 2001, **8**, 638.
46. K. Binley, Z. Askham, L. Martin, H. Spearman, D. Day, S. Kingsman and S. Naylor, *Gene Therapy*, 2003, **10**, 540.
47. J. L. Yu, B. L. Coomber and R. S. Kerbel, *Differentiation*, 2002, **70**, 599.
48. R. A. Brekken and P. E. Thorpe, *Anticancer Research*, 2001, **21**, 4221.
49. P. Workman and I. J. Stratford, *Cancer and Metastasis Reviews*, 1993, **12**, 73.
50. F. C. De Abreu, P. A. D. Ferraz and M. O. F. Goulart, *Journal of the Brazilian Chemical Society*, 2002, **13**, 19.
51. S. L. Winski, E. Swann, R. H. J. Hargreaves, D. L. Dehn, J. Butler, C. J. Moody and D. Ross, *Biochemical Pharmacology*, 2001, **61**, 1509.
52. W. A. Denny, W. R. Wilson and M. P. Hay, *British Journal of Cancer*, 1996, **74**, S32.
53. D. P. Naughton, *Advanced Drug Delivery Reviews*, 2001, **53**, 229.

54. S. V. Jovanovic, S. Steenken, M. Tomic, B. Marjanovic and M. G. Simic, *Journal of the American Chemical Society*, 1994, **116**, 4846.
55. L. H. Patterson and S. R. Mckeown, *British Journal of Cancer*, 2000, **83**, 1589.
56. Y. Fukuda, H. Furuta, Y. Kusama, H. Ebisu, Y. Oomori and S. Terashima, *Journal of Medicinal Chemistry*, 1999, **42**, 1448.
57. L. H. Li, T. F. Dekoning, R. C. Kelly, W. C. Krueger, J. P. McGovren, G. E. Padbury, G. L. Petzold, T. L. Wallace, R. J. Ouding, M. D. Prairie and I. Gebhard, *Cancer Research*, 1992, **52**, 4904.
58. M. D. I. Sessa, *Expert Opinion on Investigational Drugs*, 1997, **6**, 875
59. C. J. Moody, N. Osullivan, I. J. Stratford, M. A. Stephens, P. Workman, S. M. Bailey and A. Lewis, *Anti-Cancer Drugs*, 1994, **5**, 367.
60. P. M. Cullis, R. E. Green and M. E. Malone, *Journal of the Chemical Society, Perkin Transactions 2*, 1995, 1503.
61. W. R. Wilson, J. W. Moselen, S. Cliffe, W. A. Denny and D. C. Ware, *International Journal of Radiation Oncology Biology Physics*, 1994, **29**, 323.
62. B. D. Palmer, P. Vanzijl, W. A. Denny and W. R. Wilson, *Journal of Medicinal Chemistry*, 1995, **38**, 1229.
63. M. D. Threadgill, P. Webb, P. Oneill, M. A. Naylor, M. A. Stephens, I. J. Stratford, S. Cole, G. E. Adams and E. M. Fielden, *Journal of Medicinal Chemistry*, 1991, **34**, 2112.
64. M. P. Hay, H. H. Lee, W. R. Wilson, P. B. Roberts and W. A. Denny, *Journal of Medicinal Chemistry*, 1995, **38**, 1928.
65. J. M. Berry, C. Y. Watson, W. J. D. Whish and M. D. Threadgill, *Journal of the Chemical Society, Perkin Transactions 1*, 1997, 1147.
66. M. P. Hay, W. R. Wilson and W. A. Denny, *Tetrahedron*, 2000, **56**, 645.
67. M. Tercel, W. R. Wilson and W. A. Denny, *Journal of Medicinal Chemistry*, 1993, **36**, 2578.
68. M. Tercel, W. R. Wilson, R. F. Anderson and W. A. Denny, *Journal of Medicinal Chemistry*, 1996, **39**, 1084.
69. M. Tercel, A. E. Lee, A. Hogg, R. F. Anderson, H. H. Lee, B. G. Siim, W. A. Denny and W. R. Wilson, *Journal of Medicinal Chemistry*, 2001, **44**, 3511.
70. M. P. Hay, S. A. Gamage, M. S. Kovacs, F. B. Pruijn, R. F. Anderson, A. V. Patterson, W. R. Wilson, J. M. Brown and W. A. Denny, *Journal of Medicinal Chemistry*, 2003, **46**, 169.
71. M. Tercel, W. R. Wilson and W. A. Denny, *Journal of Medicinal Chemistry*, 1995, **38**, 1247.
72. D. C. Ware, B. D. Palmer, W. R. Wilson and W. A. Denny, *Journal of Medicinal Chemistry*, 1993, **36**, 1839.
73. B. A. Teicher, M. J. Abrams, K. W. Rosbe and T. S. Herman, *Cancer Research*, 1990, **50**, 6971.
74. D. C. Ware, W. R. Wilson, W. A. Denny and C. E. F. Rickard, *Journal of the Chemical Society, Chemical Communications*, 1991, 1171.
75. R. F. Anderson, W. A. Denny, D. C. Ware and W. R. Wilson, *British Journal of Cancer*, 1996, **74**, S48.
76. Y. Fujibayashi, H. Taniuchi, Y. Yonekura, H. Ohtani, J. Konishi and A. Yokoyama, *Journal of Nuclear Medicine*, 1997, **38**, 1155.
77. R. I. Maurer, P. J. Blower, J. R. Dilworth, C. A. Reynolds, Y. F. Zheng and G. E. D. Mullen, *Journal of Medicinal Chemistry*, 2002, **45**, 1420.

78. F. Dehdashti, M. A. Mintun, J. S. Lewis, R. Govindan and M. J. Welch, *Journal of Nuclear Medicine*, 2000, **41**, 130.
79. M. A. Mintun, K. L. Berger, F. Dehdashti, J. S. Lewis, C. Chao and M. J. Welch, *Journal of Nuclear Medicine*, 2000, **41**, 229.
80. N. Takahashi, Y. Fujibayashi, Y. Yonekura, M. J. Welch, W. Tsuchida, S. Nakamura, N. Sadato, K. Sugimoto, K. Yamamoto, A. Yokoyama and Y. Ishii, *Journal of Nuclear Medicine*, 1998, **39**, 200.
81. B. E. Rogers, C. J. Anderson, J. M. Connett, L. W. Guo, W. B. Edwards, E. L. C. Sherman, K. R. Zinn and M. J. Welch, *Bioconjugate Chemistry*, 1996, **7**, 511.
82. D. Ross, H. D. Beall, D. Siegel, R. D. Traver and D. L. Gustafson, *British Journal of Cancer*, 1996, **74**, S1.
83. P. Workman and M. I. Walton, in *Selective Activation of Drugs by Redox Processes* (Ed.: G. E. Adams, Breccia, A., Fielden, E. M., Wardman, P.), Plenum, New York, 1990, pp. 173.
84. F. Zappa, T. Ward, J. Butler, E. Pedrinis and A. McGown, *Journal of Histochemistry & Cytochemistry*, 2001, **49**, 1187.
85. P. J. Odwyer, R. P. Perez, K. S. Yao, A. K. Godwin and T. C. Hamilton, *Biochemical Pharmacology*, 1996, **52**, 21.
86. K. S. Yao and P. J. Odwyer, *Biochemical Pharmacology*, 1995, **49**, 275.
87. K. S. Yao, S. Xanthoudakis, T. Curran and P. J. Odwyer, *Molecular and Cellular Biology*, 1994, **14**, 5997.
88. G. Cavelier and L. M. Amzel, *Proteins-Structure Function and Genetics*, 2001, **43**, 420.
89. R. B. Li, M. A. Bianchet, P. Talalay and L. M. Amzel, *Proceedings of the National Academy of Sciences of the United States of America*, 1995, **92**, 8846.
90. Nci, *NCI Human Tumor Cell Lines Database*,
<http://www.atcc.org/SearchCatalogs/ncisearch.cfm>
91. P. Hlavica, J. Schulze and D. F. V. Lewis, *Journal of Inorganic Biochemistry*, 2003, **96**, 279.
92. J. C. M. Bremner, I. J. Stratford, J. Bowler and G. E. Adams, *British Journal of Cancer*, 1990, **61**, 717.
93. P. R. Norman, *Inorganica Chimica Acta*, 1987, **130**, 1.
94. S. E. Castilloblum and M. E. Sosatorres, *Polyhedron*, 1995, **14**, 223.
95. A. D. Kirk and L. Z. Cai, *Inorganic Chemistry*, 1995, **34**, 3986.
96. E. L. Hegg, S. H. Mortimore, C. L. Cheung, J. E. Huyett, D. R. Powell and J. N. Burstyn, *Inorganic Chemistry*, 1999, **38**, 2961.
97. R. D. Hancock, H. Maumela and A. S. Desousa, *Coordination Chemistry Reviews*, 1996, **148**, 315.
98. R. D. Hancock, P. W. Wade, M. P. Ngwenya, A. S. Desousa and K. V. Damu, *Inorganic Chemistry*, 1990, **29**, 1968.
99. A. E. Martell and R. J. Motekaitis, *The Determination and Use of Stability Constants, Vol. 1*, VCH, New York, 1988.
100. S. A. Grando, *Life Sciences*, 2003, **72**, 2135.
101. W. B. Mattes, J. A. Hartley and K. W. Kohn, *Nucleic Acids Research*, 1986, **14**, 2971.
102. N. J. Birdsall, A. S. Burgen and E. C. Hulme, *Molecular Pharmacology*, 1978, **14**, 723.

103. S. M. Rink and P. B. Hopkins, *Bioorganic & Medicinal Chemistry Letters*, 1995, **5**, 2845.
104. J. A. Hartley, M. D. Berardini and R. L. Souhami, *Analytical Biochemistry*, 1991, **193**, 131.
105. P. J. Mchugh, R. D. Gill, R. Waters and J. A. Hartley, *Nucleic Acids Research*, 1999, **27**, 3259.
106. M. R. Middleton and G. P. Margison, *Lancet Oncology*, 2003, **4**, 37.
107. K. T. Douglas, *Chemistry & Industry*, 1984, 738.
108. *Alkylating Agents: The Janus Effect*,
<http://www.chemheritage.org/EducationalServices/pharm/chemo/readings/alkyl.htm>
109. M. Ritchie, *BIOGRAPHICAL MEMOIRS: Alfred Gilman*,
<http://www.nap.edu/html/biomems/agilman.html>
110. H. H. Yang, R. Vescio, D. Schenkein and J. R. Berenson, *Clinical Lymphoma*, 2003, **4**, 119.
111. S. Davis-Perry, E. Hernandez, K. L. Houck and R. Shank, *American Journal of Clinical Oncology-Cancer Clinical Trials*, 2003, **26**, 429.
112. W. A. Remers, in *Antineoplastic Agents, Vol. 3* (Ed.: W. A. Remers), John Wiley & Sons, New York, 1984, p. 117.
113. G. M. Cohen, P. M. Cullis, J. A. Hartley, A. Mather, M. C. R. Symons and R. T. Wheelhouse, *Journal of the Chemical Society, Chemical Communications*, 1992, 298.
114. P. M. Cullis, L. Mersondavies and R. Weaver, *Journal of the American Chemical Society*, 1995, **117**, 8033.
115. G. J. Atwell, B. M. Yaghi, P. R. Turner, M. Boyd, C. J. Oconnor, L. R. Ferguson, B. C. Baguley and W. A. Denny, *Bioorganic & Medicinal Chemistry*, 1995, **3**, 679.
116. Y. D. Wang, J. Dziegielewski, N. R. Wurtz, B. Dziegielewska, P. B. Dervan and T. A. Beerman, *Nucleic Acids Research*, 2003, **31**, 1208.
117. Y. Q. Wang, S. C. Wright and J. W. Larrick, *Bioorganic & Medicinal Chemistry Letters*, 2003, **13**, 459.
118. N. D. Henderson, *Synthesis and biological evaluation of novel anti-cancer agents*, PhD thesis, University of Glasgow (Glasgow), 1994.
119. N. D. Henderson, J. A. Plumb, D. J. Robins and P. Workman, *Anti-Cancer Drug Design*, 1996, **11**, 421.
120. N. D. Henderson, S. M. Lacy, C. C. O'hare, J. A. Hartley, S. McClean, L. P. G. Wakelin, L. R. Kelland and D. J. Robins, *Anti-Cancer Drug Design*, 1998, **13**, 749.
121. F. M. Anderson, *Synthesis of Novel Alkylating Agents for Biological Evaluation as Anti-Cancer Prodrugs*, PhD thesis, University of Glasgow (Glasgow), 1999.
122. F. M. Anderson, C. C. O'hare, J. A. Hartley and D. J. Robins, *Anti-Cancer Drug Design*, 2000, **15**, 119.
123. V. Alexander, *Chemical Reviews*, 1995, **95**, 273.
124. R. J. Motekaitis, B. E. Rogers, D. E. Reichert, A. E. Martell and M. J. Welch, *Inorganic Chemistry*, 1996, **35**, 3821.
125. F. L. Weitz and K. N. Raymond, *Journal of the American Chemical Society*, 1979, **101**, 2728.
126. L. L. Parker, F. M. Anderson, S. M. Lacy, D. J. Robins and J. A. Hartley, *manuscript in preparation*.

127. J. A. Richman and T. J. Atkins, *Journal of the American Chemical Society*, 1974, **96**, 2268.
128. J. Van Alphen, *Recueil Travail Chimie Pays-Bas*, 1936, **55**, 835.
129. J. Van Alphen, *Recueil Travail Chimie Pays-Bas*, 1937, **56**, 343.
130. B. Bosnich, C. K. Poon and M. L. Tobe, *Inorganic Chemistry*, 1965, **4**, 1102.
131. H. Stetter and E. E. Roos, *Chemische Berichte*, 1954, **87**, 566.
132. H. Stetter and E. E. Roos, *Chemische Berichte*, 1955, **88**, 1390.
133. H. Stetter and K. Mayer, *Chemische Berichte*, 1961, **94**, 1410.
134. J. S. Bradshaw, K. E. Krakowiak, R. M. Izatt and D. J. Zameckakrakowiak, *Tetrahedron Letters*, 1990, **31**, 1077.
135. D. Parker, in *Macrocyclic Synthesis: A Practical Approach*, Oxford University Press, Oxford, 1996, p. 17.
136. S. C. Rawle, A. J. Clarke, P. Moore and N. W. Alcock, *Journal of the Chemical Society, Dalton Transactions*, 1992, 2755.
137. N. F. Curtis, Y. M. Curtis and H. J. K. Powell, *Journal of the Chemical Society A*, 1966, 1015.
138. I. Meunier, A. K. Mishra, B. Hanquet, P. Cocolios and R. Guillard, *Canadian Journal of Chemistry*, 1995, **73**, 685.
139. E. K. Barefield, F. Wagner, A. W. Herlinger and A. R. Dahl, *Inorganic Synthesis*, 1976, **16**, 220.
140. A. Bayada, G. A. Lawrance, M. Maeder and M. A. O'Leary, *Journal of the Chemical Society, Dalton Transactions*, 1994, 3107.
141. F. P. Schmidtchen, *Chemische Berichte*, 1980, **113**, 2175.
142. A. F. McKay and M. E. Kreyling, *Canadian Journal of Chemistry*, 1957, **35**, 1438.
143. G. R. Weisman, D. J. Vachan, V. B. Johnson and D. A. Gronbeck, *Journal of the Chemical Society, Chemical Communications*, 1989, 794.
144. R. W. Alder, R. W. Mowlam, D. J. Vachon and G. R. Weisman, *Journal of the Chemical Society, Chemical Communications*, 1992, 507.
145. G. R. Weisman and D. P. Reed, *Journal of Organic Chemistry*, 1996, **61**, 5186.
146. J. Rohovec, R. Gyepes, I. Cisarova, J. Rudovsky and I. Lukes, *Tetrahedron Letters*, 2000, **41**, 1249.
147. G. Herve, H. Bernard, N. Le Bris, M. Le Baccon, J. J. Yaouanc and H. Handel, *Tetrahedron Letters*, 1999, **40**, 2517.
148. G. Herve, H. Bernard, N. Le Bris, J. J. Yaouanc, H. Handel and L. Toupet, *Tetrahedron Letters*, 1998, **39**, 6861.
149. P. S. Athey and G. E. Kiefer, *Journal of Organic Chemistry*, 2002, **67**, 4081.
150. P. S. Athey and G. E. Kiefer, 'Process for preparing polyazamacrocycles', U. S. Patent 5,587,451, USA, Dow Chemical, 1996.
151. R. C. Hoye, J. E. Richman, G. A. Dantas, M. F. Lightbourne and L. S. Shinneman, *Journal of Organic Chemistry*, 2001, **66**, 2722.
152. M. I. Burguete, B. Escuder, S. V. Luis, J. F. Miravet, M. Querol and E. Garcia-Espana, *Tetrahedron Letters*, 1998, **39**, 3799.
153. H. Y. An, L. L. Cummins, R. H. Griffey, R. Bharadwaj, B. D. Haly, A. S. Fraser, L. Wilsonlingardo, L. M. Risen, J. R. Wyatt and P. D. Cook, *Journal of the American Chemical Society*, 1997, **119**, 3696.
154. F. Chavez and A. D. Sherry, *Journal of Organic Chemistry*, 1989, **54**, 2990.
155. A. V. Bogatsky, N. G. Lukyanenko, S. S. Basok and L. K. Ostrovskaya, *Synthesis*, 1983, 138.

156. B. K. Vriesema, J. Buter and R. M. Kellogg, *Journal of Organic Chemistry*, 1984, **49**, 110.
157. S. Pulacchini and M. Watkinson, *Tetrahedron Letters*, 1999, **40**, 9363.
158. S. Pulacchini and M. Watkinson, *European Journal of Organic Chemistry*, 2001, 4233.
159. V. Panetta-Le Mer, J. J. Yaouanc and H. Handel, *Tetrahedron Letters*, 1994, **35**, 2337.
160. J. W. Sibert, A. H. Cory and J. G. Cory, *Chemical Communications*, 2002, 154.
161. G. J. Bridger, R. T. Skerlj, S. Padmanabhan and D. Thornton, *Journal of Organic Chemistry*, 1996, **61**, 1519.
162. H. C. Joao, K. Devreese, R. Pauwels, E. Declercq, G. W. Henson and G. J. Bridger, *Journal of Medicinal Chemistry*, 1995, **38**, 3865.
163. Y. Inouye, T. Kanamori, M. Sugiyama, T. Yoshida, T. Koike, M. Shionoya, K. Enomoto, K. Suehiro and E. Kimura, *Antiviral Chemistry & Chemotherapy*, 1995, **6**, 337.
164. D. R. Morris, in *Polyamines in biomedical research* (Ed.: J. Gaugas), John Wiley & Sons, Chichester, 1980, pp. 1.
165. K. Nishioka, in *Polyamines in cancer: basic mechanisms and clinical approaches* (Ed.: K. Nishioka), R. G. Landes Company, Austin, Texas, 1996, pp. 1.
166. G. Karigiannis and D. Papaioannou, *European Journal of Organic Chemistry*, 2000, 1841.
167. B. Martin, F. Posseme, C. Le Barbier, F. Carreaux, B. Carboni, N. Seiler, J. P. Moulinoux and J. G. Delcros, *Journal of Medicinal Chemistry*, 2001, **44**, 3653.
168. L. Wang, H. L. Price, J. Juusola, M. Kline and O. Phanstiel, *Journal of Medicinal Chemistry*, 2001, **44**, 3682.
169. R. J. Bergeron, Y. Feng, W. R. Weimar, J. S. Mcmanis, H. Dimova, C. Porter, B. Raisler and O. Phanstiel, *Journal of Medicinal Chemistry*, 1997, **40**, 1475.
170. V. K. Reddy, A. Valasinas, A. Sarkar, H. S. Basu, L. J. Marton and B. Frydman, *Journal of Medicinal Chemistry*, 1998, **41**, 4723.
171. M. C. O' Sullivan, Q. Zhou, Z. Li, T. B. Durham, D. Rattendi, S. Lane, C. J. Bacchi, *Bioorganic & Medicinal Chemistry Letters*, 1997, **5**, 2145.
172. H. K. Webb, Z. Q. Wu, N. Sirisoma, H. C. Ha, R. A. Casero and P. M. Woster, *Journal of Medicinal Chemistry*, 1999, **42**, 1415.
173. S. Girault, P. Grellier, A. Berecibar, L. Maes, P. Lemièrre, E. Mouray, E. Davioud-Charvet and C. Sergheraert, *Journal of Medicinal Chemistry*, 2001, **44**, 1658.
174. V. Pavlov, P. K. T. Lin and V. Rodilla, *Chemico-Biological Interactions*, 2001, **137**, 15.
175. H. S. Winchell, J. Y. Klein, E. D. Simhon, R. L. Cyjon, O. Klein and H. Zaklad, *Compounds with chelation affinity and selectivity for first transition elements and their use in cosmetics and personal care products, inhibition of metalloenzymes, and inhibition of reperfusion injury*, U. S. Patent 6,387,891, Canada, Concat, Ltd., 2002.
176. M. J. Abrams, S. P. Fricker, B. A. Murrer and O. J. Vaughan, *Pharmaceutical compositions comprising metal complexes*, U. S. Patent 6,284,752, USA, Procter & Gamble, 2001.

177. E. Kimura, *Accounts of Chemical Research*, 2001, **34**, 171.
178. E. Kimura, I. Nakamura, T. Koike, M. Shionoya, Y. Kodama, T. Ikeda and M. Shiro, *Journal of the American Chemical Society*, 1994, **116**, 4764.
179. S. A. Li, D. X. Yang, D. F. Li, J. Huang and W. X. Tang, *New Journal of Chemistry*, 2002, **26**, 1831.
180. J. A. Cowan, *Current Opinion in Chemical Biology*, 2001, **5**, 634.
181. C. S. Jeung, J. B. Song, Y. H. Kim and J. Suh, *Bioorganic & Medicinal Chemistry Letters*, 2001, **11**, 3061.
182. C. S. Jeung, C. H. Kim, K. Min, S. W. Suh and J. Suh, *Bioorganic & Medicinal Chemistry Letters*, 2001, **11**, 2401.
183. K. A. Deal, G. Park, J. Shao, N. D. Chasteen, M. W. Brechbiel and R. P. Planalp, *Inorganic Chemistry*, 2001, **40**, 4176.
184. K. M. Deck, T. A. Tseng and J. N. Burstyn, *Inorganic Chemistry*, 2002, **41**, 669.
185. D. Y. Kong, L. H. Meng, J. Ding, Y. Y. Xie and X. Y. Huang, *Polyhedron*, 2000, **19**, 217.
186. A. A. Neverov, P. J. Montoya-Pelaez and R. S. Brown, *Journal of the American Chemical Society*, 2001, **123**, 210.
187. J. Suh and S. J. Moon, *Inorganic Chemistry*, 2001, **40**, 4890.
188. B. B. Jang, K. P. Lee, D. H. Min and J. Suh, *Journal of the American Chemical Society*, 1998, **120**, 12008.
189. J. W. Jeon, S. J. Son, C. E. Yoo, I. S. Hong, J. B. Song and J. Suh, *Organic Letters*, 2002, **4**, 4155.
190. J. W. Jeon, S. J. Son, C. E. Yoo, I. S. Hong and J. Suh, *Bioorganic & Medicinal Chemistry*, 2003, **11**, 2901.
191. R. J. Bergeron, J. S. Mcmanis, C. Z. Liu, Y. Feng, W. R. Weimar, G. R. Luchetta, Q. H. Wu, J. Ortizocasio, J. R. T. Vinson, D. Kramer and C. Porter, *Journal of Medicinal Chemistry*, 1994, **37**, 3464.
192. S. M. Weinreb, D. M. Demko, T. A. Lessen and J. P. Demers, *Tetrahedron Letters*, 1986, **27**, 2099.
193. J. M. Siaugue, F. Segat-Dioury, I. Sylvestre, A. Favre-Reguillon, J. Foos, C. Madic and A. Guy, *Tetrahedron*, 2001, **57**, 4713.
194. T. Fukuyama, C. K. Jow and M. Cheung, *Tetrahedron Letters*, 1995, **36**, 6373.
195. S. M. Weinreb, C. E. Chase, P. Wipf and S. Venkatraman, *Organic Syntheses*, 1997, **75**, 161.
196. R. J. Bergeron, P. S. Burton, K. A. McGovern and S. J. Kline, *Synthesis*, 1981, 732.
197. Y. B. Lee, M. H. Park and J. E. Folk, *Journal of Medicinal Chemistry*, 1995, **38**, 3053.
198. G. Gokel, *Crown Ethers & Cryptands*, The Royal Society of Chemistry, Cambridge, U.K., 1991.
199. M. F. Brana, M. Cacho, A. Gradillas, B. De Pascual-Teresa and A. Ramos, *Current Pharmaceutical Design*, 2001, **7**, 1745.
200. M. Koyama, T. R. Kelly and K. A. Watanabe, *Journal of Medicinal Chemistry*, 1988, **31**, 283.
201. G. R. Martinez, J. L. Ravanat, M. H. G. Medeiros, J. Cadet and P. Di Mascio, *Journal of the American Chemical Society*, 2000, **122**, 10212.
202. H.-D. Scharf and R. Weitz, *Tetrahedron*, 1979, **35**, 2263.

203. S. Kotha and E. Brahmachary, *Bioorganic & Medicinal Chemistry Letters*, 1997, **7**, 2719.
204. L. L. Parker, N. D. Gowans, S. W. Jones and D. J. Robins, *Tetrahedron*, 2003, **in press**.
205. M. Lee and B. J. Garbiras, *Synthetic Communications*, 1994, **24**, 3129.
206. T. Watanabe, I. Kinoyama, A. Kakefuda, T. Okazaki, K. Takizawa, S. Hirano, H. Shibata and I. Yanagisawa, *Chemical & Pharmaceutical Bulletin*, 1997, **45**, 996.
207. C. Geraldes, A. D. Sherry, M. P. M. Marques, M. C. Alpoim and S. Cortes, *Journal of the Chemical Society, Perkin Transactions 2*, 1991, 137.
208. B. A. Boyce, A. Carroy, J. M. Lehn and D. Parker, *Journal of the Chemical Society, Chemical Communications*, 1984, 1546.
209. C. M. Madeyski, J. P. Michael and R. D. Hancock, *Inorganic Chemistry*, 1984, **23**, 1487.
210. M. Rejzek, Z. Wimmer, D. Saman, M. Ricankova and V. Nemec, *Helvetica Chimica Acta*, 1994, **77**, 1241.
211. X. K. Sun, M. Wuest, G. R. Weisman, E. H. Wong, D. P. Reed, C. A. Boswell, R. Motekaitis, A. E. Martell, M. J. Welch and C. J. Anderson, *Journal of Medicinal Chemistry*, 2002, **45**, 469.
212. C. H. Hamann, A. Hamnett and W. Vielstich, *Electrochemistry*, Wiley-VCH, Weinheim, **1998**.
213. M. Cardosi, *A Cyclic Voltammetry Primer*, http://www-biol.paisley.ac.uk/marco/Enzyme_Electrode/Chapter1/Cyclic_Voltammetry1.htm
214. A. E. Kaifer and M. Gomez-Kaifer, *Supramolecular Electrochemistry*, Wiley-VCH, Weinheim, **1999**.
215. A. E. Martell and R. M. Smith, *Critical stability constants, Vol. 1-6*, Plenum Press, New York ; London, **1974-present**.
216. S. M. Lacy, D. J. Robins and J. A. Hartley, *unpublished results*, **1996**.
217. D. Osella, M. Ferrali, P. Zanello, F. Laschi, M. Fontani, C. Nervi and G. Cavigiolio, *Inorganica Chimica Acta*, 2000, **306**, 42.
218. R. Rogers, *Converting Potentials to Another Reference Electrode*, <http://www.consultsr.com/resources/ref/refpotls2.htm>
219. A. M. Bond, G. A. Lawrance, P. A. Lay and A. M. Sargeson, *Inorganic Chemistry*, 1983, **22**, 2010.
220. Y. H. Fan and B. Gold, *Journal of the American Chemical Society*, 1999, **121**, 11942.
221. B. Raz, M. Iten, Y. Gretherbuhler, R. Kaminsky and R. Brun, *Acta Tropica*, 1997, **68**, 139.
222. K. Augustyns, K. Amssoms, A. Yamani, P. K. Rajan and A. Haemers, *Current Pharmaceutical Design*, 2001, **7**, 1117.
223. S. R. Wilkinson, N. J. Temperton, A. Mondragon and J. M. Kelly, *Journal of Biological Chemistry*, 2000, **275**, 8220.
224. A. R. Bello, B. Nare, D. Freedman, L. Hardy and S. M. Beverley, *Proceedings of the National Academy of Sciences of the United States of America*, 1994, **91**, 11442.
225. H. Vial, *Parasite-Journal De La Societe Francaise De Parasitologie*, 1996, **3**, 3.
226. M. Foley and L. Tilley, *Pharmacology & Therapeutics*, 1998, **79**, 55.

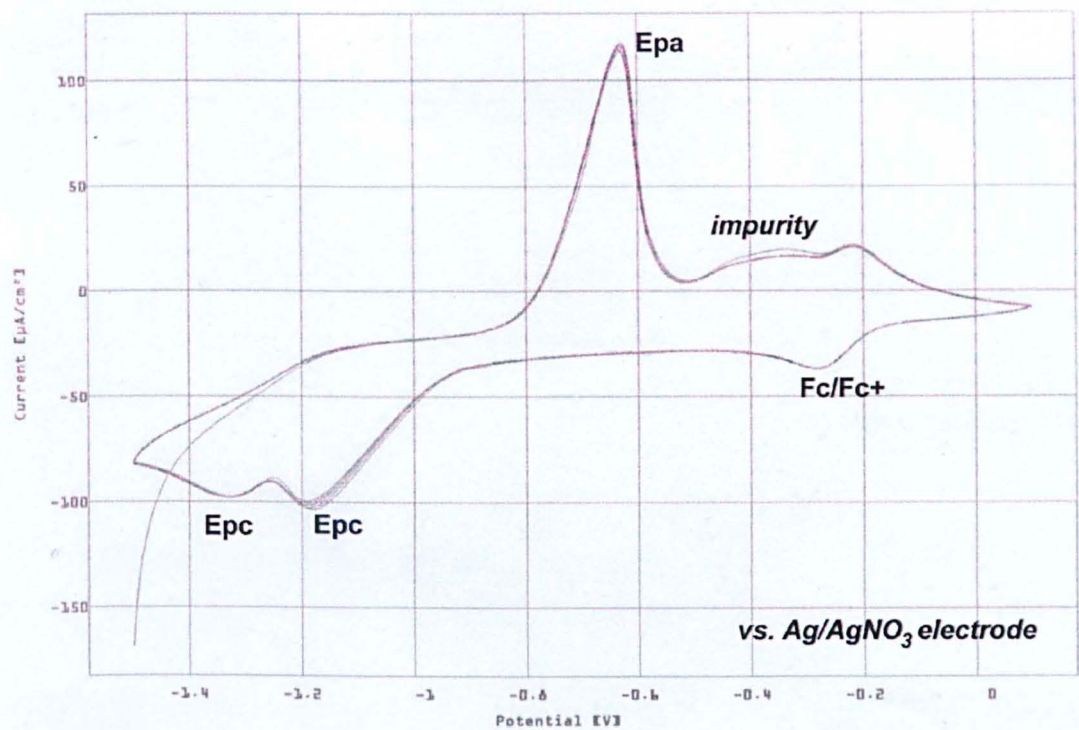
227. P. Grellier, J. Sarlauskas, Z. Anusevicius, A. Maroziene, C. Houee-Levin, J. Schrevel and N. Cenas, *Archives of Biochemistry and Biophysics*, 2001, **393**, 199.
228. J. Drummelsmith, V. Brochu, I. Girard, N. Messier and M. Ouellette, *Molecular & Cellular Proteomics*, 2003, **2**, 146.
229. F. G. Drakesmith, R. D. Richardson, O. J. Stewart and P. Tarrant, *Journal of Organic Chemistry*, 1968, **33**, 286.
230. P. G. Gassman and C. K. Harrington, *Journal of Organic Chemistry*, 1984, **49**, 2258.
231. A. Demiel, *Journal of Organic Chemistry*, 1960, **25**, 993.
232. J. B. Lambert, E. G. Larson, R. J. Bosch and M. L. E. Tevrucht, *Journal of the American Chemical Society*, 1985, **107**, 5443.
233. F. Degerbeck, B. Fransson, L. Grehn and U. Ragnarsson, *Journal of the Chemical Society, Perkin Transactions 1*, 1992, 245.
234. Y. Takeuchi, R. Masamoto, T. Hagi and T. Koizumi, *Journal of Fluorine Chemistry*, 1985, **29**, 179.
235. O. Schrems, H. M. Oberhoffer and W. A. P. Luck, *Journal of Physical Chemistry*, 1984, **88**, 4335.
236. T. Fuchigami and S. Ichikawa, *Journal of Organic Chemistry*, 1994, **59**, 607.
237. K. Aoki, K. Tomioka, H. Noguchi and K. Koga, *Tetrahedron*, 1997, **53**, 13641.
238. K. Aoki and K. Koga, *Chemical & Pharmaceutical Bulletin*, 2000, **48**, 571.
239. D. R. Burfield and R. H. Smithers, *Journal of Organic Chemistry*, 1978, **43**, 3966.
240. G. H. Searle and R. J. Geue, *Australian Journal of Chemistry*, 1984, **37**, 959.
241. S. Nagarajan and B. Ganem, *Journal of Organic Chemistry*, 1986, **51**, 4856.
242. A. E. Martin, T. M. Ford and J. E. Bulkowski, *Journal of Organic Chemistry*, 1982, **47**, 412.
243. D. H. Busch, D. J. Olszanski, J. C. Stevens, W. P. Schammel, M. Kojima, N. Herron, L. L. Zimmer, K. A. Holter and J. Mocak, *Journal of the American Chemical Society*, 1981, **103**, 1472.
244. J. M. Erhardt, E. R. Grover and J. D. Wuest, *Journal of the American Chemical Society*, 1980, **102**, 6365.
245. W. H. Hunter and B. E. Sorenson, *Journal of the American Chemical Society*, 1932, **54**, 3364.
246. M. Briellmann, S. Kaderli, C. J. Meyer and A. D. Zuberbuhler, *Helvetica Chimica Acta*, 1987, **70**, 680.
247. N. G. Lukyanenko, S. S. Basok and L. K. Filanova, *Journal of Organic Chemistry of the U.S.S.R. (English Translation)*, 1988, **24**, 1562.
248. O. P. Gladkikh, H. Inwood, D. Nicholls and D. C. Weatherburn, *Inorganica Chimica Acta*, 2002, **331**, 131.
249. M. W. Hosseini and J. M. Lehn, *Journal of the American Chemical Society*, 1987, **109**, 7047.
250. H. S. Brown, C. P. Muenchausen and L. R. Sousa, *Journal of Organic Chemistry*, 1980, **45**, 1682.
251. K. Ravichandran, F. A. J. Kerdesky and M. P. Cava, *Journal of Organic Chemistry*, 1986, **51**, 2044.
252. L. Y. Martin, L. J. Dehayes, L. J. Zompa and D. H. Busch, *Journal of the American Chemical Society*, 1974, **96**, 4046.
253. B. Alici, E. Cetinkaya and B. Cetinkaya, *Heterocycles*, 1997, **45**, 29.

254. J. D. Chartres, A. M. Groth, L. F. Lindoy, M. P. Lowe and G. V. Meehan, *Journal of the Chemical Society-Perkin Transactions 1*, 2000, 3444.
255. J. Huskens and A. D. Sherry, *Journal of the Chemical Society, Dalton Transactions*, 1998, 177.
256. M. R. Malachowski, L. J. Tomlinson, M. J. Parker and J. D. Davis, *Tetrahedron Letters*, 1992, **33**, 1395.
257. R. W. Hay and D. M. S. Clark, *Inorganica Chimica Acta*, 1984, **83**, L23.
258. Z. Otwinowski and W. Minor, in *Macromolecular Crystallography, part A*, Vol. 276 (Ed.: C. W. a. R. M. S. Carter Jr), 1997, pp. 307.
259. R. H. Blessing, *DENZOX - Program for processing Denzo x files*, Modified for KappaCCD data, L.J. Farrugia and K.W. Muir (2001), 1997.
260. P. Coppens, L. Leiserowitz and D. Rabinovich, *Acta Crystallographica*, 1965, **18**, 1035.
261. R. H. Blessing, *Journal of Applied Crystallography*, 1997, **30**, 421.
262. R. H. Blessing, *Acta Crystallographica*, 1995, **A51**, 33.
263. P. T. Beurskens, G. Beurskens, R. De Gelder, S. Garcia-Granda, R. O. Gould, R. Israel and J. M. M. Smits, *DIRDIF-99 program system*, Crystallography Laboratory, University of Nijmegen, The Netherlands, 1999.
264. A. Altomare, G. Cascarano, C. Giacovazzo and A. Guagliardi, *Journal of Applied Crystallography*, 1993, **26**, 343.
265. G. M. Sheldrick, *SHELXL-97 a program for crystal structure refinement*, University of Göttingen, Germany. Release 97-2, 1997.
266. Tables 4.2.4.2, 4.2.6.8 and 6.1.1.4, in *International Tables for Crystallography, Volume C Mathematical, Physical and Chemical Tables*, Kluwer, Dordrecht, 1995.
267. A. L. Spek, *Acta Crystallographica*, 1990, **A46**, C34.
268. L. J. Farrugia, *Journal of Applied Crystallography*, 1997, **30**, 565.
269. L. J. Farrugia, *Journal of Applied Crystallography*, 1999, **32**, 837.
270. T. Mosmann, *Journal of Immunological Methods*, 1983, **65**, 55.
271. M. Lee, A. L. Rhodes, M. D. Wyatt, S. Forrow and J. A. Hartley, *Anti-Cancer Drug Design*, 1993, **8**, 173.
272. I. J. Stratford and M. A. Stephens, *International Journal of Radiation Oncology Biology Physics*, 1989, **16**, 973.

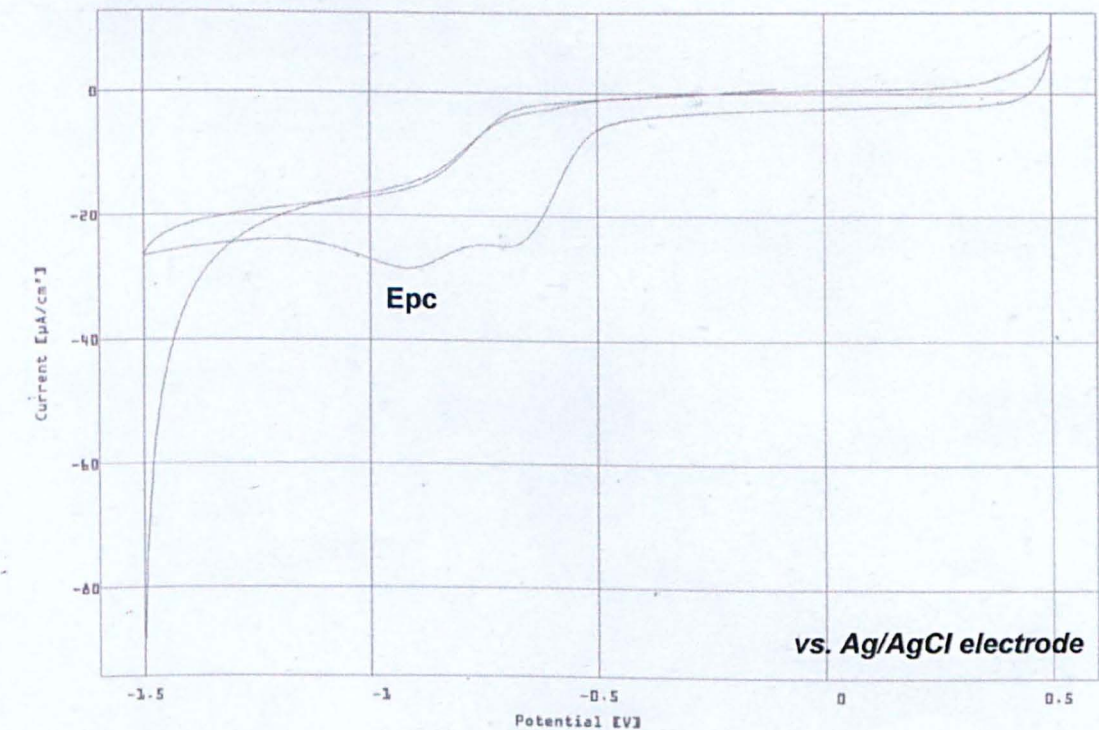
Appendix 1

Cyclic voltammograms for all complexes

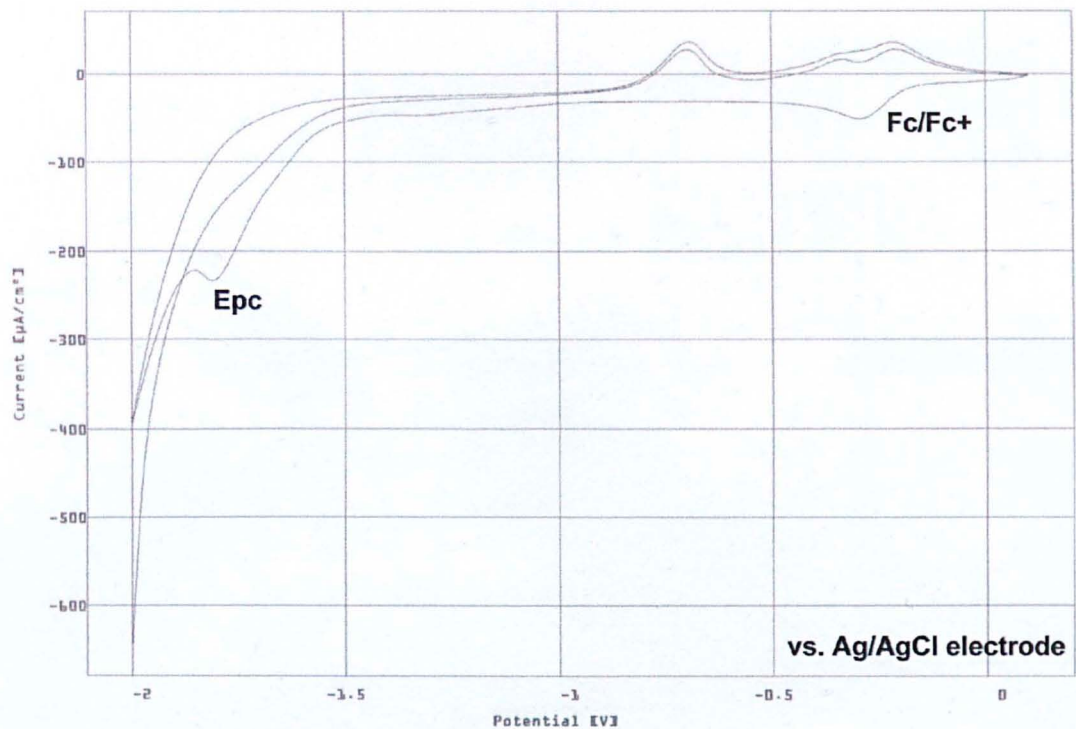
a. Cyclen[Cu(II)]Cl₂ (200) in phosphate buffer



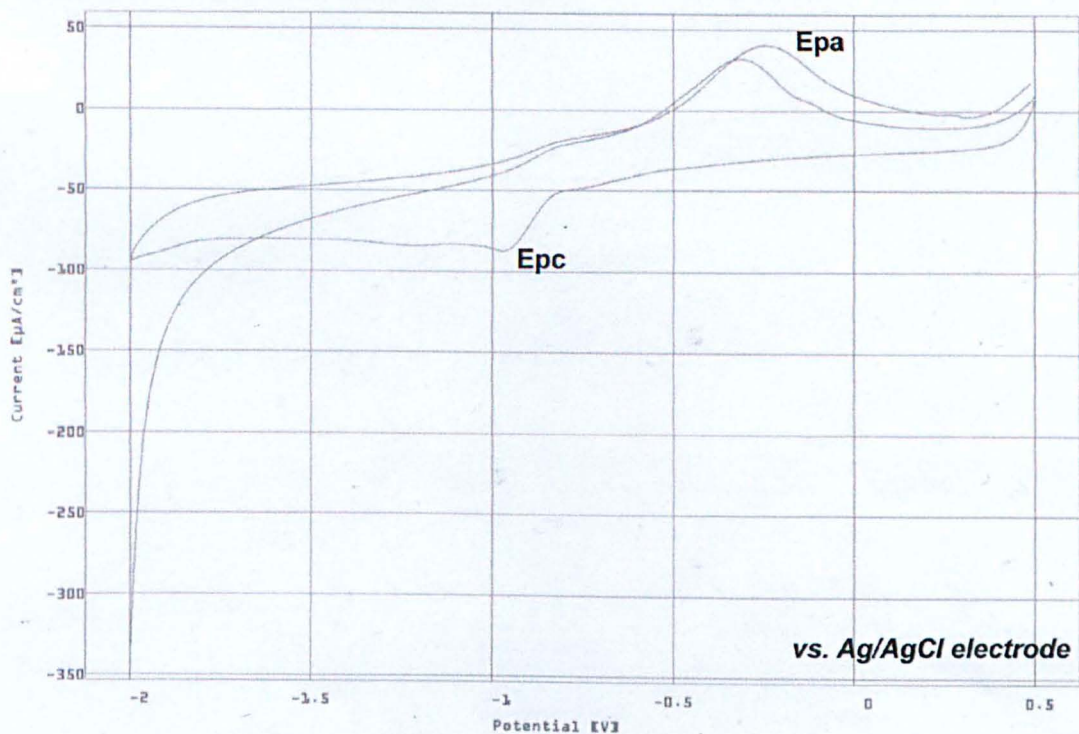
b. Cyclen[Cu(II)]Cl₂ (200) in DMF



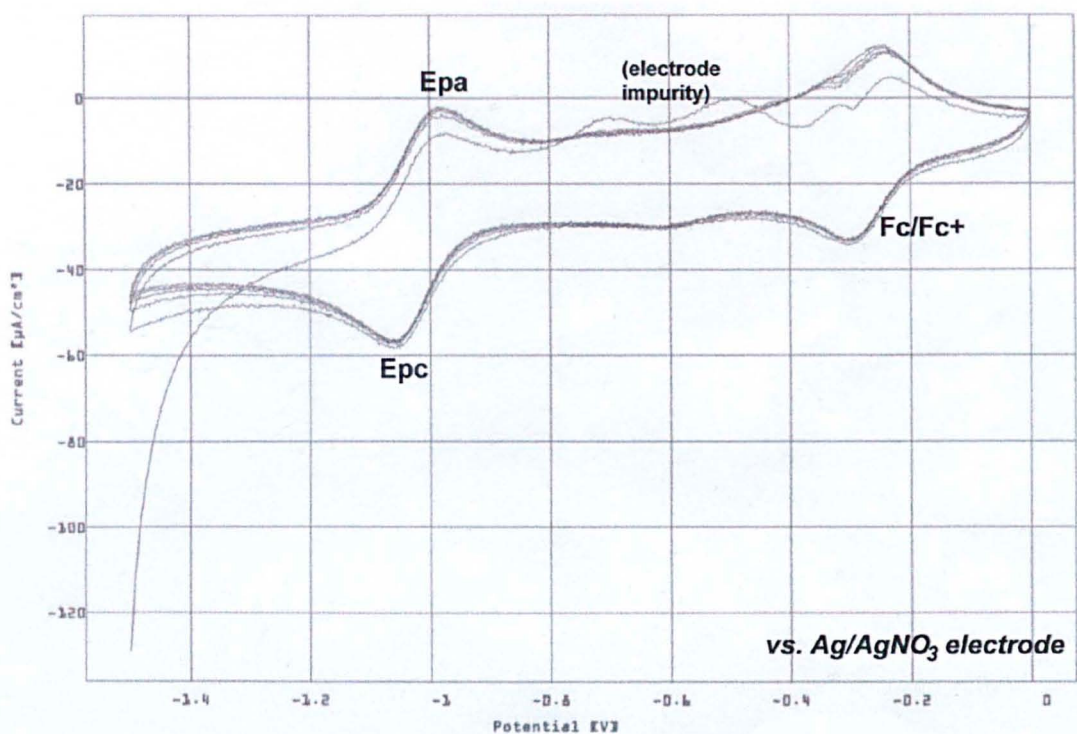
c. Cyclam[Cu(II)]Cl₂ (202) in phosphate buffer



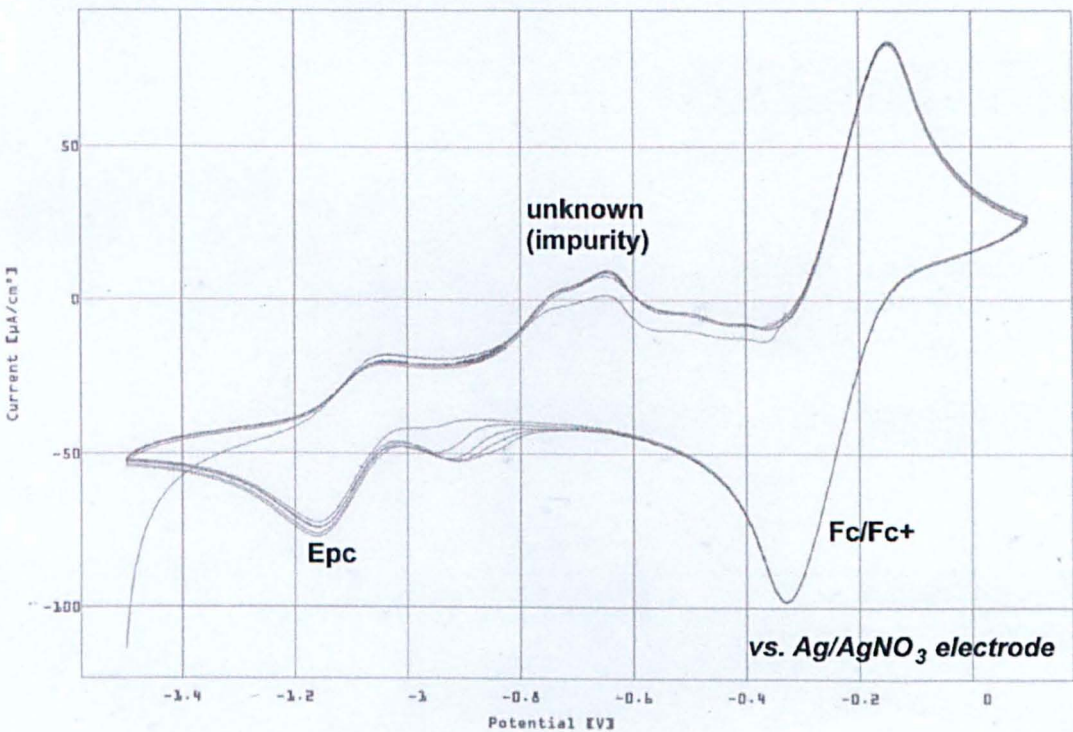
d. Cyclam[Cu(II)]Cl₂ (202) in DMF



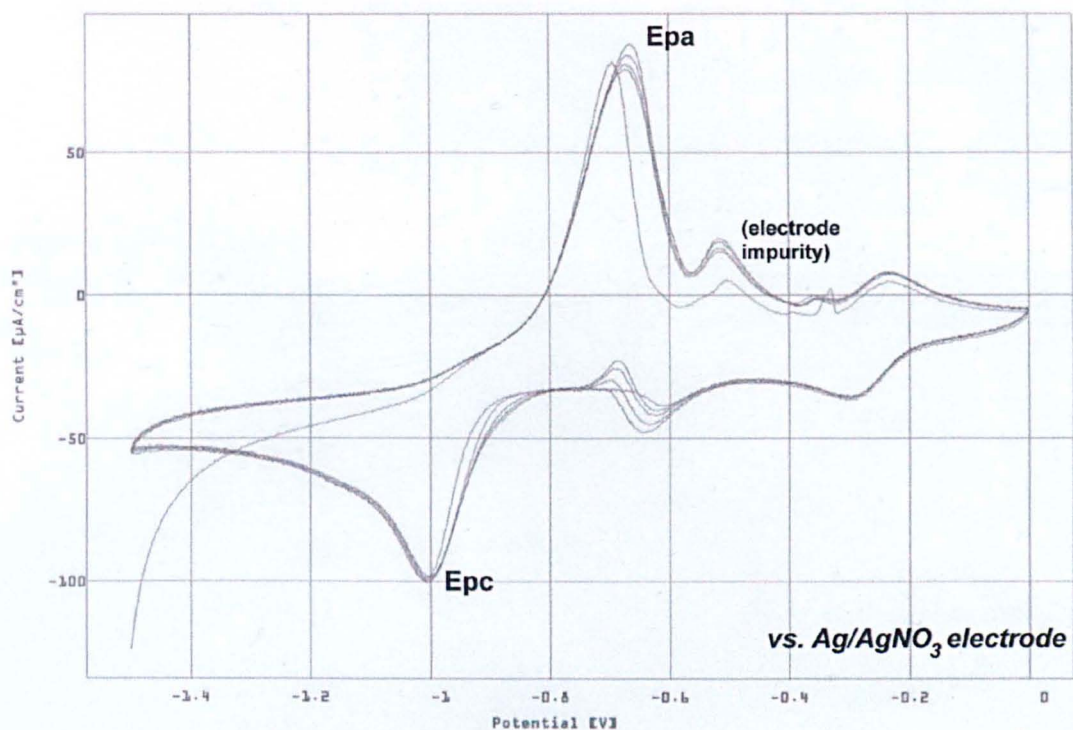
e. 1,4,7,10-Tetra(2-hydroxyethyl)cyclen[Cu(II)]Cl₂ (192) in phosphate buffer



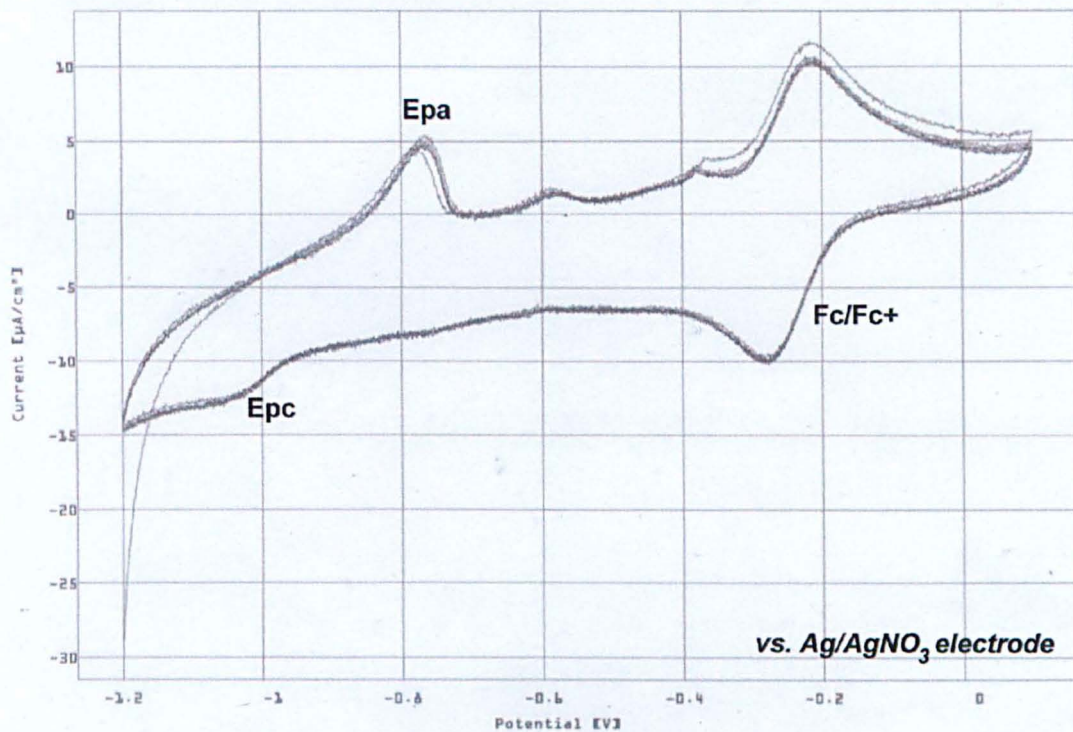
f. 1,4,7,10-Tetra(2-hydroxyethyl)homocyclen[Cu(II)]Cl₂ (193) in phosphate buffer



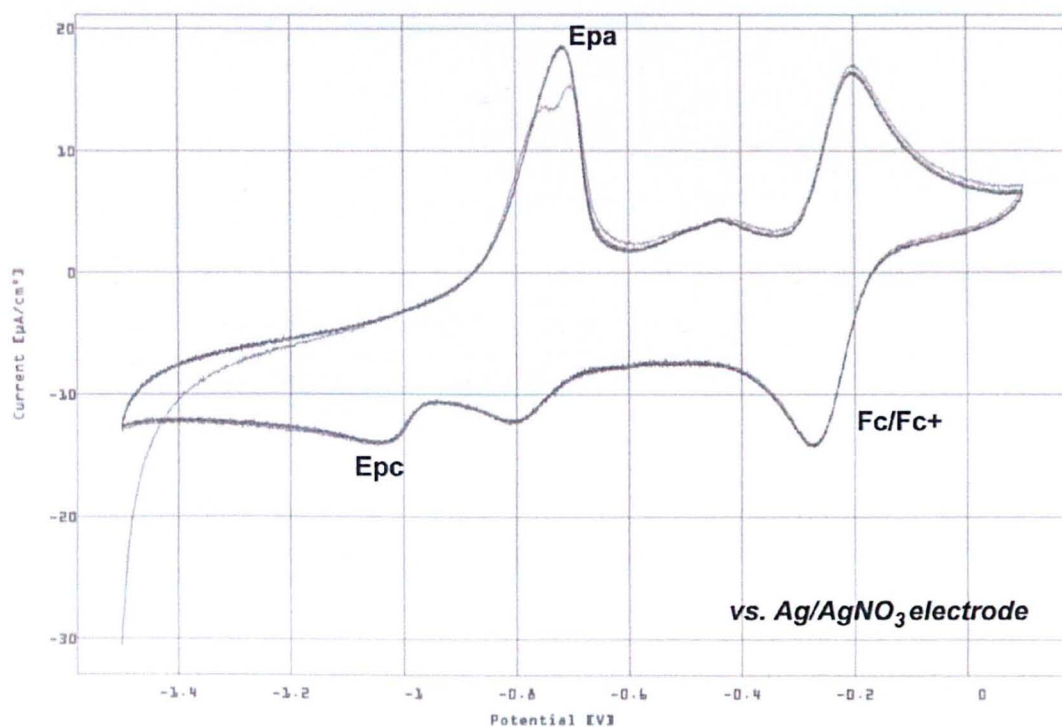
g. 1,4,8,11-Tetra(2-hydroxyethyl)cyclam[Cu(II)]Cl₂ (188) in phosphate buffer



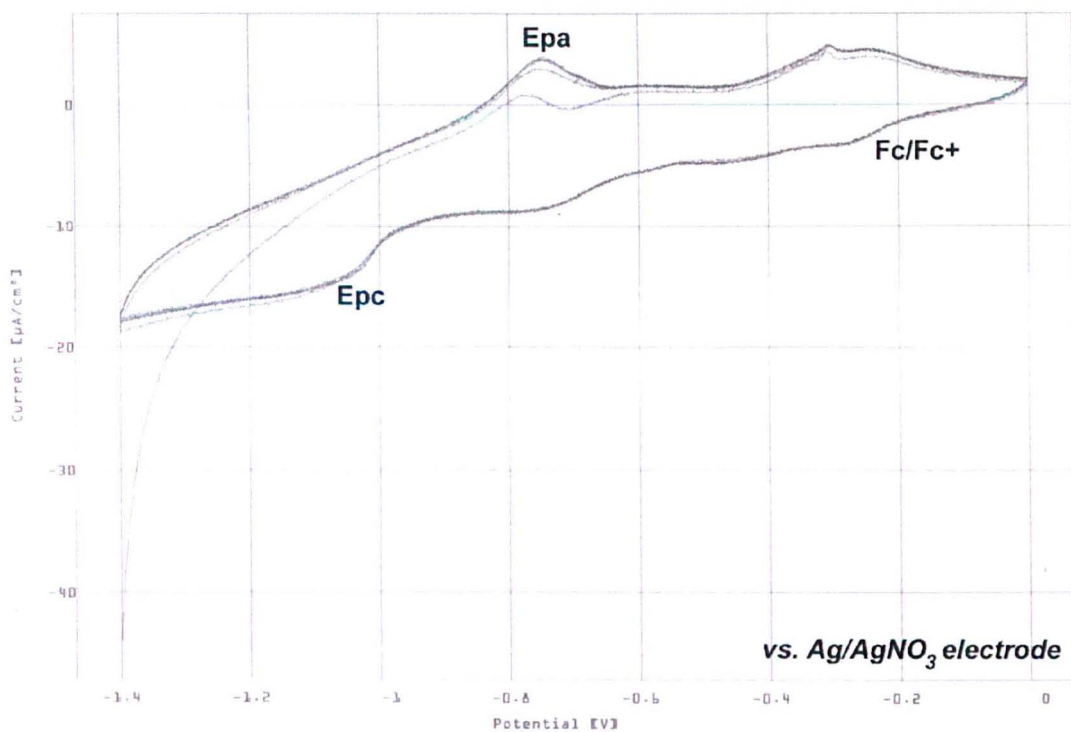
h. 1,4,8,11-Tetra-N-ethyl Cyclam[Cu(II)]Cl₂ (204) in phosphate buffer



i. 1,4,7,10-Tetra(2-chloroethyl)homocyclen[Cu(II)]Cl₂ (187) in phosphate buffer



j. 1-(2-hydroxyethyl)-4,7-(2-chloroethyl)-tacn[Cu(II)]Cl₂ (191) in phosphate buffer

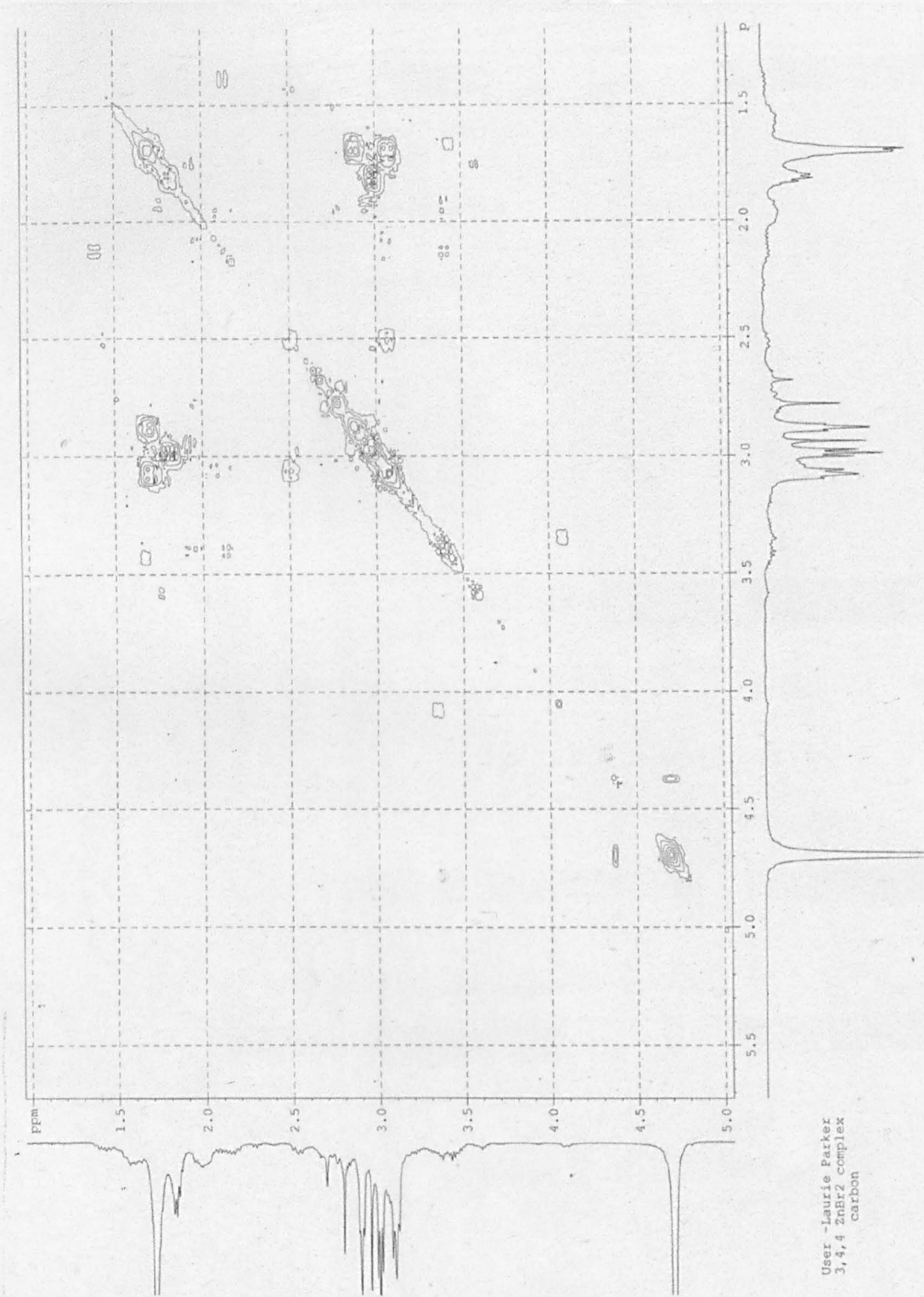


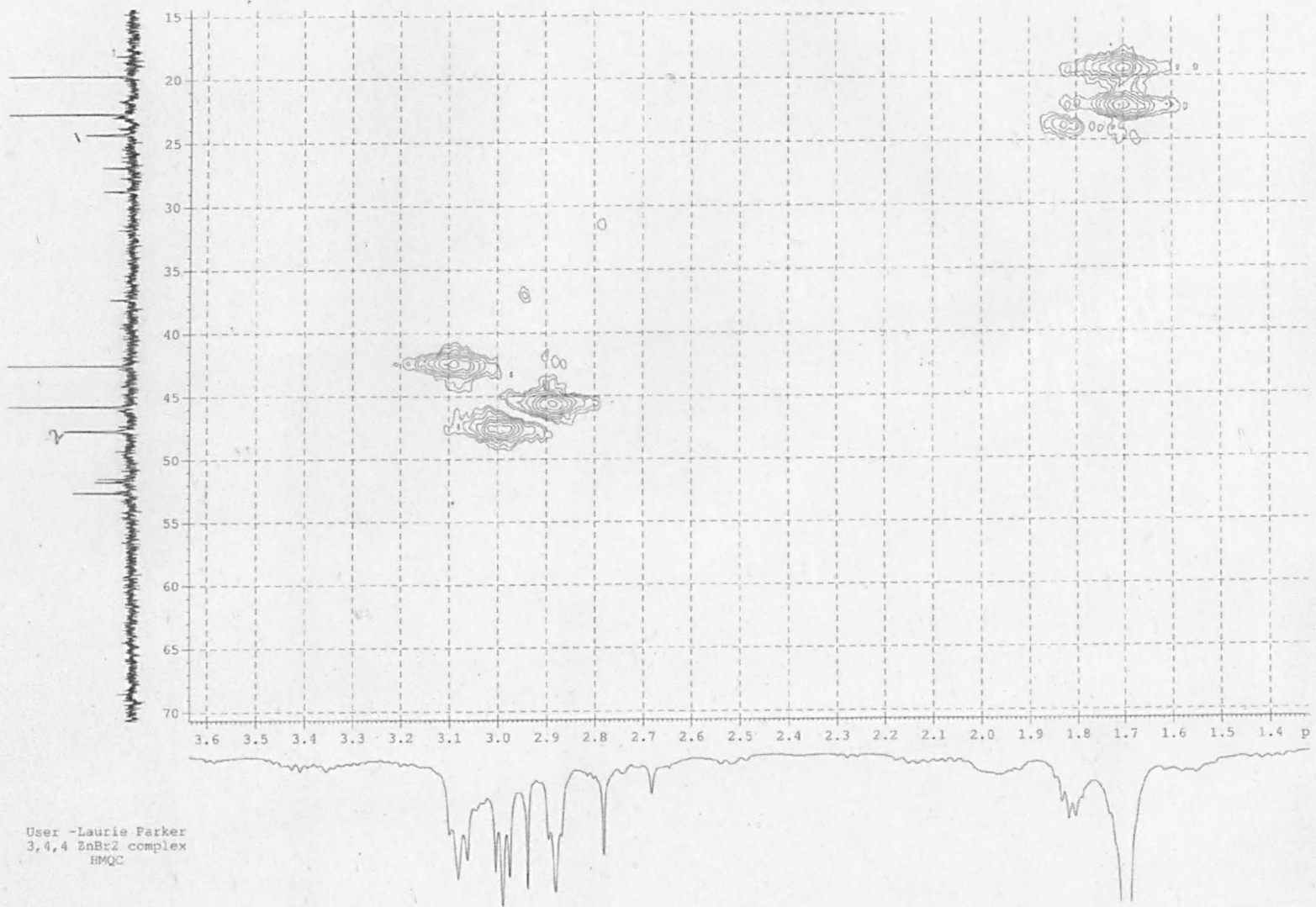
Appendix 2

Two-dimensional NMR spectra of Zn(II) titrations

1. 206: COSY, HMQC and HMBC

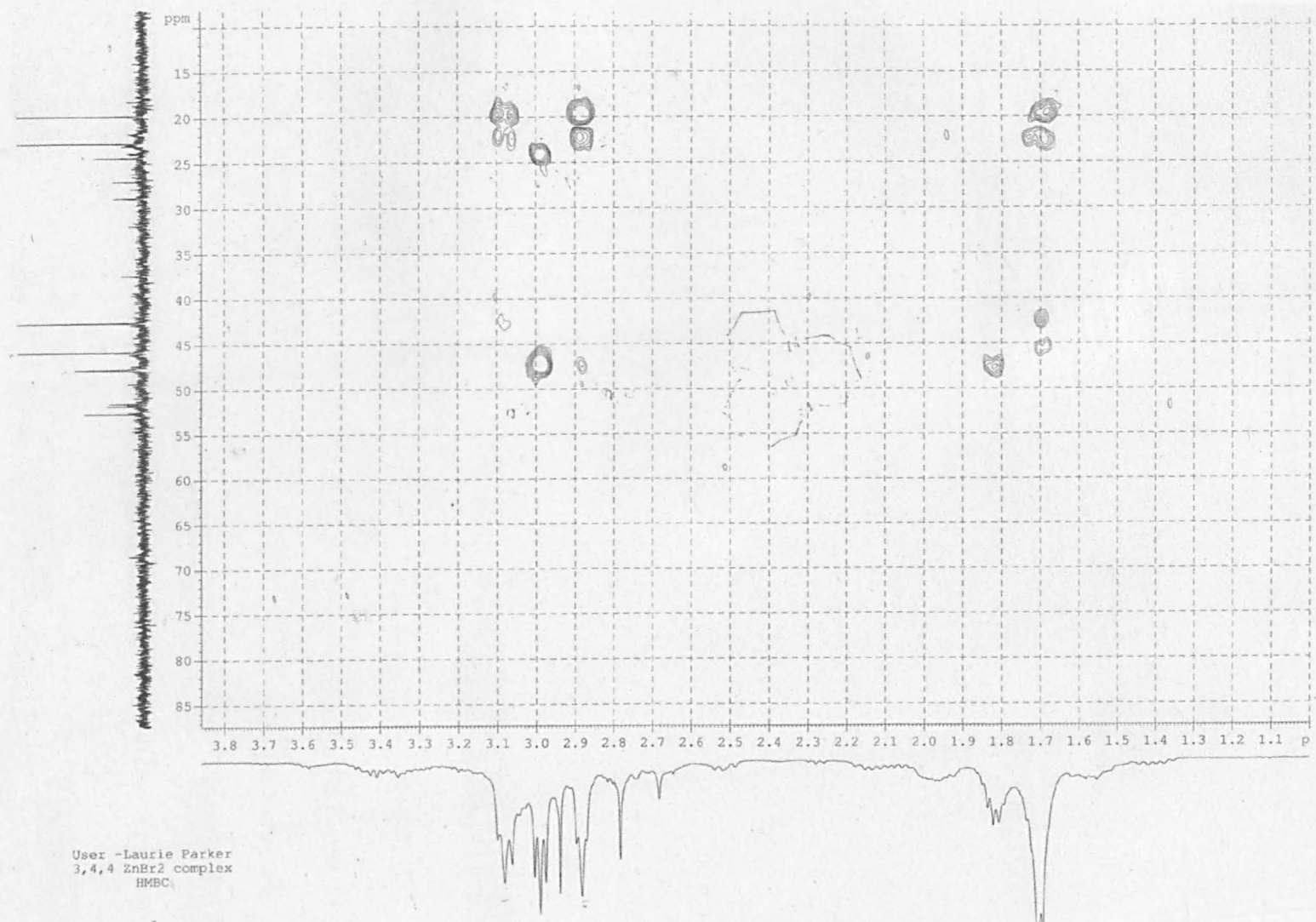
A. COSY spectrum for 206 (refer to section 6.2.6 for assignments)





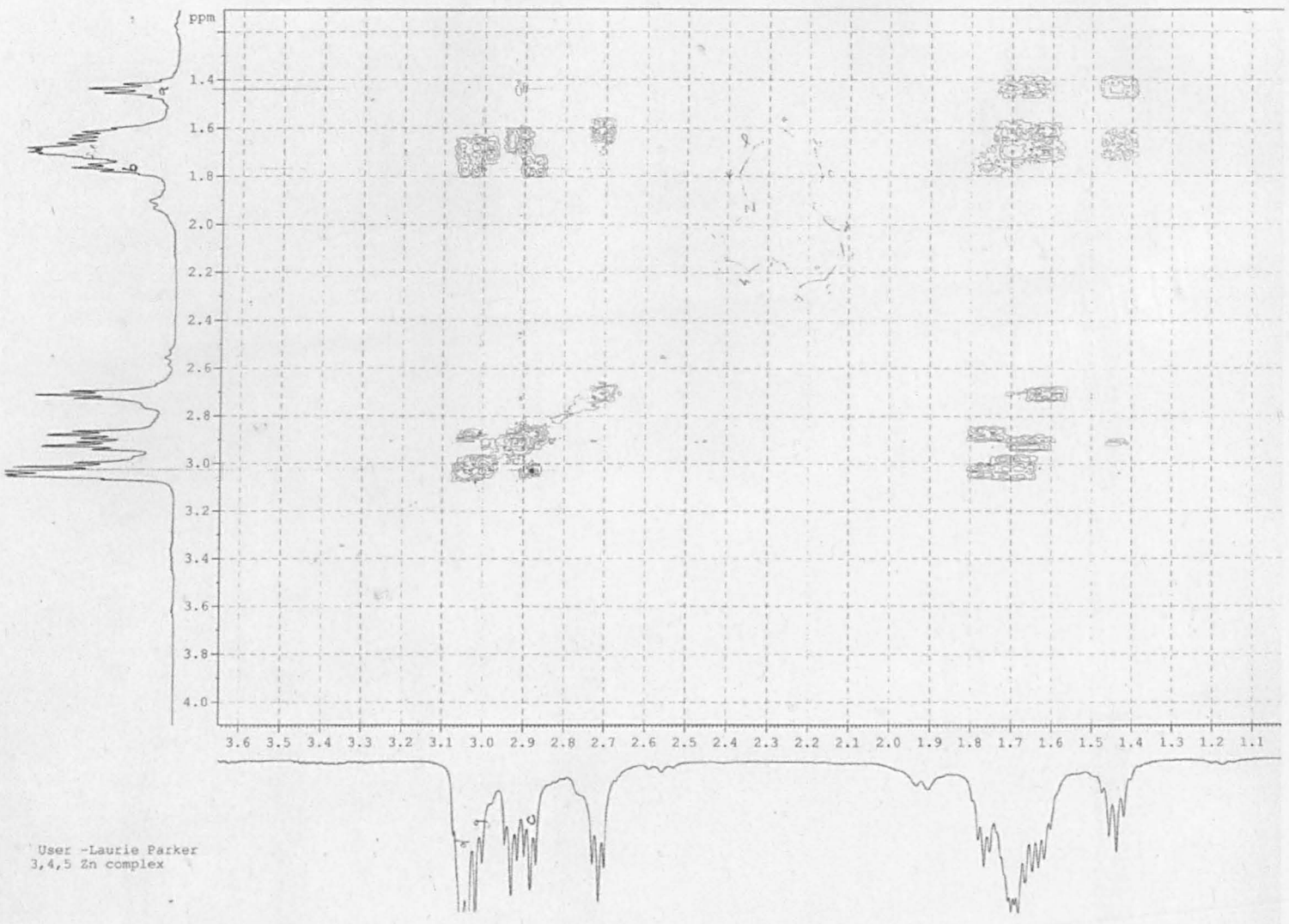
User -Laurie Parker
3,4,4 ZnBr₂ complex
HMQC

C. HMBC spectrum for 206

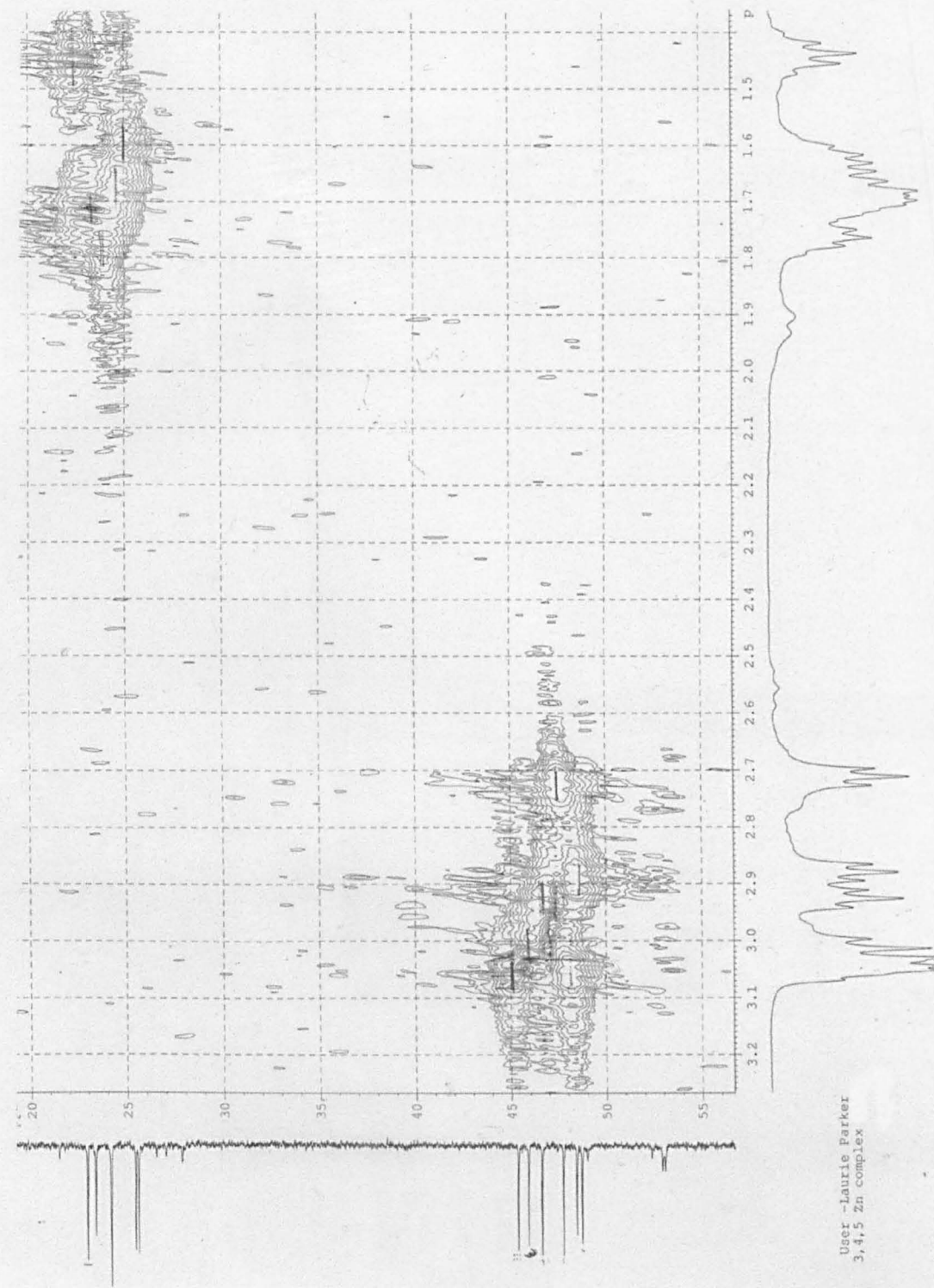


2. 207: COSY, HMQC and HMBC

1. COSY spectrum for 207 (refer to section 6.2.6 for assignments)



B. HMQC spectrum for 207



C. HMBC spectrum for 207

